Developing risk-based approaches to modelling phosphorus contamination in agricultural catchments

A thesis submitted for the degree of Doctor of Philosophy

School of Archaeology, Geography and Environmental Science,

University of Reading

Camilla Negri

June 2024

Dedication

A mia nonna Diva.

Declaration

I confirm that this is my own work and the use of all material from other sources has been properly and fully acknowledged.

Camilla Negri

June 2024

Contents

Acknowledgments

My parents and extended family: mamma, papà, Haotian, nonna Veronica, le mie zie Betty e Veronica, Federica ed Eli.

My supervisory team: Miriam, Per-Erik, Andrew, Nick, and my mentor Eulyn.

My friends who are scattered across Europe and the globe: Marti, Cami, Luke, Marta, Francesca, Joe, Irma, Hans, Eva, David, Doug, Betsy, Gabrielle, Carla, Layla, Rover, Lucas, Pippa, Anna, Daniele, Tommaso, Lorenzo, Francesco, Azuki, Oscar, Mara, Monica, Flora, and Daniela.

My fellow PhD students, Imelda, Kerr, Andy, Sofie, Matthias, Carolin, Felipe, Chisha, and Kate.

My teachers, data handlers, and co-authors across Teagasc, Hutton, BioSS, and SLU: Eddie, Simon, Una, Golnaz, Daniel, Oggy, Marc B., Marc S., Zisis, Ken, Rebecca, and Magda.

Thank you.

Abstract

Bayesian Belief Networks (BBNs) are a promising but underutilized probabilistic graphical tool for modelling water quality for Environmental Impact Assessment, with their ability to include uncertainty in the predictions being relevant to catchment and water managers. This thesis explores the application of these tools to predict phosphorus (P) losses in terms of total reactive phosphorus (TRP) concentrations in four Irish agricultural catchments, with high P concentrations being a major concern in at least three of them. A hybrid Bayesian Belief Network combining discrete and continuous variables was developed for a surface hydrology-dominated grassland catchment, using daily concentration data to build the BBN priors and assess model performance. The step-wise introduction of different P sources, combined with high-frequency data and detailed catchment understanding improved the first model iteration's predictive ability. In all model applications, the models' predictions presented wider distributions than the observations, which was noted in similar work, and remains a property of BBNs. Transferring the BBN across catchments allowed testing the model's structural uncertainty and showed that the developed BBN could perform well in surface-driven catchments. The BBN was enhanced by improved process representation and catchment-specific parameterization. Model transferability across catchment typologies (surface vs groundwater-dominated, grassland vs tillage land use) is explored, and the BBNs are used to predict future P concentrations under climate change scenarios. The application of the catchment-specific BBNs to predict future P concentrations under climate change revealed the need for further BBN sensitivity analysis to aid result interpretation. The potential for BBNs to be used as a tool to inform compliance with regulatory standards is discussed. The discussion considers learnings from current BBN research, P processes represented in both BBNs and process-based models, and the model application in this study. Limitations of the approach and future research avenues are explored.

Plain language summary

Bayesian Belief Networks (BBNs) are a useful but not widely used tool for predicting water quality. They can account for uncertainty, making them valuable for water and catchment managers. This study looks at using BBNs to predict phosphorus (P) levels in four agricultural catchments in Ireland, where high P levels are a big concern. The first model development focused on a grassland area where P losses in surface water flow are significant, examining how data availability affects the BBN's performance. The model's predictions improved by gradually adding different P sources. However, the BBN's predictions were generally more spread out than the actual observations, a common trait of BBNs. Testing the model in different catchments showed that it worked well in surface-driven ones, needing improvements (more detailed processes and catchment-specific data) to work well in groundwater-dominated catchments. When using the BBN to predict future P levels under climate change, it became clear that BBN sensitivity analysis is needed to understand the results better. We discuss if BBNs can help to inform regulatory standards, whether they can be adapted to different types of catchments (surface vs. groundwater-dominated and grassland vs. crop), and their utility in predicting future P levels under climate change. The study compares current BBN research with traditional models and discusses the strengths and weaknesses of using BBNs. Finally, areas for future research are suggested.

Supporting publications

Models and Code: the model described in Chapter 3, together with example data for the Ballycanew catchment, the R code for the data analysis and figures is available to download from GitHub at: https://github.com/CamillaNegri/Ballycanew_Ptool

The models described in Chapter 4 together with the code for the Sensitivity Analysis carried out in the same chapter are available from GitHub at: https://github.com/CamillaNegri/Transferability_Ptool

Supporting data: the data supporting Chapter 4 is available to download at: https://figshare.com/articles/online_resource/Evidence_dossier_for_the_workshop_titled_In-stream_phosphorus_cycling_in_agricultural_catchments_a_workshop_to_quantify_abiotic_and_biotic_P_uptake_/25055165/1 (CC BY 4.0) and can be cited as

Negri, C., Mellander, P.-E., 2024. Evidence dossier for the workshop titled "In-stream phosphorus cycling in agricultural catchments: a workshop to quantify abiotic and biotic P uptake". https://doi.org/10.6084/m9.figshare.25055165.v1

Supporting publication: Bieroza, M., Acharya, S., Benisch, J., ter Borg, R.N., Hallberg, L., **Negri, C.**, Pruitt, A., Pucher, M., Saavedra, F., Staniszewska, K., van't Veen, S.G.M., Vincent, A., Winter, C., Basu, N.B., Jarvie, H.P., Kirchner, J.W., 2023. Advances in Catchment Science, Hydrochemistry, and Aquatic Ecology Enabled by High-Frequency Water Quality Measurements. Environ. Sci. Technol. https://doi.org/10.1021/acs.est.2c07798, CC BY 4.0.

Peer-reviewed publications included in the thesis

Negri, C., Mellander, P.-E., Schurch, N.J., Wade, A.J., Gagkas, Z., Wardell-Johnson, D.H., Adams, K., Glendell, M., 2024. Bayesian network modelling of phosphorus pollution in agricultural catchments with high-resolution data. Environmental Modelling & Software 106073. https://doi.org/10.1016/j.envsoft.2024.106073, CC BY 4.0.

Negri, C., Schurch, N., Wade, A.J., Mellander, P.-E., Stutter, M., Bowes, M.J., Mzyece, C.C., Glendell, M., 2024. Transferability of a Bayesian Belief Network across diverse agricultural catchments using high-frequency hydrochemistry and land management data. Science of The Total Environment 949, 174926. https://doi.org/10.1016/j.scitotenv.2024.174926, CC BY 4.0.

Publications under review included in the thesis

Negri, C., Cowdery, E., Schurch, N., Wade, A.J., Mellander, P.-E., Glendell, M., 2024. An assessment of climate change impacts on stream phosphorus using a climate model ensemble and Bayesian Belief Networks. Research Square. https://dx.doi.org/10.21203/rs.3.rs-5165980/v1, CC BY 4.0.

Acronyms and abbreviations

Acronym	Definition
RoI	Republic of Ireland
ACP	Agricultural Catchments Programme
BBN, BN	Bayesian (Belief) Network
CPTs	Conditional (Contingency) Probability Tables
DAG	Directed Acyclic Graph
P	Phosphorus
TRP	Total Reactive Phosphorus
TDP	Total Dissolved Phosphorus
SS	Suspended Sediments
SRP	Soluble Reactive Phosphorus
DRP	Dissolved Reactive P
TP	Total Phosphorus
EU	European Union
WFD	Water Framework Directive
END	European Nitrates Directive
NAP	National Action Programme
EQS	Environmental Quality Standard
BMPs	Best Management Practices
DST	Decision Support Tool
DSS	Decision Support System
PBIAS	Percentage Bias

Figure captions

Table captions

1. Introduction

Figure 1.1 Harmful algal bloom in Lake Erie, 2009. T. Archer, NOAA/Flickr, CC BY-SA, as seen on https://theconversation.com/. Lake Erie is part of the Experimental Lakes Area, originally created in response to global concerns about algal blooms due to Nitrogen and Phosphorus pollution (Elser and Haygarth, 2021).

1.1 Phosphorus impacts water quality through eutrophication

Phosphorus (P) is an essential nutrient for plant growth (Elser et al., 2000). P fertilizer utilization doubled since the 1950s (Carey, 2016), with some studies noting a four-fold increase over the past 75 years (Powers et al., 2016; Villalba et al., 2008). This scale of P application has led to accumulation in soil, water, and solid waste. Globally, agriculture is estimated to contribute 75-90% of total P in river catchments (Villalba et al., 2008; Drohan et al., 2019). Therefore, the phosphorus paradox is twofold: on one hand, agricultural production increases P demand, and on the other, this finite resource can accumulate in soils, sediments, and estuaries, which decreases the plant bioavailable P pool, increasing agronomic requirements and exacerbating eutrophication (Figure 1.1), which makes it necessary to limit its pollution potential in waters. There is historical consensus that P is the nutrient that limits eutrophication in surface waters, whilst nitrogen (N) is considered the limiting factor in estuaries and coastal waters (Hecky and Kilham, 1988; Moss et al., 2013), due to the strong relationship between P and chlorophyll-a (Mischler et al., 2014). However, there is a growing consensus that not all freshwater systems are P-limited, with some being N-limited, with co-limitation by N and P being common (Elser et al., 2007; Mischler et al., 2014; Moss et al., 2013), and N:P ratios changing seasonally, leading to a potentially prevalent N limitation during plant growth season (Edwards et al., 2000; Mischler et al., 2014). Nevertheless, this research focusses on modelling of P losses from agricultural catchments to surface waters. Testing of new modelling approaches is particularly relevant due to the complexity of P transport and the inadequacy of process-based P models (Hollaway et al., 2018; Jackson-Blake et al., 2015; Vadas et al., 2013), which will be further explored in the following chapters.

Haygarth et al., (2005) introduced the interdisciplinary concept of the phosphorus transfer continuum, where they framed the issue of diffuse P loss from land to waters as sources (P inputs), mobilization (P detachment and solubilization from soils), delivery (where P enters waters), and impact (biological and ecological impacts of P in running and/or standing waters). Phosphorus sources in agricultural catchments can be natural (soil P and atmospheric deposition) and anthropogenic (fertilizers and manure applied to the fields, fertilizers, animal feed, and manure on hard standings). A typical way to describe pollution is by discriminating between diffuse and point sources. Diffuse sources are described as

pollution generated from land use activities, followed by dispersion over a large area, such as a field or (sub-)catchment. Discharges enter surface waters at intermitted intervals and diffuse sources are related to meteorological events. The core characteristics of diffuse pollution are that 1) it transits overland before reaching the unsaturated soil, surface waters or infiltrating the aquifer, and 2) is difficult to track and monitor its point of origin (Campbell et al., 2005). On the contrary, point sources come from a precise input location, such as pipes, sewers and discharge channels. Edwards and Withers, (2007), have shown that distinguishing sources can improve the understanding of P impacts in water bodies. However, rural point sources can have intermediate behaviour and become constant P sources, independent of transfers. For example, septic tanks can behave as a diffuse source when their collective number over a catchment is high. More recently, Stutter et al., (2022), challenged the source load apportionment models and showed that examining separate P fractions (the operationally defined total P, dissolved P, particulate P, and bioavailable P, summarized in Figure 1.2), can improve understanding of nutrient dynamics. In another recent example, Vero and Doody, (2021), show how the nutrient transfer continuum can be applied to farmyards, a source that is usually modelled and conceptualized as a point source. While increasing the P supply in a stream may initially boost ecosystem biomass and diversity, the longer-term effects will be ecosystem stress due to algal growth and increased speed of the eutrophication process. In short, crossing the threshold between P subsidy (supply that is healthy to the system) and P stress, will result in an ecosystem no longer able to buffer the impacts of P supply (Jarvie et al., 2019; Withers and Jarvie, 2008). Finally, P concentration changes in response to land use change can impact the dominance of autotrophs, lead to changes to the invertebrate community (specifically, increased excretion of P from invertebrates to maintain stochiometric C:N:P balance) and reduction of species diversity. Increased algal growth can cause anoxia, which in turn impacts fish eggs survival, and soluble reactive P (SRP) release from bed sediments. Nutrient enrichment has both a chronic (constant nutrient input from point sources) and an acute (short spikes from diffuse pollution) effect on macroinvertebrates, with chronic effects being worse (Davis et al., 2019). In addition, albeit nutrients may not be the major stressor, they exacerbate the negative effects of sediment enrichment (Davis et al., 2019). Therefore, management efforts should concentrate on limiting point sources, especially at low-flow periods, when concentrations increase. This is especially important considering

that climate change will increase the frequency of droughts (therefore intensifying the effects of chronic stress), and the frequency and magnitude of storms (therefore intensifying the effects of acute stress) on macroinvertebrates.

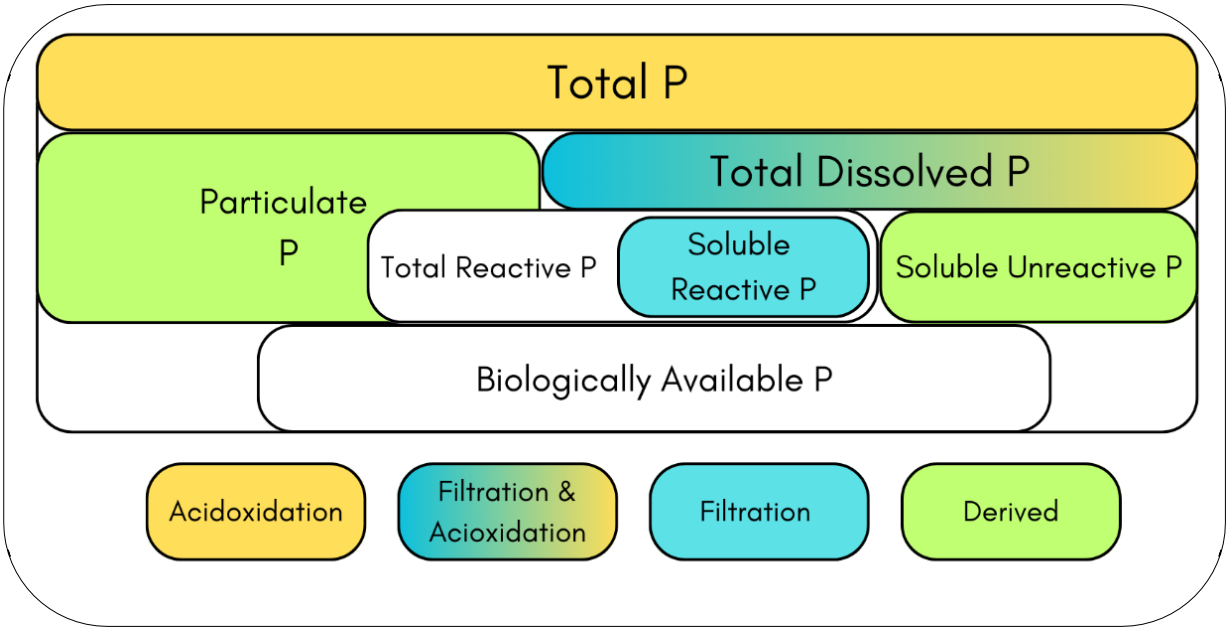

Figure 1.2 Phosphorus species and their definition by analytical methods. The filtration methods refers to filtration with 45 µm membrane. All species are derived by colorimetric determination, except Particulate P (PP) and Soluble Unereactive P SUP), which are calculated by subtraction.Figure updated and adapted from (Glendell et al., 2020).

1.2 Phosphorus pollution in Ireland: sources and key findings

The European Water Framework Directive 2000/60/EC (The European Commission, 2000), WFD hereafter, mandates that all water bodies in the European Union should have achieved a "good status" by 2015. However, only 40% of surface water bodies across the EU were in good ecological status according to the EEA report 7/2018, and Ireland had not yet reported the data relative to the River Basin Management Plan (RBMP) required by the WFD (European Environment Agency, 2018). However, the Environmental Protection Agency, (2019) reported that in 2018, 42.7% of Irish surface waters were in moderate, poor, or bad ecological status, while 52.8% had either good or high ecological status. As stated in the EEA report 7/2018, the major pressure on water body quality is diffuse pollution, particularly nitrogen and phosphorus from agriculture. Many countries have implemented legislation to address this issue. However, according to Amery and Schoumans, (2014), although the Nitrates Directive 91/676/EEC (The European Commision, 1991) states that eutrophication due to agriculture should be prevented, phosphorus is not specifically mentioned. Following Drohan et al., (2019), the need to limit soil P accumulation in Northern Ireland and in the Republic of Ireland, is written into the EU Nitrates Action Programs by the European Commission, but there is no mandatory soil test to check that farms are operating within the 170 kg ha^{1} limit of organic N application. Furthermore, support is needed to tackle P pollution, as it remains one of the major causes of water quality failure and ecological impact in Irish freshwaters (Environmental Protection Agency, 2017). In Ireland, the Environmental Quality Standard (EQS) for phosphate is equivalent to a 0.035 mg l^{-1} threshold established in Ireland to comply with the WFD (European Communities Environmental Objectives (Surface Waters) Regulations, 2009). Water quality failure becomes evident when looking at the loss of high-status sites since 2009: high-status rivers are now 8.5% compared to 13% in the WFD baseline assessment, representing an additional 115 poor-status surface bodies (Environmental Protection Agency, 2019). The decline in sites with high ecological status has been estimated at 50% since 1987 (Gaffney et al., 2021). Moreover, time lags of 15 to 20 years beyond the initial 2015 WFD deadline are estimated for P to reach the optimum index in Irish soils (Schulte et al., 2010). Time lags could further increase,

considering that Ireland is one of the few remaining EU countries where derogation from the END will be allowed until 2026 (Gleeson, The Irish Times, 2023).

Following the concept of phosphorus transfer continuum introduced by Haygarth et al., (2005), a review of the recent literature regarding the issue of P pollution in Ireland was conducted in this thesis. In this conceptual framework, pollutant sources are only delivered to receiving waters if transport pathways exist (Thomas et al., 2016a). The majority of the studies reported that the main source of P in Irish agricultural catchments was soil P content or excess plant available P, which can derive from excess manure and mineral fertilizer application (Regan et al., 2012), while a smaller number of studies pointed out the limited importance of point-source pollution (Campbell et al., 2015; Mockler et al., 2017). As a general conclusion, we could see that transport and delivery of P in Irish agricultural catchments is dominated by weather and hydrological conditions rather than initial soil P content (Mellander et al., 2015, 2018; Mockler et al., 2017). This seems to contrast with the idea that a significant correlation exists between soil test P (STP) and P loss to surface water in Ireland (Doody et al., 2012). The main pathways identified were overland flow, subsurface flow, and groundwater flow. In addition, soil chemistry and structure also play an important role in determining the preferential P pathways. In the study by Mellander et al., (2016) P colloids were proven to bypass the soil matrix and leach into the groundwater table. In a study by Fresne et al., (2022) colloidal P was found in high proportions in below-ground pathways in catchments with contrasting land use and similar hydrology. In one case (grassland-dominated catchment), colloidal P was mainly delivered by quick surface pathways (quick surface pathways, 37%) and slow below-ground pathways via groundwater (deep baseflow, 33%), while in the other (arable) it was delivered by below ground pathways (92%). Extensive research has been done with regards to P pollution risk at field and catchment scales, while a smaller number of studies considered the whole of Ireland as a study area for modelling approaches. This is confirmed by a review study conducted by Doody et al., (2012), overviewing recent literature regarding P pollution from agricultural land in Ireland, where the need for catchment management tools and Decision Support Tools (DSTs) is identified.

Since this review, decision support approaches in Ireland have focussed on the optimization of plant available P following the guidelines set out in the Teagasc green book (Wall and Plunkett, 2016), with online nutrient management calculators (e.g., Teagasc Nutrient Management Planning Online) (Teagasc - Agriculture and Food Development Authority, 2017). These calculators are usually freely available to the farmers and are used voluntarily (Drohan et al., 2019). Among these tools are high spatial resolution, field scale, P-indexes, used in USA, UK, Sweden, Republic of Ireland, and Norway (Drohan et al., 2019). In Ireland, the Nitrates Action Programme (NAP) determined by the European Nitrates Directive (END), sets limits on the agricultural use of both N and P inputs, and P regulations are based on the soil agronomic P (Morgan's phosphorus test), which is measured with a buffered acetate-acetic reagent (Daly and Casey, 2005; McDonald et al., 2019). P advice for crops and tillage is based on four categories of soil Morgan P index, where the optimum P is set at 5.1-8.0 mg l^{-1} (grassland) and 6.1-10.0 mg l^{-1} (tillage), and only maintenance fertilizer rates are required (Regan et al., 2012). A possible explanation for the observed lack of effectiveness of measures is that there are consistent lags between treatment (mitigation measure) and water quality response (Meals et al., 2010). In addition, legacy phosphorus might be so abundant as to control water quality long term (Bieroza et al., 2019, 2018). Lastly, some mitigation measures might bring about pollutant swapping, where the decrease of a pollution source might lead to the increase of another, although research has shown that reduced P can increase N concentrations, not the opposite (Bieroza et al., 2019). If flow pathways (transport) are to be taken into consideration and incorporated in P pollution mitigation strategies (Daly et al., 2016; Deakin et al., 2016), then it is clear that the DSTs and Decision Support Systems (DSSs) available should be implemented firstly at field, farm and catchment scale and secondly at regional and/or national scales. A few risk-based approaches to the management of P pollution have been undertaken by Thomas et al., (2017, 2016a). These studies have mostly been conducted at the subfield scale and applied in four Agricultural Catchments Programme catchments of ~10 km^2 in the Republic of Ireland, as well as ~100 km^2 catchment in Northern Ireland. In the first instance, a tool that accounts for microtopography, elevation and hydrological connectivity was built to predict and map the Hydrologically Sensitive Areas (HSAs). These areas generate overland flow and therefore have the highest propensity for sediment and phosphorus transport and delivery (Thomas et al., 2016a). Secondly, Thomas et al., (2016b) developed

a Geographical Information System (GIS) risk-based tool for mapping Critical Source Areas (CSAs), merging the HSA Index (which identifies high run-off generating areas and the locations for targeting mitigation measures) and field-scale soil P data. Both tools can target legacy P mitigation measures and P management best practices. More recently, Thomas et al., (2019) also applied the CSAs tool at the national scale, using a 5 m digital elevation model and the microtopographic characteristics identified in the previous study (Thomas et al., 2017). However, these are labour-intensive source-focused tools for mitigation measures, and they might be ineffective or insufficient to tackle P pollution. Hence the development of risk-based DSSs is needed (Drohan et al., 2019) to inform the choice of the most effective mitigation measures.

1.3 Bayesian Belief Networks

Bayesian Networks or Bayesian Belief Networks (BBNs) are probabilistic graphical models firstly introduced by Pearl in the 1980s (Pearl, 1986). Bayesian Networks are described as directed acyclic graphs (DAGs) of probability distributions, where the term "acyclic directed" means there is a sequential flow of information among variables and no dynamic feedback loops (Barton et al., 2012; Kragt, 2009). The relationships between variables in a BBN are parameterized using conditional probability distributions or conditional probability tables when variables are discrete (CPTs) (Borsuk et al., 2004). In a BBN, variables encoded in distributions or CPTs are defined as nodes, and the arrows pointing to nodes are called arcs, which are directed. The arcs represent the causal relationship between parent (where the arcs are directed from) and child nodes (where the arcs are directed to). Such causal relationships are calculated for a child node from the probability distribution of its parents according to Bayes' Theorem, which describes the probability of an event conditional on prior knowledge of that event (Moe et al., 2021). BBNs allow the integration of quantitative and qualitative information (e.g., experimental data, model outputs, and expert opinion) in one model. There are several advantages to the use of the Bayesian Network approach. BBNs provide a transparent representation of causal relationships between variables because such relationships are displayed graphically and the model can be built with the participation of experts; they allow better understanding of risk as variables are modelled as probability distributions rather than as mean values, and they provide understanding of the system because it is possible to learn about the effects given the causes and to know the causes given the effects. BBNs can work in data-sparse environments and can incorporate new evidence; they can be used as Decision Support Tools, as the outputs of the probabilistic analysis are often considered robust and can be used to recommend actions to policy-makers and to communicate best practices to stakeholders; they account for uncertainty without increasing calculation time, and can include both knowledge and system uncertainty (Aguilera et al., 2011; Barton et al., 2012; Brabec et al., 2019; Forio et al., 2015; Kragt, 2009; Sahlin et al., 2021; Uusitalo, 2007). However, there are still some challenges to overcome in the use of Bayesian Networks. For instance, authors have reported limitations of BBNs in handling continuous variables which leads to the necessity of discretizing data (Kragt, 2009; Landuyt

et al., 2013), and the absence of feedback loops makes the analysis of spatial and temporal variations problematic (Duespohl et al., 2012; Landuyt et al., 2013). However, Henderson and Pollino, (2010), affirm that if the feedback occurs on the same time scale as that of the dynamic BN then a feedback loop can be represented. An increased number of layers (nodes) between input nodes and output nodes can weaken the relationship between input and output (Marcot et al., 2006). Moreover, Landuyt et al., (2013), have reported on the difficulties of using commercially available software, as they are less flexible compared to open-source. However, this difficulty has been overcome by coupling such software with GIS tools (Piffady et al., 2021; Stritih et al., 2020; Troldborg et al., 2022) and using general-purpose software languages and packages (Jin et al., 2020; Scutari, 2010). Further, expert elicitation can be difficult, particularly when it comes to expressing the relationship between nodes in terms of probability distribution (Landuyt et al., 2013), and a literature review revealed that expert knowledge is more easily used to construct DAGs than to contribute to constructing CPTs (Pérez-Miñana, 2016; Phan et al., 2016). Lastly, Kaikkonen et al., (2021), recommend more transparency is needed with regards to the role of experts knowledge when building BBNs.

1.4 Bayesian Belief Networks and water quality modelling

BBNs have been used in the past in multiple decision-making setting and to understand causal relationships in different contexts, such as oil spills (Lu et al., 2019; Pascoe, 2018), medicine (Rodrigues et al., 2017; Seixas et al., 2018), epidemiology (Fuster-Parra et al., 2016; Lau et al., 2017) and machine learning (Hu et al., 2018). Furthermore, since the 1990s, BBNs have also been used to help with ecological risk-based decision-making (Barton et al., 2012), although as of 2011, the vast majority of papers published around the use of BBNs was relative to the subjects of Computer Science and Mathematics, while only 4% of the papers were published under the item “Environmental Sciences” (Aguilera et al., 2011). However, interest in the use of Bayesian probability theory in hydrogeology and environmental risk assessment has grown since (Höge et al., 2019; Kaikkonen et al., 2021). The limitations of a BBN modelling approach for environmental systems also represent an opportunity for tool development. In many settings, environmental systems represent a considerable statistical

modelling challenge both because of their complexity, their highly non-linear interlinked nature (temporally and spatially), and a relative lack of data in many scenarios. These issue may be overcome with BBNs because there is a broad range of validation tools that can be used, e.g. expert and/ or stakeholder evaluation (Landuyt et al., 2013), and BBNs can integrate various sources of data at various frequencies resolutions, thus overcoming datasets disparities (Glendell et al., 2022; Moe et al., 2021).

Analogously, modelling water quality and nutrient transport is hindered by a number of constraints associated with input data gathering, knowledge gaps in mathematically describing biogeochemical processes, the presence of highly non-linear interactions, temporal and spatial scale representation issues, as well as complications related to calibration and validation approaches (Blöschl et al., 2019; Harris and Heathwaite, 2012; Hollaway et al., 2018; Rode et al., 2010; Wellen et al., 2015). Wellen et al., (2015) set out to test whether 257 research papers applied best practices in watershed modelling. They found that 92% of the distributed models analysed were discretizing time in daily or monthly time steps, implying that biogeochemical processes that might occur in a few hours are not well represented. Other sources of uncertainty refer to the fact that there is no universal law of hydrology, because the data required to test the hypotheses would never be observable (Beven, 2006) and physical relationships used to close the water balance (e.g. hydraulic conductivity) are likely to be scale dependant (Bierkens, 1996). Furthermore, traditional water quality modelling techniques (i.e. mechanistic models) often produce over-parameterized models (Jackson-Blake et al., 2017) especially when upscaling to watershed scale (Radcliffe et al., 2009). There is therefore a need for new approaches that can incorporate available evidence with Decision Support Tools also in view of the Integrated Catchment Management (ICM) criteria promoted by European legislation (Holzkämper et al., 2012). Furthermore, there is an increasing necessity to incorporate uncertainty estimates in hydrological modelling (Beven, 2019; Pappenberger and Beven, 2006), also in view of future climatic changes (Ockenden et al., 2017; Sperotto et al., 2019a). Therefore, Bayesian Belief Networks, with their ability to incorporate uncertainty as well as disparate sources of data, are well suited to tackle these hydrological modelling issues. However, a systematic review by Phan et al., (2016) covered 111 articles (1997-2016) on the topic, and highlighted that only 7% of studies use the full functionality of BBNs, including the capacity

to learn from data. Table 1.1 reports a short literature review of studies developing BBNs targeted at water quality with regards to P pollution. Note that studies that involved Bayesian inference, Bayesian Hierarchical models, or Bayesian methods for parameter estimation were excluded from the review (e.g., Gudimov et al., (2012); Kim et al., (2017, 2014); Neumann et al., (2023); Zobrist and Reichert, (2006)). The objective of Table 1.1 was to compare existing BBNs aimed at modelling P in terms of area of interest (i.e., regulatory, ecological, economic), methods (data used, expert opinion, validation) and main results. We note here that some of the issues reported by Phan et al., (2016) are also evident when modelling P with BBNs. Firstly, the BBNs collated here are applied at a variety of scales, not just for catchments; they have been evaluated with a series of goodness of fit metrics, but often the data for validation is lacking (Ames et al., 2005; Lucci et al., 2014; McDowell et al., 2009); they have been applied spatially only in two instances (Glendell et al., 2022 and Sperotto et al, 2019a, 2019b) Additionally, these BBNs have been developed with data at low resolution, either due to the low frequency of the monitoring datasets (i.e., using weekly or monthly grab samples for laboratory analyses), or because they have been using hydrological model outputs as inputs, and therefore have been developed as yearly or seasonal BBNs. However, these low-frequency datasets will necessarily hide P variations due to changes in temperature, light, and precipitation (Bieroza et al., 2023), which can change by the hour and are likely to affect P mobilization, delivery, and in-stream uptake. Therefore, high-frequency (i.e. sub-hourly continuous sampling, even if summarized at the daily timestep) water quality datasets should be used to develop new BBNs and to test their predictive ability. Further, aside from Glendell et al., (2022) and Adams et al., (2023), these BBNs are not aimed at modelling P stream concentrations, but rather at modelling P loading, ecological processes dependent on P, or are aimed at evaluating Best Management Practices (BMPs). However, estimating P concentrations rather than loads remains important to understand future eutrophication risk and to design mitigation measures in running waters (Charlton et al., 2018; Glendell et al., 2019; Stamm et al., 2014), also given future climate and the WFD.

To date, only one BBN aimed at modelling water quality has been tested across multiple catchments. Glendell et al., (2022), tested a hybrid BBN (including both discrete and continuous variables)

predicting P concentrations in the stream and applied it with the same structure to seven Scottish catchments, showing wider predictive ranges in the BBN outputs than in the observations (a summary is given in Table 1.1). However, transferability, which involves adapting a model created for one setting to another, makes the model applicable across management scenarios and areas. Testing between-catchment transferability is necessary if we are to generalize biogeochemical models and to improve their predictive power (Mieleitner and Reichert, 2006). Transferability in geographical areas and across management applications increases confidence in the model formulation because it decreases the likelihood of the model performing well due to wrong reasons (Schuwirth et al., 2019). Models that can be applied across multiple cases are also more useful and, therefore more justifiable in terms of development and application effort (Schuwirth et al., 2019). Transferable BBNs can also inform future research by providing a clear motivation for the scope and scale of the data collection required to use the model at new sites (Hatum et al., 2022).

Table 1.1 further reports the four instances in which hybrid BBNs were used (Adams et al., 2023; Glendell et al., 2022b; Jin et al., 2020; McVittie et al., 2015). BBNs were originally developed to deal with discrete variables (expressed as CPTs). However, environmental and ecological problems involve both continuous and discrete variables, or a mix of both (Ropero, 2016). Despite this, the application of hybrid Networks in Environmental Risk Assessment is still rare, perhaps because they present several methodological challenges, including legacy software designed to deal with discrete variables only, the limited number of available distributions in such software, and the need for more assumptions and statistical expertise for the model set-up and end use (Kaikkonen et al., 2021).

Lastly, Table 1.1 reports the only three instances where the BBNs were aimed at modelling future P under climate change (Adams et al., 2023; Moe et al., 2016; Sperotto et al., 2019a), even though incorporating uncertainty is critical to water quality decision-making (Kotamäki et al., 2024).

Table 1.1 Summary of literature (2003-2023) of BBNs aimed at modelling P pollution across various scales (i.e., farm, catchment, watershed) and thematic areas (i.e., climate change and water resources management, ecology, ecosystems services). The studies are analysed in terms of methodology (use of experts, software, discretization, goodness of fit methods used), and a summary of results is given.

Study Area & Objectives	Area of interest	Methodology and BBN details	Goodness of Fit, Validation	Results	Reference
River Eden catchment in Scotland. Objective is to engage with stakeholders to consider multiple stressors in the catchment and to simulate future climate and socio-economic-driven impacts in. a single framework. Implications for five capitals (natural, social, manufactured, financial and intellectual) are considered.	Management	• BBN is iteratively built with experts and stakeholders • Conceptual model of each sub-catchment • P concentration as indicator of water quality • GeNIe software (BayesFusion, 2019a) for model development • Representative Concentration Pathways (RCPs) + Socio-economic Pathways (SSP) + land cover projections + population projections • one at a time parameter sensitivity • hybrid BN	Evaluated with percentage bias (PBIAS) against regulatory low-frequency (bimonthly) Reactive P concentrations at the catchment outlet. 43 % of observations were within the ±50 % threshold, 31 % of simulated values were above, and 26 % were below.	• BN modelling facilitates stakeholder recognition of future risks and inter-sectoral interaction • Participatory modelling methods improved the structure of the BN • BN allows systems-thinking approach for considering river basin catchment resilience	Adams et al., (2023)
Scottish agricultural catchments. Objective is to facilitate understanding of the effects of land use on P pollution risk.	Management	• co-developed with experts • *SHELF* (Oakley, 2020) elicitation framework to derive some of the nodes' parameters • two BBN version tested, one hybrid and one discretized and applied spatially with *bnspatial* (Masante 2019) • GeNIe software (BayesFusion, 2019a) for model development • seasonal discretization, static model • the model is integrated with spatial information • hybrid BN	PBIAS calculated against median annual SRP. The hybrid model version showed good agreement with the observations in 46% of cases, whilst the discrete spatial Network had a -2 ≤bias ≤.292%. A comparison between the simulated and observed probabilities of exceeding EQS was also used to evaluate the model and showed that in two catchments the agreement was high.	• management scenarios tested • importance of hydrology for P dilution in these catchments • importance of farmyard losses	Glendell et al., (2022)
Objective is to test the effects of changes in stressor levels for ecosystem services in three different catchments in Ireland. The study areas were the River Dodder (urban catchment), River Suir (agricultural catchment), River Moy (mixed land use catchment).	Ecosystem services	• calibration with data and expert judgement • P concentration is one of the parent nodes, the BBN is not aimed at modelling P • expert judgements were weighted to give a measure of confidence • climate projections included • Netica software (Norsys Software Corp, 2016) for model development • GeNIe software (BayesFusion, 2019a) for strength of influence and sensitivity analysis	N/A	• Phosphate main nutrient driver of effects on riverine ecosystem services • paper highlights how common non-linearity can be in these systems even though it is generally not represented in models	Penk et al., (2022)

Lowland streams in the Netherlands. A BN to simulate the response of macroinvertebrates to stressors.	Ecology	• model structure developed with literature + expert-based knowledge • discretization with equal intervals, then tested also equal frequency • management scenarios analysis with the best performing model. • Total P concentrations is an input node • static model assumes equilibrium • Netica software (Norsys Software Corp, 2016) for model development • discretized continuous variables	Training and testing with k-fold cross-validation. Two-thirds of the dataset for training and one third for performance. Performance evaluation was done by calculating the correlation between the observed and predicted EQS scores (predictive performance was poor).	• BN shows the positive influence of the restoration measures on ecological quality • ecological quality overall underpredicted by the model • equal frequency gave better performance • gaps in the dataset make it difficult to train knowledge-based CPTs.	de Vries et al., (2021)
The Grand River watershed of Ontario. To develop a BBN simulating the probability of TP and DRP load reductions due to BMPs and to identify which BMPs are most likely to achieve the policy objective of 40% load reductions from tributaries of Lake Erie.	Management	• ISO 31010:2009 as a framework to identify drivers, pressures, and risk pathways • Netica software (Norsys Software Corp, 2016), • P sources: mineral P application, manure P application, livestock P losses • it includes mitigation measures • social component: considers drivers such as cultural, economic, and political factors	N/A	• TP and DRP effective measures had high probability of achieving load reduction objectives at high adoption rates • The most commonly used BMPs (reduced application, reduced tillage, crop rotation grass filter strips), while reducing TP loads, had the unintended consequence of a moderate probability of increasing DRP loads	Igras and Creed, (2020)
Huaihe River Basin (HRB), China. To analyse the response of Suspended Sediments (SS) and Total Phosphorus (TP) to catchment characteristics, land use and sewage outfalls, under different rainfall patterns.	Management & Environment (land use, rainfall patterns)	• used *bnlearn* (Scutari, 2010), • rainfall intensity was inputted as discrete data, while the rest of the dataset was continuous (log-transformed TP and SS, water temperature, land use, soil erosion area, catchment area, slope, TP from sewage outfalls) • Total P as input • three models were developed: TP with and without SS (to check SS effect on TP loads), plus a SS model • variable choice was carried out with an arrow strength test • hybrid BN	Two thirds of data for calibration and one third for validation. Pearson Correlation and Nash-Sutcliffe Efficiency against observations. The observations were repeated 10000 times to match the model realizations.	• the contribution of SS is more significant when rainfall intensity is high • area, slope, soil erosion area, all have positive correlation with SS and TP, but lower than the human activity contribution • land use and sewage outfalls had a significant influence on the SS and TP loads.	Jin et al., (2020)
The Stanovice reservoir situated in North-West Bohemia, Czech Republic. Catchment area of 92 km^2. Determining whether the "good status" required by the EU WFD can be achieved with a set of selected measures.	WFD and mitigation measures	• Total P is the variable of interest, and it represents the probability of reducing the targeted amount of phosphorus • Total P is discretized only in 2 intervals (failure and success) • Netica software (Norsys Software Corp, 2016) • yearly discretization, static. • main sources of P are wastewater and agriculture • evaluation of mitigation measures	N/A	• the adjusted good status can be achieved with a 72.4% probability • the model can be used to see which combinations of measures are the most effective • model shows how effective the individual groups of measures are compared to how effective they were expected to be.	Brabec et al., (2019)

To determine catchment buffer capacity in three UK catchments with different data availability and levels of stakeholder interaction.	Management	• yearly discretization • static • software N/A	N/A	N/A	Forber et al., (2019)
Zero river basin, Northern Italy. 73% of land use is agricultural. To create an integrative tool (the BBN) for structuring and combining the information available in existing hydrological models, climate change projections, historical observations and expert opinion producing alternative risk scenarios to communicate the probability of changes in nutrients delivered from the basin under different climate change projections in mid- (2041–2070) and long-term (2071–2100) periods with respect to the baseline (1983–2012).	Climate change, scenario analysis	• seasonal discretization • BN is integrated with a climate model (Global Climate Model, Regional Climate Model, RCPs 4.5 and 8.5) • expert judgment (agronomic and irrigation practices, fertilizer use) • model training 2004-2013 • HUGIN Expert software (Bromley et al., 2005) • P as input • sources of P: wastewater treatment plants, agriculture • spatially distributed hydrological simulations. • use of an independent dataset for validation • scenario analysis with climate change projections (1976-2100) • discretized continuous variables	• Confusion matrices with available dataset • Comparison of variance and standard deviation of both predicted and observed • the BN was able to correctly classify 87.50% of instances for PO_4^{3-}.	• sensitivity analysis: PO_4^{3-} loading is mostly influenced by runoff (111% of change), P in the runoff (102%) and diffuse sources (101%) • increased temperature and decreased precipitation in spring and summer will lead to increased immobilisation of P in soil • flow reduction equals a reduction P sediment transport • increase of dry prolonged conditions might speed up the process of soil erosion • "PO_4^{3-} loadings" highly sensitive to "total P Loading", "P runoff", "P diffuse sources" • large uncertainty for spring and summer loadings • nutrient loadings sensitive to hydrological conditions.	Sperotto et al., (2019a, 2019b)
The link future climate change scenarios and land-use management to ecological status (cyanobacteria biomass) in Lake Vansjø in Norway.	Policy, Ecology	• the effects of the climate and management scenarios on river hydrology and chemistry modelled by the catchment models PERSiST (Futter et al., 2013) and INCA-P (Wade et al., 2002) • Total P produced is used as input in the lake model • outcomes of the process-based models are used as BN input and considered a source of uncertainty	Comparison of different model versions. Accuracy in terms of bias is considered for node states against the observations.	• BN helped with understanding the mismatch between process-based models and observations because it accounted for uncertainties • the BN approach allows the inclusion of biological indicators which aren't present in traditional process-based models • BNs are limited in their ability to model ecological processes due to their inability to model feedback loops.	Moe et al., (2016)
To assess and value the delivery of ecosystem services from riparian buffer strips in a generic ecosystem to investigate the general effectiveness of policy interventions with different scenarios relevant to the East and West of England.	Policy	• co-development with experts • riparian vegetation as buffer strips examined in alternative management practices • output nodes: "flood risk", "water quality" (BOD as water quality indicator). • Netica software (Norsys Software Corp, 2016) • regional scale • static model • hybrid BN	N/A	• natural vegetation optimal buffer zone management for all scenarios • riparian buffers have greater impact on flood control in scenarios with steeper slopes • utility values show little variation but that might be due to the parameterization choice (generic), more context specific parameterization may lead to different results. • further exploration of sensitivity analysis is needed.	McVittie et al., (2015)

Saginaw Bay, Lake Huron, USA. Objectives: to assess the effects of including uncertainty in predictor and response variables on parameter estimation and prediction by comparing the observation error model and simple model results and to use these models to support the development of P targets.	Ecology	• monitoring data • TP concentration was used as a driver for water quality	N/A	• compared with results from an analogous simple model using sample averages, the observation error model has a lower predictive uncertainty and predicts lower chlorophyll and P concentrations under contemporary lake conditions.	Cha and Stow, (2014)
A typical dairy farm in the south Otago region, New Zealand. The development of a robust tool that could be used to investigate and identify which sources and processes are dominating total phosphorus losses and under which conditions they occur. This information may be used to evaluate the probability of risk and reward for different mitigation strategies.	Farm management	• annual discretization • Netica software (Norsys Software Corp, 2016) • BBN incorporates expert opinion and literature data • A single finding sensitivity analysis expressed as a variance reduction • discretized continuous variables	Used data from other sites to compare.	• relative importance of network variables: annual R, average slope of the farm, proportion of overland and subsurface flow had the largest effects on TP loads exported from dairy farms • in this region farmers need to be especially attentive to hilly or steep areas of the farm by keeping Olsen P levels in the target range, grazing cows at lower stocking rates, and keeping to other BMPs (e.g., avoiding grazing during wet periods).	Lucci et al., (2014)
The Bunyip and Lang Lang rivers catchment in southern Australia; three dairy farms used as case studies.	Management of TP exports in New Zealand and Australian dairy farms	• expert knowledge of hydrological processes and point sources • BBN describes P exports • annual time step, BN defined at farm scale • Netica 3.17 (Norsys Software Corp)	Validation by expert opinion due to lack of data.	• sensitivity analysis revealed that the total exports were more sensitive to the diffuse P load than the point P loads, and that surface transport was more important than subsurface transport.	McDowell et al., (2009)
The East Canyon Reservoir, northern Utah, USA. The river is approximately 26 km long. Modelling management alternatives whilst 1. decreasing the risk of P pollution and 2. increasing the probability of recreational use.	Management	• no mention of expert elicitation in the case study, only mention of that in the generalised approach • probability distributions gathered from modelled data (water quality) and historical data • no explicit time step	Lack of independent data to validate the model.	• the optimal management scenario is non-point source reduction in the headwaters + improvement of the TP to target 0.05 mg l-1 P effluent. Results showed a probability of increased fruition of the park of 58% and a risk of violating the in-stream P standard of 17%.	Ames et al., (2005)
The lake Kanteleenjärvi basin, located in the Porvoonjoki river basin, Finland. Land use is mostly water, agriculture, or forest. To assess the effects of the buffers zones already established in the area. Two types of buffer zones were	Management	• model fully based on expert elicitation, carried out via questionnaires rather than interview in order not to influence the experts	Posterior distributions of mowing, P-status, dissolved phosphorus and plant diversity diverged significantly from prior distributions indicating inconsistency in the assessment.	• slope, soil type and plant coverage were the most influential variables on erosion and soil P for water experts, but none of the variables was predominant. Field length and orientation were also essential • gap in knowledge with respect to how much erosion affects particle bound P • Water protection experts estimated that P-status, soil fertility, management	Tattari et al., (2003)

analysed: (1) zones located along waterways and (2) dry meadows between forest and field south facing.			measures, particle bound P, and soil type influenced dissolved P. The link strength direction of the variables grazing and rotational grazing to dissolved P varied between the experts • most water protection experts strongly felt that buffer zones did not affect the P-status of the soil. On dry meadows, the P-status may decrease significantly.

1.5 Research aims and thesis structure

This research aims to develop and test the application of Bayesian Belief Networks in modelling phosphorus concentrations in four Irish agricultural catchments monitored at high frequency, described in Chapter 2. To achieve the overall aim, the thesis explores the following questions:

(1) Can high-frequency and high-resolution data, coupled with detailed understanding of catchment processes based on long-term monitoring, reduce a BBN's predictive uncertainty? Chapter 3 describes the model parameterization for a hybrid BBN aimed at predicting P concentrations at the outlet of a grassland-dominated catchment monitored at high frequency. Advantages and limitations of this modelling approach are also discussed in the chapter.

(2) Are Bayesian Belief Networks transferable across agricultural catchments with diverse land uses and hydrology? Chapter 4 describes the steps taken to parameterize the BBN to further three agricultural catchments and discusses the transferability of the approach. In this chapter, an expert elicitation exercise is deployed to fill data gaps outlined in the previous chapter.

(3) What are the projections of climate-induced changes in P concentrations for different hydrological regimes and land uses using a Bayesian Network approach? Chapter 5 explores the application of multiple downscaled discharge scenarios in the BBNs developed in Chapter 4 to predict P concentrations under climate change. Advantages and limitations of applying the scenarios are also discussed.

A summary of research achievements and limitations, as well as the implications for environmental modelling and management are discussed in Chapter 6. The conclusions are presented in Chapter 7 with recommendations for future research.

2. Study areas

Figure 2.1 View of the Castledockrell catchment, Ireland, photo taken by me during a field visit.

2.1 Introduction

This study focusses on four (< 1200 ha) agricultural catchments in the east and south of Ireland: Timoleague, Ballycanew, Castledockrell (Figure 2.1), and Dunleer, monitored by the Agricultural Catchments Programme (ACP), Teagasc (Wall et al., 2011). Ireland (Figures 2.2, 2.3, and 2.4) is located in the Northern Hemisphere, with an average altitude of 118 meters above sea level. The highest mountain peak is Carrauntoohil at 1039 meters, located in the south-west. The geology of Ireland includes metamorphic rocks, such as slates and quartzites, found in Counties Donegal, Kerry, and Wicklow. Igneous rocks are common in the north-east, while granites can be seen in Counties Donegal, Armagh, Down, Wicklow, and Galway. Sedimentary rocks are common in the south-west, while limestones cover much of Ireland, including the midlands (Geological Survey) (Figure 2.3). The mean annual precipitation in Ireland was 1230 mm for the period 1981-2010 (Walsh, 2012), which is shown for the RoI in Figure 2.4, bottom left panel. Meanwhile, the annual precipitation in 1991-2020 was 1288 mm, and the mean annual air temperature for the period 1991-2020 was 9.8°C (Curley et al., 2023).

In 2005, the agri-food sector collectively constituted approximately 8.6% of the RoI's gross domestic product (GDP) (Hynes et al., 2013). Primary agriculture retains greater significance in the Irish economy compared to many other EU member states, with agriculture contributing 2.7% to Ireland's GDP in 2005, contrasting with the EU average of 1.6% (Hynes et al., 2013). Land use (Corine Landcover released in 2018) is shown in Figure 2.4 (top left panel, data available from EPA, 2018). Agricultural outputs have increased from 313 million € per year to 8.1 billion € (2009-2019), which is linked to increased herd sizes for both total cattle and dairy cattle. This period of economic growth and change is linked with a deterioration of water quality in lakes and rivers, which are also part of the RoI's natural capital (Mellander and Jordan, 2021). The EU Water Framework Directive River Waterbody Status for the RoI is shown in Figure 2.4 (bottom right panel, data available from (EPA, 2019)).

The Agricultural Catchments Programme (ACP) was initiated to evaluate the Good Agricultural Practice measures implemented under the EU Nitrates Directive and funded by the Irish Department of Agriculture, Food and Marine (Jordan et al., 2012). The programme started in 2009 in six agricultural

catchments with contrasting hydrology and land uses, equipped with high-frequency water quality monitoring infrastructure. Within the ACP, extensive monitoring and research have been undertaken to understand the drivers and controls on nutrient loss, and catchment responses to changing weather conditions and agricultural practices, including impacts of climate change and mitigation measures (Mellander and Jordan, 2021). The catchments are located primarily along the East and Southern coast of Ireland (Figure 2.2) and have different agricultural land uses, geology, and contrasting hydrology (see Table 2.2 for baseflow and flashiness indices). The catchments were chosen because the only significant anthropogenic pressure is from agriculture, with housing density being low, and domestic waste generally treated with septic tank systems (Jordan et al., 2012). A brief description of each catchment is given in this Chapter, and further information regarding management, hydrological characteristics, phosphorus loss, and connectivity, is provided in Table 2.2. Each catchment is equipped with a bankside analyser located at the catchment outlet (marked in the figures as "Outlet Hydro-Station") to measure river discharge (Q, $m^3 s^{-1}$), total phosphorus (TP, mg l^{-1}), total reactive phosphorus (TRP, mg l^{-1}) concentrations, and turbidity (NTU) at a sub-hourly rate (every 10 minutes). The catchments are also equipped to monitor nitrate fluxes (reported for example in Mellander and Jordan, (2021)), which, however, are not an object of this study. Additional information on the catchments is also reported in Negri and Mellander, (2024).

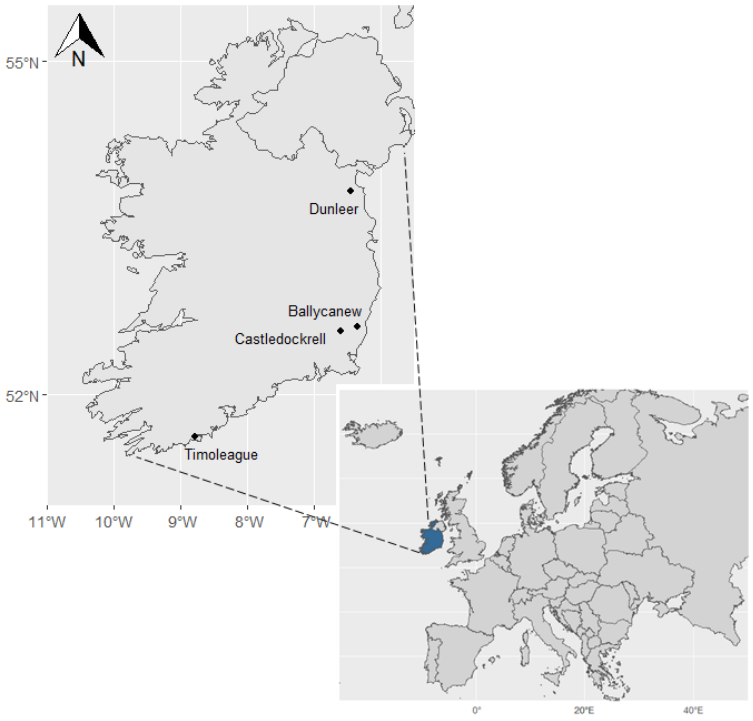

Figure 2.2 Location of the Republic of Ireland and of the four catchments. Mapped vectors are sourced from the R package naturalearthdata (South, 2017)

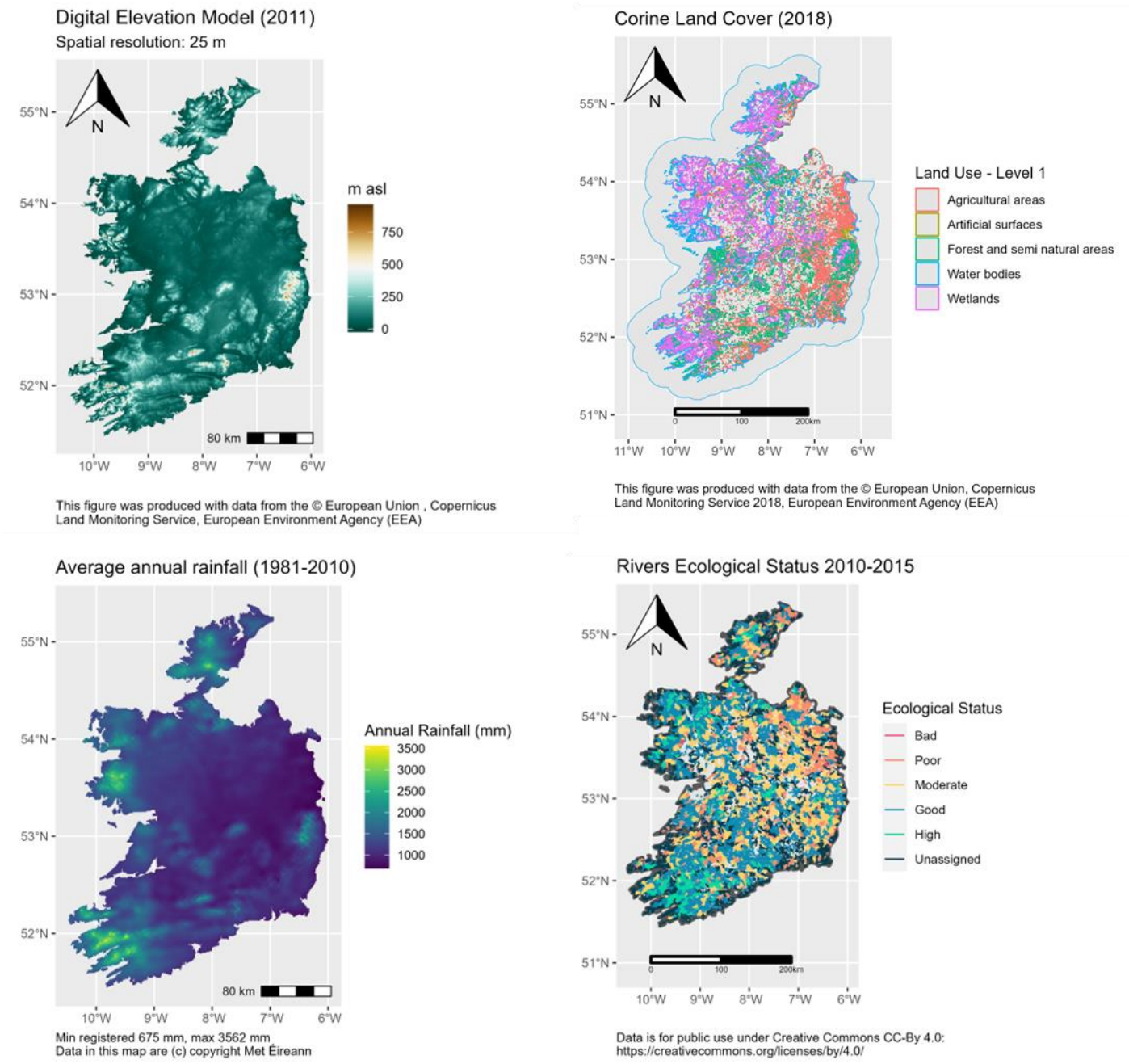

Figure 2.3 Basic information on the Republic of Ireland, including relief (top left, from the Copernicus Land Monitoring Service), the Corine Land Cover, showing 5 main categories of land use (Agricultural, Artificial, Seminatural, Water bodies and Wetlands, top right, from the Copernicus Land Monitoring Service), the average annual rainfall 1981-2010 (data from Met Eirann, bottom left), and the WFD Rivers Ecological Status (bottom right).

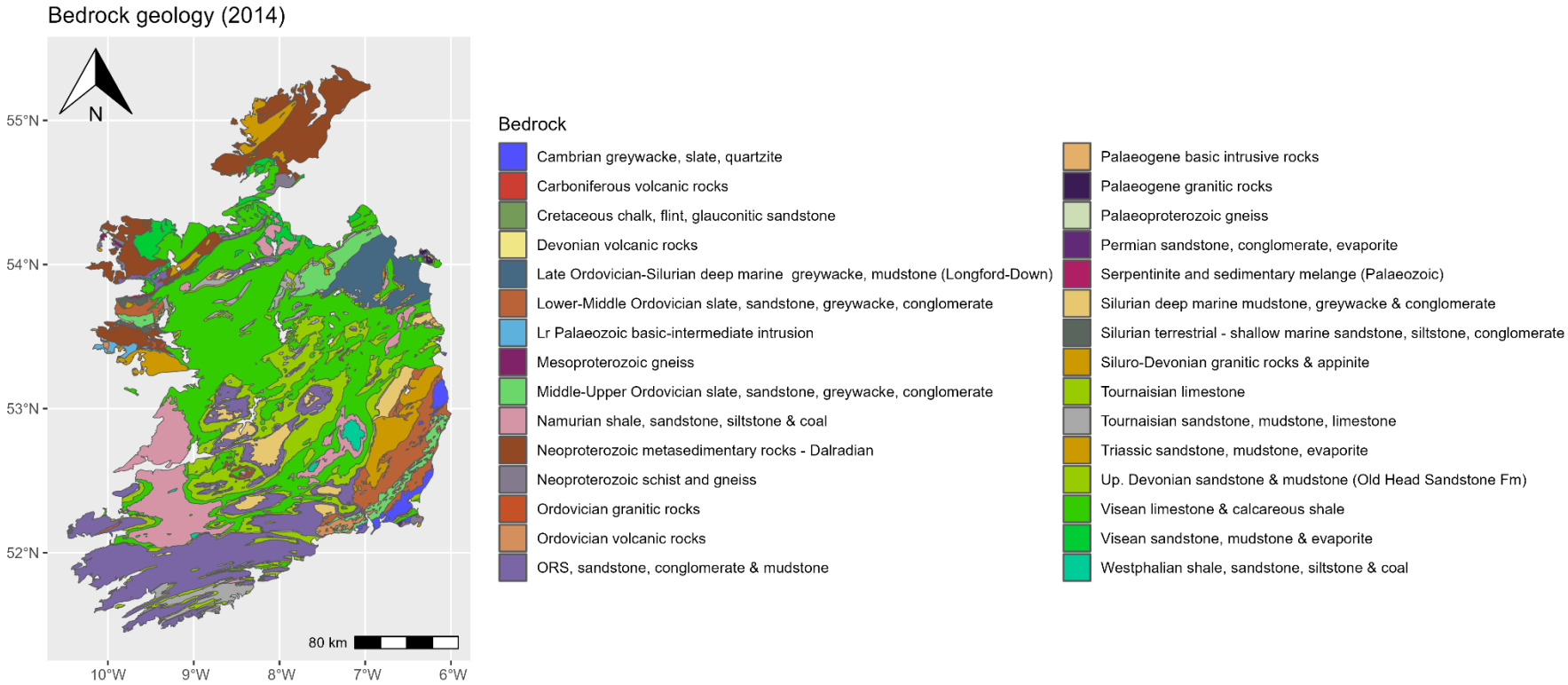

Lakes are not represented in this figure.

Figure 2.4 Bedrock geology (1:1 million) in the Republic of Ireland as published by Geological Survey Ireland in 2014.

2.2 Timoleague

The Timoleague catchment (Figures 2.5 and 2.6) is located near Clonakilty, in County Cork. It extends over 758 ha, of which 85-89% is grassland (86% of enterprises were dedicated to dairy, 14% to dry stock, in 2020) and 4-5% to tillage. This catchment, located in West Cork, is representative of the most intensively farmed area in Ireland, having the highest concentration of dairy farms (Teagasc - Agriculture and Food Development Authority, 2018). Stocking rates are estimated at 1.98 livestock units (LU) ha^{-1} (Sherriff et al., 2015) and many of the dairy farms are managing soils under derogation (i.e. deviation from the EU Nitrates Directive, with organic nitrogen (N) loading between 170 and 250 kg $ha^{-1}year^{-1}$), (Jordan et al., 2012). Dominant geology in the area is sand and siltstone. In general, the soils are well drained except for small areas neighbouring the stream at the valley bottom. Overall, this means that the catchment is mostly groundwater-fed, and more than half the P load (59%) is delivered via belowground pathways (Mellander et al., 2016). Given the predominantly free-draining nature of the soils, N is considered the main nutrient at loss risk via leaching to groundwater (Fealy et al., 2010), however, TRP (total reactive phosphorus) concentrations are above the European Environmental Quality Standards (EQS) (Mellander et al., 2022).

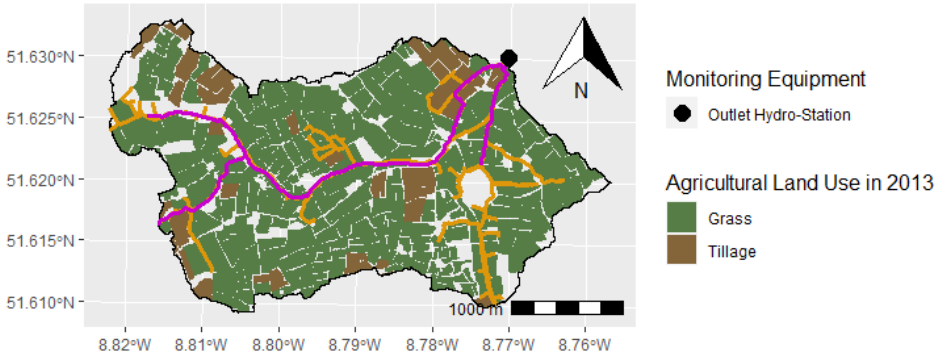

Figure 2.5 Study area: the Timoleague catchment in County Cork. Elevation varies between 2 m a.s.l. and 122 m a.s.l. Location of the monitoring equipment is shown as dot (Outlet Hydro-Station), while magenta lines represent streams, and yellow lines represent artificial drainage.

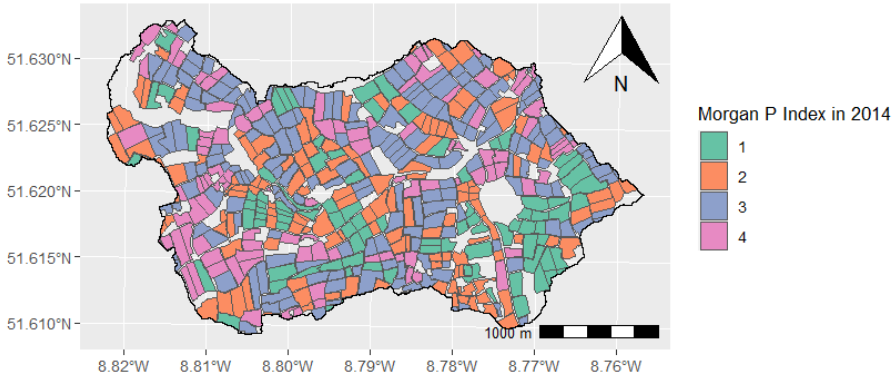

Figure 2.6 Average Morgan P index as surveyed in the catchment Timoleague in 2014. Soil Morgan P is measured every 4 years in each ACP catchment.

2.3 Ballycanew

The Ballycanew catchment (Figures 2.7 and 2.8) is located near Gorey, County Wexford, and the total area amounts to 1191 ha, with 78% grassland and approximately 20% tillage. None of the farms in this catchment are tillage only, all of them have a combination of tillage plus grassland. The dominant geology is rhyolite and slate. Here, the soils have poor drainage characteristics due to deposits of heavy clays. Landowners in the area have improved soil drainage for grass production by installing tile and mole drains (Shore et al., 2015). Due to the low soil permeability, the catchment has a flashy hydrology and a high risk of phosphorus loss to water through quick and erosive surface pathways during heavy rain events (Mellander et al., 2015). This is the catchment with the highest runoff flashiness index: Q5\Q95 was 126 for the period 2010-2020 (Mellander et al., 2022), whereby Q5 represents high- flow and Q95 represents low flow. Because it is a surface-driven catchment, the main pressure for P pollution is not related to sources but rather to transport, and TRP concentrations are above the 0.035 mg l^{-1} EQS (Mellander et al., 2022). In addition, these characteristics make the catchment less at risk of N pollution (Mellander et al., 2015), and NO_3^- concentrations are below the European Environmental Quality Standards.

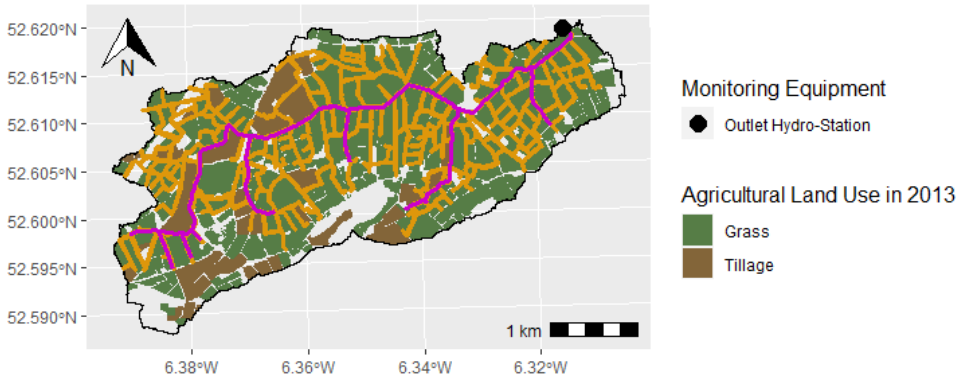

Figure 2.7 Study area: the Ballycanew catchment in County Wexford. Elevation varies between 21 m a.s.l. and 232 m a.s.l. Location of the monitoring equipment is shown as dot (Outlet Hydro-Station), while magenta lines represent streams, and yellow lines represent artificial drainage.

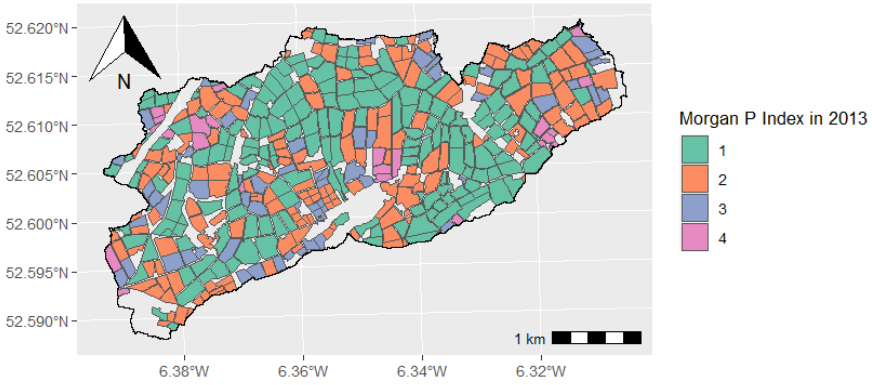

Figure 2.8 Average Morgan P index as surveyed in the Ballycanew catchment in 2013. Soil Morgan P is measured every 4 years in each ACP catchment.

2.4 Castledockrell

This catchment (Figures 2.9 and 2.10) is located between Enniscorty and Bunclody, also in County Wexford. Total area is 1117 ha, with approximately 54% dedicated to tillage and 39% to grassland. Soils are typically well drained: free-draining brown earths with slate and shale or siltstones beneath, which are ideal for spring barley (main tillage in this area). However, some of the lower lying areas near the stream (East- Southeast of the catchment) present poorly drained gley soils that are mostly artificially drained. Based on these characteristics, the catchment is considered at risk of N losses to water through leaching, but not at P loss risk: NO_3^- concentrations are above the European EQS. This catchment represents an exception within the ACP study catchments in that there is a single central wastewater treatment plant (Jordan et al., 2012). P concentrations in this catchment are relatively low, and the chance of TRP concentrations exceeding EQS limit was 22.5 % for the period 2010-2020 (Mellander et al., 2022).

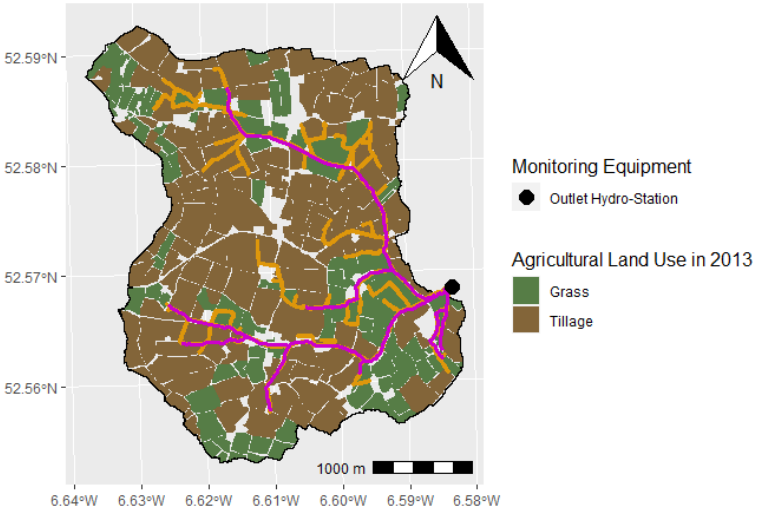

Figure 2.9 Study area: the Castledockrell catchment in County Wexford. Elevation varies between 18 m a.s.l. and 215 m a.s.l. Location of the monitoring equipment is shown as dot (Outlet Hydro-Station), while magenta lines represent streams, and yellow lines represent artificial drainage.

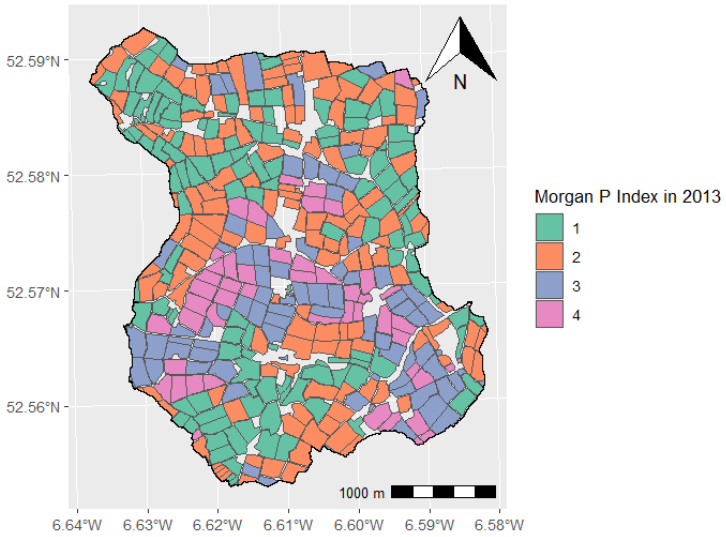

Figure 2.10 Average Morgan P index as surveyed in the Castledockrell catchment in 2013. Soil Morgan P is measured every 4 years in each ACP catchment.

2.5 Dunleer

The Dunleer catchment (Figures 2.11 and 2.12) is located near the village of Dunleer in County Louth. Total area is 948 ha with tillage (33-42%) and grassland (49%). In this catchment soil drainage classes are a mixture of well, moderately, imperfectly and poorly drained soils (Thomas et al., 2016b), the latter covering up to 70% of the total area (Teagasc - Agriculture and Food Development Authority, 2018). Soils are underlain by a mix of greywacke, mudstone, and limestone geology. Hence, P is considered the main nutrient at risk of loss though overland flow, although there is not a single dominant P transport pathway (Mellander et al., 2012). N is also considered at risk through leaching on the more freely drained part of the catchment (Eastern part of the area). This is because both TRP and NO_3^- concentrations are above the EQS.

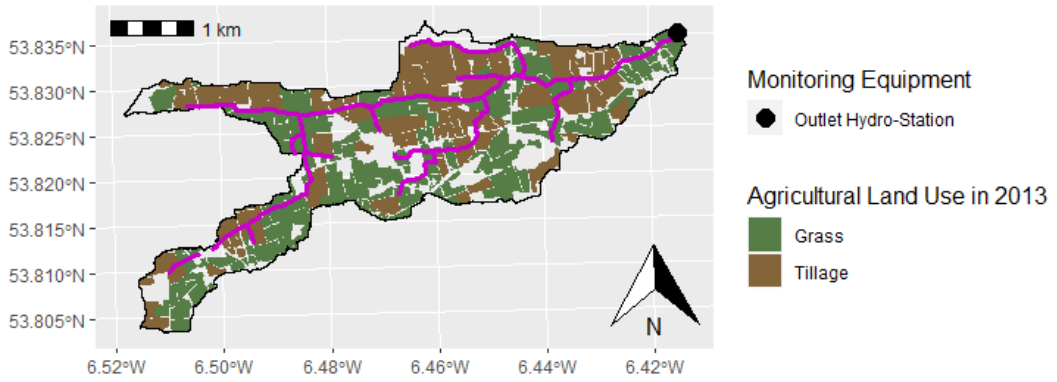

Figure 2.11 Study area: the Dunleer catchment in County Louth. Elevation varies between 26 m a.s.l. and 223 m a.s.l. Location of the monitoring equipment is shown as dot (Outlet Hydro-Station), while magenta lines represent streams (artificial drainage not mapped).

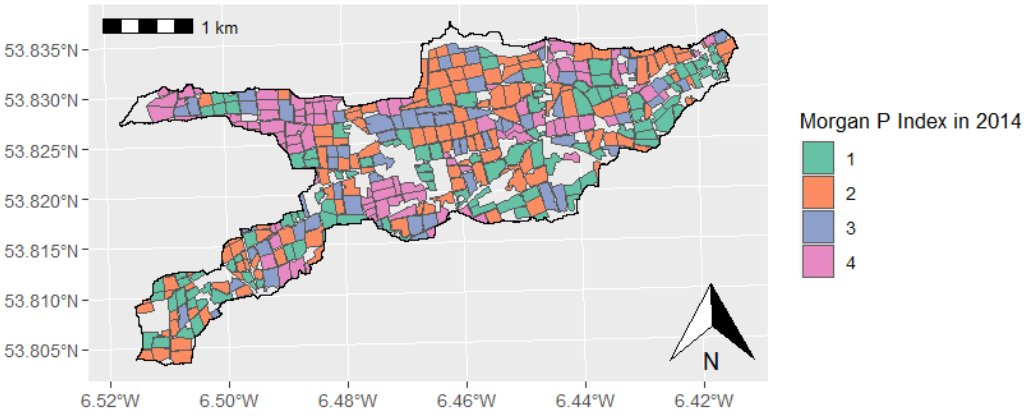

Figure 2.12 Average Morgan P index as surveyed in the Dunleer catchment in 2014. Soil Morgan P is measured every 4 years in each ACP catchment.

2.6 Soil Phosphorus in the study areas

Figures 2.6, 2.8, 2.10 and 2.12 show the Morgan P index in each catchment fields obtained in 2013 (Castledockrell and Ballycanew) and 2014 (Dunleer and Timoleague) surveys, adjusted for land use as described in Thomas et al., (2016b). Morgan P index interpretation is given in Table 2.1: Index 3 indicates optimum agronomic levels of P, while Index 4 indicates surplus levels. Morgan P is used in the National Action Programme (NAP) soil P test to determine the phosphorus allowance for each farm when the level is either 1 or 2. The P allowance quantifies Total P in terms of Organic P (produced and or imported) and Inorganic P (bought). For farms that are not under derogation from maximum permitted organic N loading up to 170 kg $ha^{-1}year^{-1}$, the allowances only allow for soil P maintenance; This means that the Total P applied should not lead to an increase in the Morgan P Index. Farms under derogation from the maximum permitted organic N loading are required to keep a soil P test inventory on grassland and not to apply any inorganic P to fields with Morgan P Index 4 (Jordan et al., 2012). In this thesis, Morgan P levels are used as a basis to characterise soil P sources, as described in the following chapter.

Table 2.1 Morgan P Index levels per land use as reported in (Wall and Plunkett, 2020).

	Grassland	**Tillage**
	P (mg l^{-1})	**P (mg l^{-1})**
Index 1 (deficient)	0.0-3.0	0.0-3.0
Index 2 (low)	3.1-5.0	3.1-6.0
Index 3 (optimum)	5.1-8.0	6.1-10.0
Index 4 (excessive)	Above 8.0	Above 10.0

Table 2.2 Characteristics of study sites.

		Grassland A*	Grassland B	Arable A	Arable B	Reference
General	**Name**	Timoleague	Ballycanew	Castledockrell	Dunleer	-
	Description	Well-drained, grassland dominated	Poorly-drained, grassland dominated	Well-drained, tillage dominated	Moderately drained, tillage dominated	-
	Location	51°38'N, 8°47'W	52°36'N, 6°20'W	52°34'N, 6°36'W	53°49'N, 6°27'W	Sherriff et al., (2015)
	Size	758 ha	1191 ha	1117 ha	948 ha	Teagasc - Agriculture and Food Development Authority, (2018)
	Median slope	4°	3°	3°	3°	Sherriff et al., (2015)
	Altitude (m a.s.l.)	2-122	19-230	18-215	26-223	Teagasc - Agriculture and Food Development Authority, (2018)
	30-year average rainfall (mm yr^{-1})[a]	1228	906	906	758	Sherriff et al., (2015)
	Average field size (ha)	2.0	3.04	3.32	2.70	Thomas et al., (2016b)
Management	**Land use**	85% grassland, 4% tillage	78% grassland, 20% tillage	54% tillage, 39% grassland	33% tillage, 49% grassland	Thomas et al., (2016a)
	Stocking rate (LU ha^{-1})	1.98	1.04	0.40	0.77	Sherriff et al., (2015)
	Mean total P fertilizer (kg ha^{-1} yr^{-1}) 2010-2013[b]	N/A	N/A	28.0	33.4	McDonald et al., (2019)
	Mean total organic P fertilizer (kg ha^{-1} yr^{-1}) 2010-2013[b]	N/A	N/A	3.43	21.9	McDonald et al., (2019)
	Surplus P range (kg ha^{-1} yr^{-1}) 2010-2013[b]	N/A	N/A	1.9 to 7.5	-0.42 to 25.5	McDonald et al., (2019)
	Average areal proportion of P applied (%) as less than, equal to or exceeding NAP limit in 2010-2013 and mean NAP limit (kg ha^{-1} yr^{-1})[b]	N/A	N/A	Less than (56%), equal (7%), exceeding (37%), allowance was 26.8.	Less than (50%), equal (17%), exceeding (33%), allowance was 26.4.	McDonald et al., (2019)
	Organic application other than farmyard manure closed period	1st October - 13th January	1st October - 13th January	1st October - 13th January	1st October - 16th January	https://www.teagasc.ie/news--events/daily/grassland/fertiliser-spreading-deadline-looms.php

	Chemical fertilizer closed period	15th September – 27th January	15th September – 27th January	15th September – 27th January	15th September – 30th January	https://www.teagasc.ie/news--events/daily/grassland/fertiliser-spreading-deadline-looms.php
	Farmyard manure application closed period	1st November -12th January	1st November -12th January	1st November -12th January	1st November -15th January	https://www.teagasc.ie/news--events/daily/grassland/fertiliser-spreading-deadline-looms.php
Hydrology	**Soil series**	Typical Brown Earths + Typical Brown Podzols (84%), Typical Surface-water Gleys (5%), Humic/ Typical Alluvial Gleys (4%)	Typical Surface-water Gleys or Groundwater Gleys (71%), Typical Brown Earths (29%)	Typical Brown Earths (88%), Gleyic Brown Earths (5%), Typical Groundwater Gleys (5%)	Stagnic Brown Earths (35%), Typical Surface-water Gleys (25%), Typical Brown Earths (22%)	Thomas et al., (2016a)
	Drainage class	Well-drained	Poorly drained, well drained in the uplands	Well drained	Well, moderately, imperfectly and poorly drained	Thomas et al., (2016a)
	Proportion of poorly drained soils on total area	N/A	85%	20.1%	N/A	Shore et al., (2014)
	Dominant flow pathway	Sub-surface	Surface	Sub-surface	Surface	Thomas et al., (2016a)
	Stream order	2	2	3	3	Mellander et al., (2012)
	Runoff coefficient 2009-2014	0.55	0.48	0.54	0.48	Thomas et al., (2016b)
	Runoff flashiness (Q5:Q95)	77	202	55	140	Thomas et al., (2016b)
	Runoff flashiness (Q5:Q95) in 2010-2020	34	126	31	61	Mellander et al., (2022)
	Baseflow index (BFi) in 2010-2020	0.73	0.63	0.78	0.66	Mellander et al., (2022)
	Ditch density (km^2km^{-2}) and area of channel network (% of catchment area)	1.7	1.3 (1.26%)	5.7 (0.53%)	2.3	Shore et al., (2015), Thomas et al., (2016a)
	Channel density (%) per sediment retention class	N/A	Low (15%), low-moderate (10%), moderate-high (26%), high (49%)	Low (44%), low-moderate (8%), moderate-high (32%), high (16%)	N/A	Shore et al., (2015)
	Stream length (m, calculated from	6515	12188	10979	16898	-

	existing spatial data, ditches are excluded)					
P loss	**Mean suspended sediments concentration 2009-2012 (mg l^{-1})**	< 6	14	< 6	17	Sherriff et al., (2015)
	Mean suspended solids loads 2009-2012 (t $km^{-2}yr^{-1}$)	15.43	26.64	11.96	24.39	Sherriff et al., (2015)
	Average P losses (kg TP ha^{-1}) 2010-2013	N/A	1.035	0.342	N/A	Mellander et al., (2015)
	Total Dissolved P (mg l^{-1}) ~ Total Reactive P (mg l^{-1}) at catchment outlet	N/A	TDP = 1.1475*TRP + 0.0078	TDP = 1.1975*TRP + 0.0058	N/A	Shore et al., (2014)
	% areas at highest risk of legacy soil P transfers in baseline and (resampled) years with CSA Index threshold ≥ 5	2.9 (2.4)	5.6 (4.1)	1.4 (1.1)	2.9 (3.0)	Thomas et al., (2016b)
	Water Extractable P (WEP) ~ Soil Morgan P	WEP = 0.57*SoilMorganP+0.22	WEP = 0.58*SoilMorganP+1.13	WEP = 0.09*SoilMorganP+2.07	WEP = 0.31*SoilMorganP+1.73	Thomas et al., (2016b)
Connectivity	**Mean HSA size m^2 (% of catchment)[c]**	216738 (2.9)	703147 (6)	215014 (1.9)	398789 (4.3)	Thomas et al., (2016a)
	% hydrologically disconnected area over total catchment area[c]	33.4	24.9	16.8	27.6	Thomas et al., (2016a)

[a]1981-2010 mean annual rainfall

[b]Calculated on an area of 1043.6 ha (Arable A) and 750.4 (Arable B)

[c]Calculated based on quick-flow and rainfall depths based on storm events (2009-2014)

*in Grassland A monitoring started in 2010 rather than 2009

3. Bayesian network modelling of phosphorus pollution in agricultural catchments with high-resolution data

To avoid repetitions, this Chapter has been redrafted from the published: Negri, C., Mellander, P.-E., Schurch, N.J., Wade, A.J., Gagkas, Z., Wardell-Johnson, D.H., Adams, K., Glendell, M., 2024. Bayesian network modelling of phosphorus pollution in agricultural catchments with high-resolution data. Environmental Modelling & Software 106073. https://doi.org/10.1016/j.envsoft.2024.106073, published under a Creative Commons License (https://creativecommons.org/licenses/by/4.0/), and the Supplementary Materials can be found in Chapter 8.

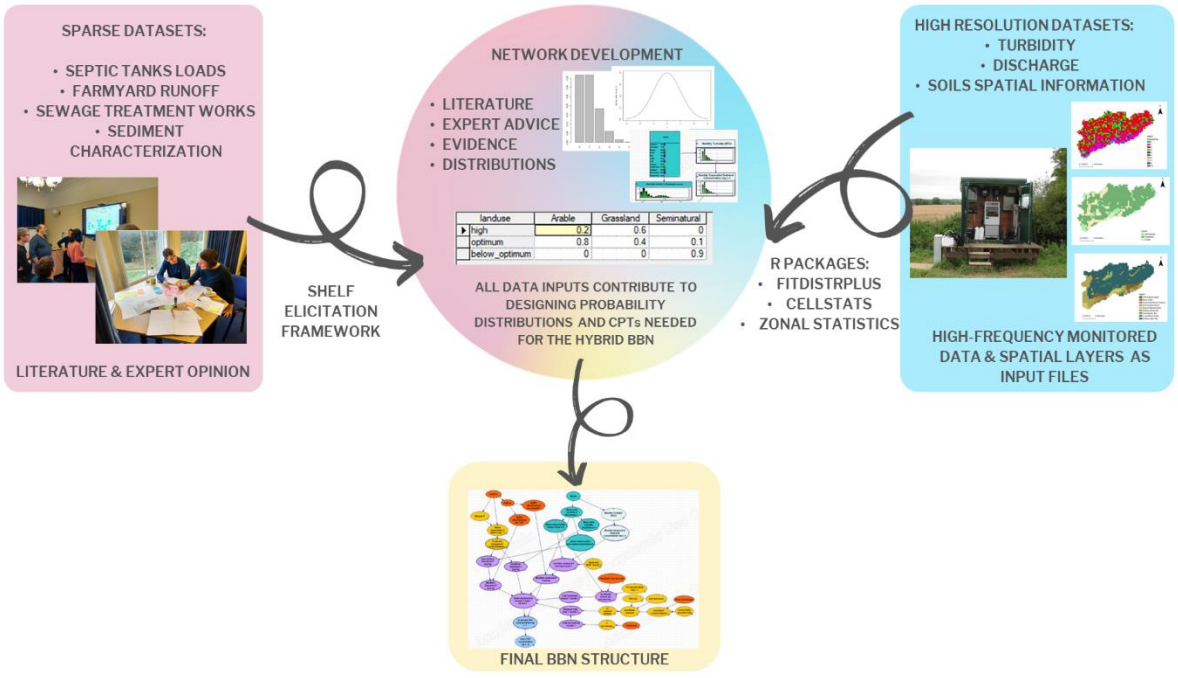

Figure 3.1 The conceptual framework underpinning Chapter 3, where high-frequency and high-resolution datasets informed the compilation of the BBN's CPTs and equations, and, where data was lacking, priors were identified through literature review and the aid of experts.

Abstract

A Bayesian Belief Network was developed to simulate phosphorus (P) loss in an Irish agricultural catchment. Septic tanks and farmyards were included to represent all P sources and assess their effect on model performance. Bayesian priors were defined using daily discharge and turbidity, high-resolution soil P data, expert opinion, and literature. Calibration was done against seven years of daily Total Reactive P concentrations. Model performance was assessed using percentage bias, summary statistics, and visually comparing distributions. Bias was within acceptable ranges, the model predicted mean and median P concentrations within the data error, with simulated distributions more variable than the observations. Considering the risk of exceeding regulatory standards, predictions showed lower P losses than observations, likely due to simulated distributions being left-skewed. We discuss model advantages and limitations, the benefits of explicitly representing uncertainty, and priorities for data collection to fill knowledge gaps present even in a highly monitored catchment.

3.1 Introduction

Phosphorus (P) losses from farmland to surface waters (diffuse P losses) continue to be a major cause of water quality deterioration and eutrophication (European Environment Agency, 2019). P remains a major source of water quality failures in Ireland, particularly due to the slow release of soil legacy P (Schulte et al., 2010), which is often unaccounted for in soil P tests (Thomas et al., 2016b). There are multiple challenges facing land managers, stakeholders, and policymakers when tackling P pollution in agricultural catchments in Northwest Europe (Bol et al., 2018). Smaller catchments (<50 km^2) vary in their vulnerability to P losses, necessitating a catchment-specific understanding of stressor-impact relationships and targeting of mitigation measures (Glendell et al., 2019). Drivers of P transfer differ across spatial scales (point, plot, field, hillslope, and catchment), and the understanding gained from laboratory or field measurements may not be directly applicable at the catchment scales represented in models (Brazier et al., 2005; Wade et al., 2008). Additionally, the understanding of key drivers of catchment vulnerability is complicated by different P sources and pathways that result in similar concentration-discharge hysteresis relationships at the catchment outlet. This confounding often makes

it difficult to determine the most important P sources and pathways to target with P reduction measures and to predict their likely effect (Bol et al., 2018).

Soil P content and excess plant available P, derived from fertilizer application, have been identified as the main sources of diffuse P in Irish agricultural catchments (Regan et al., 2012), while some studies stress the importance of point pollution sources (Campbell et al., 2015; Gill and Mockler, 2016a; Vero et al., 2019) as well as legacy P (Thomas et al., 2016b). In addition, the transport and delivery of P in Irish agricultural catchments are dominated by weather and hydrological conditions rather than initial soil P (Mellander et al., 2018, 2015b). To investigate diffuse P pollution sources in Irish agricultural catchments, modelers have used two main approaches: 1) the critical source areas (CSAs) approach (Packham et al., 2020; Thomas et al., 2021, 2016c), and 2) the load apportionment approach (Crockford et al., 2017; Mockler et al., 2017). CSAs methods aim at identifying and mapping areas of high hydrological activity connected with areas of elevated P mobilization, thus facilitating the transfer of P from terrestrial to aquatic ecosystems (Djodjic and Markensten, 2019). One of the biggest advantages of CSAs is that they provide the basis to spatially identify potential locations for mitigation measures, however, these approaches require extensive sampling and mapping of P sources and hydrological connectivity, and provide qualitative results that might be difficult to interpret for policy, to validate, or evaluate at larger scales (Djodjic and Markensten, 2019). In contrast, Load Apportionment Models (LAMs), calculate nutrient loads from all sources and then estimate factors to reduce such loads to account for treatment (e.g. wastewaters) or environmental attenuations. Estimated loads are then compared with loads calculated from measurements (Mockler et al., 2016a). This method can identify the dominant pollution contributors in catchments and sub-catchments, while also assessing management strategies (Mockler et al., 2016a). However, LAMs can be difficult to interpret for non-experts, because of the uncertainties around load estimation, especially when used with low-frequency datasets, which limits their utility as management tools (Crockford et al., 2017).

Catchment nutrient models are crucial to summarize current knowledge and process understanding, as well as to test land use and climate scenario effects on water quality, which can inform mitigation action (Jackson-Blake et al., 2015). However, mechanistic models of water quality (e.g. catchment scale P

models like INCA-P, (Jackson-Blake et al., 2016), can have parameters that are unmeasurable yet heavily influence model outputs (Jackson-Blake et al., 2017) and are often over-parameterized, especially when upscaling to watershed scales (Radcliffe et al., 2009). Additionally, P models often perform inadequately in rural catchments where diffuse sources are dominant, and model outputs' accuracy is limited by current knowledge (Jackson-Blake et al., 2015). Furthermore, water quality and nutrient transport models are frequently hindered by constraints associated with available data, the presence of non-linear interactions, and temporal and spatial scale representation issues (Blöschl et al., 2019; Harris and Heathwaite, 2012; Rode et al., 2010; Wellen et al., 2015). Hence, there is a recognition of the importance of incorporating uncertainty explicitly in hydrological and water quality modelling, not only through error bounds on output values, but by representing uncertainty as an intrinsic aspect of inexact environmental science (Beven, 2019; Pappenberger and Beven, 2006). Additionally, given the high levels of uncertainty and complexities involved in water quality mitigation and modelling, there is a pressing need to develop and apply probabilistic modelling tools for Environmental Risk Assessment (ERA) as an alternative to deterministic methods, and Bayesian Belief Networks (BBNs) are particularly well suited for this purpose (Moe et al., 2021). BBNs are a probabilistic graphical modelling framework that represents a set of variables and their conditional dependencies using a Directed Acyclic Graph (DAG) i.e., a network that has no cycles. BBNs are a powerful tool for modelling complex systems and have been used to integrate the disparate physicochemical, biotic/ abiotic, and socio-economic aspects (Penk et al., 2022) needed to simulate P in river catchments (Jarvie et al., 2019). BBNs show promise as decision support tools in water resource management (Phan et al., 2019) because they represent causal relationships between variables transparently and graphically, making it straightforward to understand and build BBNs with the participation of experts. BBNs facilitate an improved understanding of risk by explicitly representing the uncertainties and assumptions in the model as probability distributions, and they provide a systems-level understanding of a problem (Aguilera et al., 2011; Barton et al., 2012; Forio et al., 2015; Glendell et al., 2022; Kaikkonen et al., 2021; Kragt, 2009; Uusitalo, 2007). BBNs' can make predictions with sparse data (Forio et al., 2015; Glendell et al., 2022; Uusitalo, 2007); and the probabilistic outputs from BBNs can be used to recommend actions to policy makers, and to communicate best practices to stakeholders (Barton et al.,

2012; Kaikkonen et al., 2021; Uusitalo, 2007). The probability distributions used in BBNs represent (most) model parameters explicitly encoding the uncertainties in the prior knowledge, data, and parameters (Sahlin et al., 2021). These prior distributions can be assumed, elicited from expert knowledge, or quantified using prior data. However, hybrid Bayesian Networks (BBNs that have a combination of continuous and discrete variables) are rarely applied in water quality modelling, and they have not been tested in a catchment with high-resolution monitoring data. Glendell et al., (2022) found that a hybrid BBN developed using standard regulatory data in seven test catchments in Scotland performed well, albeit with relatively large predictive uncertainty. In this work, we test whether a hybrid BBN can perform better when applied and calibrated in a catchment with long-term high-resolution data to understand whether the wide predictive uncertainty can be reduced or whether it is an irreducible property of this stochastic modelling approach. Hence, in this study we developed a hybrid BBN model of in-stream P concentrations in a poorly drained Irish agricultural catchment to: (1) model P losses in a data-rich meso-scale agricultural catchment using high-resolution observational data and expert advice; (2) evaluate the impact of rural point sources (septic tanks and farmyards), which are seldom represented in catchment water quality models, on P losses, and (3) evaluate the strengths and weaknesses of using BBNs as a modelling framework for high-resolution observational hydrological data.

3.2 Materials and Methods

3.2.1 Study area and data collection

This study focusses on the Ballycanew catchment (in older papers, also referred to as Grassland B, for example in Sherriff et al., (2015), Figure 3.2) located near Gorey, county Wexford, Ireland. The catchment covers 1207 ha and comprises of 78% grassland and 20% tillage land use, while the remainder 2% is considered seminatural land use (Table 3.1). The reader is referred to Chapter 2.3 and Table 2.2 for further information on the catchment. The Ballycanew catchment is equipped with a river bank-side kiosk where the instrumentation is installed, its location is marked in Figure 3.2 as Outlet Hydro-Station (Mellander et al., 2012; Jordan et al., 2007). River water level is recorded every 10

minutes in a stilling well in the catchment outlet using an OTT Orpheus Mini vented-pressure instrument. The river discharge is calculated from a rating curve developed in a flat-V weir using an Acoustic Doppler Current meter. Total phosphorus (TP) and total reactive phosphorus (TRP) concentrations are monitored with a Hach-Lange Phosphax within the range of 0.01– 5.00 mg l^{-1}, co-located with a Solitax Hach-Lange turbidity (turbidity units, NTU, also recorded every 10 minutes) sensor field-calibrated to suspended sediment concentration (mg l^{-1}) (Sherriff et al., 2016).

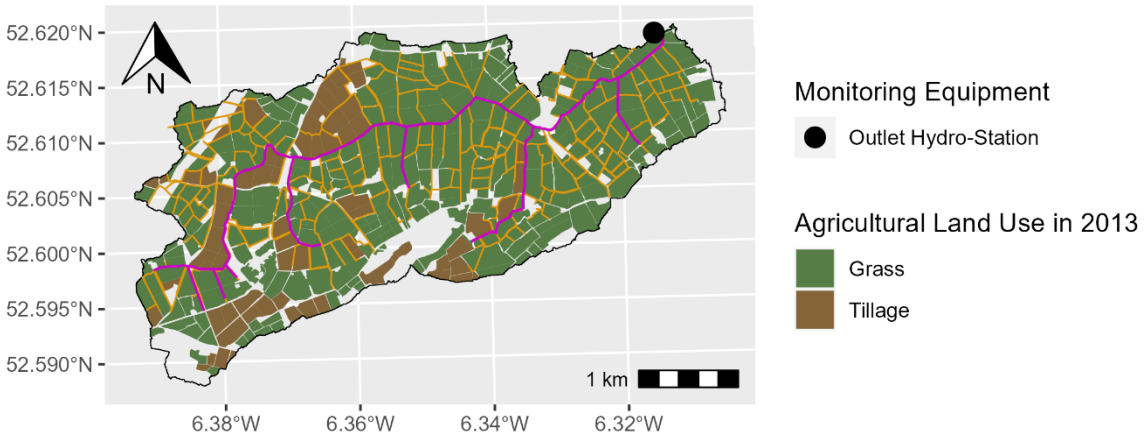

Figure 3.2 Study area: the Ballycanew catchment in County Wexford. Elevation varies between 21 m a.s.l. and 232 m a.s.l. The location of the hydrometric station is marked with the black dot, while magenta lines represent streams, and yellow lines represent artificial drainage.

Data from the bank-side monitoring station (Figure 3.2, Outlet Hydro-Station) collected every 10 minutes (total discharge, average total reactive P concentrations, and average turbidity), were aggregated to daily average values for this study.

3.2.2 Bayesian Belief Network development

Bayesian Networks are directed acyclic graphs (DAGs), that represent a set of variables and their conditional dependencies using a graphical model. The term "directed acyclic" means that there is a sequential flow of information among variables and no dynamic feedback loops (Barton et al., 2012; Kragt, 2009). An introduction to Bayesian Networks and their application in ERA can be found in Moe et al., (2021), and won't be repeated here. The relationships between variables in a BBN are

parameterised using conditional probability distributions or conditional probability tables when variables are discrete (CPTs), and the graphical network is a description of such relationships (Borsuk et al., 2004). A hybrid Bayesian network combines both discrete and continuous variables represented as probability distributions. In this study, a conceptual BBN was developed in GeNIe 2.4 (BayesFusion, 2019) visualizing the 'source-mobilisation-transport-continuum' (Haygarth et al., 2005) and identifying the main drivers of phosphorus pollution in the catchment. The initial DAG comprised of 63 nodes and 81 arcs, with 325 independent parameters out of 483, with parameter count defined as the total size of CPTs while independent parameters are those not implied by other parameters. The average number of node parents (indegree) was 1.3, and the maximum number of node parents was 5. An extensive literature review was conducted summarizing the knowledge base for the subject which was used to inform the priors (distribution shapes, parameter values, and CPTs) for key parameters in the models, as shown in Table 3.1. Catchment-specific information was also collated and used to inform the model structure and priors (Chapter 2, Table 2.2).

From the initial parameterization, two models were developed: Model A, which only accounts for diffuse reactive P sources (i.e., losses from soil matrix and topsoil), and Model B, which also includes P losses from farmyards, which is infrequent in P modelling (Harrison et al., 2019) and septic tanks, which are often overlooked as P sources, as opposed to centralized wastewater treatment centres (Withers et al., 2014). The models aim at integrating all the total reactive P losses from the different compartments at the catchment outlet ("Total catchment in-stream P load", T $month^{-1}$) and then converting the loads into concentrations (mg l^{-1}) by dividing by the monthly discharge (m^3 $month^{-1}$).

3.2.3. Expert input to inform key aspects of the model

Experts from the Agricultural Catchments Programme, the James Hutton Institute, and the Irish EPA with relevant areas of expertise (hydrology, hydrochemistry, land management, farm consultancy, policy making, and environmental modelling) were consulted in 1-to-1 meetings, and in a group workshop. Excluding the authors of this paper, whom we also consider part of the experts' pool, a total of thirteen experts were consulted, and their personal information anonymized. Before the interviews

and workshops, experts were provided with a topic information sheet describing the model and the aims and objectives of the session. The experts were asked to provide their input on the conceptual model structure to ensure that the causal dependencies between variables made sense and none were missing; parameterising variables and their relationships using equations; approving the CPT values for the "Buffers" (proportion of each type of buffer strip present in the catchment) node, as well as deciding which loads were impacted by the buffer reduction (i.e., only surface-pathway derived nodes); and were asked to provide recommendations for further information sources (e.g., reports, publications, or datasets).

3.2.4 Model structure

The model structure is presented in Figure 3.3. The complete structure and specification of both models are included in Table 3.1 to allow reproducibility and further model application in different contexts. Table 3.1 describes the model structure and the conditional probability distributions and describes which CPTs were logical, contained expert judgement, and which were derived from data or literature, highlighting which sub-models and variables are part of Model A or Model B. In particular, the "Hydrology, "Management", and "Soil erosion and soil P" sub-models are represented in both Model A and B, while the sub-models "Septic Tanks" and "Farmyards" are only represented in Model B. An illustration of the BBN showing the full distributions is reported in Figure 8.4.

Table 3.1 Model specifications organized by sub-model. The "Hydrology, "Management", and "Soil erosion and soil P" sub-models belong to both Model A and B.

<table>
<tr><th>Variable (symbol) [unit]</th><th colspan="2">Conditional Probability Table or states and discretisation boundaries for continuous nodes</th><th>Description</th></tr>
<tr><td colspan="4">Hydrology sub-model (Drivers)</td></tr>
<tr><td>Month</td><td>Each month</td><td></td><td>Calculated as No. days in the month/ 365</td></tr>
<tr><td colspan="4">Calculated variables</td></tr>
<tr><td rowspan="5">Mean total monthly Q (discharge) [m^3]</td><td>Very Low</td><td>0-109424</td><td rowspan="5">Bootstrapped from daily total discharge observations (2009-2016) to obtain a Lognormal (μ; σ) discharge distribution with base e for each month. Each month's parameters are shown in the table. Discretization of states is based on percentiles calculated from the average monthly observations (very low<= 5th percentile, low= 5th-25th percentile, medium= 25th-50th percentile, high= 50th-75th percentile, very high= 75th-100th percentile).
<table>
<tr><th></th><th>μ</th><th>σ</th></tr>
<tr><td>January</td><td>13.8</td><td>0.17</td></tr>
<tr><td>February</td><td>13.5</td><td>0.18</td></tr>
<tr><td>March</td><td>12.9</td><td>0.17</td></tr>
<tr><td>April</td><td>12.5</td><td>0.19</td></tr>
<tr><td>May</td><td>12.2</td><td>0.21</td></tr>
<tr><td>June</td><td>11.8</td><td>0.30</td></tr>
<tr><td>July</td><td>11.3</td><td>0.32</td></tr>
<tr><td>August</td><td>11.8</td><td>0.50</td></tr>
<tr><td>September</td><td>11.5</td><td>0.36</td></tr>
<tr><td>October</td><td>12.8</td><td>0.40</td></tr>
<tr><td>November</td><td>13.7</td><td>0.21</td></tr>
<tr><td>December</td><td>13.8</td><td>0.21</td></tr>
</table></td></tr>
<tr><td>Low</td><td>109424-227082</td></tr>
<tr><td>Medium</td><td>227082-373942</td></tr>
<tr><td>High</td><td>373942-806788</td></tr>
<tr><td>Very High</td><td>806788-1124380</td></tr>
<tr><td rowspan="5">Mean total monthly Surface Flow (surface runoff) [m^3]</td><td>Very Low</td><td>0-28450</td><td rowspan="5">Calculated as a portion of mean monthly runoff (26%), via hydrograph separation method described in Mellander et al., (2012). Discretization of states is based on percentiles calculated from observations (very low<= 5th percentile, low= 5th-25th percentile, medium= 25th-50th percentile, high= 50th-75th percentile, very high= 75th-100th percentile).</td></tr>
<tr><td>Low</td><td>28450-59042</td></tr>
<tr><td>Medium</td><td>59042-97225</td></tr>
<tr><td>High</td><td>97225-209765</td></tr>
<tr><td>Very High</td><td>209765-292338</td></tr>
<tr><td rowspan="5">Mean total monthly Sub-surface Stormflow (subsurface runoff) [m^3]</td><td>Very Low</td><td>0-19696</td><td rowspan="5">Calculated as a portion of mean monthly runoff (18%), via hydrograph separation method described in Mellander et al., (2012). Discretization of states is based on percentiles calculated from observations (very low<= 5th percentile, low= 5th-25th percentile, medium= 25th-50th percentile, high= 50th-75th percentile, very high= 75th-100th percentile).</td></tr>
<tr><td>Low</td><td>19696-40875</td></tr>
<tr><td>Medium</td><td>40875-67309</td></tr>
<tr><td>High</td><td>67309-145222</td></tr>
<tr><td>Very High</td><td>145222-202388</td></tr>
</table>

<table>
<tr><td rowspan="5">Mean total monthly Baseflow [m^3]</td><td>Very Low</td><td>0-61277</td><td rowspan="5">Calculated as a portion of mean monthly runoff (56%), via hydrograph separation method described in Mellander et al., (2012). Discretization of states is based on percentiles calculated from observations (very low<= 5^{th} percentile, low= 5^{th}-25^{th} percentile, medium= 25^{th}-50^{th} percentile, high= 50^{th}-75^{th} percentile, very high= 75^{th}-100^{th} percentile).</td></tr>
<tr><td>Low</td><td>61277-127166</td></tr>
<tr><td>Medium</td><td>127166-209407</td></tr>
<tr><td>High</td><td>209407-451801</td></tr>
<tr><td>Very High</td><td>451801-629651</td></tr>
<tr><td colspan="4">Management (Drivers)</td></tr>
<tr><td rowspan="3">Land use</td><td>Arable</td><td>0.20</td><td rowspan="3">As reported by Teagasc - Agriculture and Food Development Authority, (2018).</td></tr>
<tr><td>Grassland</td><td>0.78</td></tr>
<tr><td>Seminatural</td><td>0.02</td></tr>
<tr><td>Buffers</td><td colspan="2"><table><tr><th>Land use</th><th>Arable</th><th>Grassland</th><th>Seminatural</th></tr><tr><td>2 m</td><td>0.98</td><td>0.1</td><td>$1.01*10^{-6}$</td></tr><tr><td>>2 m</td><td>0.019</td><td>0.1</td><td>$1.01*10^{-6}$</td></tr><tr><td>none</td><td>0.001</td><td>0.8</td><td>0.999</td></tr></table></td><td>Buffer strips are defined as being 2 m in width, more than 2 m in width, or absent. Probabilities of having either type of buffer according to land use were agreed upon with one of the ACP advisors (expert) during consultation.</td></tr>
<tr><td colspan="4">Calculated variables</td></tr>
<tr><td rowspan="5">Buffer effectiveness for Particulate P (PP) and suspended sediments (SS)</td><td>Very Low</td><td>0-0.2</td><td rowspan="5">Dependent on the variable Buffers. For 2 m buffers, effectiveness is defined as Beta (α=2.9; β=4.5); for >2 m buffers it is defined as Beta (α=1.44; β=0.789); for no buffers, effectiveness is equal to 0. The distributions were fitted to the dataset published in Stutter et al., (2021), where negative retention data was deleted from the analysis.</td></tr>
<tr><td>Low</td><td>0.2-0.4</td></tr>
<tr><td>Medium</td><td>0.4-0.6</td></tr>
<tr><td>High</td><td>0.6-0.8</td></tr>
<tr><td>Very High</td><td>0.8-1</td></tr>
<tr><td rowspan="5">Buffer effectiveness for Total Dissolved P (TDP)</td><td>Very Low</td><td>0-0.2</td><td rowspan="5">Dependent on the variable Buffers. For Buffers 0-2 m, Buffer effectiveness is defined as Beta (α=1.8; β=2.7), for >2 m buffers it is defined as Beta (α=1; β=0.8); for no buffers, effectiveness is equal to 0. The distributions were fitted to the dataset published in Stutter et al., (2021), where negative retention data was deleted from the analysis.</td></tr>
<tr><td>Low</td><td>0.2-0.4</td></tr>
<tr><td>Medium</td><td>0.4-0.6</td></tr>
<tr><td>High</td><td>0.6-0.8</td></tr>
<tr><td>Very High</td><td>0.8-1.0</td></tr>
<tr><td colspan="4">Soil erosion and soil P sub-model</td></tr>
<tr><td>Morgan P</td><td colspan="2"><table><tr><th></th><th>Arable</th><th>Grassland</th><th>Seminatural</th></tr><tr><td>Morgan1</td><td>0.40</td><td>0.46</td><td>0</td></tr><tr><td>Morgan2</td><td>0.49</td><td>0.35</td><td>0.6</td></tr><tr><td>Morgan3</td><td>0.09</td><td>0.14</td><td>0.3</td></tr><tr><td>Morgan4</td><td>0.02</td><td>0.05</td><td>0.1</td></tr></table></td><td>Based on land use, proportions of land for each level and in each land use category were calculated based on the soil survey carried out in 2013 in the catchment. Where the Morgan P index was unknown, that proportion of land was assigned to the dominant index category. For the interpretation of the Soil Morgan P Index, the reader is referred to Regan et al., (2012).</td></tr>
<tr><td colspan="4">Calculated variables</td></tr>
<tr><td rowspan="4">Monthly Turbidity [NTU $month^{-1}$]</td><td>Very Low</td><td>0-1402</td><td rowspan="4">Bootstrapped from daily average turbidity observations (2009-2016) to obtain a Lognormal (μ; σ) turbidity distribution with base e for each month. Each month’s parameters are shown in the</td></tr>
<tr><td>Low</td><td>1402-1665</td></tr>
<tr><td>Medium</td><td>1665-2270</td></tr>
<tr><td>High</td><td>2270-3391</td></tr>
</table>

<table>
<tr><td></td><td>Very High</td><td>3391-4344</td><td>table. Discretization of states is based on percentiles calculated from the average monthly observations (very low<= 5th percentile, low= 5th-25th percentile, medium= 25th-50th percentile, high= 50th-75th percentile, very high= 75th-100th percentile).
<table><tr><th></th><th>μ</th><th>σ</th></tr><tr><td>January</td><td>6.3</td><td>0.25</td></tr><tr><td>February</td><td>6.0</td><td>0.23</td></tr><tr><td>March</td><td>5.6</td><td>0.23</td></tr><tr><td>April</td><td>5.5</td><td>0.20</td></tr><tr><td>May</td><td>5.3</td><td>0.15</td></tr><tr><td>June</td><td>5.5</td><td>0.15</td></tr><tr><td>July</td><td>5.2</td><td>0.13</td></tr><tr><td>August</td><td>5.2</td><td>0.13</td></tr><tr><td>September</td><td>5.2</td><td>0.12</td></tr><tr><td>October</td><td>5.7</td><td>0.24</td></tr><tr><td>November</td><td>6.2</td><td>0.30</td></tr><tr><td>December</td><td>6.2</td><td>0.30</td></tr></table></td></tr>
<tr><td rowspan="5">Monthly Suspended Sediment concentration [mg l^{-1} $month^{-1}$]</td><td>Very Low</td><td>0-133.3</td><td rowspan="5">Calculated as: a * Monthly Turbidity [NTU $month^{-1}$] ^{b}, where a= 0.567, and b= 1.1109, as described in Sherriff et al., (2015). Discretization of states is based on percentiles calculated from the average monthly calculated observations (very low<= 5th percentile, low= 5th-25th percentile, medium= 25th-50th percentile, high= 50th-75th percentile, very high= 75th-100th percentile).</td></tr>
<tr><td>Low</td><td>133.3-165</td></tr>
<tr><td>Medium</td><td>165-237.6</td></tr>
<tr><td>High</td><td>237.6-369.3</td></tr>
<tr><td>Very High</td><td>369.3-480.0</td></tr>
<tr><td rowspan="5">Water Extractable P (WEP) [mg l^{-1}]</td><td>Low</td><td>0-3</td><td rowspan="5">Based on variable “Morgan P levels” and “land use” (data from 2013) it is calculated with the equations available in (Thomas et al., 2016b): for Grassland, WEP=0.60 * Morgan P + 1.46, for Arable: WEP= 0.45 * Morgan P + 0.19, where Morgan P is defined as a Uniform distribution with the following parameters:
<table><tr><th>Morgan P Index</th><th>Grassland</th><th>Arable</th></tr><tr><td>Index 1</td><td>a=0; b=3</td><td>a=0; b=3</td></tr><tr><td>Index 2</td><td>a=3.1; b=5</td><td>a=3.1; b=6</td></tr><tr><td>Index 3</td><td>a=5.1; b=8</td><td>a=6.1; b=10</td></tr><tr><td>Index 4</td><td>a=8.1; b=30</td><td>a=10.1; b=30</td></tr></table></td></tr>
<tr><td>Medium</td><td>3-5</td></tr>
<tr><td>High</td><td>5-8</td></tr>
<tr><td>Very High</td><td>8-15</td></tr>
</table>

			For the Seminatural Land use, WEP was assumed constant to 0.001. Discretization is based on Morgan P discrete levels.
Sediment Water Soluble P [mg kg^{-1}]	Very Low	0-0.0995	Defined as a Lognormal distribution (μ=-0.9, σ=1), fitted with the *SHELF* R package (version 1.8.0, Oakley, 2020) to observed Water Extractable P in the catchment sediments (Shore et al., 2016). Discretization of states is based on percentiles calculated from the observations (very low<= 5^{th} percentile, low= 5^{th}-25^{th} percentile, medium= 25^{th}-50^{th} percentile, high= 50^{th}-75^{th} percentile, very high= 75^{th}-100^{th} percentile).
	Low	0.0995-0.2100	
	Medium	0.2100-0.3550	
	High	0.3550-0.9100	
	Very High	0.9100-8	
Predicted Dissolved P Concentration [mg l^{-1}]	Low	0-3	Dependant on Water Extractable P, it is defined with the linear model: Predicted Dissolved P = β(WEP)+α, where β =0.08, α =0.158, derived from (Thomas et al., 2016b). This equation is derived from data gathered during the closed period only, that is, when farmers are forbidden from spreading fertilizer. An assumption is made that when the linear model yields a negative value, that is resampled as a zero. Water Extractable P is considered a good in-stream TRP/ TDP predictor in the ACP catchments by the experts, however careful consideration is needed when choosing a soil P test in a different setting.
	Medium	3-5	
	High	5-8	
	Very High	8-15	
Sub-surface Dissolved P load [kg $month^{-1}$]	Low	0-3	Calculated as the product of Predicted Dissolved P concentration and Subsurface Storm-flow.
	High	3-200	
Baseflow Dissolved P load [kg $month^{-1}$]	Low	0-3	Calculated as the product of Predicted Dissolved P concentration and Baseflow.
	High	3-200	
Modified Dissolved P load [kg $month^{-1}$]	Low	0-3	Based on "Buffer effectiveness for Total Dissolved P", for effective buffers, modified Dissolved P load= Sub-surface Dissolved P load *(1-Buffer effectiveness for TDP). Based on expert recommendation.
	High	3-200	
Monthly Sediment P load [kg $month^{-1}$]	Low	0-3	Calculated as the product of Sediment Water Soluble P [mg kg^{-1}], Monthly Suspended Sediment concentration [mg l^{-1} $month^{-1}$], and Mean total monthly surface flow [m^3] .
	High	3-200	
Modified Sediment P load [kg $month^{-1}$]	Low	0-3	Based on "Buffer effectiveness for Suspended Sediments and Particulate P", for effective buffers, Modified Sediment P load= Monthly Sediment P load [kg $month^{-1}$]*(1-Buffer effectiveness for SS and PP). Based on expert recommendation.
	High	3-200	
Septic Tanks (ST) sub-model (Point P sources), included in Model B only			
P concentration per tank	Absent (to represent 0 STs)	0-1*10^{-8}	

<table>
<tr><td rowspan="4">[mg l^{-1}]</td><td>Low</td><td>$1*10^{-8}$-1</td><td rowspan="4">P concentration is dependent on the treatment type. If the treatment is unknown, the concentration is defined as a Lognormal distribution (μ=2.9, σ =1.25), based on a literature review of data available for Ireland (Environmental Protection Agency Ireland (EPA), 2003, 2000; Gill et al., 2005, 2007) (n=8). Fitting was done with R package fitdistrplus (version 1.1-8, Delignette-Muller et al., 2020). Otherwise, for primary and secondary treatment concentration is defined as Truncated Normal distribution (μ=10; σ=1), and (μ=5; σ=0.5) respectively, as described in Glendell et al., (2021) and derived from SEPA guidelines (Brownlie et al., 2014). All tanks are assumed to be maintained. Discretization was also based on the literature review.</td></tr>
<tr><td>Medium</td><td>1-18</td></tr>
<tr><td>High</td><td>18-35</td></tr>
<tr><td>Very High</td><td>35-100</td></tr>
<tr><td colspan="4">Management related variables</td></tr>
<tr><td rowspan="2">Direct discharge</td><td>Present</td><td>0.16</td><td rowspan="2">Probabilities are derived from the report by the Environmental Protection Agency Ireland (EPA, 2015).</td></tr>
<tr><td>Absent</td><td>0.84</td></tr>
<tr><td rowspan="3">Treatment</td><td>Unknown</td><td>0.50</td><td rowspan="3">Probability of having “unknown”, “primary” or “secondary” treatment of the effluent in a septic tank. Probabilities based on a survey conducted within WaterProtect, a research project supported by the European Union research and innovation funding programme Horizon 2020 [grant no. 727450].</td></tr>
<tr><td>Primary</td><td>0.31</td></tr>
<tr><td>Secondary</td><td>0.19</td></tr>
<tr><td colspan="4">Connectivity related variables</td></tr>
<tr><td rowspan="3">Degree of Phosphorus Saturation (DPS) [%]</td><td>Very Low_0_20</td><td>0.978</td><td rowspan="3">Discretization is equal to the $20^{th,}$ 40^{th}, 60^{th}, and 80^{th} quantiles, however 0< DPS <60 in this catchment. Probabilities were calculated from available spatial data (Wall et al., 2012).</td></tr>
<tr><td>Medium_20_40</td><td>0.017</td></tr>
<tr><td>High_40_60</td><td>0.005</td></tr>
<tr><td rowspan="6">Soil risk factor [adimensional]</td><td>Very Low</td><td>$9.9*10^{-6}$</td><td rowspan="6">An indicator to describe the combined risk of effluent leaching to the groundwater table with the risk of the effluent being transported with surface runoff. This approach is a simplification of the one adopted in Glendell et al., (2021). The risk factor was obtained by overlaying the soil series (Thomas et al., 2016b) with information on the position of the groundwater table (0- 2 m below ground or more than 2 m below ground). Because little is known regarding the septic tanks in the catchment (i.e. age, type of treatment, maintenance), and the groundwater table position (few datapoints within the catchment) experts recommended a precautionary principle. This meant that the class at most risk of effluent transfer was applied when data</td></tr>
<tr><td>Low</td><td>0.374</td></tr>
<tr><td>Medium</td><td>$9.9*10^{-6}$</td></tr>
<tr><td>High</td><td>0.620</td></tr>
<tr><td>Very High</td><td>0.006</td></tr>
<tr><td colspan="2"><table>
<tr><td></td><td colspan="2">Groundwater Table Position</td></tr>
<tr><td>Soil Series</td><td>0-2 m below surface</td><td>>2 m below surface</td></tr>
<tr><td>Brown earths</td><td>High Risk</td><td>Moderate Risk</td></tr>
<tr><td>Alluvial</td><td>High Risk</td><td>Moderate Risk</td></tr>
<tr><td>Luvisol</td><td>High Risk</td><td>Moderate Risk</td></tr>
<tr><td>Gley</td><td>Very High Risk</td><td>Very High Risk</td></tr>
</table></td></tr>
</table>

was unavailable. The table to the left represents a synthesis of the classification approach. Probabilities are based on land cover proportion.

Leachfield removal

Soil risk factor	DPS	Low	Medium	High
Very low	Very Low	0.0	0.0	1.0
	Medium	0.0	0.5	0.5
	High	0.5	0.5	0.0
Low	Very Low	0.0	0.3	0.7
	Medium	0.0	0.7	0.3
	High	0.3	0.7	0.0
Medium	Very Low	0.0	0.5	0.5
	Medium	0.0	1.0	0.0
	High	0.5	0.5	0.0
High	Very Low	0.0	0.7	0.3
	Medium	0.3	0.7	0.0
	High	0.7	0.3	0.0
Very High	Very Low	0.0	0.5	0.5
	Medium	0.5	0.5	0.0
	High	1.0	0.0	0.0

The node refers to P removal from septic drains. Conditional on P leaching risk from Degree of Phosphorus Saturation (DPS). The conditional probability table is a logical one.

Leachfield connectedness

HSA rescaled	None		Low		Medium		High	
Direct discharge	pres	abs	pres	abs	pres	abs	pres	abs
low	0	1	0	1	0	0	0	0
medium	0	0	0	0	0	1	0	0
high	1	0	1	0	1	0	1	1

Probabilities are conditional on the presence/absence of Direct ST discharge, and HSA (node: Connectivity rescaled HSA). Where Direct discharge is present, connectedness is assumed as 'high'. Where Direct discharge is absent, the risk class of the HSA is assigned.

Septic Tank connectedness

Leachfield removal	Low			Medium			High		
Leachfield connectedness	Low	Medium	High	Low	Medium	High	Low	Medium	High
Low	1.0	0.0	0.0	1.0	0.0	0.0	1.0	0.5	0.0
Medium	0.0	1.0	0.0	0.0	1.0	0.5	0.0	0.5	1.0
High	0.0	0.0	1.0	0.0	0.0	0.5	0.0	0.0	0.0

Probabilities are conditional on Leachfield removal and Leachfield connectedness. Where Leachfield removal is 'low' or 'High', Leachfield connectedness remains unaltered.

Connectivity rescaled HSA [adimensional]

None_0	0.60
Low_1_3	0.18
Medium_4_7	0.20
High_8_10	0.02

Data extracted from spatial layers of Hydrologically Sensitive Areas (HSAs) rescaled between 0 and 10 was provided by the Agricultural Catchments Programme (Thomas et al., 2016a). Discretization is also based on the spatial layers.

Calculated variables

Load per tank [kg month^{-1}]

Absent	0-1*10^{-6}
Very Low	1*10^{-6}-0.1

Specified as the product of ST density [No ha^{-1}] * ST concentration [mg l^{-1}] * 120 [L] average daily water consumption per person * 365/12 days in a

<table>
<tr><td></td><td>Low</td><td>0.1-0.5</td><td rowspan="4">month* average No of persons per household 2.7/1*10^{6}. Discretisation is based on interpolation to represent plausible probabilities for combination of extreme risk classes (e.g. High+high=high, low+low=low).</td></tr>
<tr><td></td><td>Medium</td><td>0.5-1.0</td></tr>
<tr><td></td><td>High</td><td>1.0-2.0</td></tr>
<tr><td></td><td>Very High</td><td>2.0-30</td></tr>
<tr><td rowspan="6">Total Realized load [T month^{-1}]</td><td>Very Low</td><td>0.0-0.1</td><td rowspan="6">Calculated as the product of septic tank load and delivery factors (D) related to the connectedness of a septic tank, based on the median estimated fraction to be delivered in Table 13 of the report by Glendell et al., (2021) and the number of septic tanks present within catchment boundary (N): Realised load per tank [kg month^{-1}] * N * D / 1000. In this case, N= 88. Discretisation based on interpolation to represent plausible probabilities for combination of extreme risk classes.</td></tr>
<tr><td>Low</td><td>0.1-0.5</td></tr>
<tr><td>Medium</td><td>0.5-1.0</td></tr>
<tr><td>High</td><td>1.0-2.0</td></tr>
<tr><td>Very High</td><td>2.0-12</td></tr>
<tr><td colspan="3"><table>
<tr><th>Septic tank connectedness</th><th>Delivery factor (D)</th><th>Reference</th></tr>
<tr><td>Low</td><td>0.05</td><td>“very low” category in Appendix A3, Glendell et al., (2021)</td></tr>
<tr><td>Medium</td><td>0.30</td><td>“medium” category in Appendix A3, Glendell et al., (2021)</td></tr>
<tr><td>High</td><td>0.80</td><td>“very high” category in Appendix A3, Glendell et al., (2021)</td></tr>
</table></td></tr>
<tr><td colspan="4">Farmyards sub-model (Point P sources), included in Model B only</td></tr>
<tr><td rowspan="5">Farmyard size area [m^{2}]</td><td>Very Low</td><td>0-56</td><td rowspan="5">Based on available farmyard survey, a distribution was fitted to farmyard area data: Lognormal (μ=-5.6; σ=0.98). Discretization of states is based on percentiles calculated from the observations (very low<= 5th percentile, low= 5th-25th percentile, medium= 25th-50th percentile, high= 50th-75th percentile, very high= 75th-100th percentile).</td></tr>
<tr><td>Low</td><td>56-127</td></tr>
<tr><td>Medium</td><td>127-277</td></tr>
<tr><td>High</td><td>277-586</td></tr>
<tr><td>Very High</td><td>586-4500</td></tr>
<tr><td rowspan="5">Farmyard P concentration [mg l^{-1}]</td><td>Very Low</td><td>0-0.01</td><td rowspan="5">Using the SHELF R package (version 1.8.0, Oakley, 2020), a distribution was fitted to the data in Table 2 in Harrison et al., (2019): Lognormal (μ=-1.8; σ=1.6). The best fit would have been the LogT distribution, however, that is not available for GeNIe, so we opted for Lognormal. Discretization is also based on the literature. For simplicity, here we have used SRP to mean TRP.</td></tr>
<tr><td>Low</td><td>0.01-0.50</td></tr>
<tr><td>Medium</td><td>0.50-1.00</td></tr>
<tr><td>High</td><td>1.00-2.50</td></tr>
<tr><td>Very High</td><td>2.50-60</td></tr>
<tr><td rowspan="5">Incidental losses per average yard [kg month^{-1}]</td><td>Very Low</td><td>0-1*10^{-9}</td><td rowspan="5">Based on average farmyard size, losses are calculated as Surface runoff [m^{3}] / catchment area [m^{2}]* Farmyard size area [m^{2}]* Farmyard P concentration [mg l^{-1}]/ 10^{3}.</td></tr>
<tr><td>Low</td><td>1*10^{-9}-0.001</td></tr>
<tr><td>Medium</td><td>0.001-0.01</td></tr>
<tr><td>High</td><td>0.01-0.10</td></tr>
<tr><td>Very High</td><td>0.10-60</td></tr>
<tr><td rowspan="3">Total incidental losses [T month^{-1}]</td><td>Very Low</td><td>0-1*10^{-5}</td><td rowspan="3">Incidental losses per average yard [kg month^{-1}] * N, where N is the total number of yards present within the catchment boundary. In this case, N =70.</td></tr>
<tr><td>Low</td><td>1e-05-0.007</td></tr>
<tr><td>Medium</td><td>0.007-0.070</td></tr>
</table>

<table>
<tr><td></td><td>High</td><td>0.07-0.700</td><td></td></tr>
<tr><td></td><td>Very High</td><td>0.700-10</td><td></td></tr>
<tr><td colspan="4">Catchment outlet integration sub-model</td></tr>
<tr><td rowspan="3">Total catchment in-stream P load [T month^{-1}]</td><td>Low</td><td>0-0.02</td><td rowspan="3">Equal to the sum of Baseflow Dissolved P load [kg month^{-1}], Modified Dissolved P load [kg month-^{1}], Modified Sediment P load [kg month^{-1}], Total incidental losses [T month^{-1}], and Total Realized load [T month^{-1}], all converted to appropriate units.</td></tr>
<tr><td>Medium</td><td>0.02-1</td></tr>
<tr><td>High</td><td>1-10</td></tr>
<tr><td rowspan="2">In-stream P concentration [mg l^{-1}]</td><td>Good</td><td>0-0.035</td><td rowspan="2">Defined as the Total catchment in-stream P load [T] * 10^9 / Mean total monthly Q (discharge) [m^3] * 1000, where mean monthly discharge is equal to the total catchment discharge measured at the outlet.</td></tr>
<tr><td>Bad</td><td>0.035-10</td></tr>
<tr><td>Environmental Quality Standard [TRP concentration mg l^{-1}]</td><td colspan="2"><table><tr><th>TRP concentration</th><th>Good</th><th>Bad</th></tr><tr><td>Good</td><td>1</td><td>0</td></tr><tr><td>Bad</td><td>0</td><td>1</td></tr></table></td><td>Discretization of the variable “In-stream TRP concentration [mg l^{-1}]”. For simplicity, in-stream TRP is here considered equal to in-stream Dissolved Reactive Phosphorus, as in previous studies the mean DRP accounted for 98–99% of the flow-weighted mean TRP (Shore et al., 2014).</td></tr>
</table>

3.2.5 Model evaluation

P models typically struggle to produce positive performance indicators (Jackson-Blake et al., 2015). Additionally, BBNs cannot be evaluated with the traditional metrics used for hydrological models (for example, Nash-Sutcliffe Efficiency or Root Mean Square Error), because the number of observations does not correspond to the number of model realizations. Therefore, the model performance was evaluated following the procedures suggested by Jackson-Blake et al., (2015), using a suite of strategies comparing predicted TRP concentrations (mg l^{-1}) with the observed TRP concentrations (available as daily average, mg l^{-1}) (2009-10-01 to 2016-12-31) by 1) calculating percentage bias (PBIAS), 2) comparing summary statistics (median, mean, upper and lower limit, interquartile ranges), and 3) visually comparing the full posterior distributions with the observations. Using the R *SHELF* package (version 1.8.0, Oakley, 2020), a monthly lognormal distribution was fitted to the observed TRP concentrations using 100 quantiles and 0 as the lower limit. This distribution was used to compute the PBIAS % in the R package *hydroGOF* (version 0.4-0, Zambrano-Bigiarini, 2020). Percentage Bias is calculated in *hydroGOF* as shown in Equation 3.1:

Equation 3.1

$$PBIAS = 100\frac{\sum_{i=1}^{N}(S_i - O_i)}{\sum_{i=1}^{N} O_i}$$

Whereby S_i indicates the simulated TRP values and O_i the observed ones. Percentage bias measures the tendency of simulated values to be larger or smaller than the observations, with a zero-value indicating optimum, positive values indicating overestimation, and negative values underestimation. Additionally, a bootstrapping method was applied to the available observations to obtain a lognormal distribution fitted to each month's TRP concentration data. Percentage bias was used to evaluate the BBNs performances in each month, in this case with 10,000 data points from the posterior distribution simulated by the BBNs by selecting each month as evidence, and 10,000 data points drawn from each month's lognormal distribution fitted to the observational data using bootstrapping. For the overall and the monthly performance evaluation, data points outside the instrument's limits of detection (0.01 – 5.00 mg l^{-1}) were excluded from the model evaluation.

When computing the PBIAS, observations and simulations need to have the same dimension, and the *hydroGOF* package will return one value for each column of simulations and observations. The reader is referred to the GitHub repository accompanying this Chapter to reproduce how the PBIAS function was applied here (https://github.com/CamillaNegri/Ballycanew_Ptool/blob/main/GenieResults.Rmd).

3.3 Results and discussion

3.3.1 Model structure

As a result of the discussions with experts and the extensive data review, the final model versions (A and B) are considerably less complex than was initially conceptualized. As mentioned, the original BBN comprised 63 nodes and 81 arcs, while the resulting Model B comprises 38 nodes, 46 arcs, 106 independent parameters out of 153, average indegree of 1.2, and maximum indegree of 5. The original model structure (not shown here) included variables that were excluded from the final structure as a result of the consultations with experts. Fertilizer (organic plus inorganic) application based on stocking rates was excluded from the BBN as soil P fertilizer is applied only to maintain Morgan P levels, available at field scale. Erosion rates were also not included in the final version of the model as catchment-specific data was unavailable. Incidental losses due to animal poaching were also excluded as fencing of water courses is in place in the ACP catchments. The final BBN structure is shown in Figure 3.3, which highlights which nodes were part of Model A and which ones were added for Model B. The model structure (Table 3.1) directly reports which variables were influenced by experts, in an attempt to address some of the transparency issues raised by Kaikkonen et al., (2021) regarding expert role.

Figure 3.3 Structure of the final BBNs, including the additional nodes for Model B highlighted inside the box. The nodes in orange represent variables that pertain to Management, those in yellow represent Soil variables, those in turquoise represent the Hydrology variables, those in light blue represent the Turbidity-related variables, those in lilac represent the Loads within the catchment, and those in cyan represent the Concentrations integrated at the catchment outlet. Full distributions are illustrated in Figure 8.4.

3.3.2 Phosphorus concentrations

3.3.2.1 Phosphorus concentrations in the stream – overall performance

Overall model performance is shown in Table 3.2, where mean, lower and upper limit, and meaningful percentiles of the BBN TRP concentration distributions are shown against the average monthly distribution fitted to the observations. The 5th percentile shows that the model concentrations are more skewed towards low concentrations than the observations. This may be related to the equation used to calculate the variable "Predicted Dissolved P Concentration [mg l^{-1}]", reported in Table 3.1 and derived from Thomas et al., (2016b). The node was set up to substitute the negative values with zeroes as recommended by Thomas et al., (2016b). 25% of the simulated values for the "Predicted Dissolved P Concentration [mg l^{-1}]" node equalled zero (meaning no TRP from the soil matrix would be measured

at the catchment outlet) and currently included when computing the final TRP concentration distribution prior to censoring it by instrument's limits of detection (0.01– 5.00 mg l^{-1}), which may have skewed the model predictions. However, the model results are also skewed towards larger concentrations in the upper percentiles compared to the observations. The median modelled TRP concentration approximates the observed median, and as discussed, the tails of the modelled distributions are wider than those in observed mean daily data, which is also shown in Figure 3.4.

Table 3.2 The two models' overall performances in terms of mean, standard deviation, quantiles, and percentage bias. Data outside the instrument's limit of detection (0.01-5.00 mg l^{-1}) were excluded from the calculations. Both observed and predicted TRP concentrations were log-transformed before calculating the statistics, and then converted back to normal values.

	Observed TRP (time-weighted)	**Predicted TRP Diffuse P (flow-weighted)**	**Predicted TRP Diffuse + Point P (flow-weighted)**
	mg l^{-1}	**mg l^{-1}**	**mg l^{-1}**
lower limit (μ-1σ)	0.03	0.03	0.03
mean	0.06	0.08	0.08
upper limit (μ+1σ)	0.10	0.20	0.21
5th percentile	0.02	0.02	0.01
25th percentile	0.04	0.05	0.04
50th percentile	0.06	0.09	0.10
75th percentile	0.08	0.14	0.14
		Model A (Diffuse P)	**Model B (Diffuse + Point P)**
Percentage bias against distribution fitted to observations (%)	-	76	80

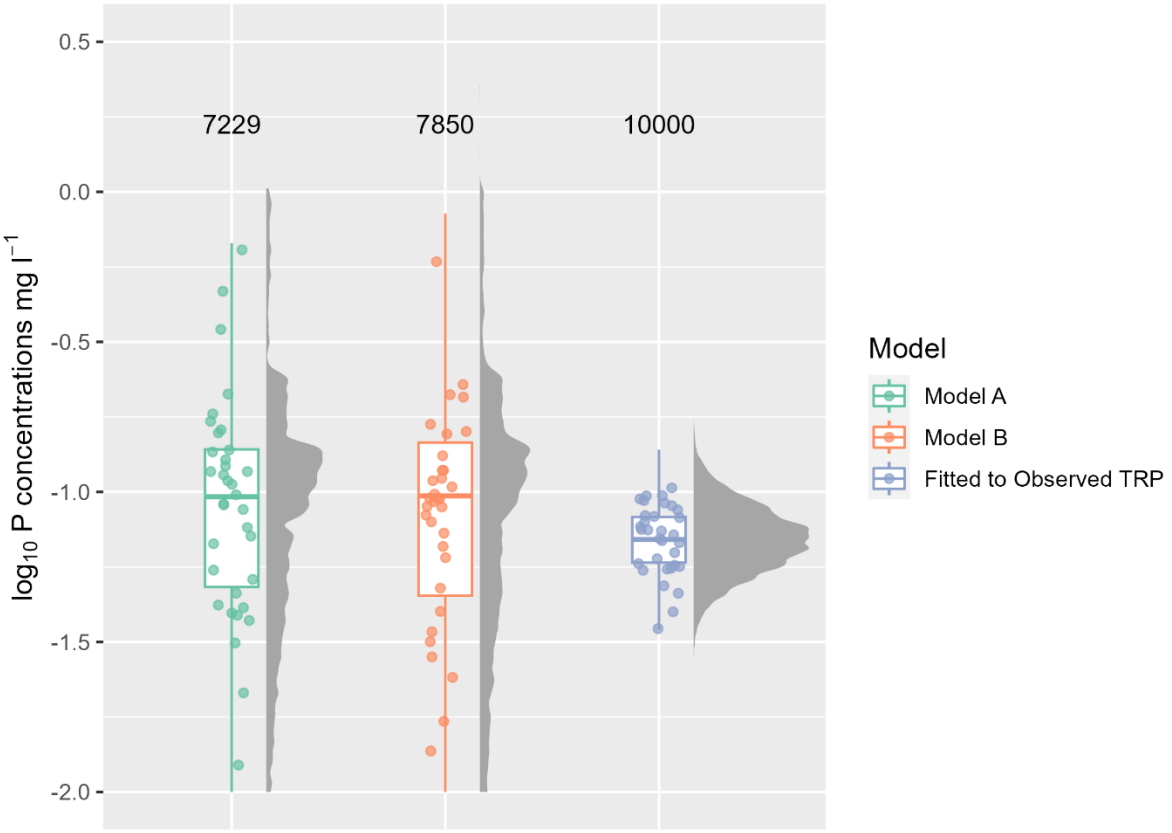

Figure 3.4 Overall distribution density of log10 TRP concentrations fitted to observations versus those predicted by the two developed BBNs. BBN predictions show a larger variance, the full extent of which is shown in the plot by the density and box plots and scattered data points. Data outside the instrument's limit of detection (0.01-5.00 mg l^{-1}) were excluded from the plot, and the text shows the number of valid samples for each model. This plot was produced with the ggdist R package version 3.3.0 (Kay, 2023).

Figure 3.4 shows the overall model distributions compared to the lognormal distribution fitted to the observations. The boxplots and the density plots at their right-hand side show the full distributions excluding data points outside the instrument's limit of detection, while the dots scattered on top of the boxplots show only a sample (n = 30).

3.3.2.2 Phosphorus concentrations in the stream – monthly performance

Each month's modelled and observed TRP concentrations are shown as histogram plots in Figure 3.5 A and as density plots in Figure 3.5 B. The histograms show that the distributions from the simulations from both models approximate the peak of the distribution of the observations, however, the simulated concentration distributions have a lower tail that is not seen in the observed data. This discrepancy could be a product of how the predicted dissolved P concentration is being calculated in the model (see 3.2.1). The observations reported are aggregated daily mean values calculated from monitoring observations taken every 10-minutes. These daily means necessarily do not reflect the full range of concentration variability in the monitoring data, especially for extreme or short duration hydrological events, and they do not show diel P variations due to changes in temperature, light, and precipitation (Bieroza et al., 2023), which are likely to affect P mobilisation, delivery, and in-stream uptake. For example, see Table 3.3 for a comparison between the daily mean P and the 10-minutes P observations. Furthermore, the detection of low P concentrations is restricted by the instrument detection limits (0.01– 5.00 mg l^{-1}). Although neither model reproduces the width of the observed data distributions, the simulated distributions from Model A are broader than those from Model B suggesting that Model B is marginally better constrained. Importantly, the models predict flow-weighted concentrations (normalized by both time and discharge) rather than time-weighted (mean concentration in stream water as it passes the sampling point), which could in some cases better represent nutrient concentrations (i.e., for lakes, Rowland et al., (2021)). This may result in the different dilution effect in the model compared to the observations (see mean (μ) total discharge (Q, m^3), in Table 3.4). Monthly density plots show little to no seasonality, probably masked by model assumptions, which are further discussed in Table 3.5. Overall, the model represents the observed distribution between the 25^{th} and 75^{th} percentile very well, indicating strong predictive performance. This is especially notable when considering the small units (P concentrations) that are being reproduced and the complexities of processes affecting P dynamics in river catchments.

Table 3.3 Monitored TRP concentrations (mg l^{-1}) characteristics (correlation between the two datasets was 0.91). The two datasets have not been censored with the instrument's detection limits for this analysis, nor log-transformed.

	10-minute concentration data	**Daily mean concentration data**
	mg l^{-1}	**mg l^{-1}**
Min	0.002	0.015
25th percentile	0.042	0.043
Median	0.057	0.058
75th percentile	0.082	0.085
Mean	0.075	0.075
Max	3.095	1.065

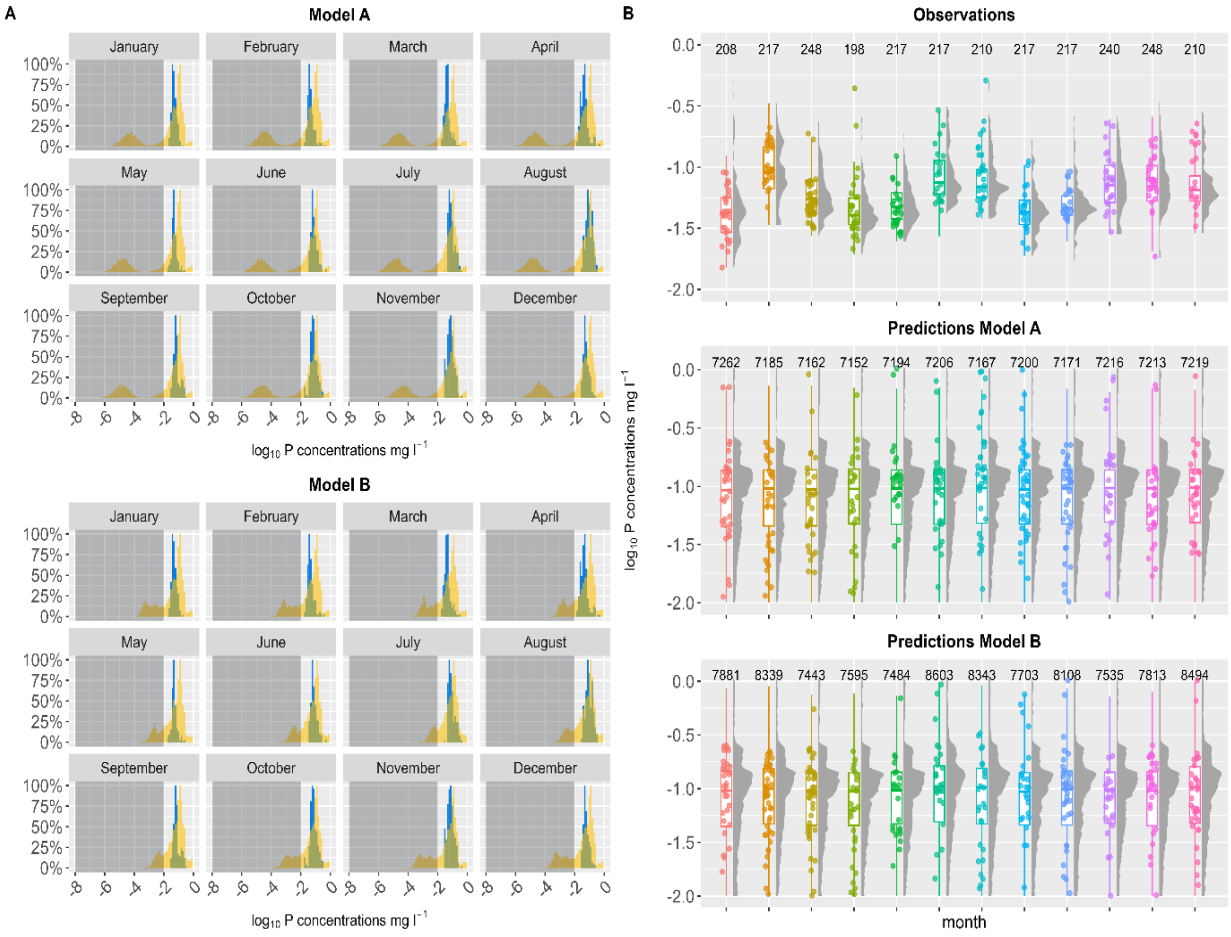

Figure 3.5 A represents the histograms of each month's log10 of TRP concentrations (mg l^{-1}), observations are shown in blue, predictions obtained from the Diffuse P model (Model A, top figure) and Diffuse + Point P model (Model B, bottom figure) are shown in yellow. The histograms placed inside the grey box show values outside the limit of detection (0.01-5.00 mg l^{-1}). B represents the monthly density plots of log10 observations (top), the Diffuse P model (middle), and the Diffuse + Point P model (bottom). Data outside the instrument's limit of detection (0.01-5.00 mg l^{-1}) were excluded from the plots in box B, and the text shows the number of valid samples for each model. The density plots in box B were produced with the ggdist R package version 3.3.0 (Kay, 2023).

Table 3.4 summarizes each month's characteristics in terms of mean and median P concentrations, as well as mean discharge and model percentage bias calculated for the two BBNs. Percentage bias shows that the difference between the two models is minimal, corroborated by the nearly identical performance in terms of mean predicted concentrations. Mean total discharge (Q, m^3) is shown for Model B and the observations, assuming to be the same for Model A. The ratio between the modelled and the observed discharge shows how the models simulate 80-100% of flow correctly in most cases, except the summer months, when the modelled discharge is 60-70% of the observed. This underprediction can explain why the model average concentrations are higher than the80-100% of flow correctly in most cases, except the summer months, when the modelled discharge is 60-70% of the observed. This underprediction can explain why the model average concentrations are higher than the than the observed ones (less discharge, less dilution).

Table 3.4 Summary of monthly characteristics and results, including model bias. Percentage bias and TRP concentrations have been calculated excluding data outside the instrument's limit of detection (0.01-5.00 mg l^{-1}). "A" columns show results for Model A and "B" columns show results for Model B. Both observed and predicted TRP concentrations were log-transformed before calculating the statistics, and then converted back to normal values.

	Percentage bias of simulations against distribution fitted to observed		**mean (μ) concentrations**			**median concentrations**			**lower limit concentrations (μ-1σ)**			**upper limit concentrations (μ+1σ)**			**Mean total discharge (Q)**		
			(mg l^{-1})			**(mg l^{-1})**			**(mg l^{-1})**			**(mg l^{-1})**			**m^3**		
	A	**B**	**A**	**B**	**obs**	**A**	**B**	**obs**	**A**	**B**	**obs**	**A**	**B**	**obs**	**Models**	**obs**	**model/ observations ratio**
Jan	69.4	74.5	0.08	0.08	0.05	0.09	0.10	0.04	0.03	0.03	0.03	0.20	0.21	0.07	$9.99*10^5$	$11.0*10^5$	0.9
Feb	74.5	70.9	0.08	0.08	0.04	0.09	0.09	0.04	0.03	0.03	0.03	0.21	0.20	0.07	$7.42*10^5$	$7.48*10^5$	1
Mar	67.5	70.7	0.08	0.08	0.04	0.09	0.09	0.04	0.03	0.03	0.03	0.20	0.20	0.07	$4.07*10^5$	$4.83*10^5$	0.8
Apr	69.9	77.9	0.08	0.08	0.05	0.09	0.09	0.04	0.03	0.03	0.03	0.20	0.21	0.09	$2.73*10^5$	$3.06*10^5$	0.9
May	69	81	0.08	0.08	0.05	0.10	0.10	0.05	0.03	0.03	0.02	0.20	0.22	0.07	$2.03*10^5$	$2.28*10^5$	0.9
Jun	73.5	89.2	0.08	0.09	0.07	0.10	0.10	0.07	0.03	0.03	0.03	0.20	0.23	0.13	$1.40*10^5$	$2.24*10^5$	0.6
Jul	70.3	101	0.08	0.09	0.09	0.09	0.10	0.07	0.03	0.03	0.05	0.20	0.24	0.14	$0.85*10^5$	$1.15*10^5$	0.7
Aug	68.5	89.1	0.08	0.09	0.09	0.09	0.10	0.09	0.03	0.03	0.05	0.20	0.23	0.16	$1.51*10^5$	$2.52*10^5$	0.6
Sept	76.5	95.6	0.09	0.09	0.07	0.10	0.10	0.06	0.04	0.03	0.04	0.21	0.24	0.12	$1.05*10^5$	$1.03*10^5$	1
Oct	72.2	73.8	0.08	0.08	0.07	0.10	0.09	0.07	0.03	0.03	0.04	0.2	0.21	0.13	$3.94*10^5$	$4.41*10^5$	0.9
Nov	73.8	71.8	0.09	0.08	0.07	0.10	0.10	0.07	0.03	0.03	0.04	0.21	0.21	0.12	$9.10*10^5$	$9.83*10^5$	0.9
Dec	73.8	72.5	0.08	0.08	0.06	0.09	0.09	0.05	0.03	0.03	0.04	0.20	0.20	0.09	$10.10*10^5$	$11.20*10^5$	0.9

3.3.2.3 Phosphorus concentrations in the stream – risk of exceeding WFD standards

For a speedy evaluation of the P loss risk, in-stream P concentrations were discretized according to the Environmental Quality Standard (EQS) for both models and evaluated against similarly discretised lognormal distribution fitted to the observed in-stream TRP. The EQS was classified as good (between 0 and 0.035 mg l^{-1}) and bad (above 0.035 mg l^{-1}), as 0.035 mg l^{-1} is the phosphate threshold established in Ireland to comply with the Water Framework Directive (European Communities Environmental Objectives (Surface Waters) Regulations, 2009). The comparison was done by censoring the concentrations for the instrument's limit of detection (0.01 – 5.00 mg l^{-1}). Overall, both models show a repartition good/bad threshold close to 40/60 % (data not shown), however, that is lower than the monthly EQS in the distribution fitted to the observations. The fitted observations agree with Mellander et al., (2022), who also showed that the probability of exceeding the EQS in this catchment was 93.7% of the time (data from 2010 to 2020). This discrepancy may be explained by the model's predicted TRP concentration distribution's inherent shape, which was left-skewed in comparison to the observed data, and by the censoring process, which might have caused a shift of the distribution towards 0.01 mg l^{-1}.

3.3.3 Model strengths and limitations

We designed a BBN to describe and calculate TRP losses at the catchment outlet in a grassland-dominated Irish agricultural catchment. As compared to the steady-state probabilistic conceptual catchment model of P pollution risk by Glendell et al., (2022), the present model was parameterized using high-resolution datasets, including seven years of daily turbidity (NTU) and discharge (m^3) data at the catchment outlet, average soil Morgan P at field scale, and average measured farmyard size (instead of using a proxy of size). Using high-resolution turbidity data to calculate sediment losses at catchment outlet simplified the representation of erosion processes, thus avoiding assumptions regarding erosion rates, delivery, and the contribution of agricultural drains. Furthermore, the model was calibrated using seven years of daily observed TRP concentrations.

Model performance in terms of percentage bias (76-85% depending on which model version) was close to the 50% acceptable range recommended by Glendell et al., (2022), and appears small, given the small

concentration values being simulated. Additionally, in terms of inter-quantile ranges, this BBN's performance approximates that of Glendell et al., (2022) BBN in the best performing catchments (Linkwood, Rough, and Lunan catchments) but is better constrained than the previous study's model in worse-performing catchments.

We offer an overview of the model assumption and subsequent potential limitations that we deem relevant in Table 3.5, highlighting several research gaps around P modelling in agricultural catchments. Specifically, there is still uncertainty around point sources, where weak priors from the literature were introduced due to a lack of monitoring data, as well as a simplification of soil P sources (Morgan P), which, albeit measured at high spatial resolution, were represented at discrete levels (indexes) used for monitoring, which may lead to loss of information. Table 3.5 also introduces the lack of in-stream biological P uptake, a process that could be significant in spring and summer, and could improve the model's representation of reality (Jackson-Blake et al., 2015). Lastly, a future enhancement to this study would be the use of a sensitivity analysis, which would improve understanding of which variables contribute the most to P losses at the catchment outlet. We note that the current method to implement a sensitivity analysis in GeNIe is only available for discrete BBNs. Discretization leads to a loss of information (Landuyt et al., 2013) and makes the sensitivity analysis dependent on the discretization method. In our case, a discretized network would not allow the calculation of quantiles from the model predictions for comparison with those from the observations, countering the utility of the high-frequency dataset used here. Thus, further work is required to implement a suitable sensitivity analysis methodology.

Table 3.5 Model assumptions, limitations, and strengths.

Model assumptions	Consequences
Due to a lack of data, in-stream P removal by biota or sediment absorption is not represented.	In-stream P concentrations may be overestimated. However, these processes are secondary, especially considering the extreme flashiness of this catchment.
The main soil P source is spatially available at field resolution; however, the "Morgan P" node was implemented using the categorical classification used in field monitoring.	The categorical variable "Morgan P" can be used for testing management scenarios, however, discretization can lead to loss of information and impact decision making (Landuyt et al., 2013; Nojavan et al., 2017).
Amount of WEP transported to stream "Predicted Dissolved P Concentration" based on the equation for the closed period only, from the 15th of October to the 12th of January, when farmers are forbidden from spreading fertilizer on land in Ireland (Thomas et al., 2016b). The equation is applied to all months, and negative values are substituted with zeroes (see Table 3.1).	25% of the simulated values of this variable were zeroes, which probably skewed the in-stream concentration posterior distribution as discussed in section 3.2.1. This could be a contributing factor in the masking of seasonality in the model.
Experts noted that the septic tanks were modelled as a surface process, although soil risk classes have been included (Glendell et al., 2021), see variable "Soil risk factor" in section 3.2.4.	Might be underestimating P losses from STs.
P concentrations in septic tanks after primary or secondary treatment are based on (optimistic) Scottish EPA guidelines of Total P concentration reduction (Brownlie et al., 2014) even though the objective of the modelling was TRP.	There is uncertainty surrounding the actual TP/ TRP concentration in a septic tank after primary or secondary treatment, and therefore more data is needed for this model compartment, as well as sensitivity testing.
Septic tanks were assumed to be working, no hypothesis was made regarding failure.	Might be underestimating P losses from STs.
There is no measured data for septic tank P concentration or loads, thus each month the load from septic tanks "Realised total load" is the same, as it is not dependent on discharge (Q).	Septic tank loads are not expected to vary seasonally; therefore, the model could be representing the domestic wastewater systems well, however, this could be one of the factors masking any seasonality in the model. However, septic tank loads have temporal patterns too, and are considered to be an important source of nutrients during spring and summer (Withers et al., 2014).
P concentrations from farmyards are modelled according to literature, however Moloney et al., (2020) found higher concentrations of TP in farmyard drains than that found by Harrison et al., (2019) (about 37 times).	Farmyard losses in the catchment cannot be estimated, and the uncertainty around these losses in the literature is very high, thus the model may be under or overestimating these losses. Further data collection is needed to test these assumptions.
The hydrology compartment, and consequently the rest of the model, was set up at a monthly time step.	This allows the integration of both sparse and high-resolution datasets, as well as the chance for future evaluation of management actions and mitigation measures. This also means that the model does not represent events and hot moments, which usually represent the larger contribution of P losses in a catchment, with climate change expected to increase their contribution (Ockenden et al., 2016).
Both models are calibrated and validated against daily averages of TRP concentration. The daily resolution data may not represent the full variability of the in-stream concentrations (statistics on the two datasets are shown in Table 3.3).	The model appears to simulate higher TRP concentrations in the upper quartiles than the observations (Table 2), but these may be realistic if compared against the sub-hourly dataset.

3.4 Conclusions

In this study, we combined different methodologies for using high-frequency water quality datasets to inform the priors of a BBN aimed at modelling P losses in Irish agricultural catchments. Different sources of P were introduced in the modelling exercise in a step-wise fashion, thus improving the model predictive ability and testing the model structural uncertainty. The two developed BBNs were able to

predict the mean and median P concentrations in the stream well overall, with some limitations apparent in performance at the monthly time-step. However, the models' predictions presented wider distributions than the observations, which was noted in a similar work, and remains a property of this stochastic modelling approach. The BBN modelling approach allowed the inclusion of all the known P sources in the agricultural catchment, including farmyards, which is rare in P modelling, and septic tanks, which are often overlooked as P sources. In addition, this study directly reported on experts' role and selection as an effort to increase transparency. The probabilistic modelling highlighted the need for further targeted data collection to fill important knowledge gaps, even in a catchment with state-of-the-art high-resolution and long-term monitoring, such as the one used in this study. Furthermore, the work informed future research steps, which will include testing of model transferability, the influence of in-stream P cycling (i.e., estimation of removal by biota, and/or sediment uptake) on model performance, and understanding of P losses under future climate change scenarios

4. Transferability of a Bayesian Belief Network across diverse agricultural catchments using high-frequency hydrochemistry and land management data

To avoid repetitions, this Chapter has been redrafted from Negri, C., Schurch, N., Wade, A.J., Mellander, P.-E., Stutter, M., Bowes, M.J., Mzyece, C.C., Glendell, M., 2024. Transferability of a Bayesian Belief Network across diverse agricultural catchments using high-frequency hydrochemistry and land management data. Science of The Total Environment 949, 174926. https://doi.org/10.1016/j.scitotenv.2024.174926, published under a Creative Commons License (https://creativecommons.org/licenses/by/4.0/), and the Supplementary Materials can be found in Chapter 9.

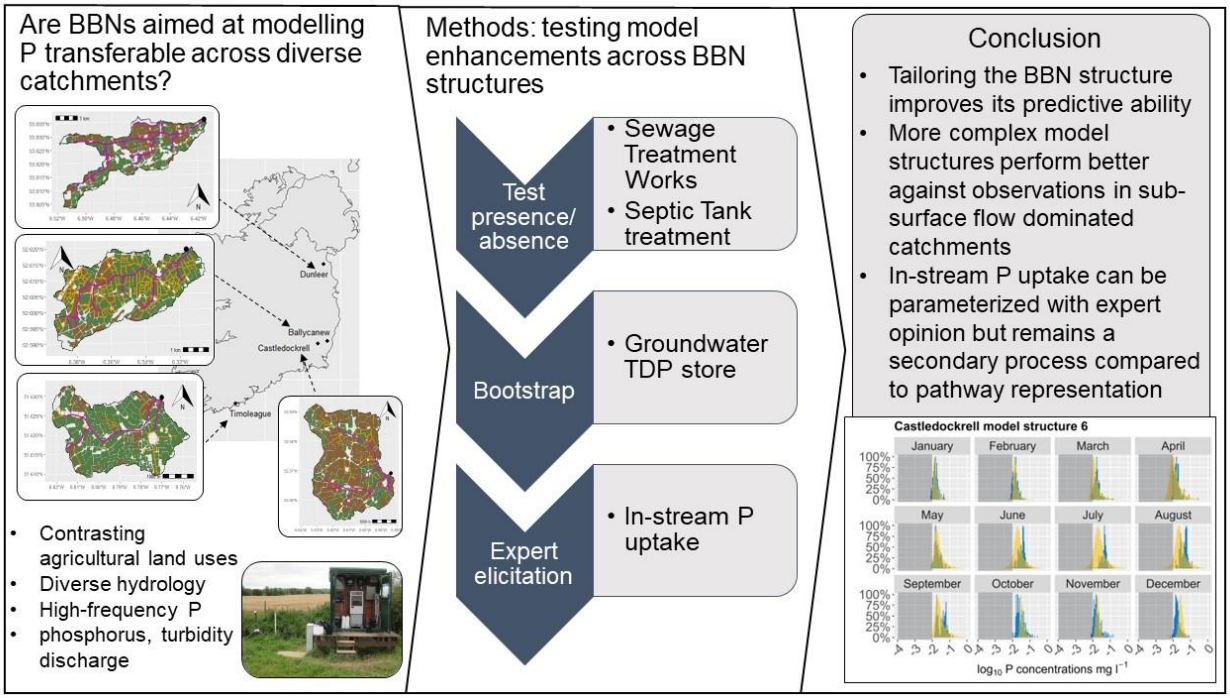

Figure 4.1 Graphical abstract summarizing the findings in Chapter 4, as submitted to the journal.

Abstract

Biogeochemical catchment models are often developed for a single catchment and, as a result, often generalize poorly beyond this. Evaluating their transferability is an important step in improving their predictive power and application range. We assess the transferability of a recently developed Bayesian Belief Network (BBN) that simulated monthly stream phosphorus (P) concentrations in a poorly-drained grassland catchment through application to three further catchments with different hydrological regimes and agricultural land uses. In all catchments, flow and turbidity were measured sub-hourly from 2009 to 2016 and supplemented with 400 – 500 soil P test measurements. In addition to a previously parameterized BBN, five further model structures were implemented to incorporate in a stepwise way: in-stream P removal using expert elicitation, additional groundwater P stores and delivery, and the presence or absence of septic tank treatment, and, in one case, Sewage Treatment Works. Model performance was tested through comparison of predicted and observed total reactive P (TRP) concentrations and percentage bias (PBIAS). The original BBN accurately simulated the absolute values of observed flow and TRP concentrations in the poorly and moderately drained catchments (albeit with poor apparent percentage bias scores; 76%≤PBIAS≤94%) irrespective of the dominant land use but performed less well in the groundwater-dominated catchments. However, including groundwater total dissolved P (TDP) and Sewage Treatment Works (STWs) inputs, and in-stream P uptake improved model performance (-5%≤PBIAS≤18%). A sensitivity analysis identified redundant variables further helping to streamline the model applications. An enhanced BBN model capable for wider application and generalisation resulted.

4.1 Introduction

Generalised scientific theories are the most powerful and ideally, water quality models should be applicable to all catchments. A transferable model will likely have greater predictive power and utility, greater confidence that the model performs well for the right reasons, and an ability to help inform data collection for the model's application (Hatum et al., 2022; Mieleitner and Reichert, 2006; Schuwirth et al., 2019).

Testing model transferability is therefore important. Hatum et al., (2022) demonstrated that transferring a model across different seagrass ecosystems, using expert elicitation to support model formulation, enabled forecasting and decision-making. To date, only one Bayesian Belief Network (BBN) aimed at modelling water quality has been tested across multiple catchments. Glendell et al., (2022), tested a hybrid BBN (including both discrete and continuous variables) to predict stream P concentrations and applied the model to seven Scottish catchments. The outcomes demonstrated wider ranges in the BBN predictions than in the observations and, given that inadequate water quality data constrains the calibration and validation of P models (Drohan et al., 2019), the use of high-frequency data was suggested as a means to reduce model predictive uncertainty (Glendell et al. 2022).

Phosphorus retention in river catchments results from a combination of biological, physical, and chemical processes (Withers and Jarvie, 2008) and there is uncertainty around the retention rate in different catchments due to variations in P uptake and release by plants, adsorption to and desorption from sediment, co-precipitation, dissolution, and advection. Both biotic and abiotic in-stream P uptake can be significant, especially during low-flows and effluent exposure (Stutter et al., 2010). Its inclusion could improve process representation, and therefore transferability, in process-based semi-distributed P models (Jackson-Blake et al., 2015) and stochastic P models (Negri et al., 2024a).

Mechanistic P models typically include processes such as calcite-P co-precipitation, sorption and desorption to and from suspended sediments, P exchange between the pore water and the water column, P entering the reach from upstream or Sewage Treatment Works (STWs), and epiphyte uptake (for example, the INCA-P model, (Jackson-Blake et al., 2016; Wade et al., 2002)). Similarly, stochastic P models include estimating numerous P sources, their transport through the land-water continuum, and delivery to surface waters (for example, Glendell et al., 2022; Igras and Creed, 2020; Neumann et al., 2023). However, some BBNs modelling P concentrations in the stream lack representation of processes such as stream P retention, as well as groundwater P stores (Glendell et al. 2022, Negri et al., 2024a).

The observational evidence to quantify in-stream retention processes is difficult to find in a single catchment, stream, or study area, therefore gathering data and comparing across diverse catchments

with different P pressures strengthens findings. Expert elicitation (acquiring experts' opinions using formal protocols, e.g., Krueger et al., (2012) is a route to help model parameterization without having to set up costly site-specific experiments and is often used to inform on model parameter uncertainty (O'Hagan, 2019).

The overall study aim was to test the transferability of a recently developed BBN (Negri et al., 2024a) in a grassland catchment in Ireland, and make enhancements as necessary. The aim was addressed through three research objectives: application of the BBN to three additional catchments in Ireland with performance assessment using daily total reactive P (TRP) observations; addition of in-stream P removal processes using expert elicitation; and the assessment of whether step-wise addition of in-stream P uptake, groundwater dissolved P concentration, and the presence or absence of septic tank treatment or Sewage Treatment Works improved model performance and transferability (in terms of reduced percentage bias across all four catchments).

4.2 Study Areas

This study focuses on four (< 1200 ha) agricultural catchments in the east and south of Ireland: Timoleague, Ballycanew, Castledockrell, and Dunleer, that are monitored by the Agricultural catchments Programme (ACP) from Teagasc; a programme created to monitor the effectiveness of Ireland's National Action Programme under the European Union Nitrates Directive (Wall et al., 2011). These catchments have different agricultural land uses and contrasting hydrology. The catchments were chosen because agriculture is the only significant anthropogenic pressure (housing density is low and domestic waste is treated with septic tanks) (Jordan et al., 2012). The location of the four catchments is shown in Chapter 2 (Figure 2.2) and further information about the catchments is given in Negri and Mellander, (2024) and Chapter 2.

4.3 Methods

4.3.1 BBN parameterization

We developed a catchment-specific Bayesian Belief Network that simulates flow-weighted P concentrations and parameterized the model using high-frequency data from the Ballycanew catchment (Negri et al., 2024a). The BBN was parameterized with high-frequency discharge and turbidity data (collected every 10 minutes and summarized at daily time-step), as well as 515 (Timoleague), 406 (Ballycanew), 408 (Castledockrell), and 392 (Dunleer) samples of soil Morgan P (McDonald et al., 2019; Thomas et al., 2016b), and calibrated against high- frequency TRP concentrations (Mellander et al., 2012). In this study, we test the BBN transferability by parametrizing the model for the first time for three further (8-12 km^2) Irish ACP catchments. The initial BBN parametrization for each catchment was identical to that presented in Negri et al., (2024a) and referred to here as "Structure 1". Structures are the graphical definitions of BBNs, also referred to as Directed Acyclic Graphs (DAGs) (Henderson and Pollino, 2010) encoding the causal (in)dependencies between variables (Aguilera et al., 2011). In this case, the structure represents the BBN's P inputs, processes, pathways, and outputs, describing their relationships. When discussing uncertainty in environmental models, the word structure indicates the conceptual model (Refsgaard et al., 2006). Where the information was available the BBN variables were parameterized with catchment-specific datasets (these are specified in the Supplementary Information). However, catchment-specific parametrization was not possible for the following nodes (i.e., BBN variables): "Direct Discharge", "Septic Tank Treatment", "Sediment Water Soluble P", "Predicted Dissolved P concentration" (i.e., P that is dissolved from the soil matrix into the stream), and the total number of septic tanks in the catchment needed to calculate the total septic tank load. A detailed description of these nodes is given in Table 4.1. Additionally, data was not available for the "Septic Tank Treatment" node for Timoleague and Dunleer, and therefore an additional BBN structure was tested where the treatment was not implemented, and the distribution of P concentration across the catchment's septic tanks was set up as equal to the "Unknown treatment" option (Structure 3). For the Timoleague and Castledockrell catchments, further model structure implementations (Structure 4, 5, 6)

saw the addition of the node "Groundwater Dissolved P Concentration mg l^{-1}" to describe the groundwater total dissolved phosphorus (TDP) concentration contributing to the total in-stream TRP concentration at catchment outlet (the details of Structure 2 will be introduced later on in this section). This was done with the same bootstrapping methodology that was applied to observed in-stream TRP concentrations in Negri et al., (2024a), here applied to monthly samples of groundwater total dissolved P (TDP, 2009-2016) monitored in multi-level wells described in Mellander et al., (2016). An assumption was made that the wells near the stream (less than 40 m from the stream) contribute the most to stream TRP (Mellander et al., 2016), hence we only used data from these wells for the parameterization. For all catchments, a model structure including the in-stream P uptake derived in the expert elicitation workshop was parameterized, and labelled Structure 2 for the Ballycanew and Dunleer catchments, Structure 5 for the Timoleague catchment, and Structure 5 and 6 for the Castledockrell catchment. For the Castledockrell catchment the Sewage Treatment Works loads were included in the finalized BBN labelled Structure 6. This was done by incorporating the P concentration (mg l^{-1}) after tertiary treatment (Truncated Normal (μ= 1.44; σ= 1.61, (Glendell et al., 2022), in this case truncated at 0), and the design size (130 people) found through the Irish Environmental Protection Agency (EPA) data. This is consistent with the fact that STWs with tertiary treatment are required to keep the orthophosphate concentration below 2 mg l^{-1} for their effluent discharge (Fitzsimons et al., 2016). The model structure and the datasets used for the finalized parametrization are specified for each catchment in the Supplementary Information, and a summary of each Structure's specifications is given in Table 4.3.

Table 4.1 Variables for which catchment-specific data was unavailable in the Timoleague, Castledockrell, and Dunleer catchments. These nodes were chosen for a preliminary sensitivity analysis to understand their effects on the targeted P concentration and inform model transferability.

Node	Septic Tank Treatment	Direct Discharge	Number of Septic Tanks	Sediment Water Soluble P (WSP) [mg kg^{-1}]	Predicted Dissolved P Concentration [mg l^{-1}]
Description	Probability of having "unknown", "primary" or "secondary" treatment of the effluent in a septic tank.	Probability of ST discharging directly into the stream.	Septic tanks within catchment boundary.	Describes the phosphorus released from the sediments into the stream. Defined as the best fitting distribution, fitted with the *SHELF* R package version 1.8.0 (Oakley, 2020) to observed Water Extractable P in the catchment sediments (Shore et al., 2016) when data was available.	Describes the Water Extractable Phosphorus (WEP) dissolved from the soil matrix into the stream. Defined with the linear model: Predicted Dissolved P = β(WEP)-α, where β =0.08, α =0.158, derived from (Thomas et al., 2016b), whereby WEP stands for Water Extractable P. An assumption is made that when the linear model yields a negative value, that is resampled as a zero. This equation is not catchment specific.
Timoleague	Unavailable.	As Ballycanew.	As Ballycanew.	As Ballycanew.	Same everywhere.
Ballycanew	Probabilities based on a survey conducted within WaterProtect, a research project supported by the European Union research and innovation funding programme Horizon 2020 [grant no. 727450]. Probabilities are reported in Negri et al., (2024a)	Assumed.	Available from data (88 tanks).	Defined as a Lognormal (base e) distribution (μ=-0.9, σ=1), fitted with the *SHELF* R package (version 1.8.0, Oakley, 2020) to observed Water Extractable P in the catchment sediments (Shore et al., 2016).	Same everywhere.
Castledockrell	Probabilities based on a survey conducted within WaterProtect, a research project supported by the European Union research and innovation funding programme Horizon 2020 [grant no. 727450].	As Ballycanew.	As Ballycanew.	Defined as a Gamma distribution (k=1.03, ~~ɵ~~=0.44).fitted with the *SHELF* R package (version 1.8.0, Oakley, 2020) to observed Water Extractable P in the catchment sediments (Shore et al., 2016).	Same everywhere.
Dunleer	Unavailable.	As Ballycanew.	As Ballycanew.	As Ballycanew.	Same everywhere.

4.3.2 In-stream P uptake

P uptake is complex with multiple components based on physical, chemical, and biological processes (Withers and Jarvie, 2008). Whilst uptake rates might be available for specific components (e.g., algal uptake, large plant uptake, sediment uptake), this study focusses on providing an overall effect from the combined processes in each catchment for each season via expert elicitation because the necessary data to quantify uptake rates was not available for the catchments. Here P uptake was framed as the percentage (%) of in-stream P that is removed by both biotic and abiotic uptake. A simplified version of the methodology presented in Mzyece et al., (2024) for expert elicitation was used to determine P uptake for the four catchments for four seasons. We selected 6 key papers describing UK-led experiments on this topic (Bowes et al., 2016; Jarvie et al., 2002; Stutter et al., 2021b, 2010; Wade et al., 2001; Withers and Jarvie, 2008), and invited four authors of these papers to contribute to our elicitation exercise as experts who have published on the topic of P uptake in rivers. Three accepted, one declined. The elicitation process then comprised of three steps: 1) The Sheffield Elicitation Framework (SHELF) e-learning course for experts (Gosling, 2018), which the experts took on their own, 2) a preliminary exercise where the experts were asked to complete an elicitation table per catchment, providing their personal judgement on the two tertiles, T1 and T2, (33^{th} and 66^{th} quantiles) and the median M (50^{th} quantile) percentage in-stream P uptake for each season. Initially, the upper limit of the distribution was fixed at 100% removal and the lower limit at 0% removal. To aid the experts with their judgements, supporting documentation containing both a summary of the literature on in-stream P removal and information on the four catchments, was provided to the experts ahead of time (published in an evidence dossier in Negri and Mellander, 2024). For the scope of this elicitation, we aimed to quantify global uptake (see, for example, the quantities in bold under the column 'P retained' in Table 1 Negri and Mellander, (2024)) and asked the experts to provide judgement on what was the likely P uptake based on their experience of other river systems. 3) Preliminary prior Normal distributions were fitted with the *SHELF* R package version 1.8.0 (Oakley, 2020) to the elicited distributions at Step 2 and presented to the experts during the workshop. In the workshop, the experts were asked to discuss the preliminary distributions and to agree on a single consensus distribution per

season per catchment. Based on what emerged during the discussion, and to facilitate consensus, distributions were re-fitted and plotted in real time for the experts to examine. The final consensus distributions were then used to parameterize the "In-stream P uptake" node in the BBNs, and the updated BBN was subsequently tested against in-stream TRP observations.

4.3.3 Sensitivity Analysis

Sensitivity analysis was done to understand the effect of using non-catchment specific data on model transferability for the variables listed in Table 4.1. For direct discharge presence (0-100%) or absence (0-100%), the relative fraction of direct discharge presence/absence was varied in 5% steps, with the probabilities for the two categories summing to 100%. To assess the impact of number of septic tanks within each catchment boundary on in-stream P concentration, increases of two septic tanks per step were applied, ranging from 30 to 150 septic tanks. This range assumed 2.4 people per household (and therefore per tank) for these scarcely populated catchments. To understand the effects of varying the Water Soluble P (WSP, described in Table 4.1) we applied a stepwise variation (0.1 increments) on the parameters of the Lognormal distribution used in the Ballycanew catchment: the mean ($-2 \leq \mu \leq 2$) and, separately, the same variation on the standard deviation ($0.1 \leq \sigma \leq 2$). The Gamma distribution has two parameters (shape, k, and scale, θ) that together control the shape of the distribution. These parameters do not correspond directly to physical values (unlike, for example, the mean value of a Normal or Poisson distribution) and are always >0. Here we stepped through these parameters in increments of 0.1 over the range $0.1 \leq k \leq 2$ and 0.005 increments over the range $0.05 \leq \theta \leq 1$ for the WSP node parameterized for Castledockrell. For the "Predicted Dissolved P Concentration, 0.02 stepwise increases were applied to the β parameter ($-1 \leq \beta \leq 1$), and 0.005 stepwise increases were applied to the α ($0 \leq \alpha \leq 0.2$). The sensitivity analysis was conducted independently for each parameter in each catchment, (no nodes were varied simultaneously) and carried out only for the finalized and best performing model structure in each catchment (specifically, Structure 5 for Timoleague, Structure 6 for Castledockrell, and Structure 2 for Dunleer). The analysis was performed using *rSMILE* version 2.0.10 (BayesFusion, 2019a), an API engine available in R which can perform the same Bayesian inference operations performed by GeNIe Modeler (BayesFusion, 2019b), the software used to design the BBNs. In each catchment, the parameter

variations were applied to predict the TRP concentration (in the model, the target node is called "In-stream P concentration [mg l^{-1}]" and it describes the variable of interest). The effects of changing the input parameters on the full distributions was assessed visually by comparison against the distribution from "simulation 0" (the initial BBN parameterization). The effects of the presence of the nodes "Septic Tank Treatment", "Groundwater Dissolved P Concentration mg l^{-1}", the nodes relative to in-stream P uptake, and those pertaining to the STWs in Castledockrell were tested by comparing distributions derived from different model structures to those obtained from the original BBN.

4.3.4 Model evaluation

The model structures were evaluated by comparing the predicted TRP concentrations with the available observed TRP concentrations (available as daily mean, mg l^{-1}) (2009-10-01 to 2016-12-31) by: calculating percentage bias (PBIAS) in the R package *hydroGOF* version 0.4-0 (Zambrano-Bigiarini, 2020), plotting and visually comparing the full posterior distributions, and comparing median concentrations. PBIAS calculation and visual assessment are recommended when modelling P in catchments with a prevalence of diffuse sources, as in these instances models struggle to produce good Nash-Sutcliffe statistics (Jackson-Blake et al., 2015). In addition, for the model version containing the "In-stream P removal", the Normal distribution allows for negative concentrations due to the potential for release of in-stream P (considered to be plausible by the expert elicitation). For the purposes of model evaluation these were resampled into zeros prior to analysis.

4.4 Results and Discussion

4.4.1 BBN Parameterization

The results of the preliminary BBN parametrization are shown in Figure 4.3, where the density plots from all model structures are shown against the distribution fitted to the observations. When comparing the TRP distributions and boxplots of Structure 1 (in green) against the observed (light brown), the figure shows that the model performs well for Ballycanew and Dunleer, and less well for the Timoleague and Castledockrell catchments. For Timoleague and Castledockrell, the initial

parameterization (Structure 1) overpredicts the stream P concentration by 65-82% (data not shown), which is a consequence of the parameterization being tailored for a surface-driven catchment instead of a groundwater-driven one. Specific details of the each of the models' performances are discussed in section 4.4.4. The state-of-the-art high-resolution and long-term monitoring data available in these catchments could also facilitate other model structures besides the ones considered in this study. For example, soil chemistry data could be leveraged to improve process representation for the groundwater-driven catchments, because the presence of aluminium-rich or iron-rich soils is known to impact P solubilization and transfer to the groundwater table (Mellander et al., 2016).

4.4.2 In-stream P uptake

During elicitation, consensus was reached by initially focusing on the first catchment (Timoleague), first comparing summer and winter, then spring and autumn. Consensus about the other three catchments was then reached by comparison with the first. For wintertime, the experts agreed to use -100% as the lower limit which represents complete sediment P release into the water column and biotic uptake close to zero. For wintertime in Timoleague, averaged values (tertiles and median) and fitted a Normal distribution were used (Figure 4.2). For summertime in Timoleague, expert consensus had the probability density centred on a 43% removal rate, and this was the same for autumn and spring. For Ballycanew, the experts decided to reduce P removal by 30%, due to the high flashiness of the catchment. The experts considered the catchment P saturation and loading to be the most influential factors in determining in-stream uptake, catchment flashiness was considered less important. As a result, the mean P uptake was similar across catchments (Table 4.2). The consensus also reflected that, even though Castledockrell is less flashy than Ballycanew, the two catchments have similar P uptake because high loading in Castledockrell due to a Sewage Treatment Works and septic tanks. An exception is made for Castledockrell in the wintertime, with tertiles and median values similar to Timoleague, and therefore the same parameterization (Table 4.2). For Dunleer, the wintertime uptake was considered very low, then the rest of the seasons were considered comparable to Timoleague. Overall, the experts had greater confidence estimating P removal in the colder seasons (winter and autumn), than in the warmer ones, where the distributions are wider and more uncertain (Figure 4.2).

Furthermore, the experts suggested that visual aids such as photos of the river corridor could assist in estimating uptake, allowing the approximate width and depth of ditches and rivers to be estimated, as well as the presence of submerged and emergent vegetation and algae to be assessed. This is especially important because increased riparian vegetation and algae can lead to decreased dissolved P concentrations (Bowes et al., 2016; Chase et al., 2016). The distributions obtained were used in each catchment model to calculate the in-stream P load reduction (Equation 4.1):

Equation 4.1

$$r = (1 - Normal\ (\mu_s; \sigma_s)) * L$$

where r is the in-stream reduced load, L the total catchment load, and N $(\mu_s; \sigma_s)$ is a Normal distribution with a seasonal dependent mean and standard deviation (specified in Table 4.2), and the loads are expressed in T month^{-1}. In the BBN, the seasonal monthly distributions are child nodes of a deterministic node termed "Season", which indicates the meteorological seasons.

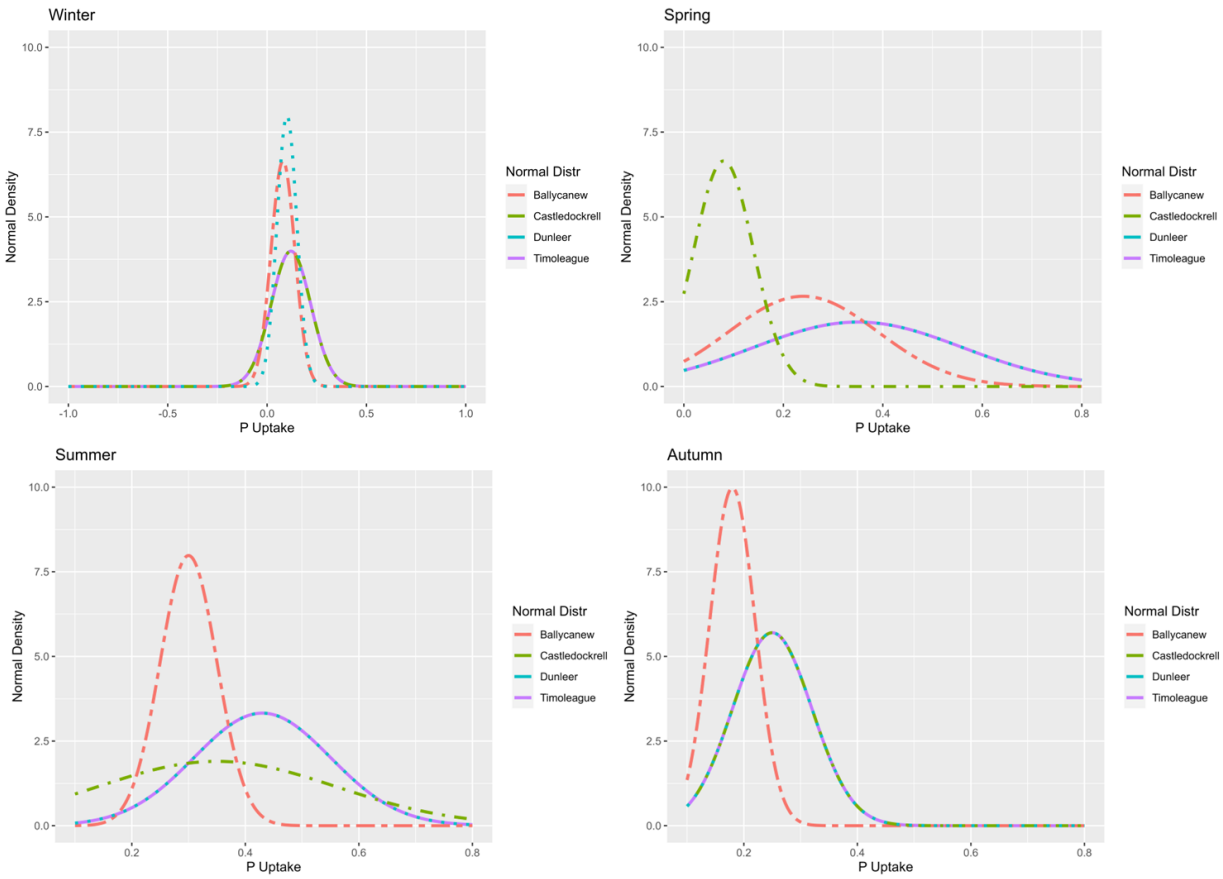

Figure 4.2 Consensus Normal distributions grouped by season. The y axis shows the probability density function, the x axis is the agreed upon plausible range for in-stream P uptake (%). Different colours show the distributions for each catchment. For the winter season, Castledockrell and Timoleague are overlapping; for spring and summer, Timoleague and Dunleer are overlapping; and for the autumn, Timoleague, Castledockrell, and Dunleer are overlapping.

Table 4.2 Characteristics of seasonal P uptake as discussed by the experts during the workshop, including re-defined lower and upper limits of uptake, and the elicited parameters for the Normal distributions. A mean (μ) of 0.10 corresponds to 10% mean uptake.

	% P uptake		justification	Normal distributions parameters fitted from consensus							
				Timoleague		Ballycanew		Castledockrell		Dunleer	
	lower limit consensus	upper limit consensus		μ	σ	μ	σ	μ	σ	μ	σ
Winter	-100	+100	To describe the fact that there can be release of P (-100%) rather than uptake (+100%)	0.12	0.10	0.08	0.06	0.12	0.10	0.10	0.05
Spring	0	80	Uptake can never be 100%, but the experts agree on absent or negligible P release	0.35	0.21	0.24	0.15	0.08	0.06	0.35	0.21
Summer	10	80	Biological uptake always present, so lower limit cannot be 0%	0.43	0.12	0.30	0.05	0.35	0.21	0.43	0.12
Autumn	0	65	Uptake can never be 100% and is lower than in spring, but the experts agree on absent or negligible P release	0.25	0.07	0.18	0.04	0.25	0.07	0.25	0.07

4.4.3 Sensitivity Analysis

The sensitivity analysis showed that the three tested BBNs are not sensitive to changes in the variables representing septic tank "Direct Discharge" (% of tanks that discharge the effluent directly into the stream), and "Sediment Water Soluble P" (that is, P released into the stream by sediments). One BBN showed sensitivity to changes in the β parameter used for the node "Predicted Dissolved P concentration". Details of the sensitivity to the Predicted Dissolved P concentration" node are shown for one catchment (Dunleer) in Figure 9.2. This shows the $\log_{10}$(TRP) concentration boxplot for each parameter value against the "simulation 0" (in light green) overlayed with a sample of the full distribution plotted as dots. The equation in the node "Predicted Dissolved P concentration" was derived from Thomas et al., (2016b), and is an aggregated result of catchment-specific regression models, which were not available at the time of model parametrization. It would be instructive to reparametrize the BBN if/when these individual models become available, and to compare the results of a corresponding sensitivity analysis on this new model structure with these results.

Sensitivity analysis is a pivotal component of model calibration and design, however, methodologies for conducting it for hybrid BBNs aren't readily accessible in the software used for BBN parameterization or in R packages, and therefore require bespoke coding for implementation. For example, Glendell et al., (2022), conducted a sensitivity analysis on a discretized version of their hybrid

network, which causes loss of information (Uusitalo, 2007), and makes the BBN sensitive to the chosen discretization. Similarly, Piffady et al., (2021) tested the sensitivity of a discretized BBN by varying nodes deemed important across a reasonable range. Here we provided a preliminary approach to the sensitivity analysis of a hybrid BBN without triggering discretization.

4.4.4 Model evaluation

Results of the model evaluation are shown in Figure 4.3, which shows boxplots with the median, interquartile range with the whiskers extending to the highest and lowest datapoints, and a representative selection of datapoints, from ten-thousand simulated realizations of each BBN structure tested. These are summarized in Table 4.3, where predicted $\log_{10}$ TRP concentrations are compared to the observations (daily time-step, data from 2009 to 2016). In the surface-drained catchments (Figure 4.3, Ballycanew and Dunleer, right-hand side), the distribution of $\log_{10}$(TRP) concentrations predicted by the BBN models is not sensitive to the structure of the BBN. The BBN parameterized in Negri et al., (2024a) (Structure 1) can reproduce the mean and median observed P concentrations in the Ballycanew and Dunleer catchments. For Ballycanew, the percentage bias is within acceptable ranges (close to the 50% departure from observations or less, shown in Table 4.3). For Dunleer, a bias of 94% is still considered acceptable because the mean predicted concentration was 0.11, whilst the observed was 0.10 mg l^{-1}. The addition of an in-stream P removal node improved the ability of the model to replicate the mean and median in-stream P concentration in these two catchments (Table 4.3, comparing Structure 1 and 2), by introducing a linear scaling factor. Further, the percentage bias in Dunleer went from 94% to 45% with the addition of removal, however, because the concentrations being predicted are small, small changes in their absolute values represent large changes in bias, therefore bias values should be looked at critically in context with mean TRP concentrations, as shown in Table 4.3. For the two groundwater-dominated catchments (Timoleague and Castledockrell), the introduction of groundwater TDP concentration (Structures 4, 5, and 6) improved the simulated TRP concentrations: in the final structure, the predicted median was the same as the observed, 0.05 (Timoleague) and 0.02 mg l^{-1} (Castledockrell). This could not be achieved in the Castledockrell catchment with a process-based model such as SimplyP

(Hawtree et al., 2023), even though the BBN and SimplyP deploy similar strategies to represent below-ground processes. An improvement in percentage bias (from 40% to -5%) is provided by the addition of in-stream P removal in the Timoleague catchment (also in Table 4.3, comparing Structure 4 and 5), however, the bias was already within the 50% departure from observations, which indicates that this remains a secondary process, at least if compared to correctly representing groundwater concentrations (Structure 4).

Knowledge of the type of septic tank treatment adopted (i.e., comparing Structure 1 to Structure 3), provides little to no advantage (concentrations remain unvaried), except for better representing the available datasets. Increasing the structural complexity of the BBN had the most impact in the Castledockrell catchment, where the percentage bias of posterior simulations has decreased more than twenty-fold (Table 4.3, comparing Structure 1 with Structure 6). To further demonstrate this, monthly predicted $\log_{10}$(TRP) concentrations (yellow bars) are plotted as histograms against daily observed $\log_{10}$(TRP) concentrations (blue bars, grouped by month) across all model structures developed for the Castledockrell catchment in Figure 4.4. This shows the progress made in adapting Structure 1 in this catchment (top histograms), where yellow and blue are not overlapping, up to the last model structure (Structure 6, bottom panel), which shows good correspondence between predicted and observed TRP concentrations. The addition of P removal had the added benefit of improving seasonality in the BBN predictions, which was not a behaviour that emerged in the first parameterization; however, the observations still show stronger seasonality patterns than the simulations. A summary table of these results is reported in the Supplementary Information, where, for each catchment, monthly predictions from the first versus the final model version are compared against the observations. Percentage bias shows that the final and best performing model in each catchment performs best in dry conditions (summer months). However, in Dunleer and Ballycanew, the model predicts the mean concentration better in winter than in summer. This is notable, as predicting P concentrations correctly in summer may be more relevant from the point of view of assessing ecological impacts in running waters than predicting them during the ecologically less active winter period. In the groundwater-dominated catchments, the final model is better constrained than in the runoff-dominated catchments (Ballycanew

and Dunleer), as evident when comparing the predicted upper (μ+σ) concentrations versus the observed in Table 8.5 of Supplementary Information. Table 4.5 shows both the observed and the marginal probabilities of Environmental Quality Standard of 0.035 mg l^{-1} (EQS) exceedance in each catchment and across two model structures. The Table shows that even though the models can work for two catchments and is improved by the inclusion of P removal, the model predicts a lower probability of exceeding the EQS than the observational data in the two P risky catchments (Ballycanew and Dunleer). Meanwhile, the prediction of EQS exceedance for the Timoleague catchment is either under- or over-predicting by 8%, depending on BBN model structure, while at Castledockrell, the prediction of exceedance for the final model is 10% lower than the observed. These findings suggest that the BBN may be best used as Decision Support Tool by calculating the quantiles of monthly predicted concentrations as seen in Negri et al., (2024a) or the monthly mean and upper and lower limits (μ±σ, as shown in the Supplementary) rather than as a discrete probability of EQS exceedance, due to the predicted distributions being wider and more skewed than the observations, also seen in Negri et al., (2024a).

Table 4.3 Overall results of the different BBN versions for the four catchments, concentrations (mg l^{-1}) outside the instrument limit of detection (0.01-5.00 mg l^{-1}) have been excluded from the analysis. Both observed and predicted TRP concentrations were log-transformed before calculating the statistics, and then converted back to normal values. A positive bias indicates overestimation. Abbreviations: ST septic tanks; GW TDP groundwater total dissolved phosphorus; STWs sewage treatment works; p.e. people equivalent.

			Structure 1	**Structure 2**	**Structure 3**	**Structure 4**	**Structure 5**	**Structure 6**	
			Negri et al., (2024a)	Negri et al., (2024a)+ in- stream removal (no ST treatment in Dunleer)	Negri et al., (2024a), no ST treatment	no ST treatment + GW TDP	no ST treatment + GW TDP + in-stream P removal	no ST treatment + GW TDP + in-stream P removal + STWs 130 p.e.	observations
Timoleague	**mean**		0.14	-	0.14	0.08	0.05	-	0.05
	lower limit (μ-1σ)		0.05	-	0.05	0.05	0.03	-	0.03
	upper limit (μ+1σ)		0.40	-	0.41	0.11	0.08	-	0.09
	median	**mg l^{-1}**	0.14	-	0.15	0.07	0.05	-	0.05
	5th quantile		0.02	-	0.02	0.05	0.03	-	0.02
	25th quantile		0.08	-	0.07	0.06	0.04	-	0.04
	75th quantile		0.21	-	0.21	0.09	0.08	-	0.08
	PBIAS	**%**	285	-	291	40	-5	-	-
Ballycanew	**mean**		0.08	0.07	-	-	-	-	0.06
	lower limit (μ-1σ)		0.03	0.03	-	-	-	-	0.03
	upper limit (μ+1σ)		0.21	0.17	-	-	-	-	0.11
	median	**mg l^{-1}**	0.10	0.08	-	-	-	-	0.06
	5th quantile		0.02	0.02	-	-	-	-	0.01
	25th quantile		0.05	0.04	-	-	-	-	0.04
	75th quantile		0.14	0.12	-	-	-	-	0.14
	PBIAS	**%**	80	49	-	-	-	-	-
Castledockrell	**mean**		0.11	-	0.10	0.03	0.02	0.02	0.02
	lower limit (μ-1σ)		0.04	-	0.04	0.01	0.01	0.01	0.01
	upper limit (μ+1σ)		0.29	-	0.29	0.05	0.04	0.05	0.04
	median	**mg l^{-1}**	0.13	-	0.13	0.02	0.02	0.02	0.02
	5th quantile		0.02	-	0.02	0.01	0.01	0.01	0.01
	25th quantile		0.07	-	0.06	0.02	0.01	0.02	0.02
	75th quantile		0.18	-	0.19	0.04	0.03	0.03	0.04
	PBIAS	**%**	445	-	453	34	12	18	-
Dunleer	**mean**		0.11	0.09	0.11	-	-	-	0.10
	lower limit (μ-1σ)		0.03	0.03	0.03	-	-	-	0.06
	upper limit (μ+1σ)		0.38	0.28	0.39	-	-	-	0.16
	median	**mg l^{-1}**	0.12	0.09	0.12	-	-	-	0.09
	5th quantile		0.01	0.01	0.01	-	-	-	0.05
	25th quantile		0.05	0.04	0.05	-	-	-	0.06
	75th quantile		0.27	0.20	0.28	-	-	-	0.14
	PBIAS	**%**	94	45	97	-	-	-	-

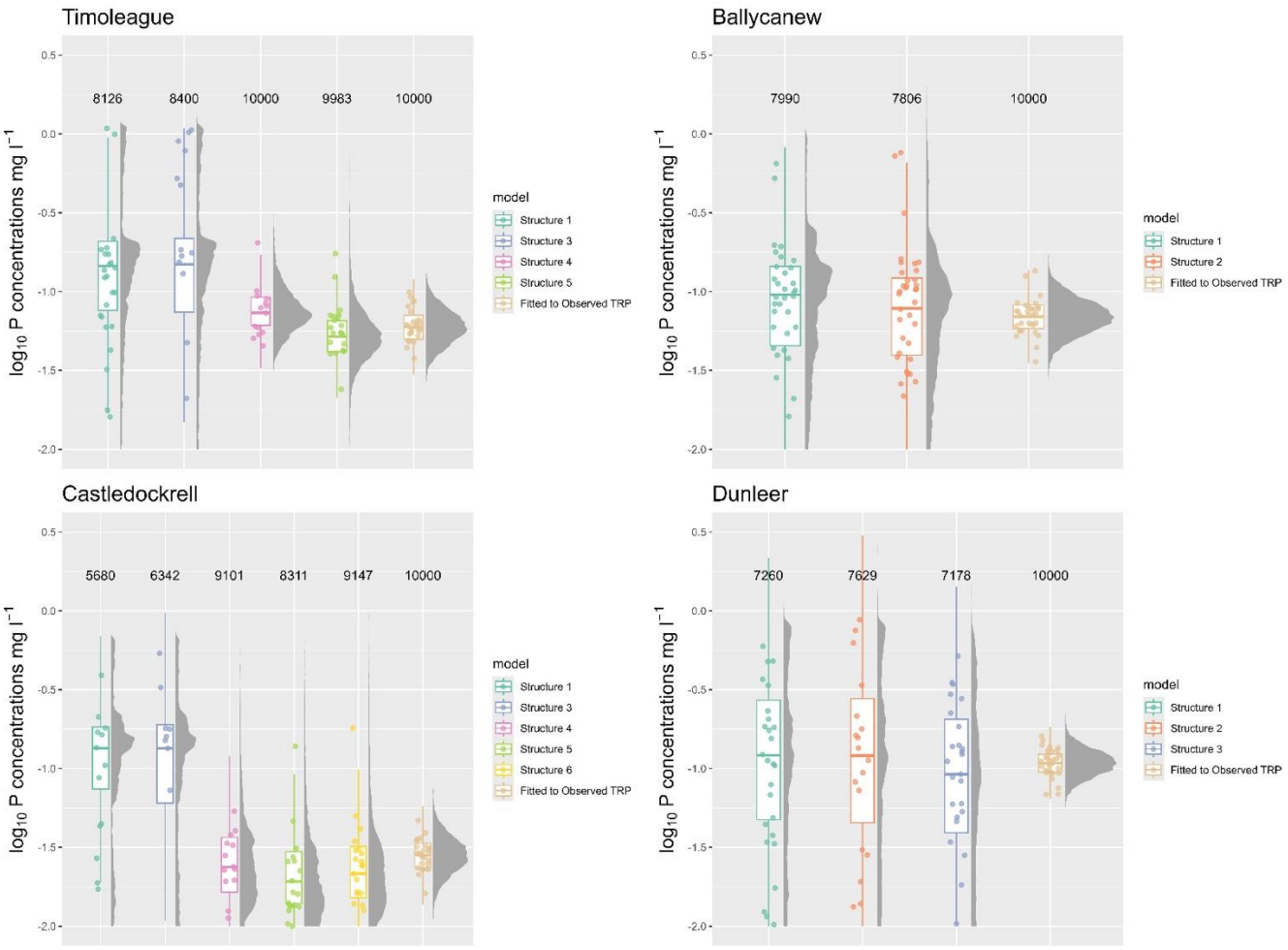

Figure 4.3 Predicted and observed log$_{10}$(TRP) concentrations for each of the four catchments. The grey density shows the distribution obtained by simulated realizations from the BBN (all plots except the rightmost of each panel), filled points the scatter of the realizations (100 samples per catchment), coloured boxplots show the median (central line), interquartile range (box) and highest and lowest datapoints (shown by the whiskers). Observations are shown in the rightmost plot in each panel, where the grey density shows the distribution fitted to the full suite of observations, filled points the scatter of the realizations, the light brown boxplots show the median (central line), interquartile range (box) and the 95% quantile range for the distribution. Data outside the instrument's limit of detection (0.01-5.00 mg l^{-1}) were excluded from the plot, and the text shows the number of valid samples for each model (with 10000 being the maximum number of available samples generated by the model). This plot was produced with the ggdist R package version 3.3.0 (Kay, 2023). A complete description of the finalized model structures is given in the Supplementary Information for the Timoleague, Dunleer, and Castledockrell catchments, a description of Structure 1 is given in Negri et al., (2024a).

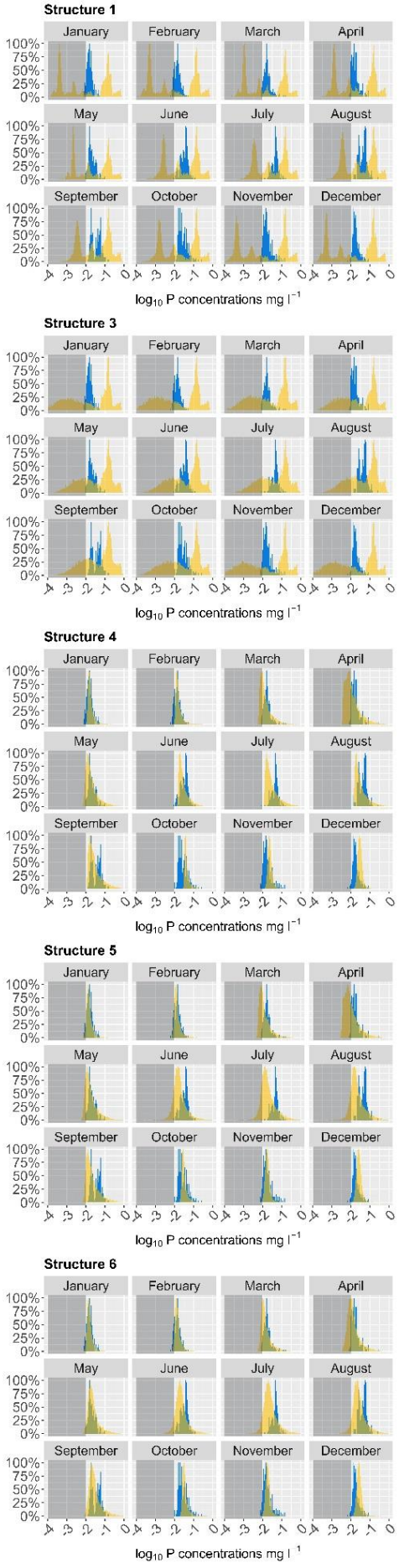

Figure 4.4 Histograms of monthly log10(TRP) concentrations (mg l^{-1}). Observations are shown in blue, predictions obtained from each model structure adapted for the Castledockrell catchment are shown in yellow. The dark grey box indicates concentration values below the limit of detection (0.01 mg l^{-1}).

Table 4.4 Marginal probability of exceeding EQS limits in the four catchments.

	Probability to exceed EQS limits			
	2010-2020 data (Mellander et al., 2022)	**2009-2016 data**	**model in Negri et al., (2024a)**	**model with in-stream P removal**
	Hourly mean concentration	**Daily mean concentration**	**Structure 1**	**Final structure (a different one for each catchment)**
TIMOLEAGUE	81%	80%	72%	88%
BALLYCANEW	94%	88%	65%	61%
CASTLEDOCKRELL	29%	28%	46%	18%
DUNLEER	99%	99%	58%	55%

4.5 Conclusions

This study is the first application of a BBN aimed at predicting stream P concentrations in four Irish agricultural catchments. We set out to test the transferability of a hybrid BBN targeting P pollution across agricultural catchments with diverse dominant hydrological processes. The initial BBN proved to be transferrable between catchments dominated by surface or mixed hydrological pathways, irrespective of land use, but less so between catchments dominated by sub-surface delivery. Inclusion of groundwater total dissolved P (TDP), Sewage Treatment Works (STWs) inputs, and in-stream P uptake improved model performance in all four catchments and made the BBN more transferable, though at the cost of increased complexity and data requirements.

In this work, we explored two strategies to improve model structure: bootstrapping to estimate the groundwater TDP concentration, and expert elicitation to assess in-stream P removal. The addition of groundwater TDP loads improved the predictions in sub-surface-driven catchments. Expert elicitation aided the P uptake parameterization, which lacked generalizable data, highlighting a research gap. However, we found that in-stream P uptake remained a secondary process compared to the representation of P transfers via both surface and subsurface pathways when simulating daily P concentrations.

To avoid discretizing the continuous distributions that form critical components of the BBN nodes prior to sensitivity analysis, we implemented a method to evaluate the effects of parameter variation on the full posterior distribution of the target node, by varying the parameters of interest while holding the

others fixed. This demonstrated the transferability of non-catchment specific data to further catchments and found redundant parameters in the sediments and septic tanks components of the model.

Testing BBN applicability also revealed constraints in this study related to the limited presence of BBN studies conducted in catchments comparable to those examined in this research, and the fact that few modelling studies have been performed in our study catchments. Therefore, future work should involve the use of other modelling approaches in these catchments, allowing the intercomparison of models parameterized with high-frequency datasets. Given the scope of the Agricultural Catchments Programme, in the future, the BBNs developed here present an effective tool for modelling of catchment-scale effects of water quality mitigation measures.

5. Climate change impacts on phosphorus concentrations in four Irish catchments: a Bayesian Belief Network approach

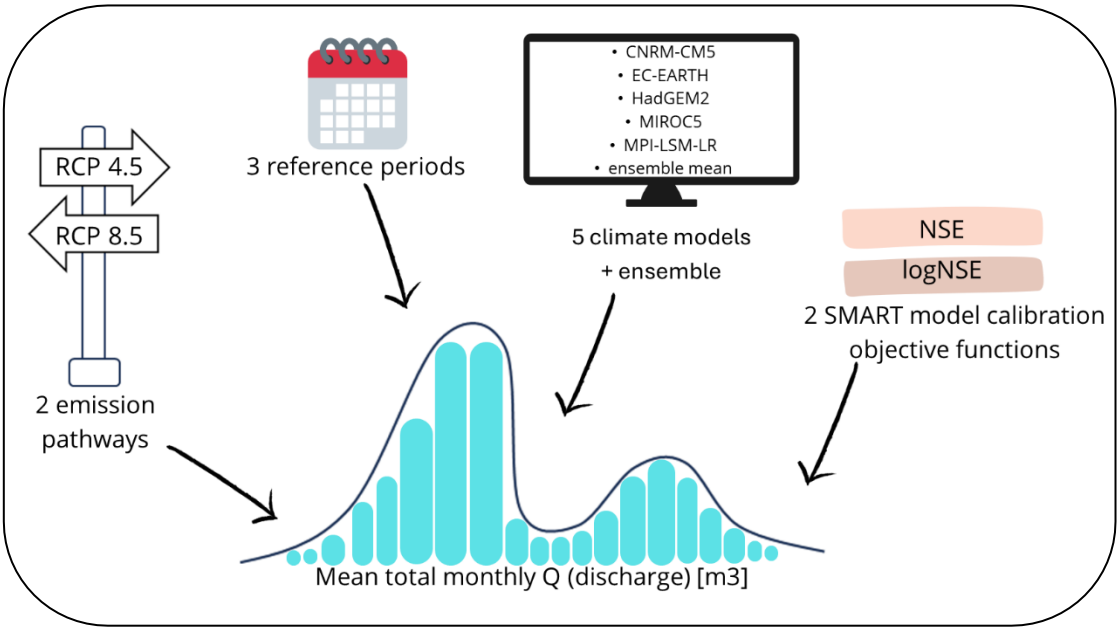

Figure 5.1 Schematic representation of the combined information required to create the seventy-two scenarios (per catchment) used to drive the BBN's TRP predictions in this chapter.

Abstract

Climate-induced changes in precipitation and river flows are expected to cause changes in river phosphorus loadings. The uncertainty associated with climate-induced changes to water quality is rarely represented in models. Bayesian Belief Networks (BBNs) are probabilistic graphical models incorporating uncertainty in their model parameters, making them ideal frameworks for communicating climate risk. This study presents a BBN to simulate total reactive phosphorus (P) concentrations in four agricultural catchments under projected climate change. Six climate models (five models plus the ensemble mean), two objective functions (NSE vs log NSE), two Representative Concentration Pathways (RCP 4.5 and 8.5), and three time periods (the 2020s, the 2040s, and the 2080s) were used to create scenarios as model inputs. The simulated monthly mean P concentrations show no obvious trends over time or differences between the two RCP scenarios, with the model ensemble essentially replicating the results obtained for the baseline period. However, the P concentration distributions simulated using the outputs from the HadGem-2 model rather than the ensemble, showed significant differences from the baseline in the drier months. A sensitivity analysis demonstrated that this difference occurred because the catchment-specific BBNs were sensitive to changes in the mean total monthly discharge which were captured in the HadGem-2 projections but not by the ensemble mean. BBNs in the surface-dominated study catchments showed sensitivity to changes in agricultural land use type.

5.1 Introduction

Intensive farming in Ireland has caused freshwater eutrophication through phosphorus (P) over-enrichment (Ulén et al., 2007). P losses in rural catchments are complex, being determined by multiple sources, including legacy P, manure and mineral fertiliser applications and effluent discharges, and multiple pathways such as overland flow, farm drains and groundwater flow; all of which vary with location (Bowes et al., 2015; Mellander et al., 2016; Thomas et al., 2016b). Phosphorus bound to soil and stream sediment can also be later released further confounding P reduction efforts. For these

reasons, whilst reducing P losses from land to water is expected to reduce freshwater eutrophication overall, determining the focus and priorities for effective policy and catchment management to achieve such reductions is difficult.

Climate change further complicates the management challenge (Bol et al., 2018). Projections for Ireland suggest increased winter precipitation and reduced summer precipitation (Murphy et al., 2023). Against this backdrop, P models have been applied to quantify P sources, transport and the in-stream concentrations and loads to identify appropriate management strategies to continue recent progress in the reduction of stream water P concentrations and loads (Charlton et al., 2018; Ockenden et al., 2017; Wade et al., 2022). Modelled outcomes in small UK river catchments suggest increased and more intense winter storms which will result in greater mobilisation and delivery of P loads to surface waters (Ockenden et al., 2017), whilst summer reductions in precipitation will reduce the dilution of point source and groundwater inputs. Studies have shown increased P loads from agricultural diffuse source under climate change (e.g., (Jennings et al., 2009; Ockenden et al., 2016, 2017)), despite the fact that concentrations are the relevant water quality standard in running waters (Stamm et al., 2014) and estimating the effects of climate on P concentrations remains crucial to understand future eutrophication risk and to design mitigation measures (Charlton et al., 2018), also in light of the European Union Water Framework Directive (WFD). Catchment area, the relative inputs from diffuse and point sources, and land use are also important factors that determine how stream water P concentrations will respond to future land cover and climate change, and must accounted for (Wade et al., 2022). Furthermore, the commensurate changes in chlorophyll-a concentrations, which are a measure of algal production, in response to stream water phosphate alterations are also complicated with growing evidence that stream water residence-time and the prevailing light conditions are equally, if not more important than P (and nitrogen in headwater catchments), as controls on algal bloom initiation and development (Bowes et al., 2012; Neal et al., 2006; Smith et al., 2017). Inadequate data resolution to describe the flow and phosphorus dynamics, particularly under extreme high and low flow conditions, and the lack of uncertainty analysis in model applications have been cited as current limitations when simulating future changes in phosphorus (Ockenden et al., 2017). The lack of suitable data means that the testing of the

assumptions to construct P models is limited. Incorporating uncertainty is critical to help decision-makers to assess models and to make informed decisions about water quality management (Kotamäki et al., 2024). Bayesian Belief Networks (BBNs) are probabilistic graphical models that due to their stochastic nature can help bridge uncertainty knowledge gaps as they provide robust quantitative uncertainty estimates, including epistemic and aleatoric uncertainty (Glendell et al., 2022; Sahlin et al., 2021) and can facilitate the identification of uncertainty sources within the model (Sperotto et al., 2017). Given this, BBNs are an alternative to the widely-used process-informed catchment P models such as HYPE, SWAT, and INCA-P (Negri et al., 2024a), and are advantageous because they incorporate P sources, processes and delivery pathways in a way that is interpretable and accessible to wider audiences. Incorporating uncertainty is also inherent in BBNs through the specification, by measurements or expert elicitation, of the conditional probability tables (CPTs), distributions, and equations describing P processes and transport pathways.

A new hybrid BBN has been developed and applied to four catchments in Ireland, representative of contrasting land cover and hydrological regimes, with good performance when simulating total reactive P concentrations (TRP) (Negri et al., 2024b). Here, we take the science further and present the application of the BBN to simulate future phosphorus losses in the same four catchments under scenarios of climate change. All four catchments have extensive datasets of in-stream TRP, discharge (Q), and turbidity measured sub-hourly since 2009, supplemented by field-scale data from over 400-500 soil P tests. These have been used previously to construct and test the catchment-specific BBNs, which have been further enhanced to include septic tank inputs, in-stream P processes, and groundwater pathways. The aim of this study is to quantify stream TRP concentrations under future projections of climate change and to achieve this overall aim there are three research objectives:

1. To use projected future flows as input to the BBN model to determine TRP concentrations based on outputs from five climate models and the ensemble mean, considering two RCPs (4.5 and 8.5) and present day (2020s), near (2040s) and far future (2080s) time periods.

2. To evaluate the sensitivity of the BBN outputs to changes in flow inputs and land use.

3. To use the sensitivity analysis results to understand the response of the BBN to altered flow and land use, and thereby better understand the relative importance of flow and land cover as drivers of change.

5.2 Study Areas

This study focusses on four agricultural catchments located in the Republic of Ireland. These have contrasting land uses (grassland or arable dominated) and hydrology (from poorly to moderately to well drained) and have been described in more detail elsewhere (Jordan et al., 2012), including Chapter 2 of this thesis. The catchments included are Ballycanew and Castledockrell in County Wexford, Timoleague in County Cork, and Dunleer in County Louth. The catchments have been monitored since 2009 to oversee the environmental and economic effectiveness of the Programme of Measures and derogation under the Nitrates Direction National Action Programmes (NAPs) of the European Union (Fealy et al., 2010). Specifically, the monitoring included high-frequency (sub-hourly) measurements of hydro-chemo-metrics at the catchment outlet such as discharge (Q, m^3), turbidity (NTU), and total reactive P (TRP, mg l^{-1}) concentrations aggregated at the daily time step (Negri et al., 2024a) and field-scale soil sampling including agronomic soil P (Wall et al., 2013).

Murphy et al., (2023) have simulated future flows under climate change scenarios in twenty-six Irish catchments, including those in this study by using the Irish Centre for High-End Computing (ICHEC) ensemble (Nolan and Flanagan, 2020) to drive the Soil Moisture Accounting and Routing for Transport (SMART) hydrological model (Hallouin et al., 2020; Mockler et al., 2016b). Annual mean flows were projected to increase across Irish catchments under RCP 8.5 (a fossil fuel-intensive emissions pathway), and the largest increase was expected in Castledockrell by the 2080s (23.8%) (Murphy et al., 2023). Under RCP 8.5 in the 2080s, Timoleague, Ballycanew, and Castledockrell showed increased winter mean flow (>30%). Large summer flow decreases were predicted for Ballycanew and Dunleer (up to -50%). The Castledockrell catchment was also expected to experience up to 114% increase in autumn mean flow under RCP 8.5 (Murphy et al., 2023). Changes to the mean seasonal and annual flows are

also expected under RCP 4.5 (an intermediate pathway with emissions peaking around the year 2040), albeit less marked.

5.3 Methods

5.3.1 Bayesian Belief Network development

The BBNs used in this study were developed in the software GeNIe, version 2.4 (BayesFusion, 2019) by Negri et al., (2024b) for the four catchments. The final best-fitting catchment-tailored BBNs were used in the present study. The four BBN structures are all aimed at quantifying monthly in-stream P concentration at the catchment outlet by integrating the TRP loads from different compartments (soils, sediments, septic tanks, farmyards, groundwater, and a wastewater treatment plant) and then converting the loads into concentrations by dividing by the monthly discharge. Catchment-specific datasets were used wherever possible, including the quantification of the different discharge (Q) components, namely quick-flow, interflow, and baseflow (Mellander et al., 2012) (specified as mean total monthly surface flow [m^3], mean total monthly sub-surface stormflow [m^3], and mean total monthly baseflow [m^3] in Tables 3.1, 9.2, 9.3, and 9.4). The finalized BBNs achieved good performance in all four catchments in terms of percentage bias ($-5\% \leq PBIAS \leq 49\%$) when compared to the observed TRP concentrations (2009-2016) (Negri et al., 2024b). The BBNs reproduced the mean monthly TRP concentration relatively well in Castledockrell and Timoleague, less accurately in Ballycanew and Dunleer, where the model predicted the mean concentration better in winter than in summer. A summary of the BBNs' performance is given in Table 5.1, whilst further detail, including the monthly performance, is reported in the previous Chapter.

Table 5.1 Summary performance of the BBNs developed in Negri et al., 2024b, including mean marginal TRP, the lower limit of the distribution (μ-1σ, superscript), the upper limit (μ+1σ, subscript), and percentage bias (PBIAS). Both observed and predicted TRP concentrations were log-transformed before calculating the statistics and then converted back to normal values. The marginal distribution mean can reproduce the observed mean TRP concentration in the reference period (2009-2016).

	PBIAS	mean predicted	mean observed
	%	TRP mg l^{-1}	
TIMOLEAGUE	-5	$0.05^{0.03}_{0.08}$	$0.05^{0.03}_{0.09}$
BALLYCANEW	49	$0.07^{0.03}_{0.17}$	$0.06^{0.03}_{0.11}$
CASTLEDOCKRELL	18	$0.02^{0.01}_{0.05}$	$0.02^{0.01}_{0.04}$
DUNLEER	45	$0.09^{0.03}_{0.28}$	$0.10^{0.06}_{0.16}$

5.3.2 Climate Scenarios and their implementation in the BBN

Nolan and Flanagan, (2020) developed high-resolution climate scenarios for Ireland by downscaling the outputs of five Global Climate Models, namely, CNRM-CM5 (Voldoire et al., 2013), EC-Earth (Hazeleger et al., 2012), HadGEM2-ES (Collins et al., 2011), MIROC5 (Watanabe et al., 2010), and MPI-ES-LR (Giorgetta et al., 2013). Future climate was simulated under Representative Concentration Pathway 2.6, 4.5, 6.0, and 8.5, of which RCP 4.5 and 8.5 are included in this study to represent an intermediate (4.5) and an extreme scenario (8.5). Murphy et al., (2023) used these climate scenarios to drive the SMART hydrological model, calibrated independently with both the Nash-Sutcliffe Efficiency (NSE) and the log Nash-Sutcliffe Efficiency (log NSE) as objective functions. Through the SMART model, Murphy et al., (2023) obtained the simulated river flows (discharge, Q) up to 2100, used in the present study. The available daily discharge (Q, mm) timeseries were summed into total monthly Q (m^3) for each model and reference period. This was used to implement a bootstrapping procedure that fits a Lognormal distribution to the data distributions from each month using *fitdistrplus* (Delignette-Muller et al., 2020). These monthly lognormal parameters (mean, μ, standard deviation, σ) per each scenario were then used to specify the distributions for the BBN node "Mean total monthly Q (discharge) [m^3]" using the same procedure used to parametrize the BBN baseline in Negri et al., (2024a). A scenario for the ensemble mean was also included, whereby monthly discharge was averaged between the five climate models prior to distribution fitting. This was done in view of the recommendation to use a multi-model ensemble approach to address model formulation and climate variability-related uncertainties as explained in Nolan and Flanagan, (2020). The combination of two

emission pathways, three reference periods, the 2020s (2010-2039), the 2050s (2040-2069), and the 2080s (2070-2099), six model options (five models plus the mean of the ensemble), and two calibration functions gave seventy-two scenarios of monthly discharge per catchment. These were used to simulate monthly TRP concentrations at the catchment outlet. The posterior probability for the target node "In-stream P concentration [mg l^{-1}]" was simulated using *rSMILE* version 2.2.1 (BayesFusion, 2019c), an API engine available in R which can perform the same operations as GeNIe Modeler (BayesFusion, 2019), the software used to develop the BBN model structure in each catchment. Mean monthly posterior TRP concentrations (μ±σ, mg l^{-1}) for each scenario were plotted alongside mean total precipitation (μ±σ, mm), observed TRP (μ±σ, mg l^{-1}) as well as the TRP (μ±σ, mg l^{-1}) predicted by the BBN in baseline period (2009-2016) (Negri et al., 2024b).

5.3.3 Sensitivity Analysis

To help us interpret the results, we conducted a sensitivity analysis on the model parameters for discharge (Q) and land use variables by adapting the methodology developed in *rSMILE* 2.0.1 in Negri et al., (2024b), but using *rSMILE* version 2.2.1. The "Mean total monthly Q (discharge) [m^3]" was defined as a series of monthly Lognormal (μ, σ) distributions. For each catchment, we tested varying the mean ($9 \leq \mu \leq 17$) and standard deviation ($0.1 \leq \sigma \leq 1$) of the Lognormal discharge (Q) on the median $\log_{10}$(TRP) concentration (mg l^{-1}). Additionally, we tested the effects of land use changes by varying the proportions of the three potential land uses (arable, grassland, and seminatural), with the proportions for the three categories summing to 1.

5.4 Results and Discussion

5.4.1 Phosphorus concentrations under future climate

Marginal mean TRP concentrations are predicted by each catchment's BBNs using the model ensemble across the three reference periods: the 2020s (2010-2039), the 2050s (2040-2069), and the 2080s (2070-2099). These show no differences against the observed reference period (2009-2016) nor obvious trend

over time, nor differences when using the two different SMART model calibrations (log NSE vs NSE) (shown Table 10.1 of Supplementary Information as $\log_{10}$(TRP)). However, here we applied a model ensemble consisting of the mean discharge simulated by five climate models which progresses previous work using a single climate scenario in a BBN (Mentzel et al., 2022).

The marginal TRP results driven by the ensemble could mask seasonal variation, therefore, monthly mean TRP ($\mu \pm \sigma$, mg l^{-1}) predictions in the Ballycanew (top plots) and Castledockrell (bottom plots) catchments are shown in Figure 5.2, while Figure 5.3 shows the same for Timoleague (top plots) and Dunleer (bottom plots). Simulated future TRP concentrations are plotted against the precipitation (mm) predicted by the different models (on the left-hand side) and against the observed and predicted TRP for the baseline period (2009-2016), as well as BBN predictions when using the model ensemble mean and the BBN baseline. In Ballycanew and Castledockrell, the HadGEM2-ES model predicts higher TRP concentrations under future scenarios, likely due to lower predicted precipitation and therefore discharge, and a subsequent dilution reduction. This concurs with Wade et al., (2022), whereby the change in future SRP concentrations depended on the choice of climate model. However, the HadGEM2-ES model also shows higher uncertainty, made evident by the wider upper ($\mu+\sigma$) and lower limit ($\mu-\sigma$) in Figure 5.2 and 5.3 (see Table 10.2 and Figure 10.1 in the Supplementary Materials which show the mean (μ) TRP concentrations under the different scenarios). In all catchments, the predicted TRP concentration remained at levels similar to those simulated during the baseline period. Differences in climate-driven mean concentrations were negligible, especially when accounting for uncertainty by considering the upper and lower simulated concentrations (see for example, the differences between figures 5.2 and 5.3 and Figure 10.1). An exception was found in Castledockrell, with a higher mean TRP in August, September, and October for HadGEM2-ES RCP 8.5, irrespective of time period (Table 10.2 and Figure 10.1). Further, it should be noted that the uncertainty in the Ballycanew catchment is larger, due to a worse fit of the BBN to the data from the reference period than in the other catchments (Negri et al., 2024b). Similarly, the uncertainty in the Timoleague and Dunleer catchments shows a large spread in predicted stream TRP concentrations. The precipitation plots show differences and therefore large uncertainty between climate models, which could probably explain the uncertainty in

TRP predictions. In Castledockrell, the least P-vulnerable catchment, the uncertainty in the observed and baseline TRP concentrations is smaller than the range of TRP concentrations predicted under the climate change scenarios. This is because the climate model ensemble performance during calibration and validation was best (NSE_{cal} was 0.87, NSE_{val} was 0.83) in Castledockrell (Murphy et al., 2023). Further, the BBN specified for the Castledockrell catchment perfectly represented the mean TRP concentration at the catchment outlet (Table 5.1). While all the BBNs achieved good performance in predicting the marginal mean concentrations across the four catchments (Table 5.1), the BBNs did not represent seasonality well in the Ballycanew and Dunleer (Negri et al., 2024b). However, the ability to reproduce seasonal variation in discharge, and therefore dilution, correctly during ecological sensitive periods is important, for example, to determine algal bloom development and persistence.

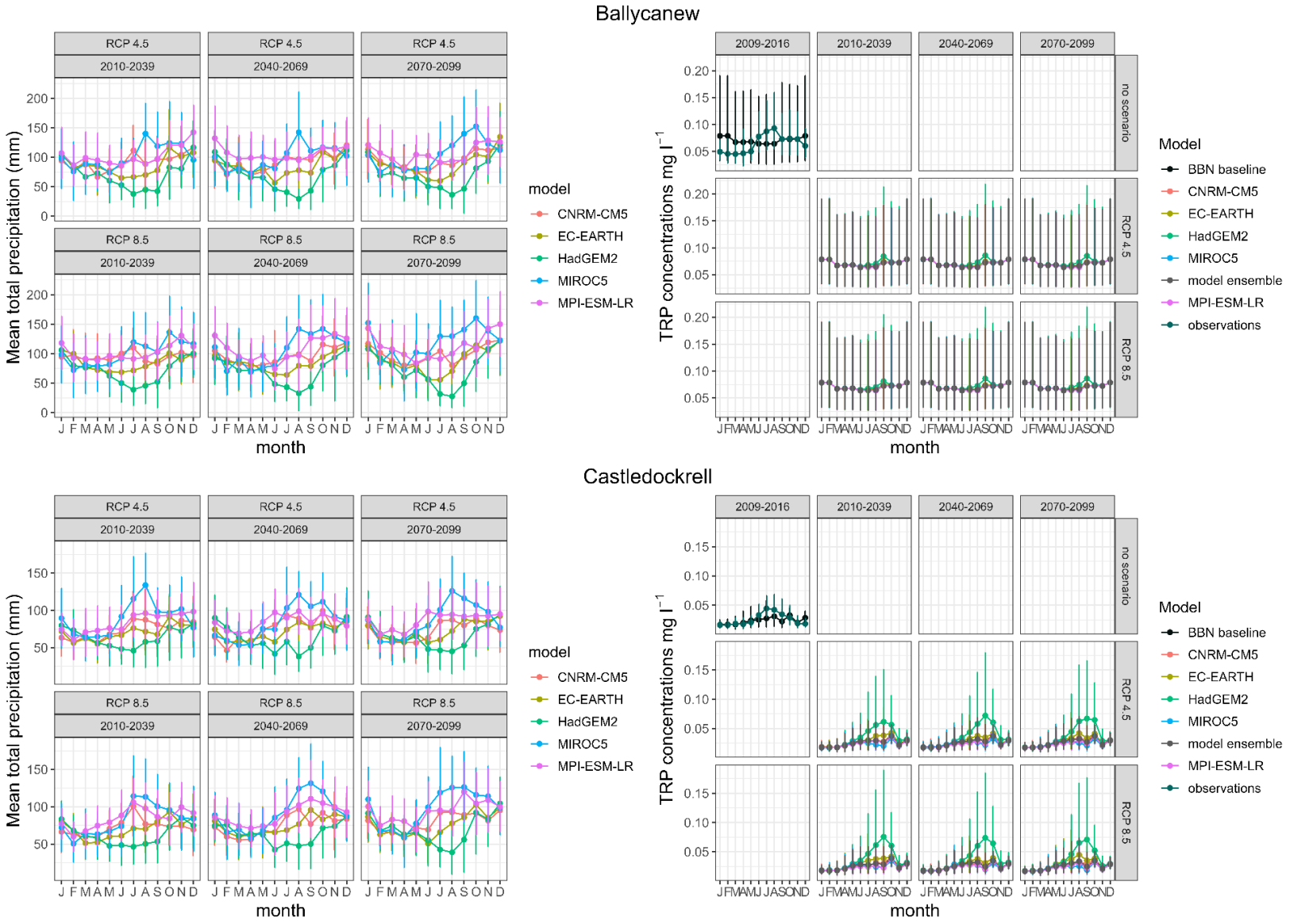

Figure 5.2 Mean monthly predicted precipitation (left-hand side) in Ballycanew (top left) and Castledockrell (bottom left) driven by five climate models and the ensemble mean. The predicted and observed means (mg l^{-1}) ± standard deviation are shown to demonstrate the full range of uncertainty in the predictions and observations. Predicted TRP concentrations were log-transformed before calculating the statistics, and then converted back to normal values. Results are shown for the NSE calibration of the SMART model only.

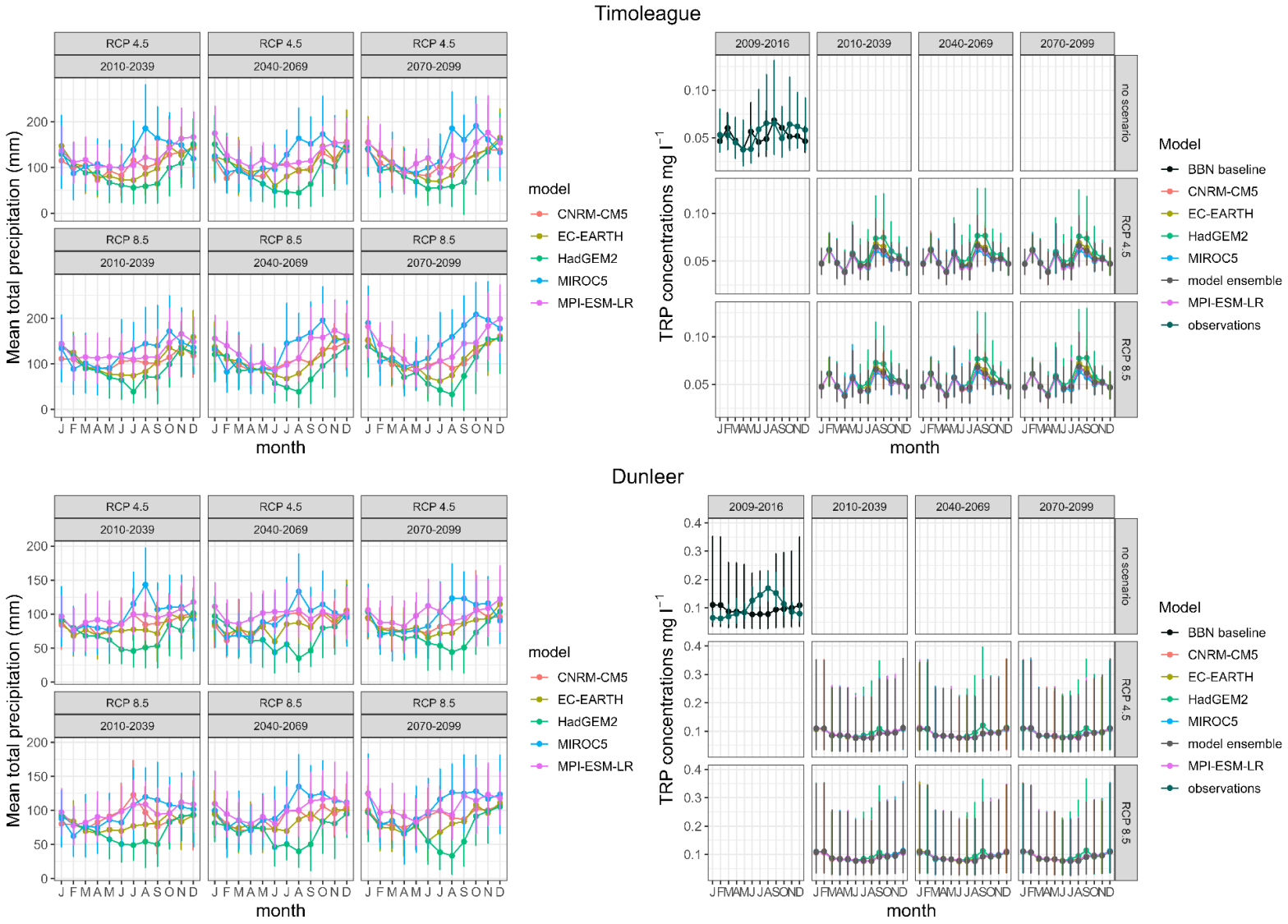

Figure 5.3 Mean monthly predicted precipitation (left-hand side) in Timoleague (top left) and Dunleer (bottom left) driven by five climate models and the ensemble mean. The predicted and observed means (mg l^{-1}) ± standard deviation are shown to demonstrate the full range of uncertainty in the predictions and observations. Predicted TRP concentrations were log-transformed before calculating the statistics, and then converted back to normal values. Results are shown for the NSE calibration of the SMART model only.

5.4.2 Sensitivity to discharge

The sensitivity analysis showed that the BBNs developed for the four catchments are somewhat sensitive to a variation in the monthly mean discharge, but not to variations in the standard deviation (Figure 10.2 in Supplementary Information). Specifically, the model was sensitive to variations mean (μ) of the Lognormal discharge in the range $9 \leq \mu \leq 12$ (these are specified in the $\log_e$ scale in the BBN), which is equivalent to a variation between 8000 and $1.6*10^5$ m^3. Variations outside this range (Lognormal $\mu \geq 12$) were shown not to have an impact on the median $\log_{10}$(TRP) concentration (mg l^{-1}). The sensitivity analysis explains why the BBNs under climate change show TRP concentrations similar to those shown in the baseline when using the model ensemble.

Table 5.2 Mean (μ), lower (μ-σ), and upper limit (μ+σ) of discharge (total monthly Q, m^3) in the month of January for the model ensemble across the two climate scenarios (RCP 4.5 and RCP 8.5) against the same for the BBN baseline (Negri et al., 2024b) for each of the four catchments. Here, only results derived from the NSE calibration driving the SMART model are shown. Mean monthly discharge is represented in the model with a Lognormal(μ, σ) distribution (base e). In this table, all Lognormal distributions have a mean of $13.36 \leq \mu \leq 13.92$, and a standard deviation of $0.04 \leq \sigma \leq 0.17$ which is a range the model is not sensitive to (shown in Supplementary Information).

	Timoleague								
	RCP 4.5			**RCP 8.5**			**BBN baseline (Negri et al., 2024b)**		
	μ-σ	**μ**	**μ+σ**	**μ-σ**	**μ**	**μ+σ**	**μ-σ**	**μ**	**μ+σ**
	$m^3*10^6 month^{-1}$								
2009-2016	-	-	-	-	-	-	0.89	0.98	1.09
2010-2039	0.81	0.84	0.88	0.75	0.78	0.81	-	-	-
2040-2069	0.85	0.89	0.93	0.85	0.88	0.92	-	-	-
2070-2099	0.89	0.92	0.96	0.98	1.02	1.07	-	-	-
	Ballycanew								
	RCP 4.5			**RCP 8.5**			**BBN baseline (Negri et al., 2024b)**		
	μ-σ	**μ**	**μ+σ**	**μ-σ**	**μ**	**μ+σ**	**μ-σ**	**μ**	**μ+σ**
	$m^3*10^6 month^{-1}$								
2009-2016	-	-	-	-	-	-	0.83	0.98	1.17
2010-2039	0.84	0.89	0.96	0.85	0.91	1.88	-	-	-
2040-2069	0.88	0.94	1.01	0.87	0.93	1.00	-	-	-
2070-2099	0.91	0.97	1.04	1.03	1.11	1.20	-	-	-
	Castledockrell								
	RCP 4.5			**RCP 8.5**			**BBN baseline (Negri et al., 2024b)**		
	μ-σ	**μ**	**μ+σ**	**μ-σ**	**μ**	**μ+σ**	**μ-σ**	**μ**	**μ+σ**
	$m^3*10^6 month^{-1}$								
2009-2016	-	-	-	-	-	-	0.97	1.09	1.21
2010-2039	0.61	0.63	0.66	0.60	0.63	0.65	-	-	-
2040-2069	0.63	0.66	0.69	0.66	0.69	1.02	-	-	-
2070-2099	0.67	0.70	0.73	0.76	0.79	0.82	-	-	-
	Dunleer								
	RCP 4.5			**RCP 8.5**			**BBN baseline (Negri et al., 2024b)**		
	μ-σ	**μ**	**μ+σ**	**μ-σ**	**μ**	**μ+σ**	**μ-σ**	**μ**	**μ+σ**
	$m^3*10^6 month^{-1}$								
2009-2016	-	-	-	-	-	-	0.60	0.66	0.73
2010-2039	0.71	0.75	0.79	0.71	0.74	0.78	-	-	-
2040-2069	0.73	0.77	0.81	0.76	0.81	0.85	-	-	-
2070-2099	0.78	0.83	0.88	0.84	0.89	0.95	-	-	-

A comparison of the discharge (Q) for the month of January is shown in Table 5.2 across the model ensemble scenarios (NSE calibration only) and the BBN baseline parameterized in Negri et al., (2024b). The same results were obtained when testing the model sensitivity in a drier month (August, data not shown). The ensemble-driven discharge in the scenarios was comparable to that in the BBN baseline (Table 5.2). Meanwhile, the climate models (rather than the ensemble) predict total monthly Q in ranges that the BBN is sensitive to (Lognormal $\mu \leq 9$). The analysis suggests that the sensitivity of the target node (TRP concentrations at the catchment outlet) to parents (discharge, Q) that are far away from the target node itself is low. In these BBNs, discharge is used to calculate both the concentrations at the catchment outlet and the loads from the different model compartments, therefore it's considered to be distant from the target node because there is an increased number of variables between input (parent nodes) and output (target child node). This confirms the finding that an increased number of variables between input (parent nodes) and output (target nodes) weakens the relationship between input and output (Marcot et al., 2006). However, due to time constraints, the sensitivity to nodes closer to the target was not tested here, albeit a previous analysis showed that the BBNs are sensitive to the P dissolved from the soil matrix into the stream (Negri et al., 2024b).

5.4.3 Sensitivity to land use

When testing land use change scenarios, only two of the BBNs showed sensitivity to changes in land use proportions in the land use node, as shown in Figure 5.4 for the two surface-driven catchments, Ballycanew (top right) and Dunleer (bottom right). The models for the other two catchments (which include groundwater inputs), did not show a sensitivity to changes in land use proportions (Figure 5.4, Timoleague and the top left and Castledockrell at the bottom left). The BBNs for the groundwater-driven catchments parameterized in Negri et al., (2024b), Chapter 4, represent more P processes than the models in the other two surface-driven catchments, which could have contributed to a smaller spread of predicted posterior $\log_{10}$(TRP) concentrations (mg l^{-1}), shown in Chapter 4, Figure 4.3 and 4.4 and Figures 5.2 and 5.3 in this chapter. The two models in groundwater-driven catchment support a simplified representation of the causal relationship between land use and groundwater P concentrations

(the full structures are shown in Negri et al., (2024b)), which explains the low sensitivity of in-stream TRP concentrations to changes in land use in these two study catchments. In addition, BBNs are limited in their ability to represent temporal dynamics (Moe et al., 2021), which represents an issue for climate applications (Sperotto et al., 2017). Specifically, in this study, in the groundwater-dominated catchments Castledockrell and Timoleague, P transit time from land use to groundwater far exceeds the BBN monthly timestep, and therefore a Dynamic Bayesian Network (DBN) might be better suited to represent these catchments both under the current conditions and future climate scenarios.

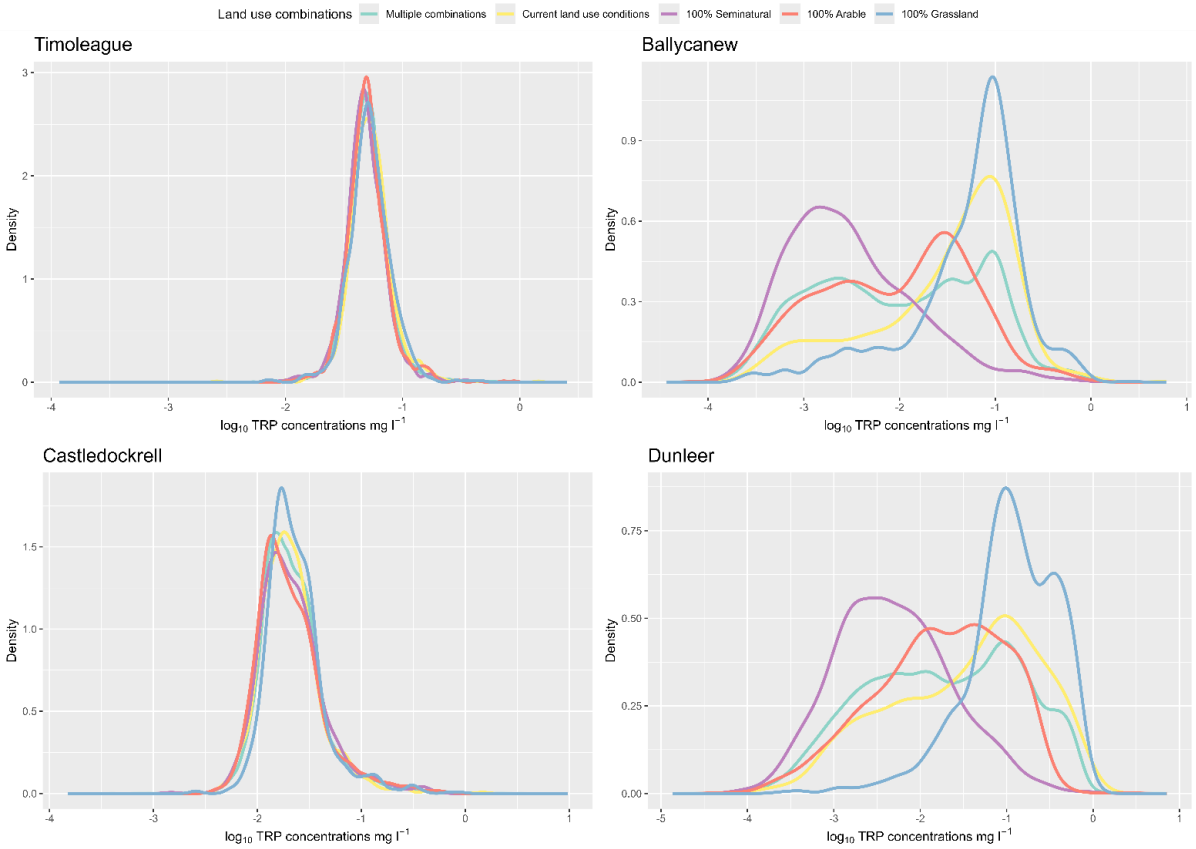

Figure 5.4 BBN sensitivity to changes in land use shown in the four catchments as Kernel Density Estimates of the probability density (y-axis) of log_{10}(TRP) concentrations (mg l^{-1}) on the x-axis corresponding to different land use scenarios. Current catchment land use is represented by the yellow density, 100% seminatural land use is represented in purple, 100% arable in red, and 100% grassland in blue. 57 different combinations of proportions of the three land uses are shown in green under "multiple combinations". Kernel Density Estimate peak densities can exceed 1 but are constrained to integrate to 1. The surface water-dominated catchments (right hand-side, top and bottom) on the right show sensitivity to land use change, whilst the groundwater-dominated catchments (left-hand-side, top and bottom) do not.

5.5 Conclusions and further research

Downscaled climate-driven discharge (Q) time series up to the year 2099 were used as input to the catchment-specific Bayesian Belief Networks, to quantify future TRP concentrations in the four study catchments for the first time. The results driven by an ensemble of five climate models showed no evident trends in stream TRP concentration in either catchment, regardless of concentration pathway (RCP 4.5 vs RCP 8.5) and future time periods. This outcome is consistent with similar research conducted using process-based models. This suggests that the impacts of climate change alone might not be significant when evaluating TRP concentrations in rivers and streams; however, effects may become apparent elsewhere, for example in terms of total loads entering standing waters, or at different time steps. The sensitivity analysis suggested that simulated changes in monthly Q driven by an ensemble of climate models are insufficient to drive stream TRP concentration changes in the studied catchments. The sensitivity analysis also demonstrated that in-depth knowledge of the BBN model response is necessary to interpret the results of future scenario simulations. Designing scenarios where the discharge was driven by the individual climate models rather than the ensemble proved to be an effective tool into understanding the drivers of the ensemble and helped results interpretation. This also suggested that future research should focus on testing different ensemble sets, or ensembles made of a larger number of climate models, as suggested by Moe et al., (2022), and on developing new strategies to implement climate information in these BBNs. Further investigation of the combined effects of climate and land use changes in the ACP catchments is needed to fully understand what controls TRP concentrations in these catchments.

6. Discussion

The uniqueness and richness of the Agricultural Catchments Programme dataset prompted advancements in BBN and water quality research that would not have been possible otherwise, as discussed in sections 6.1 and 6.2. Using a Bayesian Belief Network to model P losses in the ACP catchments allowed the representation of all P sources: measured ones such as soil P and stream sediments, and unmeasured ones (farmyard, septic tanks, and sewage treatment works); as well as measured drivers (discharge, land use, agronomic management) and unknown ones such as those related to point sources. This approach enabled the systematic mapping and detailing of all data available (Tables 2.2, 3.1, 4.1, 9.1, 9.2, 9.3, 9.4), and the combination of datasets with disparate spatial and temporal resolutions in a single model, pinpointing research gaps present even in highly monitored catchments. Implications for management and suggestions for further model development for stakeholder use are laid out in section 6.3. Finally, the limitations of the BBN approach are discussed in section 6.4.

6.1 Addressing Bayesian Networks and process-based models' knowledge gaps

Whilst developing the catchments-specific BBNs (chapters 3 and 4), the step-wise inclusion and parameterization of point sources P inputs, in-stream P processes, and groundwater pathways improved model performance and P processes and loss pathway representation. Specifically, the inclusion of groundwater pathways provided the greatest improvement. This addresses the general omission of in-stream P processing from catchment P models raised by Jackson-Blake et al., (2015), and the lack of groundwater processes in BBNs developed in Negri et al.,(2024a) (Chapter 3) and Glendell et al., (2022). Other issues related to P modelling with process-based models addressed in this thesis are discussed in the introduction of Negri et al., (2024a) (Chapter 3), and in Chapter 4. These encompass the inclusion of point P sources in the model and the addition of uncertainty estimation embedded in the BBN modelling framework, which is relevant to modelling future water quality (Ockenden et al., 2017; Sperotto et al., 2019a). Such improvements were enabled by the Bayesian framework and by

addressing four knowledge gaps regarding BBN application for Environmental Risk Assessment (described in section 1.4): 1) BBN validation with monitoring data (Table 1.1), 2) the use of high-frequency data to develop hybrid BBNs, 3) transferability testing, and 4) transparency of expert elicitation. A brief description of how these were addressed is given below.

(1) and (2): Given the state-of-the-art high-frequency monitoring in operation at the Agricultural Catchments Programme, the issue of BBN validation (Death et al., 2015; Moe et al., 2021) was addressed in Chapter 3 and 4, where simulated TRP concentrations were compared against daily TRP observations, both quantitatively (using percentage bias) and qualitatively (visual assessment) in four ACP catchments, showing that the BBNs developed in this study performed better than those built using low-frequency regulatory datasets (e.g., Glendell et al., 2022). The development of hybrid BBNs through the use of high-frequency and resolution ACP data further addresses the issue of scarcity of BBNs in Environmental Risk Assessment (Kaikkonen et al., 2021).

(3) Testing the BBN transferability (Negri et al., 2024b, Chapter 4) showed that for the BBN to be more widely applicable, additional key processes needed to be represented (e.g., groundwater P inputs, in-stream P removal processes, and sewage treatment works inputs). Therefore, these sources need to be monitored for more accurate and reliable P assessment and scenario modelling.

(4) In Negri et al., (2024a), Chapter 3, I address the issue raised by Kaikkonen et al., (2021) around the role of experts in BBN modelling by providing information on the experts' background and credentials; noting which variables (nodes) were constrained using expert judgment, publishing the full model structure both in an Open Access journal and in an open GitHub repository, and providing supplementary information regarding the background information received by the experts prior to the interviews and workshops. Similarly, in Chapter 4, the reasoning behind the selected experts was made clear. Building upon recent research (Mzyece et al., 2024), to further address transparency concerns as well as to clarify the background information received by the experts, the methodology and supporting information regarding the elicitation workshop were published in an evidence dossier (Negri and Mellander, 2024).

6.2 Advancing Sensitivity Analysis in BBNs

In chapters 4 and 5 I describe the extensive sensitivity analysis carried out for the hybrid BBNs, which revealed redundant parameters. The strategy deployed to conduct such analysis is an extension of previous approaches, shown by Piffady et al., (2021). However, in the code published alongside Chapter 4, we showed how the same procedure could be applied in a hybrid network without triggering discretization. The redundant parameters pertained to the release of P from sediments into the stream ("Soil erosion and soil P" sub-model) and the septic tanks components ("Septic Tanks (ST)" sub-model) of the BBNs. This is consistent with the finding that in some of the ACP catchments soil erosion losses are lower comparatively to other catchments in Europe (Sherriff et al., 2019). However, removing the nodes relative to erosion might not always be the best choice as these could be needed if the BBNs are applied to other catchments where these processes are more dominant. Keeping the less important components (nodes) at zero results in computational issues in my experience, therefore, it's best to parameterize them to local conditions so that the causal relationships remain discernible in the graph.

Furthermore, the sensitivity analysis in Chapter 5 aided with understanding the results of the climate scenarios analyses. The sensitivity analyses conducted in chapters 4 and 5 are an advancement in this area of research and could be further enhanced by developing methods to conduct a global sensitivity analysis or to explore the effects of varying multiple nodes simultaneously on the full posterior distribution of the target node, which requires more computing power. Even though we carried out a sensitivity analysis on the hybrid BBN, the parameter space was explored based on the literature and the modellers' experience, therefore other methods could be developed to further extend this area of research. Lastly, the sensitivity analyses carried out here are still contingent on the proprietary software *GeNIe* and its API engine *rSMILE* (BayesFusion, 2019a, 2019c). This is a design choice dictated by the ease of use of the software which allowed the rapid design of multiple BBNs (Chapter 4) and analysis of numerous climate scenarios (Chapter 5).

Another strategy to evaluate the BBN's sensitivity to certain nodes (variables) was addressed using the progressive addition of nodes to the original model structure, which enabled a preliminary assessment

of the model's structural uncertainty. In Chapter 3, the step-wise addition of septic tank nodes has shown that the BBN has low sensitivity to these inputs. These nodes were kept in the model as they describe our current understanding of P transport from septic tanks to surface waters. These nodes present broad priors informed by the literature as opposed to the other variables informed by measured data. Due to time constraints, they have been parameterized subjectively, that is, they have been informed by the modeller(s). These steps have been described in chapters 3 and 4 and the CPTs of these nodes ("Leachfield removal", "Leachfield connectedness", "Septic Tank connectedness") have been described as "logical". Chapters 3 and 4 have demonstrated that these variables have a small influence on the posterior TRP distribution. A possible reason for observing low sensitivity to a particular node or parameter could be that the variability of other, less well-known parameters tends to dominate the output TRP distribution, regardless of the specific value of the parameter in question. For example, we might have observed low sensitivity to discharge (Q), even though it's a data-driven node in which we have reasonable confidence, because there are so many other nodes that are not as well characterized, either because logically derived, or because informed by few literature-derived data points (e.g., P concentrations in soils, septic tanks, and farmyards, see also Table 3.5).

Regardless, in Chapter 4 we demonstrated an improved approach whereby the nodes of interest were parameterized through expert elicitation. Alternatively, CPTs can be validated by experts, as was done for some of the CPTs in Chapter 3 (e.g., Table 3.1), and as shown by McDowell et al., (2009).

6.3 Implications for management

This research highlighted avenues for further data collection even in highly monitored catchments such as those in the ACP, and I have summarized them in Table 6.1. However, considering that some of these relate to point sources that are not very influential on the total P losses at the catchment outlet in these BBN models, improved data collection and management interventions should still prioritise targeting diffuse P sources such as soil, legacy, and groundwater P.

Presently, these BBN models can be used to test a limited range of management interventions, including changes in soil Morgan P levels. As BBNs are well suited to include disparate sources of information, including information about mitigation measures, as done in Igras and Creed, (2020), the models developed in this study should be expanded to include further measures and their effectiveness (besides the already included buffer strips). This would fully exploit the BBNs' potential as DSTs, given that understanding the full potential of mitigation at catchment scale and under future conditions rather than at the plot scale is a knowledge gap farmers and land managers are interested in (Adams et al., 2022). For example, the database in Stutter et al., (2021) could be leveraged to evaluate the effectiveness of measures at the catchment scale, rather than at the local scale, to aid managers with decision-making. Further, given that BBNs can model socio-economic aspects (Penk et al., 2022), these could be used to leverage already existing Teagasc research (e.g., regarding farmer's attitude toward mitigation, (Osawe and Curtis, 2024)) and potential policy options (e.g., Stewart et al., 2021).

Table 6.1 Model assumptions regarding P sources in the ACP catchments.

P source	Model assumptions	Consequences
Septic Tanks (STs)	• assumed concentrations and loads • assumed pathways • assumed age and working conditions.	Over/underestimation of STs loads.
Farmyards (FYs)	Assumed initial concentrations.	Over/underestimation of FYs loads.
Soils	• soil P to in-stream P relationship is assumed constant in time • soil P to in-stream P relationship unspecific to catchment • agronomic soil P available as categorical.	• Masking seasonality • Over/underestimation of diffuse loads • Loss of information.

A further implication for catchment managers is that the developed BBNs are best utilized as Decision Support Tools by calculating quantiles of the posterior TRP distributions (chapters 3 and 4) rather than calculating the probability of discrete EQS exceedance, due to the predicted distributions being inherently wider than the observations. However, point values do not make full use of the BBN's capability of predicting probability distributions which are useful when quantifying risk. Rather than a shortcoming of Bayesian Belief Networks as modelling tools, this issue reflects a broader limitation in regulatory practices, where single-point standards are still favoured over probabilistic approaches (Moe

et al., 2022). In my view, this highlights the need for regulators to evolve beyond point values to fully leverage probabilistic methods that can better inform risk under uncertain conditions.

6.4 Limitations of the BBN approach

Whilst the BBNs developed in this thesis can predict the marginal median and mean TRP concentration during the reference period (2009-2016) well (chapters 3 and 4), the monthly TRP concentrations at the catchment outlet are not as well represented, and the simulations look relatively constant throughout the year. This contrasts with the observed TRP concentrations that show a seasonal pattern (e.g. in Figure 3.5 A and Table 9.5) and is especially evident in the surface-runoff driven catchments (Dunleer and Ballycanew), albeit there is a small improvement in the representation of seasonality when the in-stream P removal process is added (Chapter 4). This lack of seasonality is likely due to two main factors regarding the P sources and how they are represented. Firstly, the equation predicting P release from the soil to the stream developed by Thomas et al., (2016b) is not catchment-specific and is applied equally every month (section 3.3.2.1, and Table 6.1, this section). This is important, as it is a variable the BBNs are sensitive to (section 4.4.3 and Figure 9.2). Secondly, the BBNs for Ballycanew and Dunleer do not represent temporal changes in P sources. Conversely, in the Castledockrell and Timoleague catchments (the groundwater-driven ones), the sources have a monthly signal in groundwater TDP concentration used to derive the groundwater load (discussed in Chapter 4). The groundwater-driven catchments and the surface-driven catchments owe different proportions of stream TRP load to the groundwater component. This proportion is low in Ballycanew and Dunleer, with 45-88% of P transported via quick-flow instead (Mellander et al., 2012), therefore a simpler model structure was adopted in these two catchments. These considerations give the posterior TRP concentrations in Ballycanew and Dunleer a flatter and wider distribution than in the groundwater-pathway-dominated catchments (shown in Chapter 4, Figure 4.3). Nevertheless, the seasonal differences in the observations are mostly evident when comparing summer and winter, at least in the Ballycanew catchment (Chapter 3, Table 3.4). In Chapter 3 we hypothesized that the lack of seasonality shown in the first model iteration could also be due to the model's worse performance in predicting total monthly discharge, especially

evident in June, July, and August. However, in Chapter 5, we demonstrated that the developed BBNs have low sensitivity to the total monthly discharge node used to calculate the target flow-weighted TRP concentration. The lack of seasonality is not important when modelling the status quo with the marginal concentrations (models performed well in the reference period 2009-2016, Chapter 4) for regulatory purposes. However, it remains a hindrance if the objective is to model future seasonal TRP concentrations under climate and land use change scenarios. In the case of Timoleague and Castledockrell, the stream TRP is heavily influenced by the groundwater store: about 60% of stream TRP comes from the baseflow (Mellander et al., 2016), but Chapter 5 highlighted how the two groundwater-driven catchment BBNs do not represent the causal relationship between land use and groundwater P concentrations. As the results of BBN simulations do not depend on what happened in the previous time step, in the BBN the groundwater mixes with the stream water instantaneously and therefore there is no interaction between different stores. This is not because a causal relationship does not exist but rather this reflects our current (in)ability to represent it in the BBN. P transit time from land use to groundwater far exceeds these BBNs' timesteps, and generally BBNs (with the exception Hidden Markov Models) have limited ability to represent temporal dynamics (Moe et al., 2021). Therefore, other research avenues, such as Dynamic Bayesian Networks (DBNs) should be explored, as they might be better suited to represent the groundwater-driven catchments in the present and under future climate scenarios.

Lastly, there are some limitations when using a hybrid BBN compared to a fully continuous or discrete one. Because nodes are represented by probabilities, each model realization propagates uncertainty through the network, thus impacting the shape of the target node. This means that the target node might have the same summary statistics for two different catchments while also showing different distribution shapes, potentially making the BBNs more accurate, but less transferable. Additionally, even when model simulations are "stable", the stochastic nature of the approach makes it so that each posterior distribution drawn will differ slightly from the previous, thus impacting goodness of fit metrics, albeit in the case of the catchment BBNs these were negligible (1% PBIAS variation with each draw).

7. Conclusions and directions for future research

This thesis explored the application of Bayesian Belief Networks to predict phosphorus losses in four Irish agricultural catchments with contrasting agricultural land uses and dominant hydrology. Briefly, catchment-specific BBNs were parameterized with high-frequency (sub-daily) discharge and turbidity measurements (summarized at the daily time step) and high-resolution (field scale) soil data and management information. These were supplemented with data from the literature and EPA reports, expert elicitation, and data at a lower temporal resolution (i.e., piezometer grab data at the monthly scale) when high-resolution and frequency datasets were not available. Sub-hourly stream TRP concentrations summarized at the daily time step were then used to validate the BBNs. The validated BBNs were used to carry out a sensitivity analysis and to integrate multiple climate models to predict future P concentrations. The three research questions (section 1.5) are reported below with a summary of the results obtained. Finally, suggestions for future research are explored in section 7.4.

7.1 Can high-frequency and high-resolution data, coupled with detailed understanding of catchment processes based on long-term monitoring, reduce a BBN's predictive uncertainty?

High-frequency water quality data and high-resolution field-scale management and soil data were used for BBN parameterization and validation. High-frequency data enabled a good performance against a similarly developed BBN evaluated against low-resolution data (Glendell et al., 2022), with the BBNs tested in chapters 3 and 4 being better constrained, especially when considering the last model iterations parameterized for Timoleague and Castledockrell. The data-rich monitoring programme enabled the parameterization of further stores (groundwater P, Chapter 4) and processes (in-stream P uptake, Chapter 4), while simplifying the erosion sub-model and farmyards runoff losses (Chapter 3). However, the BBNs developed here have not been tested and evaluated using low-resolution datasets. Therefore, further research could focus on testing the same BBNs without high-frequency data or with depleted datasets. Specific to the BBNs developed in the ACP, these could be evaluated against the next

monitoring period. Further high-frequency data collection could help to inform priors for the parameters that were developed in this study using weak priors (the septic tanks components) or with non-catchment specific datasets. In the future, high-frequency monitoring can support the validation of already developed BBNs, by either validating already existing priors, or setting up new priors entirely.

7.2 Are Bayesian Belief Networks transferable across agricultural catchments with diverse land uses and hydrology?

We tested the transferability of a BBN developed for a surface-driven grassland catchment and simulating phosphorus concentrations to three Irish agricultural catchments. Without modifications, the model performance was poor in the new catchments, but enhancing the BBN structure to better represent the catchment dynamics improved the performance. BBN enhancements were done by step-wise addition of inputs (sewage treatment works), processes (in-stream P uptake), and groundwater phosphorus pathways. These enhancements are recommended for future applications of the model and demonstrated that the BBN structure developed in Chapter 3, is not transferrable and needs to be further modified besides the parameterization to local conditions. A sensitivity analysis demonstrated parameter redundancy for stream sediments P content, type of effluent treatment in the septic tank (i.e., unknown, primary, or secondary), presence or absence of septic tanks discharging directly into the stream, and number of septic tanks within the catchment. However, further model testing is required to confirm the general redundancy of these parameters or whether this was specific to the catchments considered here.

7.3 What are the projections of climate-induced changes in P concentrations for different hydrological regimes and land uses using a Bayesian Network approach?

The application of climate-driven discharge ensembles with a Bayesian Network framework to predict future P showed no evident trends in stream TRP concentrations regardless of catchment, period, or RCP analysed, with the BBNs essentially replicating the trends shown in the baseline period in Chapter 4. However, the test showed that the model ensemble masked the effects of climate on future TRP

concentrations, as opposed to using single climate models. The sensitivity analysis carried out in Chapter 5 supported the understanding of the modelling framework and aided results interpretation. The ensemble used to drive the SMART hydrological model (Hallouin et al., 2020; Mockler et al., 2016b) obtained different results in terms of NSE and log NSE during both calibration and validation across the four ACP catchments, with only one catchment (Castledockrell) having an acceptable performance in both calibration and validation across the two objective functions (Murphy et al., 2023). At present, it is not possible to disentangle this uncertainty from that associated with the developed BBN model structure, therefore, future research should test the effects of climate-induced changes in these BBN models using a different climate models suite. Ideally, downscaled climate projections from a larger number of models will be tested, with Moe et al., (2022), suggesting ensembles should have at least 30 - 100 climate models. Alternatively, water quality process-based models under climate scenarios can be linked with BBNs to predict the probability of exceeding good ecological status thresholds, as done in Couture et al., (2018).

Finally, future research in modelling climate change in the ACP catchments should focus on developing catchment-specific future land use scenarios and studying the combined effects of both land use and climate change on stream P concentrations.

7.4 Future research

- **BBN upscaling.** This thesis represents the first study to test BBN transferability targeting P losses across catchment types (diverse hydrology and agricultural land uses) using high temporal and spatial resolution data. The major implication for research is that it constitutes a blueprint for the development of an upscaled BBN (i.e., national, or regional scale), to address future water quality requirements from European Union legislation. This upscaling could be based on catchment types (i.e. surface-driven vs groundwater-driven, different land uses, soil types, and management intensities) and be further enhanced with catchment typologies not represented in this study, such as karst catchments (e.g., Mellander et al., 2013).

- **Model intercomparison.** The models developed in chapter 3 and 4 represent the first P model application developed and tested in four ACP catchments. Therefore, with the exception of the ongoing work regarding the parameterization of SimplyP (Hawtree et al., 2023), there was a lack of models to compare this work to. The ACP has been created specifically to monitor measures implemented under the EU Nitrates Directive in terms of monitoring water quality, therefore, modelling was not a priority in the first three phases of the programme. However, the research in this thesis is grounded in the fourth phase of the ACP (2020-2023). The objectives of this phase relevant to this thesis include 1) the catchments intercomparison through the use of models and 2) the analysis of the National Action Programme (NAP) measures (Teagasc - Agriculture and Food Development Authority, 2020). To deliver on these objectives, it was necessary to set up and run the models and the analyses (including the ones conducted here) first, therefore these are becoming available at the end of this PhD project. Phan et al., (2016), highlighted a lack of studies comparing BBN performance with other models. Future work should involve further modelling approaches including statistical and process-based ones in the ACP catchments, allowing the intercomparison of the developed BBNs with models parameterized with high-frequency datasets.
- **BBN intercomparison.** The literature review conducted in Chapter 1.4 (Table 1.1) showed that BBN studies have been carried out in catchments and basins that are not comparable to the ACP in terms of size and climate e.g., China and Italy (Jin et al., 2020; Sperotto et al., 2019a, 2019b). Although in chapters 3 and 4 a comparison was made with results presented in Glendell et al., (2022), it was not possible to verify whether the catchments in the two studies have comparable hydrological processes. Similarly, Lucci et al., (2014), used data from other sites for comparison of their modelling results. BBN intercomparison is not always possible as different criteria are used to evaluate the goodness of fit of models (Chapter 1.4) and when models included P pollution, the final target node (or the node of interest) was not always stream P concentration (de Vries et al., 2021; Jin et al., 2020; Penk et al., 2022).

- **Spatial BBN applications.** In the first phases of BBN development, a preliminary spatial application of the model was tested using the R package *bnspatial* (Masante, 2019). This package allows the modeler to run any discrete BBN spatially, using any resolution of spatial unit. During the research, it became evident that discretizing the BBN developed using high-frequency data would be a labour-intensive task whose results would be unpredictable, with the results of the spatial application entirely dependent on the discretization methodology. It would also defeat the purpose of using the high-frequency dataset. Further, Glendell et al., (2022) have shown that two model conceptualizations (and possibly two parameterizations) are necessary when running both a hybrid and a spatially applied discrete BBN. If *bnspatial* is used to map the expected value (or most likely state) of the target node, this is akin to considering significant quantiles of the target distribution (as was done in chapters 3 and 4) at the desired spatial scale (i.e. field scale or raster cell). Given that there is stream data available at the sub-catchment scale for the ACP, using *bnspatial* isn't advantageous, because the BBN could simply be run for the sub-catchments, making the BBN semi-distributed. Meanwhile, a spatial application where interactions among spatial units would be an interesting avenue of research (such as the platform developed by Stritih et al., 2020), but is not possible using *bnspatial* as the package hasn't been further developed or maintained (CRAN, 2023), therefore future research should focus on expanding the available spatial tools.
- **Bayesian updating.** As discussed in Chapter 4, the predicted TRP distributions are wider and more skewed than the observations, therefore the current BBNs could be improved upon by making the posterior distributions more representative of the observations, perhaps by using Bayesian updating, i.e. iteratively incorporating new data to calculate the posterior, with the new posterior serving as the prior for the next update cycle. Bayesian updating could also be used to improve the current BBNs' TRP predictions under climate change, because it allows for continuous refinement of impact estimates as new climate data emerges, which leads to more accurate predictions than traditional frequentist methods (Mann et al., 2017).

8. Supplementary Materials to Chapter 3

A tool to reduce phosphorus pollution in the Agricultural Catchment Programme catchments: model screening

8.1 Aim

To develop a Bayesian Belief Network (BBN) to use as Decision Support Tool (DST) for stakeholders, decision, and policy makers to help predict phosphorus (P) losses in Irish agricultural catchments.

8.2 Background

Bayesian Networks or Bayesian Belief Networks (BBNs) are probabilistic graphical models that allow the integration of quantitative and qualitative information from different sources (e.g., experimental data, other model outputs and expert opinion) in one model (Barton et al., 2012; Kragt, 2009). The graphs in the BBN provide a transparent and interpretable representation of the causal relationships between the response variable, i.e., in this study, phosphorus concentrations in the stream, and the explanatory variables, meaning causes of phosphorus loss to waters**.** These relationships can be built with the participation of experts and stakeholders.

The causal relationships are represented using probability distributions for variables that explicitly capture assumptions about how the explanatory variables relate to phosphorus losses and the associated uncertainly. This results in transparent and explicit model of phosphorus loss to the stream, with an improved understanding and representation of risk and variability in the model outcome enabling interpretation and transparency in the approach and assumptions made. The relationships between variables (nodes) in a BBN are described with conditional probability distributions rather than through deterministic relationships (Borsuk et al., 2004). Relationships between discrete variables may be represented and quantified with **conditional probability tables (CPTs)**. The probability distribution of a node is calculated from the probability of the causes combined according to Bayes' rule, which describes the probability of an event happening given a prior knowledge around the event (Moe et al., 2021). In CPTs, the probability of an event occurring is expressed on a scale from 0 to 1, where 0 represents impossible events and 1 represents certain events. Examples of CPTs are given in Figure 8.1 and 8.2.

▶	yes	0.0013333...
	no	0.99866667

Figure 8.1 Example of CPT. According to the Breast Cancer Surveillance Consortium, 4 in 3000 women in their forties have cancer, which translates in a 0.001 probability to have it (yes), and a 0.99 probability not to have it (no).

Breast Cancer	yes	no
▶ positive	0.75	0.12016021
negative	0.25	0.87983979

Figure 8.2 Another example of CPT. What is the probability of having a positive test? If a woman in her forties has breast cancer (yes column), the probability of a positive test is 0.75, while the probability of having a negative test (false negative) is 0.75. When there is no cancer (no column), the probability of having a positive test (false positive) is 0.12, and the probability of a negative test is 0.88.

8.3 Topic

The proposed model is a module of the tool being developed, and it is focussed on phosphorus pollution within the Ballycanew agricultural catchment. Figure 8.3 provides an overview of the main sub-models (parts of the model thematically grouped together), and during the workshop the participants will have the chance to explore all the variables in detail.

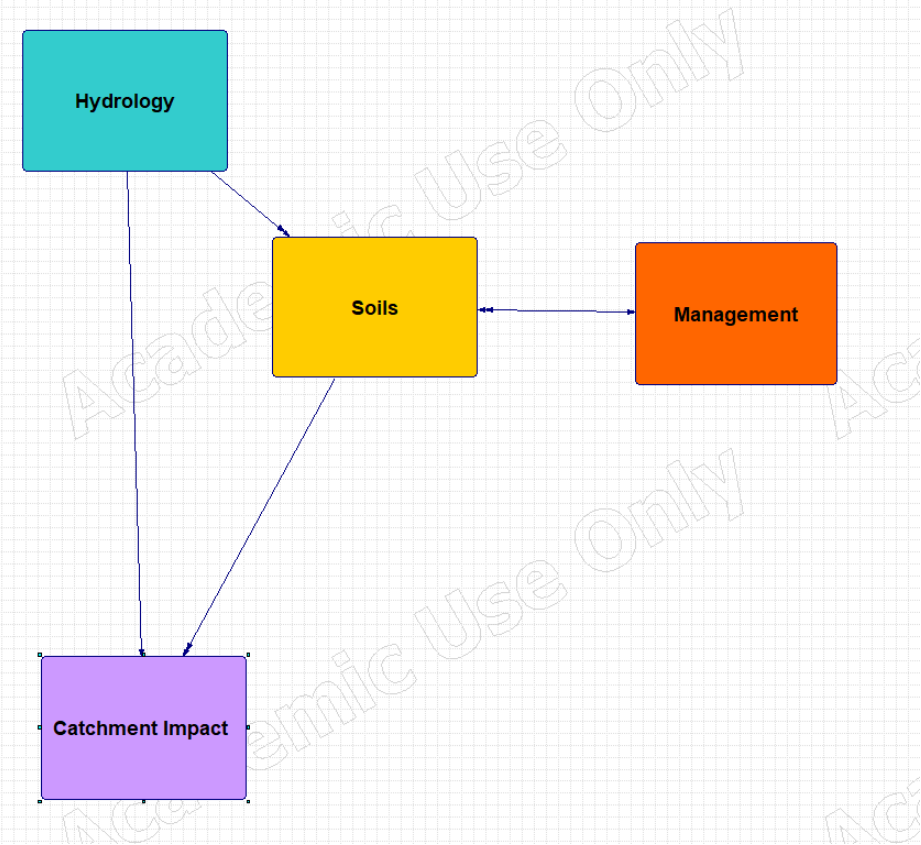

Figure 8.3 Variables determining phosphorus concentrations in the stream were group together in three main sub-models: hydrology, Soils, and Management. The Catchment Impact sub-model describes phosphorus loads at catchment scale, as well as phosphorus concentrations in the stream.

8.4 Workshop Objectives

We would like you to screen the proposed model and consider the causal relationships between variables.

After the workshops

We would like you to take part in an anonymous survey and provide feedback on the session. We would also like to hear if you have any additional comments that you might have not had at the time of the workshop.

8.5 Participants' role

We would like you to provide feedback on:

- the conceptual model structure, ensuring that the causal dependencies between variables make sense and none are missing
- characterizing the causal relationships
- the appropriate datasets in support of model variables and recommendations for further information sources (e.g. reports, publications, datasets etc)

8.6 Personal data

This research is being conducted as part of Camilla Negri's PhD research at the University of Reading and is funded by the Teagasc Walsh Fellowship Ref. No 2019021, in partnership with the James Hutton Institute (JHI) and the University of Reading (UoR). The supervisory Team includes Dr Miriam Glendell (JHI), Dr Per-Erik Mellander (Agricultural Catchments Programme, Teagasc), Dr Nicholas J. Schurch (JHI/ Biomathemathics and Statistics Scotland), and Prof. Andrew J. Wade (UoR).

The experts' (you) personal data will be stored in a pseudonymized form on Hutton servers, and notes from the workshop will be shared exclusively with the supervisory team. In addition, the data gathered in this research will be published in the PhD thesis (all UoR thesis can be downloaded from an online repository (http://centaur.reading.ac.uk/), as well as in (Open Access) scientific journals. Any summary workshop content, that will made available through the PhD thesis or other academic outlets will be anonymized prior to publication, so that you cannot be identified, and care will be taken to ensure that other information in the interview that could identify yourself is not revealed.

This research has been approved by the Research Ethics Committee at the James Hutton Institute.

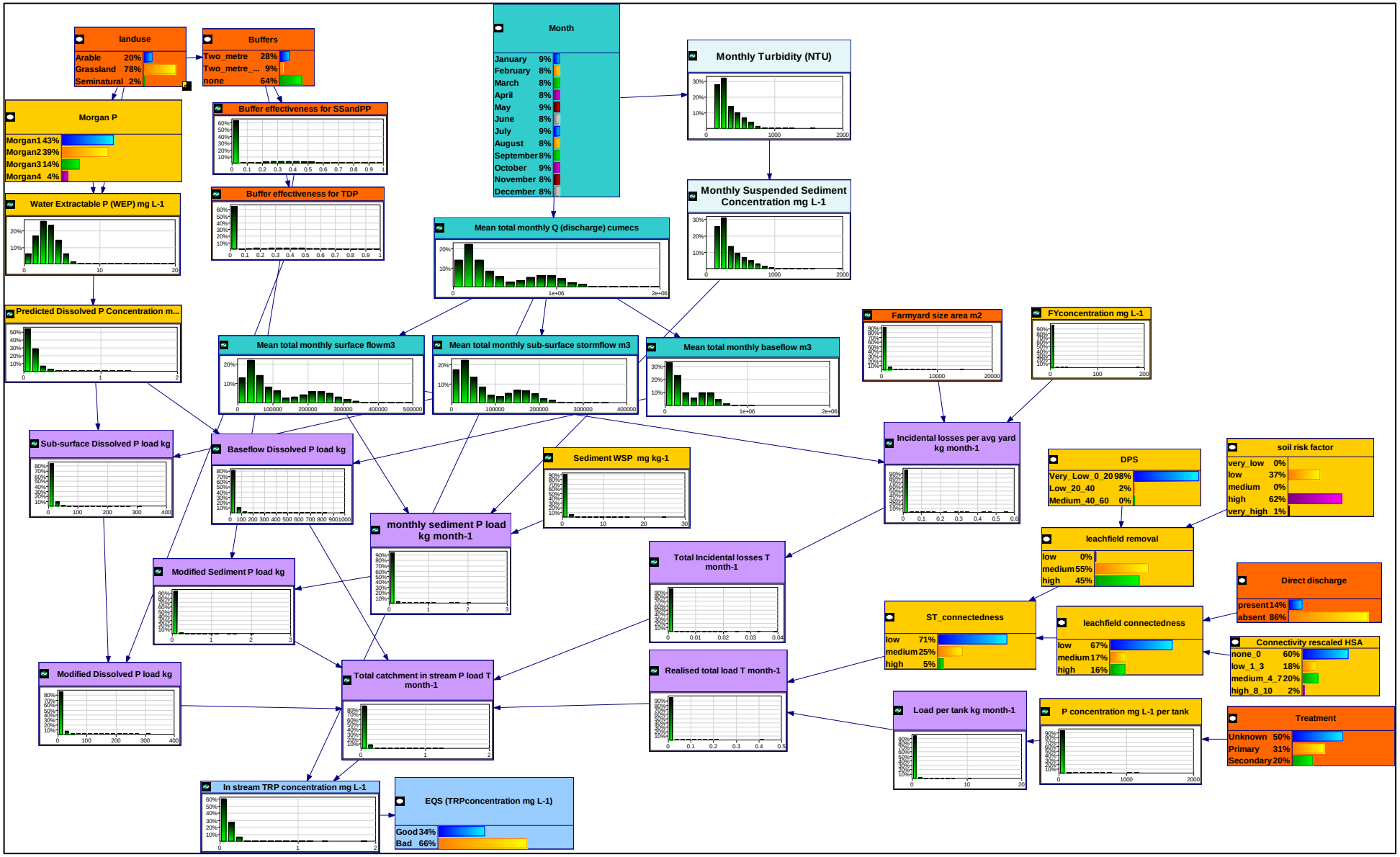

Figure 8.1 Illustration of the BBN developed in Chapter 3 for the Ballycanew catchment, this time showing histograms and bar charts of the full distributions.

9. Supplementary Materials to Chapter 4

Table 9.1 Data availability for the BBN nodes. Variables pertaining to the calculated loads and those nodes parametrized as logical Conditional Probability Tables are not reported here but specified for each catchment.

Node or variable name	**Data availability**	**Model structure implementing the variable**
Mean total monthly Q (discharge) [m^3]	Catchment specific	All model structures
Mean total monthly Surface Flow (surface runoff) [m^3]	Catchment specific	All model structures
Mean total monthly Sub-surface Stormflow (subsurface runoff) [m^3]	Catchment specific	All model structures
Mean total monthly Baseflow [m^3]	Catchment specific	All model structures
Land use	Catchment specific	All model structures
Buffers	Not catchment specific	All model structures
Buffer effectiveness for Particulate P (PP) and suspended sediments (SS)	Not catchment specific	All model structures
Buffer effectiveness for Total Dissolved P (TDP)	Not catchment specific	All model structures
Morgan P	Catchment specific	All model structures
Monthly Turbidity [NTU $month^{-1}$]	Catchment specific	All model structures
Monthly Suspended Sediment concentration [mg l^{-1} $month^{-1}$]	Catchment specific	All model structures
Water Extractable P (WEP) [mg l^{-1}]	Catchment specific	All model structures
Sediment Water Soluble P [mg kg^{-1}]	Only available for Ballycanew and Castledockrell	All model structures
Predicted Dissolved P Concentration [mg l^{-1}]	Not catchment specific	All model structures
P concentration per tank [mg l^{-1}]	Not catchment specific	All model structures
Direct discharge	Not catchment specific	All model structures
Degree of Phosphorus Saturation (DPS) [%]	Catchment specific	All model structures
Soil risk factor	Catchment specific	All model structures
Connectivity rescaled (Hydrologically Sensitive Areas, HSA)	Catchment specific	All model structures
Farmyard size area [m^2]	Catchment specific	All model structures
Farmyard P concentration [mg l^{-1}]	Catchment specific	All model structures
Number of Septic Tanks	Only available for Ballycanew	All model structures
Septic Tank Treatment	Only available for Ballycanew and Castledockrell	Structure 1 only
Groundwater Dissolved P Concentration [mg l^{-1}]	Implemented for Timoleague and Castledockrell	Structure 4 and 5 (Timoleague and Castledockrell), Structure 6 (Castledockrell)
In-stream winter P removal	From expert elicitation, catchment specific	Structure 2 (Ballycanew and Dunleer), Structure 5 (Timoleague and Castledockrell), Structure 6 (Castledockrell)
In-stream spring P removal	From expert elicitation, catchment specific	
In-stream summer P removal	From expert elicitation, catchment specific	
In-stream autumn P removal	From expert elicitation, catchment specific	
Sewage Treatment Works (STWs) P concentration [mg l^{-1}]	Castledockrell only	Structure 6 (Castledockrell)

9.1 Timoleague model specifications

Table 9.2 Timoleague model structure (filename Ptool_pointanddiffuse_v7_Timoleague.xdsl)

<table>
<tr><th>Variable (symbol) [unit]</th><th colspan="2">Conditional Probability Table or states and discretisation boundaries for continuous nodes</th><th>Description</th></tr>
<tr><td colspan="4">Hydrology sub-model (Drivers)</td></tr>
<tr><td>Month</td><td>Each month</td><td></td><td>Calculated as No. days in the month/ 365</td></tr>
<tr><td rowspan="5">Mean total monthly Q (discharge) [m^3]</td><td>Very Low</td><td>0-202577</td><td rowspan="5">Bootstrapped from daily total discharge observations (2009-2016) to obtain a Lognormal (μ; σ) discharge distribution with base e for each month. Each month’s parameters are shown in the table. Discretization of states is based on percentiles calculated from the average monthly observations (very low<= 5th percentile, low= 5th-25th percentile, medium= 25th-50th percentile, high= 50th-75th percentile, very high= 75th-100th percentile).
<table><tr><th></th><th>μ</th><th>σ</th></tr><tr><td>January</td><td>13.8</td><td>0.1</td></tr><tr><td>February</td><td>13.8</td><td>0.1</td></tr><tr><td>March</td><td>12.8</td><td>0.1</td></tr><tr><td>April</td><td>12.6</td><td>0.1</td></tr><tr><td>May</td><td>12.2</td><td>0.1</td></tr><tr><td>June</td><td>12.2</td><td>0.2</td></tr><tr><td>July</td><td>12.2</td><td>0.3</td></tr><tr><td>August</td><td>12.1</td><td>0.4</td></tr><tr><td>September</td><td>12.1</td><td>0.4</td></tr><tr><td>October</td><td>12.4</td><td>0.2</td></tr><tr><td>November</td><td>13.4</td><td>0.1</td></tr><tr><td>December</td><td>13.6</td><td>0.2</td></tr></table></td></tr>
<tr><td>Low</td><td>202577-277340</td></tr>
<tr><td>Medium</td><td>277340-603944</td></tr>
<tr><td>High</td><td>603944-934347</td></tr>
<tr><td>Very High</td><td>934347-990000</td></tr>
<tr><td rowspan="5">Mean total monthly Surface Flow (surface runoff) [m^3]</td><td>Very Low</td><td>0-16207</td><td rowspan="5">Calculated as a portion of mean monthly runoff (8%), via hydrograph separation method described in Mellander et al., (2012). Discretization of states is based on percentiles calculated from observations.</td></tr>
<tr><td>Low</td><td>16207-22188</td></tr>
<tr><td>Medium</td><td>22188-48316</td></tr>
<tr><td>High</td><td>48316-74748</td></tr>
<tr><td>Very High</td><td>74748-79070</td></tr>
<tr><td rowspan="5">Mean total monthly Sub-surface Stormflow (subsurface runoff) [m^3]</td><td>Very Low</td><td>0-8104</td><td rowspan="5">Calculated as a portion of mean monthly runoff (4%), via hydrograph separation method described in Mellander et al., (2012). Discretization of states is based on percentiles calculated from observations.</td></tr>
<tr><td>Low</td><td>8104-11094</td></tr>
<tr><td>Medium</td><td>11094-24158</td></tr>
<tr><td>High</td><td>24158-37374</td></tr>
<tr><td>Very High</td><td>37374-39540</td></tr>
<tr><td rowspan="5">Mean total monthly Baseflow [m^3]</td><td>Very Low</td><td>0-178268</td><td rowspan="5">Calculated as a portion of mean monthly runoff (56%), via hydrograph separation method described in Mellander et al., (2012). Discretization of states is based on percentiles calculated from observations .</td></tr>
<tr><td>Low</td><td>178268-244060</td></tr>
<tr><td>Medium</td><td>244060-531471</td></tr>
<tr><td>High</td><td>531471-822225</td></tr>
<tr><td>Very High</td><td>822225-869748</td></tr>
</table>

<table>
<tr><td colspan="4">Management (Drivers)</td></tr>
<tr><td rowspan="3">Land use</td><td colspan="2">Arable</td><td>0.04</td><td rowspan="3">As reported by Teagasc - Agriculture and Food Development Authority, (2018).</td></tr>
<tr><td colspan="2">Grassland</td><td>0.89</td></tr>
<tr><td colspan="2">Seminatural</td><td>0.07</td></tr>
<tr><td>Buffers</td><td colspan="2"><table><tr><th>Land use</th><th>Arable</th><th>Grassland</th><th>Seminatural</th></tr><tr><td>2 m</td><td>0.98</td><td>0.01</td><td>$1.01*10^{-6}$</td></tr><tr><td>>2 m</td><td>0.019</td><td>0.01</td><td>$1.01*10^{-6}$</td></tr><tr><td>none</td><td>0.001</td><td>0.08</td><td>0.999</td></tr></table></td><td></td><td>Buffer strips are defined as being 2 m in width, more than 2 m in width, or absent. Probabilities of having either type of buffer according to land use were agreed upon with one of the ACP advisors (expert) during consultation.</td></tr>
<tr><td rowspan="5">Buffer effectiveness for Particulate P (PP) and suspended sediments (SS)</td><td colspan="2">Very Low</td><td>0-0.2</td><td rowspan="5">Dependent on the variable Buffers. For 2 m buffers, effectiveness is defined as Beta (α=2.9; β=4.5); for >2 m buffers it is defined as Beta (α=1.44; β=0.789); for no buffers, effectiveness is equal to 0. The distributions were fitted to the dataset published in Stutter et al., (2021), where negative retention data was deleted from the analysis.</td></tr>
<tr><td colspan="2">Low</td><td>0.2-0.4</td></tr>
<tr><td colspan="2">Medium</td><td>0.4-0.6</td></tr>
<tr><td colspan="2">High</td><td>0.6-0.8</td></tr>
<tr><td colspan="2">Very High</td><td>0.8-1</td></tr>
<tr><td rowspan="5">Buffer effectiveness for Total Dissolved P (TDP)</td><td colspan="2">Very Low</td><td>0-0.2</td><td rowspan="5">Dependent on the variable Buffers. For Buffers 0-2 m, Buffer effectiveness is defined as Beta (α=1.8; β=2.7), for >2 m buffers it is defined as Beta (α=1; β=0.8); for no buffers, effectiveness is equal to 0. The distributions were fitted to the dataset published in Stutter et al., (2021), where negative retention data was deleted from the analysis.</td></tr>
<tr><td colspan="2">Low</td><td>0.2-0.4</td></tr>
<tr><td colspan="2">Medium</td><td>0.4-0.6</td></tr>
<tr><td colspan="2">High</td><td>0.6-0.8</td></tr>
<tr><td colspan="2">Very High</td><td>0.8-1.0</td></tr>
<tr><td colspan="4">Soil erosion and soil P sub-model</td></tr>
<tr><td>Morgan P</td><td colspan="2"><table><tr><th></th><th>Arable</th><th>Grassland</th><th>Seminatural</th></tr><tr><td>Morgan1</td><td>0.163</td><td>0.163</td><td>0</td></tr><tr><td>Morgan2</td><td>0.442</td><td>0.225</td><td>0.6</td></tr><tr><td>Morgan3</td><td>0.289</td><td>0.42</td><td>0.3</td></tr><tr><td>Morgan4</td><td>0.106</td><td>0.192</td><td>0.1</td></tr></table></td><td></td><td>Based on land use, proportions of land for each level and in each land use category were calculated based on the soil survey carried out in 2013 in the catchment. Where the Morgan P index was unknown, that proportion of land was assigned to the dominant index category. For the interpretation of the Soil Morgan P Index, the reader is referred to Regan et al., (2012).</td></tr>
<tr><td rowspan="6">Monthly Turbidity [NTU $month^{-1}$]</td><td colspan="2">Very Very Low</td><td>0-500</td><td rowspan="6">Bootstrapped from daily average turbidity observations (2009-2016) to obtain a Lognormal (μ; σ) turbidity distribution with base e for each month. Each month’s parameters are shown in the table. Discretization of states is based on percentiles calculated from the average monthly observations.</td></tr>
<tr><td colspan="2">Very Low</td><td>500-664</td></tr>
<tr><td colspan="2">Low</td><td>664-946</td></tr>
<tr><td colspan="2">Medium</td><td>946-1115</td></tr>
<tr><td colspan="2">High</td><td>1115-2060</td></tr>
<tr><td colspan="2">Very High</td><td>2060-2680</td></tr>
</table>

<table>
<tr><td></td><td></td><td></td><td></td></tr>
<tr><td>Monthly Suspended Sediment concentration [mg l^{-1} $month^{-1}$]</td><td>Very Very Low</td><td>0-52</td><td rowspan="6">Calculated as: a * Monthly Turbidity [NTU $month^{-1}$] ^{b}, where a= 0.6636, and b= 1.1045, as described in Sherriff et al., (2015). Discretization of states is based on percentiles calculated from the average monthly calculated observations.</td></tr>
<tr><td>Very Low</td><td>52-73</td></tr>
<tr><td>Low</td><td>73-104</td></tr>
<tr><td>Medium</td><td>104-124</td></tr>
<tr><td>High</td><td>124-268</td></tr>
<tr><td>Very High</td><td>268-380</td></tr>
<tr><td rowspan="4">Water Extractable P (WEP) [mg l^{-1}]</td><td>Low</td><td>0-3</td><td rowspan="4">Based on variable “Morgan P levels” and “land use” (data from 2013) it is calculated with the equations available in (Thomas et al., 2016b): for Grassland, WEP=0.57 * Morgan P + 0.29, for Arable: WEP= 0.36 * Morgan P + 0.89, where Morgan P is defined as a Uniform distribution with the following parameters:
<table><tr><th>Morgan P Index</th><th>Grassland</th><th>Arable</th></tr><tr><td>Index 1</td><td>a=0; b=3</td><td>a=0; b=3</td></tr><tr><td>Index 2</td><td>a=3.1; b=5</td><td>a=3.1; b=6</td></tr><tr><td>Index 3</td><td>a=5.1; b=8</td><td>a=6.1; b=10</td></tr><tr><td>Index 4</td><td>a=8.1; b=30</td><td>a=10.1; b=30</td></tr></table>
For the Seminatural Land use, WEP was assumed constant to 0.001. Discretization is based on Morgan P discrete levels.</td></tr>
<tr><td>Medium</td><td>3-5</td></tr>
<tr><td>High</td><td>5-8</td></tr>
<tr><td>Very High</td><td>8-15</td></tr>
<tr><td rowspan="5">Sediment Water Soluble P [mg kg^{-1}]</td><td>Very Low</td><td>0-0.0995</td><td rowspan="5">Defined as a Lognormal distribution (μ=-0.9, σ=1), fitted with the SHELF R package (version 1.8.0, Oakley, 2020) to observed Water Extractable P in the catchment sediments (Shore et al., 2016). Discretization of states is based on percentiles calculated from the observations. Based on Ballycanew data.</td></tr>
<tr><td>Low</td><td>0.0995-0.2100</td></tr>
<tr><td>Medium</td><td>0.2100-0.3550</td></tr>
<tr><td>High</td><td>0.3550-0.9100</td></tr>
<tr><td>Very High</td><td>0.9100-8</td></tr>
</table>

	μ	σ
January	5.42	0.17
February	5.23	0.14
March	5.07	0.15
April	4.92	0.13
May	4.75	0.17
June	4.58	0.14
July	4.32	0.14
August	4.29	0.18
September	3.80	0.16
October	4.31	0.22
November	4.71	0.20
December	5.48	0.30

<table>
<tr><td rowspan="6">Predicted Dissolved P Concentration [mg l^{-1}]</td><td>Very Very Low</td><td>0-0.1</td><td rowspan="6">Dependant on Water Extractable P, it is defined with the linear model: Predicted Dissolved P = β(WEP)+α, where β =0.08, α =0.158, derived from (Thomas et al., 2016b). This equation is derived from data gathered during the closed period only, that is, when farmers are forbidden from spreading fertilizer. An assumption is made that when the linear model yields a negative value, that is resampled as a zero. Water Extractable P is considered a good in-stream TRP/ TDP predictor in the ACP catchments by the experts, however careful consideration is needed when choosing a soil P test in a different setting.</td></tr>
<tr><td>Very Low</td><td>0.1-0.5</td></tr>
<tr><td>Low</td><td>0.5-1.5</td></tr>
<tr><td>Medium</td><td>1.5-5</td></tr>
<tr><td>High</td><td>5-8</td></tr>
<tr><td>Very High</td><td>8-15</td></tr>
<tr><td rowspan="6">Groundwater Dissolved P Concentration [mg l^{-1}]</td><td>Very Very Low</td><td>0-0.1</td><td rowspan="6">Derived from monthly piezometer data of TDP concentrations (2009-2016) monitored in multi-level wells described in Mellander et al., (2016).
<table><tr><th></th><th>μ</th><th>σ</th></tr><tr><td>January</td><td>-3.00</td><td>0.16</td></tr><tr><td>February</td><td>-2.70</td><td>0.12</td></tr><tr><td>March</td><td>-2.60</td><td>0.12</td></tr><tr><td>April</td><td>-2.90</td><td>0.10</td></tr><tr><td>May</td><td>-2.45</td><td>0.10</td></tr><tr><td>June</td><td>-2.67</td><td>0.06</td></tr><tr><td>July</td><td>-2.69</td><td>0.06</td></tr><tr><td>August</td><td>-2.22</td><td>0.21</td></tr><tr><td>September</td><td>-2.62</td><td>0.07</td></tr><tr><td>October</td><td>-2.74</td><td>0.17</td></tr><tr><td>November</td><td>-2.70</td><td>0.20</td></tr><tr><td>December</td><td>-3.00</td><td>0.20</td></tr></table></td></tr>
<tr><td>Very Low</td><td>0.1-0.5</td></tr>
<tr><td>Low</td><td>0.5-1.5</td></tr>
<tr><td>Medium</td><td>1.5-5</td></tr>
<tr><td>High</td><td>5-8</td></tr>
<tr><td>Very High</td><td>8-15</td></tr>
<tr><td rowspan="2">Sub-surface Dissolved P load [kg $month^{-1}$]</td><td>Low</td><td>0-3</td><td rowspan="2">Calculated as the product of Predicted Dissolved P concentration and Subsurface Storm-flow.</td></tr>
<tr><td>High</td><td>3-200</td></tr>
<tr><td rowspan="2">Baseflow Dissolved P load [kg $month^{-1}$]</td><td>Low</td><td>0-3</td><td rowspan="2">Calculated as the product of Predicted Dissolved P concentration and Baseflow.</td></tr>
<tr><td>High</td><td>3-200</td></tr>
<tr><td rowspan="2">Modified Dissolved P load [kg $month^{-1}$]</td><td>Low</td><td>0-3</td><td rowspan="2">Based on “Buffer effectiveness for Total Dissolved P”, for effective buffers, modified Dissolved P load= Sub-surface Dissolved P load *(1-Buffer effectiveness for TDP). Based on expert recommendation.</td></tr>
<tr><td>High</td><td>3-200</td></tr>
<tr><td rowspan="2">Monthly Sediment P load [kg $month^{-1}$]</td><td>Low</td><td>0-3</td><td rowspan="2">Calculated as the product of Sediment Water Soluble P [mg kg^{-1}], Monthly Suspended Sediment concentration [mg l^{-1} $month^{-1}$] , and Mean total monthly surface flow [m^3] .</td></tr>
<tr><td>High</td><td>3-200</td></tr>
<tr><td rowspan="2">Modified Sediment P load [kg $month^{-1}$]</td><td>Low</td><td>0-3</td><td rowspan="2">Based on “Buffer effectiveness for Suspended Sediments and Particulate P”, for effective buffers, Modified Sediment P load=</td></tr>
<tr><td>High</td><td>3-200</td></tr>
</table>

<table>
<tr><td></td><td></td><td></td><td>Monthly Sediment P load [kg month^{-1}]*(1-Buffer effectiveness for SS and PP). Based on expert recommendation.</td></tr>
<tr><td colspan="4">Septic Tanks (ST) sub-model (Point P sources)</td></tr>
<tr><td rowspan="5">P concentration per tank [mg l^{-1}]</td><td>Absent (to represent 0 STs)</td><td>0-1*10^{-8}</td><td rowspan="5">P concentration is dependent on the treatment type. If the treatment is unknown, the concentration is defined as a Lognormal distribution (μ=2.9, σ =1.25), based on a literature review of data available for Ireland (Environmental Protection Agency Ireland (EPA), 2003, 2000; Gill et al., 2005, 2007) (n=8). Fitting was done with R package fitdistrplus (version 1.1-8, Delignette-Muller et al., 2020). Otherwise, for primary and secondary treatment concentration is defined as Truncated Normal distribution (μ=10; σ=1), and (μ=5; σ=0.5) respectively, as described in Glendell et al., (2021) and derived from SEPA guidelines (Brownlie et al., 2014). All tanks are assumed to be maintained. Discretization was also based on the literature review.</td></tr>
<tr><td>Low</td><td>1*10^{-8}-1</td></tr>
<tr><td>Medium</td><td>1-18</td></tr>
<tr><td>High</td><td>18-35</td></tr>
<tr><td>Very High</td><td>35-100</td></tr>
<tr><td rowspan="2">Direct discharge</td><td>Present</td><td>0.16</td><td rowspan="2">Probabilities are derived from the report by the Environmental Protection Agency Ireland (EPA, 2015).</td></tr>
<tr><td>Absent</td><td>0.84</td></tr>
<tr><td rowspan="3">Degree of Phosphorus Saturation (DPS) [%]</td><td>Very Low_0-20</td><td>0.674</td><td rowspan="3">Discretization is equal to the 20^{th,} 40th, 60th, and 80th quantiles, however 0< DPS <60 in this catchment. Probabilities were calculated from available spatial data (Wall et al., 2012).</td></tr>
<tr><td>Medium_20-40</td><td>0.324</td></tr>
<tr><td>High_40-60</td><td>0.002</td></tr>
<tr><td rowspan="5">Soil risk factor [adimensional]</td><td>Low</td><td>0.766</td><td rowspan="5">An indicator to describe the combined risk of effluent leaching to the groundwater table with the risk of the effluent being transported with surface runoff. This approach is a simplification of the one adopted in Glendell et al., (2021). The risk factor was obtained by overlaying the soil series (Thomas et al., 2016b) with information on the position of the groundwater table (0- 2 m below ground or more than 2 m below ground). Because little is known regarding the septic tanks in the catchment (i.e. age, type of treatment, maintenance), and the groundwater table position (few datapoints within the catchment) experts recommended a precautionary principle. This meant that the class at most risk of effluent transfer was applied when data was unavailable. The table to the left represents a synthesis of the classification approach. Probabilities are based on land cover proportion.</td></tr>
<tr><td>Medium</td><td>0.118</td></tr>
<tr><td>High</td><td>0</td></tr>
<tr><td>Very High</td><td>0.116</td></tr>
<tr><td colspan="2"><table>
<tr><td></td><td colspan="2">Groundwater Table Position</td></tr>
<tr><td>Soil Series</td><td>0-2 m below surface</td><td>>2 m below surface</td></tr>
<tr><td>Brown earths</td><td>High Risk</td><td>Moderate Risk</td></tr>
<tr><td>Gleys</td><td>Very High Risk</td><td>Very High Risk</td></tr>
</table></td></tr>
<tr><td>Leachfield removal</td><td colspan="2"><table>
<tr><th>Soil risk factor</th><th>DPS</th><th>Low</th><th>Medium</th><th>High</th></tr>
<tr><td rowspan="3">Low</td><td>Very Low</td><td>0</td><td>0.3</td><td>0.7</td></tr>
<tr><td>Medium</td><td>0</td><td>0.7</td><td>0.3</td></tr>
<tr><td>High</td><td>0.3</td><td>0.7</td><td>0</td></tr>
<tr><td rowspan="3">Medium</td><td>Very Low</td><td>0</td><td>0.5</td><td>0.5</td></tr>
<tr><td>Medium</td><td>0</td><td>1</td><td>0</td></tr>
<tr><td>High</td><td>0.5</td><td>0.5</td><td>0</td></tr>
</table></td><td>The node refers to P removal from septic drains. Conditional on P leaching risk from Degree of Phosphorus Saturation (DPS). The conditional probability table is a logical one.</td></tr>
</table>

		High	**Very Low**	0	0.7	0.3	
			Medium	0.3	0.7	0	
			High	0.7	0.3	0	
		Very High	**Very Low**	0	0.5	0.5	
			Medium	0.5	0.5	0	
			High	1	0	0	

Leachfield connectedness	**HSA rescaled**	**None**		**Low**		**Medium**		**High**		Probabilities are conditional on the presence/absence of Direct ST discharge, and HSA (node: Connectivity rescaled HSA). Where Direct discharge is present, connectedness is assumed as 'high'. Where Direct discharge is absent, the risk class of the HSA is assigned.
	Direct discharge	**pres**	**abs**	**pres**	**abs**	**pres**	**abs**	**pres**	**abs**	
	low	0	1	0	1	0	0	0	0	
	medium	0	0	0	0	0	1	0	0	
	high	1	0	1	0	1	0	1	1	

Septic Tank connectedness	**Leachfield removal**	**Low**			**Medium**			**High**			Probabilities are conditional on Leachfield removal and Leachfield connectedness. Where Leachfield removal is 'low' or 'High', Leachfield connectedness remains unaltered.
	Leachfield connectedness	**Low**	**Medium**	**High**	**Low**	**Medium**	**High**	**Low**	**Medium**	**High**	
	Low	1.0	0.0	0.0	1.0	0.0	0.0	1.0	0.5	0.0	
	Medium	0.0	1.0	0.0	0.0	1.0	0.5	0.0	0.5	1.0	
	High	0.0	0.0	1.0	0.0	0.0	0.5	0.0	0.0	0.0	

Connectivity rescaled HSA [adimensional]	None_0	0.09	Data extracted from spatial layers of Hydrologically Sensitive Areas (HSAs) rescaled between 0 and 10 was provided by the Agricultural Catchments Programme (Thomas et al., 2016a). Discretization is also based on the spatial layers.
	Low_1-3	0.78	
	Medium_4-7	0.12	
	High_8-10	0.01	
Load per tank [kg month^{-1}]	Absent	0-1*10^{-6}	Specified as the product of ST density [No ha^{-1}] * ST concentration [mg l^{-1}] * 120 [L] average daily water consumption per person * 365/12 days in a month* average No of persons per household 2.7/1*10^{6}. Discretisation is based on interpolation to represent plausible probabilities for combination of extreme risk classes (e.g. High+high=high, low+low=low).
	Very Low	1*10^{-6}-0.1	
	Low	0.1-0.5	
	Medium	0.5-1.0	
	High	1.0-2.0	
	Very High	2.0-30	
Total Realized load [T month^{-1}]	Very Low	0.0-0.1	Calculated as the product of septic tank load and delivery factors (D) related to the connectedness of a septic tank, based on the median estimated fraction to be delivered in Table 13 of the report by Glendell et al., (2021) and the number of septic tanks present within catchment boundary (N): Realised load per tank [kg month^{-1}] * N * D / 1000. In this case, N= 88. Discretisation based on interpolation
	Low	0.1-0.5	
	Medium	0.5-1.0	
	High	1.0-2.0	
	Very High	2.0-12	

		Septic tank connectedness	**Delivery factor (D)**	**Reference**	to represent plausible probabilities for combination of extreme risk classes.
		Low	0.05	"very low" category in Appendix A3, Glendell et al., (2021)	
		Medium	0.30	"medium" category in Appendix A3, Glendell et al., (2021)	
		High	0.80	"very high" category in Appendix A3, Glendell et al., (2021)	
Farmyards sub-model (Point P sources)					
Farmyard size area [m^2]	Very Low	0-38			Based on available farmyard survey, a distribution was fitted to farmyard area data: Lognormal (μ=-5.13; σ=1.01). Discretization of states is based on percentiles calculated from the observations.
	Low	38-98			
	Medium	98-160			
	High	160-317			
	Very High	317-3100			
Farmyard P concentration [mg l^{-1}]	Very Low	0-0.01			Using the *SHELF* R package (version 1.8.0, Oakley, 2020), a distribution was fitted to the data in Table 2 in Harrison et al., (2019): Lognormal (μ=-1.8; σ=1.6). The best fit would have been the LogT distribution, however, that is not available for Genie, so we opted for Lognormal. Discretization is also based on the literature. For simplicity, here we have used SRP to mean TRP.
	Low	0.01-0.50			
	Medium	0.50-1.00			
	High	1.00-2.50			
	Very High	2.50-60			
Incidental losses per average yard [kg $month^{-1}$]	Very Low	0-1*10^{-9}			Based on average farmyard size, losses are calculated as Surface runoff [m^3] / catchment area [m^2]* Farmyard size area [m^2]* Farmyard P concentration [mg l^{-1}]/ 10^3. Catchment area is set at 758 ha.
	Low	1*10^{-9}-0.001			
	Medium	0.001-0.01			
	High	0.01-0.10			
	Very High	0.10-60			
Total incidental losses [T $month^{-1}$]	Very Low	0-1*10^{-5}			Incidental losses per average yard [kg $month^{-1}$] * N, where N is the total number of yards present within the catchment boundary. In this case, N =97.
	Low	1e-05-0.007			
	Medium	0.007-0.070			
	High	0.07-0.700			
	Very High	0.700-10			
Catchment outlet integration sub-model					
Total catchment in-stream P load [T $month^{-1}$]	Low	0-0.02			Equal to the sum of Baseflow Dissolved P load [kg $month^{-1}$], Modified Dissolved P load [kg $month^{-1}$], Modified Sediment P load [kg $month^{-1}$], Total incidental losses [T $month^{-1}$], and Total Realized load [T $month^{-1}$], all converted to appropriate units.
	Medium	0.002-1			
	High	1-10			
(meteorological) Season					Based on the node "Month".
In-stream winter P removal	Very Low	-1 to -0.5			Defined as a Normal distribution (μ=0.12; σ=0.1) derived from expert elicitation with the R package (version 1.8.0, Oakley, 2020).
	Low	-0.5-0			
	Medium	0-0.5			

<table>
<tr><td></td><td>High</td><td>0.5-1</td><td></td></tr>
<tr><td rowspan="4">In-stream spring P removal</td><td>Very Low</td><td>0-0.2</td><td rowspan="4">Defined as a Normal distribution (μ=0.35; σ=0.21) derived from expert elicitation with the R package (version 1.8.0, Oakley, 2020).</td></tr>
<tr><td>Low</td><td>0.2-0.4</td></tr>
<tr><td>Medium</td><td>0.4-0.6</td></tr>
<tr><td>High</td><td>0.6-0.8</td></tr>
<tr><td rowspan="4">In-stream summer P removal</td><td>Very Low</td><td>0.1-0.3</td><td rowspan="4">Defined as a Normal distribution (μ=0.43; σ=012) derived from expert elicitation with the R package (version 1.8.0, Oakley, 2020).</td></tr>
<tr><td>Low</td><td>0.3-0.45</td></tr>
<tr><td>Medium</td><td>0.45-0.6</td></tr>
<tr><td>High</td><td>0.6-0.8</td></tr>
<tr><td rowspan="4">In-stream autumn P removal</td><td>Very Low</td><td>0-0.2</td><td rowspan="4">Defined as a Normal distribution (μ=0.25; σ=0.07) derived from expert elicitation with the R package (version 1.8.0, Oakley, 2020).</td></tr>
<tr><td>Low</td><td>0.2-0.4</td></tr>
<tr><td>Medium</td><td>0.4-0.5</td></tr>
<tr><td>High</td><td>0.5-0.65</td></tr>
<tr><td rowspan="2">In-stream reduced P load [T month^{-1}]</td><td>Moderate</td><td>0-1</td><td rowspan="2">Calculated as the product of Total catchment in-stream P load and the seasonal removal.</td></tr>
<tr><td>Bad</td><td>1-10</td></tr>
<tr><td rowspan="2">In-stream P concentration [mg l^{-1}]</td><td>Good</td><td>0-0.035</td><td rowspan="2">Defined as the in-stream reduced P load [T] * 10^9 / Mean total monthly Q (discharge) [m^3] * 1000, where mean monthly discharge is equal to the total catchment discharge measured at the outlet.</td></tr>
<tr><td>Bad</td><td>0.035-5</td></tr>
<tr><td>Environmental Quality Standard [TRP concentration mg l^{-1}]</td><td colspan="2"><table><tr><th>TRP concentration</th><th>Good</th><th>Bad</th></tr><tr><td>Good</td><td>1</td><td>0</td></tr><tr><td>Bad</td><td>0</td><td>1</td></tr></table></td><td>Discretization of the variable “In-stream TRP concentration [mg l^{-1}]”. For simplicity, in-stream TRP is here considered equal to in-stream Dissolved Reactive Phosphorus, as in previous studies the mean DRP accounted for 98–99% of the flow-weighted mean TRP (Shore et al., 2014).</td></tr>
</table>

9.2 Castledockrell model specifications

Table 9.3 Castledockrell model structure (filename Ptool_pointanddiffuse_v8_Castledockrell)

<table>
<tr><th>Variable (symbol) [unit]</th><th colspan="2">Conditional Probability Table or states and discretisation boundaries for continuous nodes</th><th>Description</th></tr>
<tr><td colspan="4">Hydrology sub-model (Drivers)</td></tr>
<tr><td>Month</td><td>Each month</td><td></td><td>Calculated as No. days in the month/ 365</td></tr>
<tr><td rowspan="5">Mean total monthly Q (discharge) [m^3]</td><td>Very Low</td><td>0-193630</td><td rowspan="5">Bootstrapped from daily total discharge observations (2009-2016) to obtain a Lognormal (μ; σ) discharge distribution with base e for each month. Each month’s parameters are shown in the table. Discretization of states is based on percentiles calculated from the average monthly observations (very low<= 5th percentile, low= 5th-25th percentile, medium= 25th-50th percentile, high= 50th-75th percentile, very high= 75th-100th percentile).
<table>
<tr><th></th><th>μ</th><th>σ</th></tr>
<tr><td>January</td><td>13.9</td><td>0.11</td></tr>
<tr><td>February</td><td>13.7</td><td>0.13</td></tr>
<tr><td>March</td><td>12.9</td><td>0.11</td></tr>
<tr><td>April</td><td>12.7</td><td>0.13</td></tr>
<tr><td>May</td><td>12.2</td><td>0.09</td></tr>
<tr><td>June</td><td>12.0</td><td>0.18</td></tr>
<tr><td>July</td><td>11.7</td><td>0.21</td></tr>
<tr><td>August</td><td>11.7</td><td>0.21</td></tr>
<tr><td>September</td><td>11.7</td><td>0.22</td></tr>
<tr><td>October</td><td>12.5</td><td>0.19</td></tr>
<tr><td>November</td><td>13.8</td><td>0.19</td></tr>
<tr><td>December</td><td>13.7</td><td>0.15</td></tr>
</table></td></tr>
<tr><td>Low</td><td>193630-310530</td></tr>
<tr><td>Medium</td><td>310530-871120</td></tr>
<tr><td>High</td><td>871120-1080000</td></tr>
<tr><td>Very High</td><td>1080000-1200000</td></tr>
<tr><td rowspan="5">Mean total monthly Surface Flow (surface runoff) [m^3]</td><td>Very Low</td><td>0-3873</td><td rowspan="5">Calculated as a portion of mean monthly runoff (2%), via hydrograph separation method described in Mellander et al., (2012). Discretization of states is based on percentiles calculated from observations.</td></tr>
<tr><td>Low</td><td>3873-6211</td></tr>
<tr><td>Medium</td><td>6211-17425</td></tr>
<tr><td>High</td><td>17425-21556</td></tr>
<tr><td>Very High</td><td>21556-24000</td></tr>
<tr><td rowspan="5">Mean total monthly Sub-surface Stormflow (subsurface runoff) [m^3]</td><td>Very Low</td><td>0-3873</td><td rowspan="5">Calculated as a portion of mean monthly runoff (2%), via hydrograph separation method described in Mellander et al., (2012). Discretization of states is based on percentiles calculated from observations.</td></tr>
<tr><td>Low</td><td>3873-6211</td></tr>
<tr><td>Medium</td><td>6211-17425</td></tr>
<tr><td>High</td><td>17425-21556</td></tr>
<tr><td>Very High</td><td>21556-24000</td></tr>
<tr><td rowspan="5">Mean total monthly Baseflow [m^3]</td><td>Very Low</td><td>0-186000</td><td rowspan="5">Calculated as a portion of mean monthly runoff (96%), via hydrograph separation method described in Mellander et al., (2012). Discretization of states is based on percentiles calculated from observations.</td></tr>
<tr><td>Low</td><td>186000-230000</td></tr>
<tr><td>Medium</td><td>230000-837000</td></tr>
<tr><td>High</td><td>837000-1035000</td></tr>
<tr><td>Very High</td><td>1035000-1107000</td></tr>
</table>

<table>
<tr><td colspan="4">Management (Drivers)</td></tr>
<tr><td rowspan="3">Land use</td><td colspan="2">Arable</td><td>0.2</td><td rowspan="3">As reported by Teagasc - Agriculture and Food Development Authority, (2018).</td></tr>
<tr><td colspan="2">Grassland</td><td>0.78</td></tr>
<tr><td colspan="2">Seminatural</td><td>0.02</td></tr>
<tr><td>Buffers</td><td colspan="2"><table><tr><th>Land use</th><th>Arable</th><th>Grassland</th><th>Seminatural</th></tr><tr><td>2 m</td><td>0.98</td><td>0.01</td><td>$1.01*10^{-6}$</td></tr><tr><td>>2 m</td><td>0.019</td><td>0.01</td><td>$1.01*10^{-6}$</td></tr><tr><td>none</td><td>0.001</td><td>0.08</td><td>0.999</td></tr></table></td><td>Buffer strips are defined as being 2 m in width, more than 2 m in width, or absent. Probabilities of having either type of buffer according to land use were agreed upon with one of the ACP advisors (expert) during consultation.</td></tr>
<tr><td rowspan="5">Buffer effectiveness for Particulate P (PP) and suspended sediments (SS)</td><td colspan="2">Very Low</td><td>0-0.2</td><td rowspan="5">Dependent on the variable Buffers. For 2 m buffers, effectiveness is defined as Beta (α=2.9; β=4.5); for >2 m buffers it is defined as Beta (α=1.44; β=0.789); for no buffers, effectiveness is equal to 0. The distributions were fitted to the dataset published in Stutter et al., (2021), where negative retention data was deleted from the analysis.</td></tr>
<tr><td colspan="2">Low</td><td>0.2-0.4</td></tr>
<tr><td colspan="2">Medium</td><td>0.4-0.6</td></tr>
<tr><td colspan="2">High</td><td>0.6-0.8</td></tr>
<tr><td colspan="2">Very High</td><td>0.8-1</td></tr>
<tr><td rowspan="5">Buffer effectiveness for Total Dissolved P (TDP)</td><td colspan="2">Very Low</td><td>0-0.2</td><td rowspan="5">Dependent on the variable Buffers. For Buffers 0-2 m, Buffer effectiveness is defined as Beta (α=1.8; β=2.7), for >2 m buffers it is defined as Beta (α=1; β=0.8); for no buffers, effectiveness is equal to 0. The distributions were fitted to the dataset published in Stutter et al., (2021), where negative retention data was deleted from the analysis.</td></tr>
<tr><td colspan="2">Low</td><td>0.2-0.4</td></tr>
<tr><td colspan="2">Medium</td><td>0.4-0.6</td></tr>
<tr><td colspan="2">High</td><td>0.6-0.8</td></tr>
<tr><td colspan="2">Very High</td><td>0.8-1.0</td></tr>
<tr><td colspan="4">Soil erosion and soil P sub-model</td></tr>
<tr><td>Morgan P</td><td colspan="2"><table><tr><th></th><th>Arable</th><th>Grassland</th><th>Seminatural</th></tr><tr><td>Morgan1</td><td>0.29</td><td>0.29</td><td>0</td></tr><tr><td>Morgan2</td><td>0.41</td><td>0.34</td><td>0.6</td></tr><tr><td>Morgan3</td><td>0.2</td><td>0.19</td><td>0.3</td></tr><tr><td>Morgan4</td><td>0.09</td><td>0.18</td><td>0.1</td></tr></table></td><td>Based on land use, proportions of land for each level and in each land use category were calculated based on the soil survey carried out in 2013 in the catchment. Where the Morgan P index was unknown, that proportion of land was assigned to the dominant index category. For the interpretation of the Soil Morgan P Index, the reader is referred to Regan et al., (2012).</td></tr>
<tr><td colspan="4">Calculated variables</td></tr>
<tr><td rowspan="5">Monthly Turbidity [NTU $month^{-1}$]</td><td colspan="2">Very Very Low</td><td>0-707</td><td rowspan="5">Bootstrapped from daily average turbidity observations (2009-2016) to obtain a Lognormal (μ; σ) turbidity distribution with base e for each month. Each month’s parameters are shown in the table. Discretization of states is based on percentiles calculated from the average monthly observations.</td></tr>
<tr><td colspan="2">Very Low</td><td>707-780</td></tr>
<tr><td colspan="2">Low</td><td>780-1510</td></tr>
<tr><td colspan="2">Medium</td><td>1510-2770</td></tr>
<tr><td colspan="2">High</td><td>2770-5590</td></tr>
</table>

<table>
<tr><td></td><td>Very High</td><td>5590-8661</td><td></td></tr>
<tr><td>Monthly Suspended Sediment concentration [mg l^{-1} $month^{-1}$]</td><td>Very Very Low</td><td>0-50</td><td rowspan="6">Calculated as: a * Monthly Turbidity [NTU $month^{-1}$] ^{b}, where a= 0.4119, and b= 1.1456, as described in Sherriff et al., (2015). Discretization of states is based on percentiles calculated from the average monthly calculated observations.</td></tr>
<tr><td>Very Low</td><td>50-60</td></tr>
<tr><td>Low</td><td>60-130</td></tr>
<tr><td>Medium</td><td>130-262</td></tr>
<tr><td>High</td><td>262-640</td></tr>
<tr><td>Very High</td><td>640-1050</td></tr>
<tr><td>Water Extractable P (WEP) [mg l^{-1}]</td><td>Low</td><td>0-3</td><td rowspan="4">Based on variable “Morgan P levels” and “land use” (data from 2013) it is calculated with the equations available in (Thomas et al., 2016b): for Grassland, WEP=0.26 * Morgan P + 2.74, for Arable: WEP= 0.11 * Morgan P + 1.12, where Morgan P is defined as a Uniform distribution with the following parameters:
<table><tr><th>Morgan P Index</th><th>Grassland</th><th>Arable</th></tr><tr><td>Index 1</td><td>a=0; b=3</td><td>a=0; b=3</td></tr><tr><td>Index 2</td><td>a=3.1; b=5</td><td>a=3.1; b=6</td></tr><tr><td>Index 3</td><td>a=5.1; b=8</td><td>a=6.1; b=10</td></tr><tr><td>Index 4</td><td>a=8.1; b=30</td><td>a=10.1; b=30</td></tr></table>
For the Seminatural Land use, WEP was assumed constant to 0.001. Discretization is based on Morgan P discrete levels.</td></tr>
<tr><td>Medium</td><td>3-5</td></tr>
<tr><td>High</td><td>5-8</td></tr>
<tr><td>Very High</td><td>8-15</td></tr>
<tr><td>Sediment Water Soluble P [mg kg^{-1}]</td><td>Very Low</td><td>0-0.042</td><td rowspan="5">Defined as a Gamma distribution (k=1.03, ɵ=0.44), fitted with the SHELF R package (version 1.8.0, Oakley, 2020) to observed Water Extractable P in the catchment sediments (Shore et al., 2016). Discretization of states is based on percentiles calculated from the observations (very low<= 5^{th} percentile, low= 5^{th}-25^{th}</td></tr>
<tr><td>Low</td><td>0.042-0.720</td></tr>
<tr><td>Medium</td><td>0.720-1.570</td></tr>
<tr><td>High</td><td>1.570-3.350</td></tr>
<tr><td>Very High</td><td>3.350-7.000</td></tr>
</table>

	μ	σ
January	5.7	0.19
February	5.5	0.20
March	4.9	0.15
April	4.6	0.13
May	4.4	0.13
June	4.6	0.15
July	4.5	0.13
August	5.8	0.44
September	4.5	0.13
October	5.1	0.25
November	5.7	0.33
December	5.6	0.24

<table>
<tr><td></td><td></td><td></td><td>percentile, medium= 25th-50th percentile, high= 50th-75th percentile, very high= 75th-100th percentile).</td></tr>
<tr><td rowspan="6">Predicted Dissolved P Concentration [mg l^{-1}]</td><td>Very Very Low</td><td>0-0.1</td><td rowspan="6">Dependant on Water Extractable P, it is defined with the linear model: Predicted Dissolved P = β(WEP)+α, where β =0.08, α =0.158, derived from (Thomas et al., 2016b). This equation is derived from data gathered during the closed period only, that is, when farmers are forbidden from spreading fertilizer. An assumption is made that when the linear model yields a negative value, that is resampled as a zero. Water Extractable P is considered a good in-stream TRP/ TDP predictor in the ACP catchments by the experts, however careful consideration is needed when choosing a soil P test in a different setting.</td></tr>
<tr><td>Very Low</td><td>0.1-0.5</td></tr>
<tr><td>Low</td><td>0.5-1.5</td></tr>
<tr><td>Medium</td><td>1.5-5</td></tr>
<tr><td>High</td><td>5-8</td></tr>
<tr><td>Very High</td><td>8-15</td></tr>
<tr><td rowspan="6">Groundwater Dissolved P Concentration [mg l^{-1}]</td><td>Very Very Low</td><td>0-0.1</td><td rowspan="6">Derived from monthly piezometer data of TDP concentrations (2009-2016) monitored in multi-level wells described in Mellander et al., (2016).
<table><tr><th></th><th>μ</th><th>σ</th></tr><tr><td>January</td><td>-4.3</td><td>0.09</td></tr><tr><td>February</td><td>-4.4</td><td>0.07</td></tr><tr><td>March</td><td>-5.0</td><td>0.06</td></tr><tr><td>April</td><td>-5.6</td><td>0.05</td></tr><tr><td>May</td><td>-4.8</td><td>0.12</td></tr><tr><td>June</td><td>-4.1</td><td>0.08</td></tr><tr><td>July</td><td>-4.4</td><td>0.03</td></tr><tr><td>August</td><td>-4.2</td><td>0.04</td></tr><tr><td>September</td><td>-4.4</td><td>0.00</td></tr><tr><td>October</td><td>-3.4</td><td>0.06</td></tr><tr><td>November</td><td>-3.9</td><td>0.17</td></tr><tr><td>December</td><td>-3.6</td><td>0.21</td></tr></table></td></tr>
<tr><td>Low</td><td>0-0.1</td></tr>
<tr><td>Low</td><td>0.1-0.5</td></tr>
<tr><td>Low</td><td>0.5-1.5</td></tr>
<tr><td>Medium</td><td>1.5-5</td></tr>
<tr><td>High</td><td>5-8</td></tr>
<tr><td>Very High</td><td>8-15</td></tr>
<tr><td rowspan="2">Sub-surface Dissolved P load [kg $month^{-1}$]</td><td>Low</td><td>0-3</td><td rowspan="2">Calculated as the product of Predicted Dissolved P concentration and Subsurface Storm-flow.</td></tr>
<tr><td>High</td><td>3-200</td></tr>
<tr><td rowspan="2">Baseflow Dissolved P load [kg $month^{-1}$]</td><td>Low</td><td>0-3</td><td rowspan="2">Calculated as the product of Predicted Dissolved P concentration and Baseflow.</td></tr>
<tr><td>High</td><td>3-200</td></tr>
<tr><td rowspan="2">Modified Dissolved P load [kg $month^{-1}$]</td><td>Low</td><td>0-3</td><td rowspan="2">Based on “Buffer effectiveness for Total Dissolved P”, for effective buffers, modified Dissolved P load= Sub-surface Dissolved P load *(1-Buffer effectiveness for TDP). Based on expert recommendation.</td></tr>
<tr><td>High</td><td>3-200</td></tr>
<tr><td rowspan="2">Monthly Sediment P load [kg $month^{-1}$]</td><td>Low</td><td>0-3</td><td rowspan="2">Calculated as the product of Sediment Water Soluble P [mg kg^{-1}], Monthly Suspended Sediment concentration [mg l^{-1} $month^{-1}$] , and Mean total monthly surface flow [m^3] .</td></tr>
<tr><td>High</td><td>3-200</td></tr>
<tr><td>Modified Sediment P load</td><td>Low</td><td>0-3</td><td></td></tr>
</table>

<table>
<tr><td>[kg month^{-1}]</td><td>High</td><td>3-200</td><td>Based on “Buffer effectiveness for Suspended Sediments and Particulate P”, for effective buffers, Modified Sediment P load= Monthly Sediment P load [kg month^{-1}]*(1-Buffer effectiveness for SS and PP). Based on expert recommendation.</td></tr>
<tr><td colspan="4">Septic Tanks (ST) sub-model (Point P sources)</td></tr>
<tr><td rowspan="5">P concentration per tank [mg l^{-1}]</td><td>Absent (to represent 0 STs)</td><td>0-1*10^{-8}</td><td rowspan="5">P concentration is dependent on the treatment type. If the treatment is unknown, the concentration is defined as a Lognormal distribution (μ=2.9, σ =1.25), based on a literature review of data available for Ireland (Environmental Protection Agency Ireland (EPA), 2003, 2000; Gill et al., 2005, 2007) (n=8). Fitting was done with R package fitdistrplus (version 1.1-8, Delignette-Muller et al., 2020). Otherwise, for primary and secondary treatment concentration is defined as Truncated Normal distribution (μ=10; σ=1), and (μ=5; σ=0.5) respectively, as described in Glendell et al., (2021) and derived from SEPA guidelines (Brownlie et al., 2014). All tanks are assumed to be maintained. Discretization was also based on the literature review.</td></tr>
<tr><td>Low</td><td>1*10^{-8}-1</td></tr>
<tr><td>Medium</td><td>1-18</td></tr>
<tr><td>High</td><td>18-35</td></tr>
<tr><td>Very High</td><td>35-100</td></tr>
<tr><td rowspan="2">Direct discharge</td><td>Present</td><td>0.16</td><td rowspan="2">Probabilities are derived from the report by the Environmental Protection Agency Ireland (EPA, 2015).</td></tr>
<tr><td>Absent</td><td>0.84</td></tr>
<tr><td rowspan="2">Degree of Phosphorus Saturation (DPS) [%]</td><td>Very Low_0-20</td><td>0.88</td><td rowspan="2">Discretization is equal to the 20^{th,} 40th, 60th, and 80th quantiles, however 0< DPS <40 in this catchment. Probabilities were calculated from available spatial data (Wall et al., 2012).</td></tr>
<tr><td>Low 20-40</td><td>0.12</td></tr>
<tr><td rowspan="5">Soil risk factor [adimensional]</td><td>Low</td><td>0</td><td rowspan="5">An indicator to describe the combined risk of effluent leaching to the groundwater table with the risk of the effluent being transported with surface runoff. This approach is a simplification of the one adopted in Glendell et al., (2021). The risk factor was obtained by overlaying the soil series (Thomas et al., 2016b) with information on the position of the groundwater table (0- 2 m below ground or more than 2 m below ground). Because little is known regarding the septic tanks in the catchment (i.e. age, type of treatment, maintenance), and the groundwater table position (few datapoints within the catchment) experts recommended a precautionary principle. This meant that the class at most risk of effluent transfer was applied when data was unavailable. The table to the left represents a synthesis of the classification approach. Probabilities are based on land cover proportion.</td></tr>
<tr><td>Medium</td><td>0.02</td></tr>
<tr><td>High</td><td>0.98</td></tr>
<tr><td>Very High</td><td>0</td></tr>
<tr><td colspan="2"><table>
<tr><th></th><th colspan="2">Groundwater Table Position</th></tr>
<tr><th>Soil Series</th><th>0-2 m below surface</th><th>>2 m below surface</th></tr>
<tr><td>Brown earths</td><td>High Risk</td><td>Moderate Risk</td></tr>
<tr><td>Gleys</td><td>Very High Risk</td><td>Very High Risk</td></tr>
</table></td></tr>
<tr><td>Leachfield removal</td><td colspan="2"><table>
<tr><th>Soil risk factor</th><th>DPS</th><th>Low</th><th>Medium</th><th>High</th></tr>
<tr><td rowspan="2">Low</td><td>Very Low</td><td>0</td><td>0.3</td><td>0.7</td></tr>
<tr><td>Low</td><td>0</td><td>0.7</td><td>0.3</td></tr>
<tr><td rowspan="2">Medium</td><td>Very Low</td><td>0</td><td>0.5</td><td>0.5</td></tr>
<tr><td>Low</td><td>0</td><td>1</td><td>0</td></tr>
</table></td><td>The node refers to P removal from septic drains. Conditional on P leaching risk from Degree of Phosphorus Saturation (DPS). The conditional probability table is a logical one.</td></tr>
</table>

	High	**Very Low**	0	0.7	0.3	
		Low	0.3	0.7	0	
	Very High	**Very Low**	0	0.5	0.5	
		Low	0.5	0.5	0	

Leachfield connectedness	**HSA rescaled**	**None**		**Low**		**Medium**		**High**		Probabilities are conditional on the presence/absence of Direct ST discharge, and HSA (node: Connectivity rescaled HSA). Where Direct discharge is present, connectedness is assumed as 'high'. Where Direct discharge is absent, the risk class of the HSA is assigned.
	Direct discharge	**pres**	**abs**	**pres**	**abs**	**pres**	**abs**	**pres**	**abs**	
	low	0	1	0	1	0	0	0	0	
	medium	0	0	0	0	0	1	0	0	
	high	1	0	1	0	1	0	1	1	

Septic Tank connectedness	**Leachfield removal**	**Low**			**Medium**			**High**			Probabilities are conditional on Leachfield removal and Leachfield connectedness. Where Leachfield removal is 'low' or 'High', Leachfield connectedness remains unaltered.
	Leachfield connectedness	**Low**	**Medium**	**High**	**Low**	**Medium**	**High**	**Low**	**Medium**	**High**	
	Low	1.0	0.0	0.0	1.0	0.0	0.0	1.0	0.5	0.0	
	Medium	0.0	1.0	0.0	0.0	1.0	0.5	0.0	0.5	1.0	
	High	0.0	0.0	1.0	0.0	0.0	0.5	0.0	0.0	0.0	

Connectivity rescaled HSA [adimensional]	None_0	0.03	Data extracted from spatial layers of Hydrologically Sensitive Areas (HSAs) rescaled between 0 and 10 was provided by the Agricultural Catchments Programme (Thomas et al., 2016a). Discretization is also based on the spatial layers.
	Low_1-3	0.8	
	Medium_4-7	0.16	
	High_8-10	0.01	
Load per tank [kg month^{-1}]	Absent	0-1*10^{-6}	Specified as the product of ST density [No ha^{-1}] * ST concentration [mg l^{-1}] * 120 [L] average daily water consumption per person * 365/12 days in a month* average No of persons per household 2.7/1*10^{6}. Discretisation is based on interpolation to represent plausible probabilities for combination of extreme risk classes (e.g. High+high=high, low+low=low).
	Very Low	1*10^{-6}-0.1	
	Low	0.1-0.5	
	Medium	0.5-1.0	
	High	1.0-2.0	
	Very High	2.0-30	
Total Realized load [T month^{-1}]	Very Low	0.0-0.1	Calculated as the product of septic tank load and delivery factors (D) related to the connectedness of a septic tank, based on the median estimated fraction to be delivered in Table 13 of the report by Glendell et al., (2021) and the number of septic tanks present within catchment boundary (N): Realised load per tank [kg month^{-1}] * N * D / 1000. In this case, N= 88. Discretisation based on interpolation to represent plausible probabilities for combination of extreme risk classes.
	Low	0.1-0.5	
	Medium	0.5-1.0	
	High	1.0-2.0	
	Very High	2.0-12	

Septic tank connectedness	**Delivery factor (D)**	**Reference**
Low	0.05	"very low" category in Appendix A3, Glendell et al., (2021)

		Medium	0.30	"medium" category in Appendix A3, Glendell et al., (2021)		
		High	0.80	"very high" category in Appendix A3, Glendell et al., (2021)		
Sewage Treatment Works (STWs) sub-model (Point P sources)						
STWs P concentration [mg l^{-1}]	Absent			$0\text{-}1*10^{-8}$		Based on Total P concentrations after tertiary treatment and specified as a Truncated Normal distribution (μ=1.44, σ=1 .61, truncated at 0), as described in Glendell et al., (2022).
	Low			$1*10^{-8}\text{-}1$		
	Medium			1-18		
	High			18-35		
	Very High			35-100		
STWs Load [kg $month^{-1}$]	Absent			$0\text{-}1*10^{-6}$		Specified as the product of STWs P concentration [mg l^{-1}] * 120 [L] average daily water consumption per person * 365/12 days in a month* 130 people equivalent /$1*10^{6}$.
	Very Low			$1*10^{-}6\text{-}0.1$		
	Low			0.1-0.5		
	Medium			0.5-1		
	High			1-2		
	Very High			2-30		
Farmyards sub-model (Point P sources)						
Farmyard size area [m^2]	Very Low			0-35		Based on available farmyard survey, a distribution was fitted to farmyard area data: Lognormal (μ=4.9; σ=0.9). Discretization of states is based on percentiles calculated from the observations (very low<= 5^{th} percentile, low= 5^{th}-25^{th} percentile, medium= 25^{th}-50^{th} percentile, high= 50^{th}-75^{th} percentile, very high= 75^{th}-100^{th} percentile).
	Low			35-75		
	Medium			75-146		
	High			146-270		
	Very High			270-1315		
Farmyard P concentration [mg l^{-1}]	Very Low			0-0.01		Using the *SHELF* R package (version 1.8.0, Oakley, 2020), a distribution was fitted to the data in Table 2 in Harrison et al., (2019): Lognormal (μ=-1.8; σ=1.6). The best fit would have been the LogT distribution, however, that is not available for Genie, so we opted for Lognormal. Discretization is also based on the literature. For simplicity, here we have used SRP to mean TRP.
	Low			0.01-0.50		
	Medium			0.50-1.00		
	High			1.00-2.50		
	Very High			2.50-60		
Incidental losses per average yard [kg $month^{-1}$]	Very Low			$0\text{-}1*10^{-9}$		Based on average farmyard size, losses are calculated as Surface runoff [m^3] / catchment area [m^2]* Farmyard size area [m^2]* Farmyard P concentration [mg l^{-1}]/ 10^3. Catchment area is set at 758 ha.
	Low			$1*10^{-9}\text{-}0.001$		
	Medium			0.001-0.01		
	High			0.01-0.10		
	Very High			0.10-60		
Total incidental losses [T $month^{-1}$]	Very Low			$0\text{-}1*10^{-5}$		Incidental losses per average yard [kg $month^{-1}$] * N, where N is the total number of yards present within the catchment boundary. In this case, N =86.
	Low			1e-05-0.007		
	Medium			0.007-0.070		
	High			0.07-0.700		
	Very High			0.700-10		

<table>
<tr><th colspan="4">Catchment outlet integration sub-model</th></tr>
<tr><td rowspan="3">Total catchment in-stream P load [T month^{-1}]</td><td>Low</td><td>0-0.02</td><td rowspan="3">Equal to the sum of Baseflow Dissolved P load [kg month^{-1}], Modified Dissolved P load [kg month-^{1}], Modified Sediment P load [kg month^{-1}], Total incidental losses [T month^{-1}], and Total Realized load [T month^{-1}], all converted to appropriate units.</td></tr>
<tr><td>Medium</td><td>0.002-1</td></tr>
<tr><td>High</td><td>1-10</td></tr>
<tr><td>(meteorological) Season</td><td></td><td></td><td>Based on the node “Month”.</td></tr>
<tr><td rowspan="4">In-stream winter P removal</td><td>Very Low</td><td>-1, -05</td><td rowspan="4">Defined as a Normal distribution (μ=0.12; σ=0.1) derived from expert elicitation with the R package (version 1.8.0, Oakley, 2020).</td></tr>
<tr><td>Low</td><td>-0.5-0</td></tr>
<tr><td>Medium</td><td>0-0.5</td></tr>
<tr><td>High</td><td>0.5-1</td></tr>
<tr><td rowspan="4">In-stream spring P removal</td><td>Very Low</td><td>0-0.2</td><td rowspan="4">Defined as a Normal distribution (μ=0.08; σ=0.06) derived from expert elicitation with the R package (version 1.8.0, Oakley, 2020).</td></tr>
<tr><td>Low</td><td>0.2-0.4</td></tr>
<tr><td>Medium</td><td>0.4-0.6</td></tr>
<tr><td>High</td><td>0.6-0.8</td></tr>
<tr><td rowspan="4">In-stream summer P removal</td><td>Very Low</td><td>0.1-0.3</td><td rowspan="4">Defined as a Normal distribution (μ=0.; 35=0.21) derived from expert elicitation with the R package (version 1.8.0, Oakley, 2020).</td></tr>
<tr><td>Low</td><td>0.3-0.45</td></tr>
<tr><td>Medium</td><td>0.45-0.6</td></tr>
<tr><td>High</td><td>0.6-0.8</td></tr>
<tr><td rowspan="4">In-stream autumn P removal</td><td>Very Low</td><td>0-0.2</td><td rowspan="4">Defined as a Normal distribution (μ=0.25; σ=0.07) derived from expert elicitation with the R package (version 1.8.0, Oakley, 2020).</td></tr>
<tr><td>Low</td><td>0.2-0.4</td></tr>
<tr><td>Medium</td><td>0.4-0.5</td></tr>
<tr><td>High</td><td>0.5-0.65</td></tr>
<tr><td rowspan="2">In-stream reduced P load [T month^{-1}]</td><td>Moderate</td><td>0-0.5</td><td rowspan="2">Calculated as the product of Total catchment in-stream P load and the seasonal removal.</td></tr>
<tr><td>Bad</td><td>0.5-10</td></tr>
<tr><td rowspan="2">In-stream P concentration [mg l^{-1}]</td><td>Good</td><td>0-0.035</td><td rowspan="2">Defined as the in-stream reduced P load [T] * 10^9 / Mean total monthly Q (discharge) [m^3] * 1000, where mean monthly discharge is equal to the total catchment discharge measured at the outlet.</td></tr>
<tr><td>Bad</td><td>0.035-5</td></tr>
<tr><td>Environmental Quality Standard [TRP concentration mg l^{-1}]</td><td colspan="2"><table><tr><th>TRP concentration</th><th>Good</th><th>Bad</th></tr><tr><td>Good</td><td>1</td><td>0</td></tr><tr><td>Bad</td><td>0</td><td>1</td></tr></table></td><td>Discretization of the variable “In-stream TRP concentration [mg l^{-1}]”. For simplicity, in-stream TRP is here considered equal to in-stream Dissolved Reactive Phosphorus, as in previous studies the mean DRP accounted for 98–99% of the flow-weighted mean TRP (Shore et al., 2014).</td></tr>
</table>

9.3 Dunleer model specifications

Table 9.4 Dunleer model structure (filename Ptool_pointanddiffuse_v7_Dunleer)

<table>
<tr><th>Variable (symbol) [unit]</th><th colspan="2">Conditional Probability Table or states and discretisation boundaries for continuous nodes</th><th>Description</th></tr>
<tr><td colspan="4">Hydrology sub-model (Drivers)</td></tr>
<tr><td>Month</td><td>Each month</td><td></td><td>Calculated as No. days in the month/ 365</td></tr>
<tr><td rowspan="5">Mean total monthly Q (discharge) [m^3]</td><td>Very Low</td><td>0-139000</td><td rowspan="5">Bootstrapped from daily total discharge observations (2009-2016) to obtain a Lognormal (μ; σ) discharge distribution with base e for each month. Each month’s parameters are shown in the table. Discretization of states is based on percentiles calculated from the average monthly observations (very low<= 5^{th} percentile, low= 5^{th}-25^{th} percentile, medium= 25^{th}-50^{th} percentile, high= 50^{th}-75^{th} percentile, very high= 75^{th}-100^{th} percentile).

<table><tr><th></th><th>μ</th><th>σ</th></tr><tr><td>January</td><td>13.4</td><td>0.1</td></tr><tr><td>February</td><td>13.3</td><td>0.1</td></tr><tr><td>March</td><td>12.6</td><td>0.1</td></tr><tr><td>April</td><td>12.5</td><td>0.2</td></tr><tr><td>May</td><td>11.9</td><td>0.2</td></tr><tr><td>June</td><td>11.5</td><td>0.3</td></tr><tr><td>July</td><td>11.3</td><td>0.3</td></tr><tr><td>August</td><td>11.3</td><td>0.4</td></tr><tr><td>September</td><td>11.7</td><td>0.4</td></tr><tr><td>October</td><td>12.3</td><td>0.3</td></tr><tr><td>November</td><td>13.3</td><td>0.2</td></tr><tr><td>December</td><td>13.2</td><td>0.2</td></tr></table></td></tr>
<tr><td>Low</td><td>139000-274000</td></tr>
<tr><td>Medium</td><td>274000-596800</td></tr>
<tr><td>High</td><td>596800-697000</td></tr>
<tr><td>Very High</td><td>697000-720000</td></tr>
<tr><td rowspan="5">Mean total monthly Surface Flow (surface runoff) [m^3]</td><td>Very Low</td><td>0-23100</td><td rowspan="5">Calculated as a portion of mean monthly runoff (21%), via hydrograph separation method described in Mellander et al., (2012). Discretization of states is based on percentiles calculated from observations .</td></tr>
<tr><td>Low</td><td>23100-57400</td></tr>
<tr><td>Medium</td><td>57400-125400</td></tr>
<tr><td>High</td><td>125400-147000</td></tr>
<tr><td>Very High</td><td>147000-150900</td></tr>
<tr><td rowspan="5">Mean total monthly Sub-surface Stormflow (subsurface runoff) [m^3]</td><td>Very Low</td><td>0-5541</td><td rowspan="5">Calculated as a portion of mean monthly runoff (4%), via hydrograph separation method described in Mellander et al., (2012). Discretization of states is based on percentiles calculated from observations .</td></tr>
<tr><td>Low</td><td>5541-10934</td></tr>
<tr><td>Medium</td><td>10934-23870</td></tr>
<tr><td>High</td><td>23870-27860</td></tr>
<tr><td>Very High</td><td>27860-28800</td></tr>
</table>

Mean total monthly Baseflow [m^3]	Very Low			0-103887	Calculated as a portion of mean monthly runoff (75%), via hydrograph separation method described in Mellander et al., (2012). Discretization of states is based on percentiles calculated from observations.
	Low			103887-205000	
	Medium			205000-447565	
	High			447565-522370	
	Very High			522370-538900	
Management (Drivers)					
Land use	Arable			0.33	As reported by Teagasc - Agriculture and Food Development Authority, (2018).
	Grassland			0.49	
	Seminatural			0.18	
Buffers	**Land use**	**Arable**	**Grassland**	**Seminatural**	Buffer strips are defined as being 2 m in width, more than 2 m in width, or absent. Probabilities of having either type of buffer according to land use were agreed upon with one of the ACP advisors (expert) during consultation.
	2 m	0.98	0.01	$1.01*10^{-6}$	
	>2 m	0.019	0.01	$1.01*10^{-6}$	
	none	0.001	0.08	0.999	
Buffer effectiveness for Particulate P (PP) and suspended sediments (SS)	Very Low			0-0.2	Dependent on the variable Buffers. For 2 m buffers, effectiveness is defined as Beta (α=2.9; β=4.5); for >2 m buffers it is defined as Beta (α=1.44; β=0.789); for no buffers, effectiveness is equal to 0. The distributions were fitted to the dataset published in Stutter et al., (2021), where negative retention data was deleted from the analysis.
	Low			0.2-0.4	
	Medium			0.4-0.6	
	High			0.6-0.8	
	Very High			0.8-1	
Buffer effectiveness for Total Dissolved P (TDP)	Very Low			0-0.2	Dependent on the variable Buffers. For Buffers 0-2 m, Buffer effectiveness is defined as Beta (α=1.8; β=2.7), for >2 m buffers it is defined as Beta (α=1; β=0.8); for no buffers, effectiveness is equal to 0. The distributions were fitted to the dataset published in Stutter et al., (2021), where negative retention data was deleted from the analysis.
	Low			0.2-0.4	
	Medium			0.4-0.6	
	High			0.6-0.8	
	Very High			0.8-1.0	
Soil erosion and soil P sub-model					
Morgan P		**Arable**	**Grassland**	**Seminatural**	Based on land use, proportions of land for each level and in each land use category were calculated based on the soil survey carried out in 2013 in the catchment. Where the Morgan P index was unknown, that proportion of land was assigned to the dominant index category. For the interpretation of the Soil Morgan P Index, the reader is referred to Regan et al., (2012).
	Morgan1	0.224	0.224	0	
	Morgan2	0.426	0.249	0.6	
	Morgan3	0.142	0.154	0.3	
	Morgan4	0.208	0.373	0.1	
Monthly Turbidity [NTU $month^{-1}$]	Very Very Low			0-1312	Bootstrapped from daily average turbidity observations (2009-2016) to obtain a Lognormal (μ; σ) turbidity distribution with base e for each month. Each month's parameters are shown in the table. Discretization of states is based on percentiles calculated from the average monthly observations.
	Very Low			1312-1417	
	Low			1417-1792	
	Medium			1792-3004	
	High			3004-3775	

<table>
<tr><td></td><td>Very High</td><td>3775-3810</td><td></td></tr>
<tr><td>Monthly Suspended Sediment concentration [mg l^{-1} $month^{-1}$]</td><td>Very Very Low</td><td>0-186</td><td rowspan="6">Calculated as: a * Monthly Turbidity [NTU $month^{-1}$], where a= 1.132 when the monthly turbidity is <= 432.2 NTU, a * Monthly Turbidity [NTU $month^{-1}$]+b, where a= 0.6032 and b= 228.547 when the monthly turbidity is >= 432.2 NTU, as described in Sherriff et al., (2015). Discretization of states is based on percentiles calculated from the average monthly calculated observations.</td></tr>
<tr><td></td><td>Very Low</td><td>186-201</td></tr>
<tr><td></td><td>Low</td><td>201-249</td></tr>
<tr><td></td><td>Medium</td><td>249-421</td></tr>
<tr><td></td><td>High</td><td>421-527</td></tr>
<tr><td></td><td>Very High</td><td>527-531</td></tr>
<tr><td rowspan="4">Water Extractable P (WEP) [mg l^{-1}]</td><td>Low</td><td>0-3</td><td rowspan="4">Based on variable “Morgan P levels” and “land use” (data from 2013) it is calculated with the equations available in (Thomas et al., 2016b): for Grassland, WEP=0.57 * Morgan P + 0.29, for Arable: WEP= 0.36 * Morgan P + 0.89, where Morgan P is defined as a Uniform distribution with the following parameters:
<table><tr><th>Morgan P Index</th><th>Grassland</th><th>Arable</th></tr><tr><td>Index 1</td><td>a=0; b=3</td><td>a=0; b=3</td></tr><tr><td>Index 2</td><td>a=3.1; b=5</td><td>a=3.1; b=6</td></tr><tr><td>Index 3</td><td>a=5.1; b=8</td><td>a=6.1; b=10</td></tr><tr><td>Index 4</td><td>a=8.1; b=30</td><td>a=10.1; b=30</td></tr></table>
For the Seminatural Land use, WEP was assumed constant to 0.001. Discretization is based on Morgan P discrete levels.</td></tr>
<tr><td>Medium</td><td>3-5</td></tr>
<tr><td>High</td><td>5-8</td></tr>
<tr><td>Very High</td><td>8-15</td></tr>
<tr><td rowspan="5">Sediment Water Soluble P [mg kg^{-1}]</td><td>Very Low</td><td>0-0.0995</td><td rowspan="5">Defined as a Lognormal distribution (μ=-0.9, σ=1), fitted with the SHELF R package (version 1.8.0, Oakley, 2020) to observed Water Extractable P in the catchment sediments (Shore et al., 2016). Discretization of states is based on percentiles calculated from the observations (very low<= 5^{th} percentile, low= 5^{th}-25^{th} percentile, medium= 25^{th}-50^{th} percentile, high= 50^{th}-75^{th}</td></tr>
<tr><td>Low</td><td>0.0995-0.2100</td></tr>
<tr><td>Medium</td><td>0.2100-0.3550</td></tr>
<tr><td>High</td><td>0.3550-0.9100</td></tr>
<tr><td>Very High</td><td>0.9100-8</td></tr>
</table>

	μ	σ
January	5.9	0.23
February	5.9	0.26
March	5.3	0.19
April	5.4	0.16
May	5.1	0.14
June	5.2	0.14
July	5.1	0.13
August	5.3	0.15
September	5.1	0.14
October	5.4	0.23
November	6.1	0.30
December	6.0	0.28

			percentile, very high= 75th-100th percentile). Based on Ballycanew data.
Predicted Dissolved P Concentration [mg l^{-1}]	Very Very Low	0-0.1	Dependant on Water Extractable P, it is defined with the linear model: Predicted Dissolved P = β(WEP)+α, where β =0.08, α =0.158, derived from (Thomas et al., 2016b). This equation is derived from data gathered during the closed period only, that is, when farmers are forbidden from spreading fertilizer. An assumption is made that when the linear model yields a negative value, that is resampled as a zero. Water Extractable P is considered a good in-stream TRP/ TDP predictor in the ACP catchments by the experts, however careful consideration is needed when choosing a soil P test in a different setting.
	Very Low	0.1-0.5	
	Low	0.5-1.5	
	Medium	1.5-5	
	High	5-8	
	Very High	8-15	
Sub-surface Dissolved P load [kg month^{-1}]	Low	0-3	Calculated as the product of Predicted Dissolved P concentration and Subsurface Storm-flow.
	High	3-200	
Baseflow Dissolved P load [kg month^{-1}]	Low	0-3	Calculated as the product of Predicted Dissolved P concentration and Baseflow.
	High	3-200	
Modified Dissolved P load [kg month^{-1}]	Low	0-3	Based on "Buffer effectiveness for Total Dissolved P", for effective buffers, modified Dissolved P load= Sub-surface Dissolved P load *(1-Buffer effectiveness for TDP). Based on expert recommendation.
	High	3-200	
Monthly Sediment P load [kg month^{-1}]	Low	0-3	Calculated as the product of Sediment Water Soluble P [mg kg^{-1}], Monthly Suspended Sediment concentration [mg l^{-1} month^{-1}] , and Mean total monthly surface flow [m^3] .
	High	3-200	
Modified Sediment P load [kg month^{-1}]	Low	0-3	Based on "Buffer effectiveness for Suspended Sediments and Particulate P", for effective buffers, Modified Sediment P load= Monthly Sediment P load [kg month^{-1}]*(1-Buffer effectiveness for SS and PP). Based on expert recommendation.
	High	3-200	
Septic Tanks (ST) sub-model (Point P sources)			
P concentration per tank [mg l^{-1}]	Absent (to represent 0 STs)	0-1*10^{-8}	P concentration is dependent on the treatment type. If the treatment is unknown, the concentration is defined as a Lognormal distribution (μ=2.9, σ =1.25), based on a literature review of data available for Ireland (Environmental Protection Agency Ireland (EPA), 2003, 2000; Gill et al., 2005, 2007) (n=8). Fitting was done with R package *fitdistrplus* (version 1.1-8, Delignette-Muller et al., 2020). Otherwise, for primary and secondary treatment concentration is defined as Truncated Normal distribution (μ=10; σ=1), and (μ=5; σ=0.5) respectively, as described in Glendell et al., (2021) and derived from SEPA guidelines (Brownlie et al., 2014). All tanks are assumed to be maintained. Discretization was also based on the literature review.
	Low	1*10^{-8}-1	
	Medium	1-18	
	High	18-35	
	Very High	35-100	
Direct discharge	Present	0.16	Probabilities are derived from the report by the Environmental Protection Agency Ireland (EPA, 2015).
	Absent	0.84	

<table>
<tr><td rowspan="5">Degree of Phosphorus Saturation (DPS) [%]</td><td>Very_Low_0-20</td><td>0.85</td><td rowspan="5">Discretization is equal to the 20th, 40th, 60th, and 80th quantiles. Probabilities were calculated from available spatial data (Wall et al., 2012).</td></tr>
<tr><td>Low_20-40</td><td>0.117</td></tr>
<tr><td>Medium_40-60</td><td>0.0145</td></tr>
<tr><td>High_60-80</td><td>0.01</td></tr>
<tr><td>Very_High_80-100</td><td>0.0085</td></tr>
<tr><td rowspan="5">Soil risk factor [adimensional]</td><td>Low</td><td>0.639</td><td rowspan="5">An indicator to describe the combined risk of effluent leaching to the groundwater table with the risk of the effluent being transported with surface runoff. This approach is a simplification of the one adopted in Glendell et al., (2021). The risk factor was obtained by overlaying the soil series (Thomas et al., 2016b) with information on the position of the groundwater table (0- 2 m below ground or more than 2 m below ground). Because little is known regarding the septic tanks in the catchment (i.e. age, type of treatment, maintenance), and the groundwater table position (few datapoints within the catchment) experts recommended a precautionary principle. This meant that the class at most risk of effluent transfer was applied when data was unavailable. The table to the left represents a synthesis of the classification approach. Probabilities are based on land cover proportion.</td></tr>
<tr><td>Medium</td><td>0.236</td></tr>
<tr><td>High</td><td>0</td></tr>
<tr><td>Very High</td><td>0.125</td></tr>
<tr><td colspan="2"><table>
<tr><th></th><th colspan="2">Groundwater Table Position</th></tr>
<tr><th>Soil Series</th><th>0-2 m below surface</th><th>>2 m below surface</th></tr>
<tr><td>Brown earths</td><td>High Risk</td><td>Moderate Risk</td></tr>
<tr><td>Gleys</td><td>Very High Risk</td><td>Very High Risk</td></tr>
</table></td></tr>
<tr><td>Leachfield removal</td><td colspan="2"><table>
<tr><th>Soil risk factor</th><th>DPS</th><th>Low</th><th>Medium</th><th>High</th></tr>
<tr><td rowspan="5">Low</td><td>Very Low</td><td>0</td><td>0</td><td>1</td></tr>
<tr><td>Low</td><td>0</td><td>0.1</td><td>0.9</td></tr>
<tr><td>Medium</td><td>0</td><td>0.5</td><td>0.5</td></tr>
<tr><td>High</td><td>0.1</td><td>0.4</td><td>0.5</td></tr>
<tr><td>Very High</td><td>0.1</td><td>0.6</td><td>0.3</td></tr>
<tr><td rowspan="5">Medium</td><td>Very Low</td><td>0</td><td>0.4</td><td>0.6</td></tr>
<tr><td>Low</td><td>0.1</td><td>0.3</td><td>0.6</td></tr>
<tr><td>Medium</td><td>0.1</td><td>0.8</td><td>0.1</td></tr>
<tr><td>High</td><td>0.5</td><td>0.5</td><td>0</td></tr>
<tr><td>Very High</td><td>0.6</td><td>0.4</td><td>0</td></tr>
<tr><td rowspan="5">High</td><td>Very Low</td><td>0.3</td><td>0.7</td><td>0</td></tr>
<tr><td>Low</td><td>0.4</td><td>0.6</td><td>0</td></tr>
<tr><td>Medium</td><td>0.6</td><td>0.5</td><td>0</td></tr>
<tr><td>High</td><td>0.7</td><td>0.3</td><td>0</td></tr>
<tr><td>Very High</td><td>0.9</td><td>0.1</td><td>0</td></tr>
<tr><td rowspan="2">Very High</td><td>Very Low</td><td>0.4</td><td>0.6</td><td>0</td></tr>
<tr><td>Low</td><td>0.5</td><td>0.5</td><td>0</td></tr>
</table></td><td>The node refers to P removal from septic drains. Conditional on P leaching risk from Degree of Phosphorus Saturation (DPS). The conditional probability table is a logical one.</td></tr>
</table>

Medium	0.6	0.4	0			
High	0.9	0.1	0			
Very High	1	0	0			

Leachfield connectedness

HSA rescaled	**None**		**Low**		**Medium**		**High**	
Direct discharge	**pres**	**abs**	**pres**	**abs**	**pres**	**abs**	**pres**	**abs**
low	0	1	0	1	0	0	0	0
medium	0	0	0	0	0	1	0	0
high	1	0	1	0	1	0	1	1

Probabilities are conditional on the presence/absence of Direct ST discharge, and HSA (node: Connectivity rescaled HSA). Where Direct discharge is present, connectedness is assumed as 'high'. Where Direct discharge is absent, the risk class of the HSA is assigned.

Septic Tank connectedness

Leachfield removal	**Low**			**Medium**			**High**		
Leachfield connectedness	**Low**	**Medium**	**High**	**Low**	**Medium**	**High**	**Low**	**Medium**	**High**
Low	1.0	0.0	0.0	1.0	0.0	0.0	1.0	0.5	0.0
Medium	0.0	1.0	0.0	0.0	1.0	0.5	0.0	0.5	1.0
High	0.0	0.0	1.0	0.0	0.0	0.5	0.0	0.0	0.0

Probabilities are conditional on Leachfield removal and Leachfield connectedness. Where Leachfield removal is 'low' or 'High', Leachfield connectedness remains unaltered.

Connectivity rescaled HSA [adimensional]

None_0	0.06
Low_1-3	0.73
Medium_4-7	0.2
High_8-10	0.01

Data extracted from spatial layers of Hydrologically Sensitive Areas (HSAs) rescaled between 0 and 10 was provided by the Agricultural Catchments Programme (Thomas et al., 2016a). Discretization is also based on the spatial layers.

Load per tank [kg month^{-1}]

Absent	0-1*10^{-6}
Very Low	1*10^{-6}-0.1
Low	0.1-0.5
Medium	0.5-1.0
High	1.0-2.0
Very High	2.0-30

Specified as the product of ST density [No ha^{-1}] * ST concentration [mg l^{-1}] * 120 [L] average daily water consumption per person * 365/12 days in a month* average No of persons per household 2.7/1*10^{6}. Discretisation is based on interpolation to represent plausible probabilities for combination of extreme risk classes (e.g. High+high=high, low+low=low).

Total Realized load [T month^{-1}]

Very Low	0.0-0.1
Low	0.1-0.5
Medium	0.5-1.0
High	1.0-2.0
Very High	2.0-12

Septic tank connectedness	**Delivery factor (D)**	**Reference**
Low	0.05	"very low" category in Appendix A3, Glendell et al., (2021)
Medium	0.30	"medium" category in Appendix A3, Glendell et al., (2021)

Calculated as the product of septic tank load and delivery factors (D) related to the connectedness of a septic tank, based on the median estimated fraction to be delivered in Table 13 of the report by Glendell et al., (2021) and the number of septic tanks present within catchment boundary (N): Realised load per tank [kg month^{-1}] * N * D / 1000. In this case, N= 88. Discretisation based on interpolation to represent plausible probabilities for combination of extreme risk classes.

		High	0.80	"very high" category in Appendix A3, Glendell et al., (2021)	
Farmyards sub-model (Point P sources)					
Farmyard size area [m^2]	Very Low			0-99	Based on available farmyard survey, a distribution was fitted to farmyard area data: Lognormal (μ=-5.9; σ=0.83). Discretization of states is based on percentiles calculated from the observations (very low<= 5^{th} percentile, low= 5^{th}-25^{th} percentile, medium= 25^{th}-50^{th} percentile, high= 50^{th}-75^{th} percentile, very high= 75^{th}-100^{th} percentile).
	Low			99-204	
	Medium			204-378	
	High			378-665	
	Very High			665-5500	
Farmyard P concentration [mg l^{-1}]	Very Low			0-0.01	Using the *SHELF* R package (version 1.8.0, Oakley, 2020), a distribution was fitted to the data in Table 2 in Harrison et al., (2019): Lognormal (μ=-1.8; σ=1.6). The best fit would have been the LogT distribution, however, that is not available for Genie, so we opted for Lognormal. Discretization is also based on the literature. For simplicity, here we have used SRP to mean TRP.
	Low			0.01-0.50	
	Medium			0.50-1.00	
	High			1.00-2.50	
	Very High			2.50-60	
Incidental losses per average yard [kg $month^{-1}$]	Very Low			0-1*10^{-9}	Based on average farmyard size, losses are calculated as Surface runoff [m^3] / catchment area [m^2]* Farmyard size area [m^2]* Farmyard P concentration [mg l^{-1}]/ 10^3. Catchment area is set at 758 ha.
	Low			1*10^{-9}-0.001	
	Medium			0.001-0.01	
	High			0.01-0.10	
	Very High			0.10-60	
Total incidental losses [T $month^{-1}$]	Very Low			0-1*10^{-5}	Incidental losses per average yard [kg $month^{-1}$] * N, where N is the total number of yards present within the catchment boundary. In this case, N =70.
	Low			1e-05-0.007	
	Medium			0.007-0.070	
	High			0.07-0.700	
	Very High			0.700-10	
Catchment outlet integration sub-model					
Total catchment in-stream P load [T $month^{-1}$]	Low			0-0.02	Equal to the sum of Baseflow Dissolved P load [kg $month^{-1}$], Modified Dissolved P load [kg month-^{1}], Modified Sediment P load [kg $month^{-1}$], Total incidental losses [T $month^{-1}$], and Total Realized load [T $month^{-1}$], all converted to appropriate units.
	Medium			0.002-1	
	High			1-10	
(meteorological) Season					Based on the node "Month".
In-stream winter P removal	Very Low			-1, -0.5	Defined as a Normal distribution (μ=0.1; σ=0.05) derived from expert elicitation with the R package (version 1.8.0, Oakley, 2020).
	Low			-0.5-0	
	Medium			0-0.5	
	High			0.5-1	
In-stream spring P removal	Very Low			0-0.2	Defined as a Normal distribution (μ=0.35; σ=0.21) derived from expert elicitation with the R package (version 1.8.0, Oakley, 2020).
	Low			0.2-0.4	
	Medium			0.4-0.6	

<table>
<tr><td></td><td>High</td><td>0.6-0.8</td><td></td></tr>
<tr><td rowspan="5">In-stream summer P removal</td><td>Very Low</td><td>0.1-0.3</td><td rowspan="5">Defined as a Normal distribution (μ=0.43; σ=012) derived from expert elicitation with the R package (version 1.8.0, Oakley, 2020).</td></tr>
<tr><td>Low</td><td>0.3-0.45</td></tr>
<tr><td>Medium</td><td>0.45-0.6</td></tr>
<tr><td>High</td><td>0.6-0.8</td></tr>
<tr><td rowspan="5">In-stream autumn P removal</td><td>Very Low</td><td>0-0.2</td><td rowspan="5">Defined as a Normal distribution (μ=0.25; σ=0.07) derived from expert elicitation with the R package (version 1.8.0, Oakley, 2020).</td></tr>
<tr><td>Low</td><td>0.2-0.4</td></tr>
<tr><td>Medium</td><td>0.4-0.5</td></tr>
<tr><td>High</td><td>0.5-0.65</td></tr>
<tr><td rowspan="2">In-stream reduced P load [T month^{-1}]</td><td>Moderate</td><td>0-0.5</td><td rowspan="2">Calculated as the product of Total catchment in-stream P load and the seasonal removal.</td></tr>
<tr><td>Bad</td><td>0.5-10</td></tr>
<tr><td rowspan="2">In-stream P concentration [mg l^{-1}]</td><td>Good</td><td>0-0.035</td><td rowspan="2">Defined as the in-stream reduced P load [T] * 10^9 / Mean total monthly Q (discharge) [m^3] * 1000, where mean monthly discharge is equal to the total catchment discharge measured at the outlet.</td></tr>
<tr><td>Bad</td><td>0.035-5</td></tr>
<tr><td>Environmental Quality Standard [TRP concentration mg l^{-1}]</td><td colspan="2"><table><tr><th>TRP concentration</th><th>Good</th><th>Bad</th></tr><tr><td>Good</td><td>1</td><td>0</td></tr><tr><td>Bad</td><td>0</td><td>1</td></tr></table></td><td>Discretization of the variable “In-stream TRP concentration [mg l^{-1}]”. For simplicity, in-stream TRP is here considered equal to in-stream Dissolved Reactive Phosphorus, as in previous studies the mean DRP accounted for 98–99% of the flow-weighted mean TRP (Shore et al., 2014).</td></tr>
</table>

9.4 Supplementary Results

Table 9.5 Summary of months' results, including Percentage Bias and P concentrations, which have been calculated excluding data outside the instrument's limit of detection (0.01-5.00 mg l^{-1}). Both observed and predicted TRP concentrations were log-transformed before calculating the statistics, and then converted back to normal values. For each catchment, results are reported only for Structure 1 ("Str 1") and the best performing model structure which includes in-stream P removal. Therefore, the column "final" describes Structure 5 for Timoleague, Structure 2 for Ballycanew and Dunleer, and Structure 6 for Castledockrell. A positive bias indicates overestimation. Observations are shaded in grey to improve readability of text.

		Percentage bias of simulations against distribution fitted to observed		mean (μ) concentrations (mg l^{-1})			lower limit concentrations (μ-1σ) (mg l^{-1})			upper limit concentrations (μ+1σ) (mg l^{-1})		
		Str 1	final	Str 1	final	observations	Str 1	final	observations	Str 1	final	observations
Timoleague	Jan	28	-20	0.14	0.05	0.05	0.05	0.04	0.04	0.40	0.06	0.08
	Feb	289	5	0.14	0.06	0.05	0.05	0.05	0.04	0.41	0.08	0.08
	Mar	281	-10	0.14	0.05	0.04	0.05	0.03	0.03	0.40	0.08	0.07
	Apr	281	-26	0.14	0.04	0.04	0.05	0.03	0.02	0.40	0.07	0.07
	May	286	11	0.14	0.06	0.04	0.05	0.03	0.02	0.41	0.10	0.06
	Jun	283	-12	0.14	0.05	0.06	0.05	0.03	0.03	0.41	0.07	0.10
	Jul	280	-18	0.14	0.05	0.06	0.05	0.03	0.04	0.40	0.07	0.12
	Aug	290	20	0.14	0.07	0.06	0.05	0.04	0.03	0.41	0.10	0.13
	Sept	277	17	0.13	0.07	0.05	0.05	0.04	0.03	0.40	0.10	0.08
	Oct	286	-1	0.14	0.06	0.06	0.05	0.04	0.04	0.41	0.08	0.11
	Nov	285	-10	0.14	0.05	0.06	0.05	0.04	0.04	0.40	0.07	0.10
	Dec	286	-19	0.14	0.05	0.06	0.05	0.04	0.04	0.40	0.07	0.09
Ballycanew	Jan	70	57	0.08	0.08	0.05	0.03	0.03	0.03	0.20	0.19	0.07
	Feb	72	63	0.08	0.08	0.04	0.03	0.03	0.03	0.21	0.19	0.07
	Mar	75	40	0.08	0.07	0.04	0.03	0.03	0.03	0.21	0.16	0.07
	Apr	78	39	0.08	0.07	0.05	0.03	0.03	0.03	0.21	0.16	0.09
	May	78	40	0.08	0.07	0.05	0.03	0.03	0.02	0.22	0.17	0.07
	Jun	91	39	0.09	0.07	0.07	0.03	0.03	0.03	0.23	0.16	0.13
	Jul	107	47	0.09	0.07	0.09	0.04	0.03	0.05	0.25	0.17	0.14
	Aug	88	39	0.09	0.07	0.09	0.03	0.03	0.05	0.23	0.16	0.16
	Sept	99	64	0.09	0.08	0.07	0.04	0.03	0.04	0.294	0.19	0.12
	Oct	77	48	0.08	0.07	0.07	0.03	0.03	0.04	0.21	0.18	0.13
	Nov	74	47	0.08	0.07	0.07	0.03	0.03	0.04	0.21	0.17	0.12
	Dec	73	58	0.08	0.08	0.06	0.03	0.03	0.04	0.21	0.19	0.09

Castledockrell	**Jan**	485	-38	0.12	0.02	0.02	0.05	0.01	0.01	0.29	0.02	0.02
	Feb	485	-36	0.12	0.02	0.02	0.05	0.01	0.01	0.29	0.02	0.02
	Mar	461	-14	0.11	0.02	0.02	0.04	0.01	0.02	0.29	0.03	0.03
	Apr	471	10	0.11	0.02	0.02	0.04	0.01	0.01	0.29	0.04	0.03
	May	413	31	0.09	0.02	0.02	0.03	0.01	0.01	0.27	0.05	0.03
	Jun	424	27	0.09	0.03	0.03	0.03	0.01	0.02	0.27	0.05	0.05
	Jul	437	57	0.09	0.03	0.04	0.03	0.01	0.03	0.27	0.06	0.07
	Aug	420	62	0.09	0.03	0.04	0.03	0.01	0.03	0.26	0.06	0.07
	Sept	430	61	0.09	0.03	0.03	0.03	0.01	0.02	0.27	0.06	0.06
	Oct	428	51	0.09	0.03	0.03	0.03	0.02	0.02	0.28	0.06	0.05
	Nov	499	-27	0.13	0.02	0.02	0.05	0.01	0.01	0.30	0.03	0.03
	Dec	491	6	0.12	0.03	0.02	0.05	0.02	0.01	0.29	0.04	0.03
Dunleer	**Jan**	98.3	75.4	0.12	0.11	0.07	0.04	0.03	0.05	0.40	0.35	0.09
	Feb	95.6	74.1	0.12	0.11	0.06	0.04	0.03	0.04	0.39	0.34	0.09
	Mar	96.9	33.8	0.11	0.08	0.07	0.03	0.03	0.04	0.39	0.25	0.11
	Apr	87.5	31.8	0.11	0.08	0.08	0.03	0.03	0.04	0.37	0.25	0.13
	May	83.6	34.4	0.11	0.08	0.08	0.03	0.03	0.06	0.36	0.25	0.12
	Jun	94.3	23.9	0.11	0.08	0.13	0.03	0.03	0.09	0.38	0.23	0.18
	Jul	94.9	31.7	0.11	0.08	0.15	0.03	0.03	0.11	0.38	0.25	0.20
	Aug	97.9	28.3	0.11	0.08	0.17	0.03	0.03	0.12	0.38	0.24	0.23
	Sept	90.3	54.5	0.11	0.09	0.15	0.03	0.03	0.10	0.37	0.30	0.23
	Oct	91.5	49.6	0.11	0.09	0.11	0.03	0.03	0.08	0.38	0.29	0.17
	Nov	99.7	50.5	0.12	0.09	0.09	0.04	0.03	0.06	0.40	0.29	0.12
	Dec	92.4	75.4	0.12	0.11	0.08	0.04	0.03	0.05	0.38	0.34	0.12

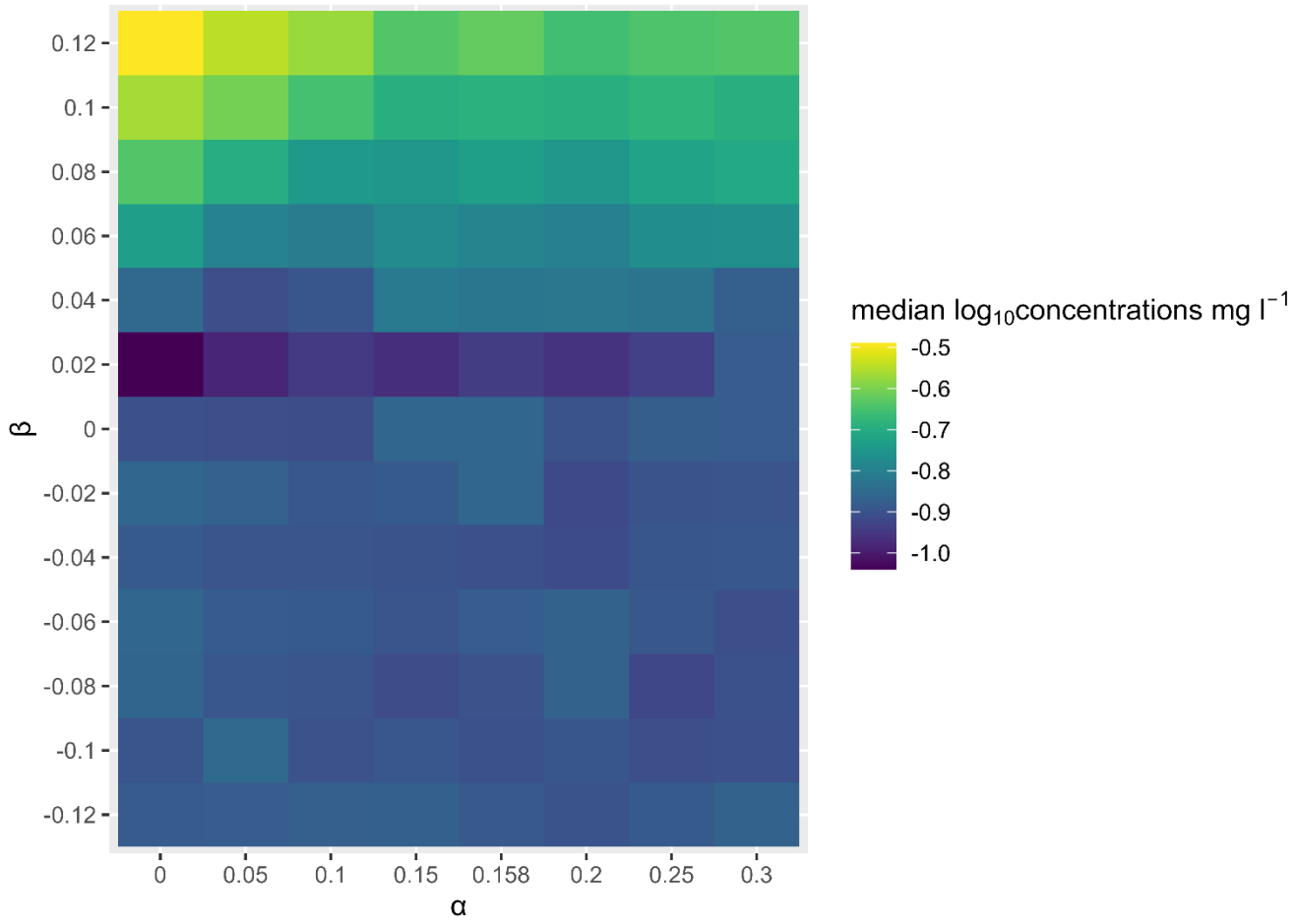

Figure 9.1 A representation of the impact of varying both α and β parameters of Predicted Dissolved P Concentration [mg l^{-1}] on the median log_{10}(TRP) concentration. In order to combine the effect of both parameters, a limited number of values were tested for both α and β. The figure shows the target TRP concentration is more sensitive to the β parameter than the α.

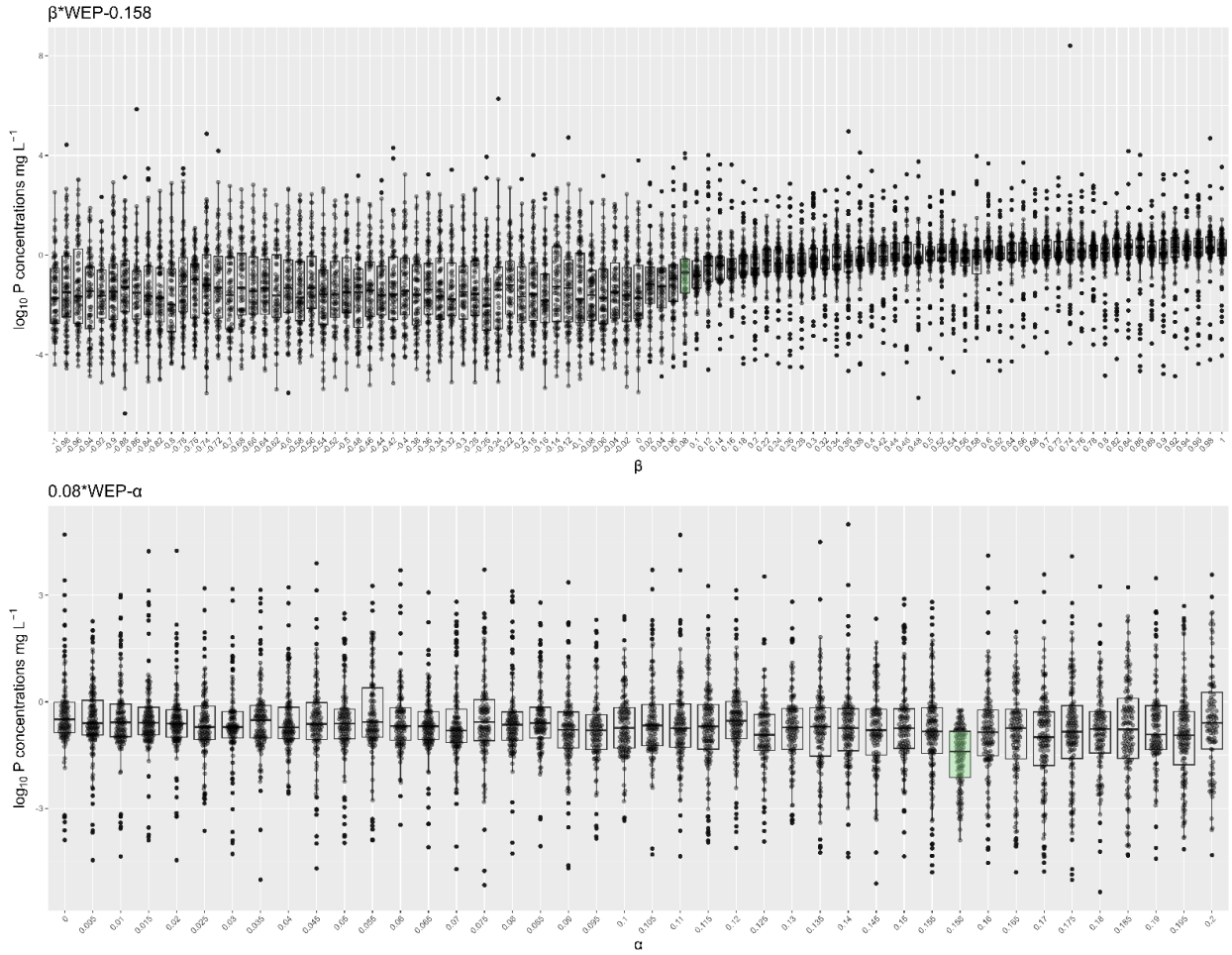

Figure 9.2 Results of the sensitivity analysis on the two parameters for the "Predicted Dissolved P concentration" node, β (slope, top plot) and α (intercept, bottom plot) displayed as boxplots showing the median (central line), interquartile range (box) for the log_{10}(TRP) concentration (mg l^{-1}) distribution of each simulation, filled black points show the scatter of the realizations. Values assumed for each parameter in each simulation are shown on the x axis, the boxplots of the "simulation 0" are shown in light green. Results are shown for the model Structure 2 for the Dunleer catchment.

10. Supplementary Materials to Chapter 5

Table 10.1 Mean log_{10}(TRP) (mg l^{-1}) predicted with model ensemble against the mean observed TRP at the catchment outlet. All concentrations have been filtered by the instrument's detection limit (0.01-5.00 mg l^{-1}).

Timoleague						
	RCP 4.5 (NSE)	**RCP 4.5 (logNSE)**	**RCP 8.5 (NSE)**	**RCP 8.5 (log NSE)**	**obs**	**BBN baseline (Chapter 4)**
2009-2016	-	-	-	-	-1.27±0.24	1.28±0.18
2010-2039	1.29±0.17	1.29±0.17	1.29±0.17	1.29±0.17	-	-
2040-2069	1.29±0.17	1.28±0.18	1.29±0.17	1.28±0.18	-	-
2070-2099	1.29±0.17	1.28±0.18	1.29±0.17	1.28±0.18	-	-
Ballycanew						
	RCP 4.5 (NSE)	**RCP 4.5 (log NSE)**	**RCP 8.5 (NSE)**	**RCP 8.5 (log NSE)**	**obs**	**BBN baseline (Chapter 4)**
2009-2016	-	-	-	-	-1.20±0.24	1.15±0.38
2010-2039	1.15±0.38	1.15±0.38	1.15±0.38	1.15±0.38	-	-
2040-2069	1.15±0.38	1.15±0.38	1.15±0.38	1.15±0.38	-	-
2070-2099	1.15±0.38	1.15±0.38	1.15±0.38	1.15±0.38	-	-
Castledockerell						
	RCP 4.5 (NSE)	**RCP 4.5 (log NSE)**	**RCP 8.5 (NSE)**	**RCP 8.5 (log NSE)**	**obs**	**BBN baseline (Chapter 4)**
2009-2016	-	-	-	-	1.62±0.28	-1.61±0.29
2010-2039	1.60±0.28	1.60±0.28	1.60±0.29	1.60±0.29	-	-
2040-2069	1.60±0.29	1.60±0.29	1.60±0.28	1.60±0.28	-	-
2070-2099	1.60±0.29	1.60±0.29	1.61±0.29	1.61±0.29	-	-
Dunleer						
	RCP 4.5 (NSE)	**RCP 4.5 (log NSE)**	**RCP 8.5 (NSE)**	**RCP 8.5 (log NSE)**	**obs**	**BBN baseline (Chapter 4)**
2009-2016	-	-	-	-	-1.02±0.22	1.05±0.49
2010-2039	1.04±0.49	1.05±0.49	1.05±0.48	1.05±0.49	-	-
2040-2069	1.04±0.49	1.05±0.49	1.05±0.49	1.05±0.49	-	-
2070-2099	1.04±0.49	1.05±0.48	1.04±0.49	1.04±0.49	-	-

Table 10.2 Mean monthly TRP concentration (mg l^{-1}) in the four catchments as predicted by each model in September using the RCP 8.5 scenarios. Predicted TRP concentrations were log-transformed before calculating the statistics, and then converted back to normal values. Results are shown for the NSE calibration of the SMART model only. Concentrations are shown for the observations (obs) and the BBN (BBN baseline) in the reference period (2009-2016).

				Timoleague				
	CNRM-CM5	**EC-EARTH**	**HadGEM2**	**MIROC5**	**MPI-ESM-LR**	**model ensemble**	**obs**	**BBN baseline (Chapter 4)**
2009-2016	-	-		-		-	0.05	0.07
2010-2039	0.06	0.06	0.07	0.06	0.06	0.06	-	-
2040-2069	0.06	0.07	0.08	0.06	0.06	0.06	-	-
2070-2099	0.06	0.07	0.08	0.06	0.06	0.06	-	-
				Ballycanew				
	CNRM-CM5	**EC-EARTH**	**HadGEM2**	**MIROC5**	**MPI-ESM-LR**	**model ensemble**	**obs**	**BBN baseline (Chapter 4)**
2009-2016	-	-		-		-	0.07	0.08
2010-2039	0.07	0.07	0.08	0.07	0.07	0.07	-	-
2040-2069	0.07	0.07	0.09	0.07	0.07	0.07	-	-
2070-2099	0.07	0.07	0.09	0.07	0.07	0.07	-	-
				Castledockerell				
	CNRM-CM5	**EC-EARTH**	**HadGEM2**	**MIROC5**	**MPI-ESM-LR**	**model ensemble**	**obs**	**BBN baseline (Chapter 4)**
2009-2016	-	-		-		-	0.03	0.03
2010-2039	0.03	0.04	0.08	0.02	0.02	0.03	-	-
2040-2069	0.03	0.03	0.07	0.02	0.02	0.02	-	-
2070-2099	0.03	0.04	0.07	0.02	0.02	0.02	-	-
				Dunleer				
	CNRM-CM5	**EC-EARTH**	**HadGEM2**	**MIROC5**	**MPI-ESM-LR**	**model ensemble**	**obs**	**BBN baseline (Chapter 4)**
2009-2016	-	-		-		-	0.15	0.09
2010-2039	0.09	0.09	0.11	0.09	0.09	0.09	-	-
2040-2069	0.09	0.09	0.11	0.09	0.09	0.09	-	-
2070-2099	0.09	0.09	0.11	0.09	0.09	0.09	-	-

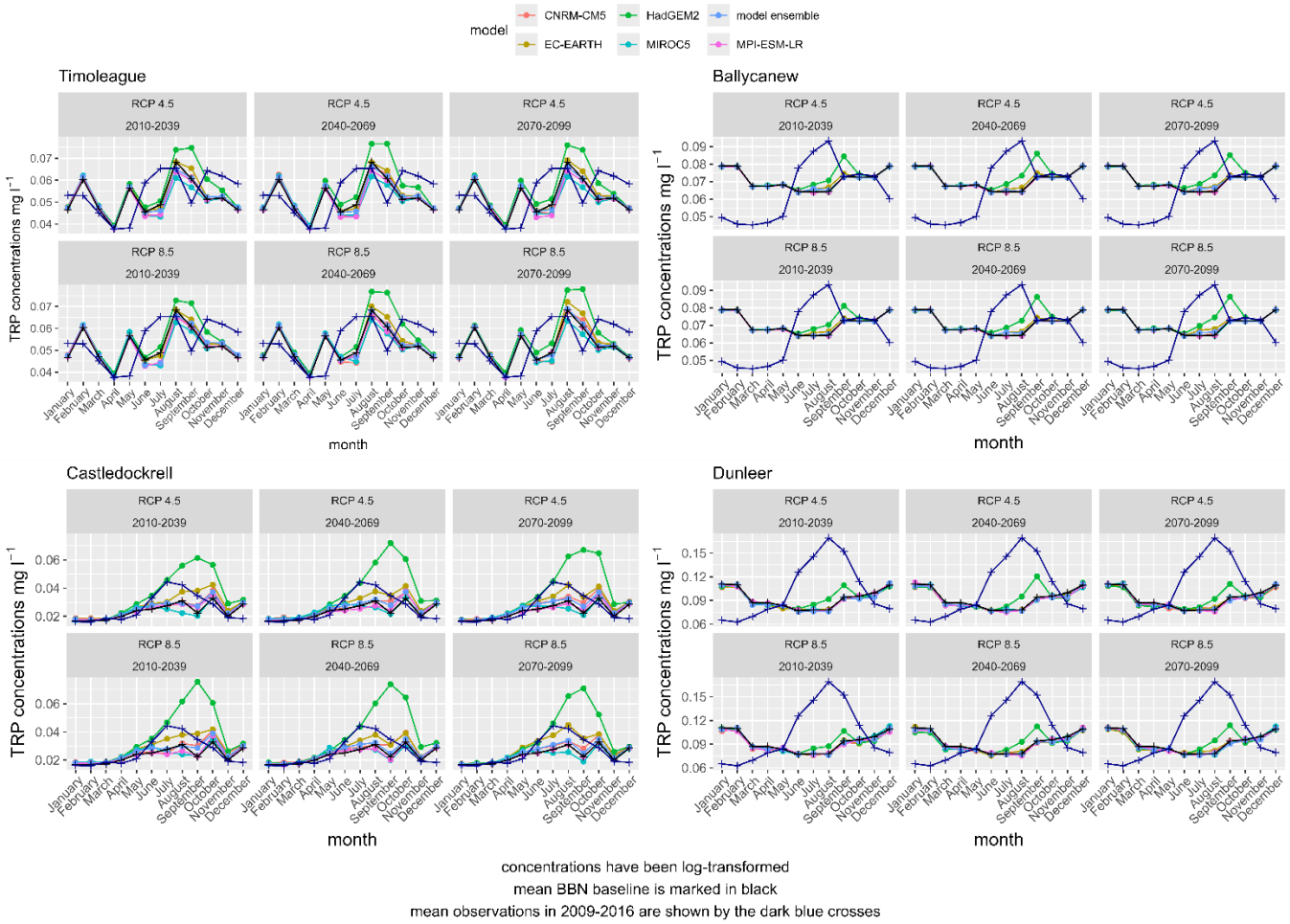

Figure 10.1 Mean monthly TRP concentration (mg l^{-1}) in the four catchments driven by five climate models, the mean of the ensemble and the BBN in the reference period are plotted with the mean observations. The predictions for the BBN baseline are shown in black and they remain the same for each catchment in each plot, the same was done for the observations (2009-2016) which are shown by the blue crosses. Predicted TRP concentrations were log-transformed before calculating the statistics, and then converted back to normal values. Results are shown for the NSE calibration of the SMART model only.

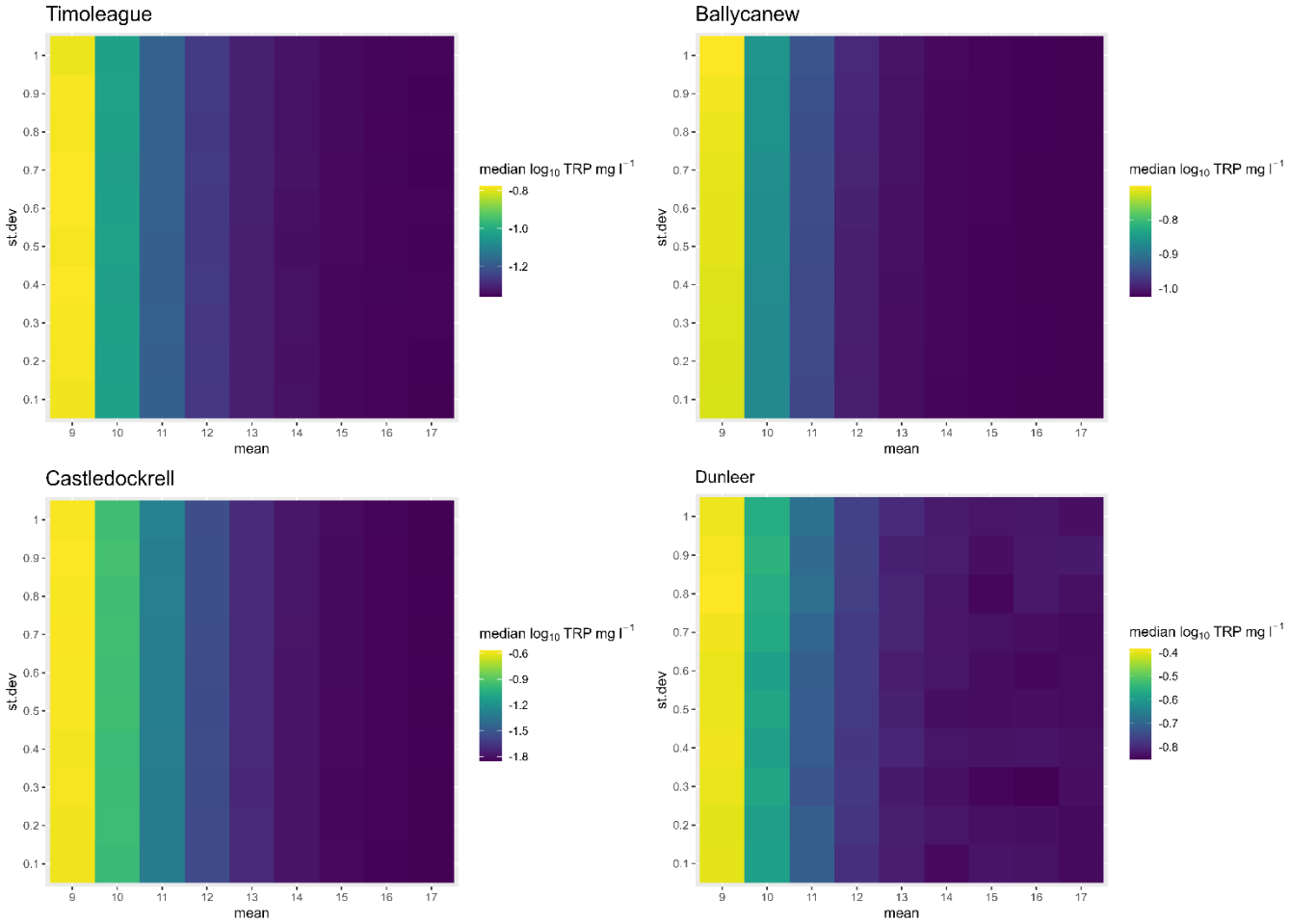

Figure 10.2 BBN Sensitivity to changes in mean and standard deviation in the discharge (Q) node across the four catchments, from top left to bottom rights: Timoleague, Ballycanew, Castledockrell, and Dunleer. The effect is shown on the median log10(TRP) concentration (mg l-1). For all catchments, sensitivity is visible along changes in the January mean Q (along the x axis), but not for changes in the January standard deviation of Q (along the y axis).

References

Adams, K.J., Macleod, C.A.J., Metzger, M.J., Melville, N., Helliwell, R.C., Pritchard, J., Glendell, M., 2023. Developing a Bayesian network model for understanding river catchment resilience under future change scenarios. Hydrol. Earth Syst. Sci. 27, 2205–2225. https://doi.org/10.5194/hess-27-2205-2023

Adams, K.J., Metzger, M.J., Macleod, C. (Kit) J.A., Helliwell, R.C., Pohle, I., 2022. Understanding knowledge needs for Scotland to become a resilient Hydro Nation: Water stakeholder perspectives. Environ. Sci. Policy 136, 157–166. https://doi.org/10.1016/j.envsci.2022.06.006

Aguilera, P.A., Fernández, A., Fernández, R., Rumí, R., Salmerón, A., 2011. Bayesian networks in environmental modelling. Environ. Model. Softw. 26, 1376–1388. https://doi.org/10.1016/j.envsoft.2011.06.004

Amery, F., Schoumans, O.F., 2014. Agricultural phosphorus legislation in Europe. Institute for Agricultural and Fisheries Research (ILVO), Merelbeke.

Ames, D.P., Neilson, B.T., Stevens, D.K., Lall, U., 2005. Using Bayesian networks to model watershed management decisions: an East Canyon Creek case study. J. Hydroinformatics 7, 267–282. https://doi.org/10.2166/hydro.2005.0023

Barton, D.N., Kuikka, S., Varis, O., Uusitalo, L., Henriksen, H.J., Borsuk, M., de la Hera, A., Farmani, R., Johnson, S., Linnell, J.D., 2012. Bayesian networks in environmental and resource management. Integr. Environ. Assess. Manag. 8, 418–429. https://doi.org/10.1002/ieam.1327

BayesFusion, 2019a. GeNIe [WWW Document]. URL https://www.bayesfusion.com/ (accessed 5.6.20).

BayesFusion, 2019b. GeNIe 2.4 [WWW Document]. URL https://www.bayesfusion.com/ (accessed 5.6.20).

BayesFusion, 2019c. SMILE Engine [WWW Document]. URL https://www.bayesfusion.com/smile/ (accessed 7.26.23).

Beven, K., 2019. Towards a methodology for testing models as hypotheses in the inexact sciences. Proc. R. Soc. Math. Phys. Eng. Sci. 475, 20180862. https://doi.org/10.1098/rspa.2018.0862

Beven, K., 2006. Searching for the Holy Grail of scientific hydrology: Qt=(S, R, ?t)A as closure. Hydrol. Earth Syst. Sci. Discuss. 10, 609–618.

Bierkens, M.F.P., 1996. Modeling Hydraulic Conductivity of a Complex Confining Layer at Various Spatial Scales. Water Resour. Res. 32, 2369–2382. https://doi.org/10.1029/96WR01465

Bieroza, M., Acharya, S., Benisch, J., ter Borg, R.N., Hallberg, L., Negri, C., Pruitt, A., Pucher, M., Saavedra, F., Staniszewska, K., van't Veen, S.G.M., Vincent, A., Winter, C., Basu, N.B., Jarvie, H.P., Kirchner, J.W., 2023. Advances in Catchment Science, Hydrochemistry, and Aquatic Ecology Enabled by High-Frequency Water Quality Measurements. Environ. Sci. Technol. https://doi.org/10.1021/acs.est.2c07798

Bieroza, M., Bergström, L., Ulén, B., Djodjic, F., Tonderski, K., Heeb, A., Svensson, J., Malgeryd, J., 2019. Hydrologic Extremes and Legacy Sources Can Override Efforts to Mitigate Nutrient and Sediment Losses at the Catchment Scale. J. Environ. Qual. 48, 1314–1324. https://doi.org/10.2134/jeq2019.02.0063

Bieroza, M.Z., Heathwaite, A.L., Bechmann, M., Kyllmar, K., Jordan, P., 2018. The concentration-discharge slope as a tool for water quality management. Sci. Total Environ. 630, 738–749. https://doi.org/10.1016/j.scitotenv.2018.02.256

Blöschl, G., Bierkens, M.F.P., Chambel, A., 2019. Twenty-three unsolved problems in hydrology (UPH) – a community perspective. Hydrol. Sci. J. 64, 1141–1158. https://doi.org/10.1080/02626667.2019.1620507

Bol, R., Gruau, G., Mellander, P.-E., Dupas, R., Bechmann, M., Skarbøvik, E., Bieroza, M., Djodjic, F., Glendell, M., Jordan, P., Van der Grift, B., Rode, M., Smolders, E., Verbeeck, M., Gu, S., Klumpp, E., Pohle, I., Fresne, M., Gascuel-Odoux, C., 2018. Challenges of Reducing

Phosphorus Based Water Eutrophication in the Agricultural Landscapes of Northwest Europe. Front. Mar. Sci. 5.
Borsuk, M.E., Stow, C.A., Reckhow, K.H., 2004. A Bayesian network of eutrophication models for synthesis, prediction, and uncertainty analysis. Ecol. Model. 173, 219–239. https://doi.org/10.1016/j.ecolmodel.2003.08.020
Bowes, M.J., Gozzard, E., Johnson, A.C., Scarlett, P.M., Roberts, C., Read, D.S., Armstrong, L.K., Harman, S.A., Wickham, H.D., 2012. Spatial and temporal changes in chlorophyll-a concentrations in the River Thames basin, UK: Are phosphorus concentrations beginning to limit phytoplankton biomass? Sci. Total Environ. 426, 45–55. https://doi.org/10.1016/j.scitotenv.2012.02.056
Bowes, M.J., Jarvie, H.P., Halliday, S.J., Skeffington, R.A., Wade, A.J., Loewenthal, M., Gozzard, E., Newman, J.R., Palmer-Felgate, E.J., 2015. Characterising phosphorus and nitrate inputs to a rural river using high-frequency concentration–flow relationships. Sci. Total Environ. 511, 608–620. https://doi.org/10.1016/j.scitotenv.2014.12.086
Bowes, M.J., Loewenthal, M., Read, D.S., Hutchins, M.G., Prudhomme, C., Armstrong, L.K., Harman, S.A., Wickham, H.D., Gozzard, E., Carvalho, L., 2016. Identifying multiple stressor controls on phytoplankton dynamics in the River Thames (UK) using high-frequency water quality data. Sci. Total Environ. 569–570, 1489–1499. https://doi.org/10.1016/j.scitotenv.2016.06.239
Brabec, Macháč, Jílková, 2019. Using Bayesian Networks to Assess Effectiveness of Phosphorus Abatement Measures under the Water Framework Directive. Water 11, 1791. https://doi.org/10.3390/w11091791
Brazier, R.E., Heathwaite, A.L., Liu, S., 2005. Scaling issues relating to phosphorus transfer from land to water in agricultural catchments. J. Hydrol., Nutrient Mobility within River Basins: A European Perspective 304, 330–342. https://doi.org/10.1016/j.jhydrol.2004.07.047
Bromley, J., Jackson, N.A., Clymer, O.J., Giacomello, A.M., Jensen, F.V., 2005. The use of Hugin® to develop Bayesian networks as an aid to integrated water resource planning. Environ. Model. Softw., Policies and Tools for Sustainable Water Management in the European Union 20, 231–242. https://doi.org/10.1016/j.envsoft.2003.12.021
Brownlie, W., May, L., McDonald, C., Roaf, S., Spears, B.M., 2014. Assessment of a novel development policy for the control of phosphorus losses from private sewage systems to the Loch Leven catchment, Scotland, UK. Environ. Sci. Policy 38, 207–216. https://doi.org/10.1016/j.envsci.2013.12.006
Campbell, J.M., Jordan, P., Arnscheidt, J., 2015. Using high-resolution phosphorus data to investigate mitigation measures in headwater river catchments. Hydrol. Earth Syst. Sci. 19, 453–464. https://doi.org/10.5194/hess-19-453-2015
Campbell, N., D'Arcy, B., Frost, A., Novotny, V., Sansom, A., 2005. Diffuse Pollution. IWA Publishing.
Carey, J., 2016. Core Concept: Are we in the "Anthropocene"? Proc. Natl. Acad. Sci. U. S. A. 113, 3908–3909. https://doi.org/10.1073/pnas.1603152113
Cha, Y., Stow, C.A., 2014. A Bayesian network incorporating observation error to predict phosphorus and chlorophyll a in Saginaw Bay. Environ. Model. Softw. 57, 90–100. https://doi.org/10.1016/j.envsoft.2014.02.010
Charlton, M.B., Bowes, M.J., Hutchins, M.G., Orr, H.G., Soley, R., Davison, P., 2018. Mapping eutrophication risk from climate change: Future phosphorus concentrations in English rivers. Sci. Total Environ. 613–614, 1510–1526. https://doi.org/10.1016/j.scitotenv.2017.07.218
Chase, J.W., Benoy, G.A., Hann, S.W.R., Culp, J.M., 2016. Small differences in riparian vegetation significantly reduce land use impacts on stream flow and water quality in small agricultural watersheds. J. Soil Water Conserv. 71, 194–205. https://doi.org/10.2489/jswc.71.3.194
Collins, W.J., Bellouin, N., Doutriaux-Boucher, M., Gedney, N., Halloran, P., Hinton, T., Hughes, J., Jones, C.D., Joshi, M., Liddicoat, S., Martin, G., O'Connor, F., Rae, J., Senior, C., Sitch, S., Totterdell, I., Wiltshire, A., Woodward, S., 2011. Development and evaluation of an Earth-System model – HadGEM2. Geosci. Model Dev. 4, 1051–1075. https://doi.org/10.5194/gmd-4-1051-2011

Couture, R.-M., Moe, S.J., Lin, Y., Kaste, Ø., Haande, S., Lyche Solheim, A., 2018. Simulating water quality and ecological status of Lake Vansjø, Norway, under land-use and climate change by linking process-oriented models with a Bayesian network. Sci. Total Environ. 621, 713–724. https://doi.org/10.1016/j.scitotenv.2017.11.303

CRAN, 2023. CRAN: Package bnspatial [WWW Document]. URL https://cran.r-project.org/web/packages/bnspatial/index.html (accessed 6.9.24).

Crockford, L., O'Riordain, S., Taylor, D., Melland, A., Shortle, G., Jordan, P., 2017. The application of high temporal resolution data in river catchment modelling and management strategies. Environ. Monit. Assess. 189, 461. https://doi.org/10.1007/s10661-017-6174-1

Curley, M., Coonan, B., Ruth, C.E., Ryan, C., 2023. Ireland's Climate Averages 1991-2020 (No. Climatological Note No. 22). Met Éireann, Ireland.

Daly, D., Deakin, J., Craig, M., Mockler, E.M., Al, E., 2016. Progress in Implementation of the Water Framework Directive in Ireland. Presented at the International Association of Hydrogeologists (IAH) (Irish Group) Sustaining Ireland's Water Future: The Role of Groundwater, Tullamore, Co. Offaly, Ireland, 12-13 April 2016.

Daly, K., Casey, A., 2005. Evaluating Morgan's Phosphorus Test as an Environmental Indicator - END OF PROJECT REPORT (No. RMIS 4976). Teagasc, Teagasc Headquarters, Oak Park, Carlow.

Davis, S.J., Ó hUallacháin, D., Mellander, P.-E., Matthaei, C.D., Piggott, J.J., Kelly-Quinn, M., 2019. Chronic nutrient inputs affect stream macroinvertebrate communities more than acute inputs: An experiment manipulating phosphorus, nitrogen and sediment. Sci. Total Environ. 683, 9–20. https://doi.org/10.1016/j.scitotenv.2019.05.031

de Vries, J., Kraak, M.H.S., Skeffington, R.A., Wade, A.J., Verdonschot, P.F.M., 2021. A Bayesian network to simulate macroinvertebrate responses to multiple stressors in lowland streams. Water Res. 194, 116952. https://doi.org/10.1016/j.watres.2021.116952

Deakin, J., Flynn, R., Archbold, M., Daly, D., O'Brien, R., Orr, A., Misstear, B., 2016. Understanding pathways transferring nutrients to streams: review of a major Irish study and its implications for determining water quality management strategies. Biol. Environ. Proc. R. Ir. Acad. 116B, 233–243. https://doi.org/10.3318/bioe.2016.19

Death, R.G., Death, F., Stubbington, R., Joy, M.K., van den Belt, M., 2015. How good are Bayesian belief networks for environmental management? A test with data from an agricultural river catchment. Freshw. Biol. 60, 2297–2309. https://doi.org/10.1111/fwb.12655

Delignette-Muller, M.-L., Dutang, C., Pouillot, R., Denis, J.-B., Siberchiot, A., 2020. Package 'fitdistrplus': Help to Fit of a Parametric Distribution to Non-Censored or Censored Data.

Djodjic, F., Markensten, H., 2019. From single fields to river basins: Identification of critical source areas for erosion and phosphorus losses at high resolution. Ambio 48, 1129–1142. https://doi.org/10.1007/s13280-018-1134-8

Doody, D.G., Archbold, M., Foy, R.H., Flynn, R., 2012. Approaches to the implementation of the Water Framework Directive: Targeting mitigation measures at critical source areas of diffuse phosphorus in Irish catchments. J. Environ. Manage. 93, 225–234. https://doi.org/10.1016/j.jenvman.2011.09.002

Drohan, P.J., Bechmann, M., Buda, A., Djodjic, F., Doody, D., Duncan, J.M., Iho, A., Jordan, P., Kleinman, P.J., McDowell, R., Mellander, P.-E., Thomas, I.A., Withers, P.J.A., 2019. A Global Perspective on Phosphorus Management Decision Support in Agriculture: Lessons Learned and Future Directions. J. Environ. Qual. 48, 1218. https://doi.org/10.2134/jeq2019.03.0107

Duespohl, M., Frank, S., Doell, P., 2012. A Review of Bayesian Networks as a Participatory Modeling Approach in Support of Sustainable Environmental Management. J. Sustain. Dev. 5, p1. https://doi.org/10.5539/jsd.v5n12p1

Edwards, A. c., Cook, Y., Smart, R., Wade, A. j., 2000. Concentrations of nitrogen and phosphorus in streams draining the mixed land-use Dee Catchment, north-east Scotland. J. Appl. Ecol. 37, 159–170. https://doi.org/10.1046/j.1365-2664.2000.00500.x

Edwards, A.C., Withers, P.J.A., 2007. Linking phosphorus sources to impacts in different types of water body. Soil Use Manag. 23, 133–143. https://doi.org/10.1111/j.1475-2743.2007.00110.x

Elser, J., Haygarth, P., 2021. Phosphorus: Past and Future. Oxford University Press, Oxford, New York.
Elser, J.J., Bracken, M.E.S., Cleland, E.E., Gruner, D.S., Harpole, W.S., Hillebrand, H., Ngai, J.T., Seabloom, E.W., Shurin, J.B., Smith, J.E., 2007. Global analysis of nitrogen and phosphorus limitation of primary producers in freshwater, marine and terrestrial ecosystems. Ecol. Lett. 10, 1135–1142. https://doi.org/10.1111/j.1461-0248.2007.01113.x
Elser, J.J., Fagan, W.F., Denno, R.F., Dobberfuhl, D.R., Folarin, A., Huberty, A., Interlandi, S., Kilham, S.S., McCauley, E., Schulz, K.L., Siemann, E.H., Sterner, R.W., 2000. Nutritional constraints in terrestrial and freshwater food webs. Nature 408, 578–580. https://doi.org/10.1038/35046058
Environmental Protection Agency, 2019. Water Quality in Ireland 2013-2018. An Ghníomhaireacht um Chaomhnú Comhshaoil PO Box 3000, Johnstown Castle, Co. Wexford, Ireland.
Environmental Protection Agency, 2017. Water Quality in Ireland 2010-2015. An Ghníomhaireacht um Chaomhnú Comhshaoil PO Box 3000, Johnstown Castle, Co. Wexford, Ireland.
Environmental Protection Agency Ireland (EPA), 2015. National Inspection Plan: Domestic Waste Water Treatment Systems: Inspection Data Report 1st July 2013 – 31st December 2014 (No. ISBN 978-1-84095-615-3). Johnstown Castle, Co. Wexford.
Environmental Protection Agency Ireland (EPA), 2003. A catchment based approach for reducing nutrient inputs from all sources to the lakes of Kilarney: final report. Lough Leane catchment monitoring and management system. Kerry County Council, Ireland.
Environmental Protection Agency Ireland (EPA), 2000. Code of Practice: Wastewater Treatment Systems for Single Houses.
EPA, 2019. WFD River Waterbody Status 2016 - 2021 [WWW Document]. URL https://gis.epa.ie/geonetwork/srv/ita/catalog.search#/metadata/b8980e24-df64-48eb-95a1-1765a286f9b0 (accessed 4.2.24).
EPA, 2018. Corine Landcover 2018 [WWW Document]. URL https://data.gov.ie/dataset/corine-landcover-2018 (accessed 4.2.24).
European Communities Environmental Objectives (Surface Waters) Regulations, 2009. S.I. No. 272 of 2009, Dublin: Stationery Office.
European Environment Agency, 2019. The European environment: state and outlook 2020 : knowledge for transition to a sustainable Europe. Publications Office, LU.
European Environment Agency, 2018. European waters assessment of status and pressures 2018.
Evans, D.M., Schoenholtz, S.H., Wigington, P.J., Griffith, S.M., Floyd, W.C., 2014. Spatial and temporal patterns of dissolved nitrogen and phosphorus in surface waters of a multi-land use basin. Environ. Monit. Assess. 186, 873–887. https://doi.org/10.1007/s10661-013-3428-4
Fealy, R.M., Buckley, C., Mechan, S., Melland, A., Mellander, P.E., Shortle, G., Wall, D., Jordan, P., 2010. The Irish Agricultural Catchments Programme: catchment selection using spatial multi-criteria decision analysis. Soil Use Manag. 26, 225–236. https://doi.org/10.1111/j.1475-2743.2010.00291.x
Fitzsimons, L., Clifford, E., McNamara, G., Doherty, E., Phelan, T., Horrigan, M., Delauré, Y., Corcoran, B., 2016. Increasing Resource Efficiency in Wastewater Treatment Plants (No. 168). Environmental Protection Agency, Ireland.
Forber, K., Doody, D., Jarvie, H., Rothwell, S., Lyon, C., Nash, D., Withers, P., 2019. Using Bayesian belief networks to infer catchment phosphorus buffering capacity, in: Geophysical Research Abstracts. Presented at the EGU Genral Assembly 2019, p. 1.
Forio, M.A.E., Landuyt, D., Bennetsen, E., Lock, K., Nguyen, T.H.T., Ambarita, M.N.D., Musonge, P.L.S., Boets, P., Everaert, G., Dominguez-Granda, L., Goethals, P.L.M., 2015. Bayesian belief network models to analyse and predict ecological water quality in rivers. Ecol. Model. 312, 222–238. https://doi.org/10.1016/j.ecolmodel.2015.05.025
Fresne, M., Jordan, P., Daly, K., Fenton, O., Mellander, P.-E., 2022. The role of colloids and other fractions in the below-ground delivery of phosphorus from agricultural hillslopes to streams. CATENA 208, 105735. https://doi.org/10.1016/j.catena.2021.105735
Fuster-Parra, P., Tauler, P., Bennasar-Veny, M., Ligęza, A., López-González, A.A., Aguiló, A., 2016. Bayesian network modeling: A case study of an epidemiologic system analysis of

cardiovascular risk. Comput. Methods Programs Biomed. 126, 128–142. https://doi.org/10.1016/j.cmpb.2015.12.010
Futter, M., Erlandsson, M., Butterfield, D., Oni, S., Wade, A., 2013. PERSiST: the precipitation, evapotranspiration and runoff simulator for solute transport. Hydrol. Earth Syst. Sci. Discuss. 10, 8635–8681. https://doi.org/10.5194/hessd-10-8635-2013
Gaffney, G., Daly, K., Jordan, P., 2021. Assessing the impact of fine sediment on high status river sites. Sci. Total Environ. 759, 143895. https://doi.org/10.1016/j.scitotenv.2020.143895
Geological Survey, n.d. Geology of Ireland [WWW Document]. URL https://www.gsi.ie/en-ie/geoscience-topics/geology/Pages/Geology-of-Ireland.aspx (accessed 4.2.24).
Gill, L., Ireland, Environmental Protection Agency, Environmental Research Technological Development and Innovation Programme, 2005. Water framework directive: an investigation into the performance of subsoils and stratified sand filters for the treatment of wastewater from on-site systems (2001-MS-15-M1) : synthesis report. Environmental Protection Agency, Johnstown Castle, Co. Wexford.
Gill, L.W., Mockler, E.M., 2016. Modeling the pathways and attenuation of nutrients from domestic wastewater treatment systems at a catchment scale. Environ. Model. Softw. 84, 363–377. https://doi.org/10.1016/j.envsoft.2016.07.006
Gill, L.W., O'Súlleabháin, C., Misstear, B.D.R., Johnston, P.J., 2007. The Treatment Performance of Different Subsoils in Ireland Receiving On-Site Wastewater Effluent. J. Environ. Qual. 36, 1843–1855. https://doi.org/10.2134/jeq2007.0064
Giorgetta, M.A., Jungclaus, J., Reick, C.H., Legutke, S., Bader, J., Böttinger, M., Brovkin, V., Crueger, T., Esch, M., Fieg, K., Glushak, K., Gayler, V., Haak, H., Hollweg, H.-D., Ilyina, T., Kinne, S., Kornblueh, L., Matei, D., Mauritsen, T., Mikolajewicz, U., Mueller, W., Notz, D., Pithan, F., Raddatz, T., Rast, S., Redler, R., Roeckner, E., Schmidt, H., Schnur, R., Segschneider, J., Six, K.D., Stockhause, M., Timmreck, C., Wegner, J., Widmann, H., Wieners, K.-H., Claussen, M., Marotzke, J., Stevens, B., 2013. Climate and carbon cycle changes from 1850 to 2100 in MPI-ESM simulations for the Coupled Model Intercomparison Project phase 5. J. Adv. Model. Earth Syst. 5, 572–597. https://doi.org/10.1002/jame.20038
Gleeson, C., 2023. Irish farmers react angrily to EU decision on nitrates derogation [WWW Document]. Ir. Times. URL https://www.irishtimes.com/environment/2023/09/06/farmers-react-angrily-to-eu-decision-on-nitrates-derogation/ (accessed 11.4.24).
Glendell, M., Gagkas, Z., Richards, S., Halliday, S., 2021. Developing a probabilistic model to estimate phosphorus, nitrogen and microbial pollution to water from septic tanks. Scotland's Centre of Expertise for Waters (CREW).
Glendell, M., Gagkas, Z., Stutter, M., Richards, S., Lilly, A., Vinten, A., Coull, M., 2022. A systems approach to modelling phosphorus pollution risk in Scottish rivers using a spatial Bayesian Belief Network helps targeting effective mitigation measures. Front. Environ. Sci. 10.
Glendell, M., Palarea-Albaladejo, J., Pohle, I., Marrero, S., McCreadie, B., Cameron, G., Stutter, M., 2019. Modeling the Ecological Impact of Phosphorus in Catchments with Multiple Environmental Stressors. J. Environ. Qual. 48, 1336–1346. https://doi.org/10.2134/jeq2019.05.0195
Glendell, M., Stutter, M., Pohle, I., Palarea-Albadejo, J., Potts, J., May, L., 2020. Factoring Ecological Significance of Sources into Phosphorus Source Apportionment Phase 2. Crew: Scotland's Centre of Expertise for Waters, Scotland.
Gosling, J.P., 2018. SHELF: The Sheffield Elicitation Framework, in: Dias, L.C., Morton, A., Quigley, J. (Eds.), Elicitation: The Science and Art of Structuring Judgement, International Series in Operations Research & Management Science. Springer International Publishing, Cham, pp. 61–93. https://doi.org/10.1007/978-3-319-65052-4_4
Gudimov, A., O'Connor, E., Dittrich, M., Jarjanazi, H., Palmer, M.E., Stainsby, E., Winter, J.G., Young, J.D., Arhonditsis, G.B., 2012. Continuous Bayesian Network for Studying the Causal Links between Phosphorus Loading and Plankton Patterns in Lake Simcoe, Ontario, Canada. Environ. Sci. Technol. 46, 7283–7292. https://doi.org/10.1021/es300983r
Hallouin, T., Bruen, M., O'Loughlin, F.E., 2020. Calibration of hydrological models for ecologically relevant streamflow predictions: a trade-off between fitting well to data and estimating

consistent parameter sets? Hydrol. Earth Syst. Sci. 24, 1031–1054. https://doi.org/10.5194/hess-24-1031-2020
Harris, G.P., Heathwaite, A.L., 2012. Why is achieving good ecological outcomes in rivers so difficult? Freshw. Biol. 57, 91–107. https://doi.org/10.1111/j.1365-2427.2011.02640.x
Harrison, S., McAree, C., Mulville, W., Sullivan, T., 2019. The problem of agricultural 'diffuse' pollution: Getting to the point. Sci. Total Environ. 677, 700–717. https://doi.org/10.1016/j.scitotenv.2019.04.169
Hatum, P.S., McMahon, K., Mengersen, K., Wu, P.P.-Y., 2022. Guidelines for model adaptation: A study of the transferability of a general seagrass ecosystem Dynamic Bayesian Networks model. Ecol. Evol. 12, e9172. https://doi.org/10.1002/ece3.9172
Hawtree, D., Galloway, J., Zurovec, O., Jackson-Blake, L., Norling, M., Mellander, P.-E., 2023. Performance of a Parsimonious Phosphorus Model (SimplyP) in Two Contrasting Agricultural Catchments in Ireland (No. EGU23-7759). Copernicus Meetings. https://doi.org/10.5194/egusphere-egu23-7759
Haygarth, P.M., Condron, L.M., Heathwaite, A.L., Turner, B.L., Harris, G.P., 2005. The phosphorus transfer continuum: Linking source to impact with an interdisciplinary and multi-scaled approach. Sci. Total Environ. 344, 5–14. https://doi.org/10.1016/j.scitotenv.2005.02.001
Hazeleger, W., Wang, X., Severijns, C., Ştefănescu, S., Bintanja, R., Sterl, A., Wyser, K., Semmler, T., Yang, S., van den Hurk, B., van Noije, T., van der Linden, E., van der Wiel, K., 2012. EC-Earth V2.2: description and validation of a new seamless earth system prediction model. Clim. Dyn. 39, 2611–2629. https://doi.org/10.1007/s00382-011-1228-5
Hecky, R.E., Kilham, P., 1988. Nutrient limitation of phytoplankton in freshwater and marine environments: A review of recent evidence on the effects of enrichment. Limnol. Oceanogr. 33, 796–822. https://doi.org/10.4319/lo.1988.33.4part2.0796
Henderson, C.M., Pollino, C.A., 2010. Bayesian networks : A guide for their application in natural resource management and policy. (No. Landscape Logic, Technical Report 14). Australian Government – Department of the Environment, Water, Heritage and the Arts.
Höge, M., Guthke, A., Nowak, W., 2019. The hydrologist's guide to Bayesian model selection, averaging and combination. J. Hydrol. 572, 96–107. https://doi.org/10.1016/j.jhydrol.2019.01.072
Hollaway, M.J., Beven, K.J., Benskin, C.McW.H., Collins, A.L., Evans, R., Falloon, P.D., Forber, K.J., Hiscock, K.M., Kahana, R., Macleod, C.J.A., Ockenden, M.C., Villamizar, M.L., Wearing, C., Withers, P.J.A., Zhou, J.G., Barber, N.J., Haygarth, P.M., 2018. The challenges of modelling phosphorus in a headwater catchment: Applying a 'limits of acceptability' uncertainty framework to a water quality model. J. Hydrol. 558, 607–624. https://doi.org/10.1016/j.jhydrol.2018.01.063
Holzkämper, A., Kumar, V., Surridge, B.W.J., Paetzold, A., Lerner, D.N., 2012. Bringing diverse knowledge sources together – A meta-model for supporting integrated catchment management. J. Environ. Manage. 96, 116–127. https://doi.org/10.1016/j.jenvman.2011.10.016
Hu, M., Chen, H., Shen, L., Li, G., Guo, Y., Li, H., Li, J., Hu, W., 2018. A machine learning bayesian network for refrigerant charge faults of variable refrigerant flow air conditioning system. Energy Build. 158, 668–676. https://doi.org/10.1016/j.enbuild.2017.10.012
Hynes, S., Morrissey, K., O'Donoghue, C., 2013. Modelling Greenhouse Gas Emissions from Agriculture, in: O'Donoghue, C., Ballas, D., Clarke, G., Hynes, S., Morrissey, K. (Eds.), Spatial Microsimulation for Rural Policy Analysis. Springer, Berlin, Heidelberg, pp. 143–157. https://doi.org/10.1007/978-3-642-30026-4_8
Igras, J.D., Creed, I.F., 2020. Uncertainty analysis of the performance of a management system for achieving phosphorus load reduction to surface waters. J. Environ. Manage. 276, 111217. https://doi.org/10.1016/j.jenvman.2020.111217
Jackson-Blake, L., Wade, A., Futter, M., Butterfield, D., Couture, R.-M., Cox, B., Crossman, J., Ekholm, P., Halliday, S., Jin, L., Lawrence, D.S.L., Lepistö, A., Lin, Y., Rankinen, K., Whitehead, P., 2016. The INtegrated CAtchment model of phosphorus dynamics (INCA-P):

Description and demonstration of new model structure and equations. Environ. Model. Softw. 83, 356–386. https://doi.org/10.1016/j.envsoft.2016.05.022
Jackson-Blake, L.A., Dunn, S.M., Helliwell, R.C., Skeffington, R.A., Stutter, M.I., Wade, A.J., 2015. How well can we model stream phosphorus concentrations in agricultural catchments? Environ. Model. Softw. 64, 31–46. https://doi.org/10.1016/j.envsoft.2014.11.002
Jackson-Blake, L.A., Sample, J.E., Wade, A.J., Helliwell, R.C., Skeffington, R.A., 2017. Are our dynamic water quality models too complex? A comparison of a new parsimonious phosphorus model, SimplyP, and INCA-P. Water Resour. Res. 53, 5382–5399. https://doi.org/10.1002/2016WR020132
Jarvie, H.P., Neal, C., Williams, R.J., Neal, M., Wickham, H.D., Hill, L.K., Wade, A.J., Warwick, A., White, J., 2002. Phosphorus sources, speciation and dynamics in the lowland eutrophic River Kennet, UK. Sci. Total Environ., Water quality functioning of lowland permeable catchments:inferences from an intensive study of the River Kennet and upper River Thames 282–283, 175–203. https://doi.org/10.1016/S0048-9697(01)00951-2
Jarvie, H.P., Sharpley, A.N., Flaten, D., Kleinman, P.J.A., 2019. Phosphorus mirabilis: Illuminating the Past and Future of Phosphorus Stewardship. J. Environ. Qual. 48, 1127–1132. https://doi.org/10.2134/jeq2019.07.0266
Jennings, E., Allott, N., Pierson, D.C., Schneiderman, E.M., Lenihan, D., Samuelsson, P., Taylor, D., 2009. Impacts of climate change on phosphorus loading from a grassland catchment: Implications for future management. Water Res. 43, 4316–4326. https://doi.org/10.1016/j.watres.2009.06.032
Jin, G., Xu, J., Mo, Y., Tang, H., Wei, T., Wang, Y.-G., Li, L., 2020. Response of sediments and phosphorus to catchment characteristics and human activities under different rainfall patterns with Bayesian Networks. J. Hydrol. 584, 124695. https://doi.org/10.1016/j.jhydrol.2020.124695
Jordan, P., Arnscheidt, A., McGrogan, H., McCormick, S., 2007. Characterising phosphorus transfers in rural catchments using a continuous bank-side analyser. Hydrol. Earth Syst. Sci. 11, 372–381. https://doi.org/10.5194/hess-11-372-2007
Jordan, P., Melland, A.R., Mellander, P.-E., Shortle, G., Wall, D., 2012. The seasonality of phosphorus transfers from land to water: Implications for trophic impacts and policy evaluation. Sci. Total Environ., Climate Change and Macronutrient Cycling along the Atmospheric, Terrestrial, Freshwater and Estuarine Continuum - A Special Issue dedicated to Professor Colin Neal 434, 101–109. https://doi.org/10.1016/j.scitotenv.2011.12.070
Kaikkonen, L., Parviainen, T., Rahikainen, M., Uusitalo, L., Lehikoinen, A., 2021. Bayesian Networks in Environmental Risk Assessment: A Review. Integr. Environ. Assess. Manag. 17, 62–78. https://doi.org/10.1002/ieam.4332
Kay, M., 2023. {ggdist}: Visualizations of Distributions and Uncertainty.
Kim, D.-K., Kaluskar, S., Mugalingam, S., Blukacz-Richards, A., Long, T., Morley, A., Arhonditsis, G.B., 2017. A Bayesian approach for estimating phosphorus export and delivery rates with the SPAtially Referenced Regression On Watershed attributes (SPARROW) model. Ecol. Inform. 37, 77–91. https://doi.org/10.1016/j.ecoinf.2016.12.003
Kim, D.-K., Zhang, W., Hiriart-Baer, V., Wellen, C., Long, T., Boyd, D., Arhonditsis, G.B., 2014. Towards the development of integrated modelling systems in aquatic biogeochemistry: a Bayesian approach. J. Gt. Lakes Res. 40, 73–87. https://doi.org/10.1016/j.jglr.2014.04.005
Kotamäki, N., Arhonditsis, G., Hjerppe, T., Hyytiäinen, K., Malve, O., Ovaskainen, O., Paloniitty, T., Similä, J., Soininen, N., Weigel, B., Heiskanen, A.-S., 2024. Strategies for integrating scientific evidence in water policy and law in the face of uncertainty. Sci. Total Environ. 931, 172855. https://doi.org/10.1016/j.scitotenv.2024.172855
Kragt, M.E., 2009. A beginners guide to Bayesian network modelling for integrated catchment management, Landscape Logic Technical Report No. 9.
Landuyt, D., Broekx, S., D'hondt, R., Engelen, G., Aertsens, J., Goethals, P.L.M., 2013. A review of Bayesian belief networks in ecosystem service modelling. Environ. Model. Softw. 46, 1–11. https://doi.org/10.1016/j.envsoft.2013.03.011

Lau, C.L., Mayfield, H.J., Lowry, J.H., Watson, C.H., Kama, M., Nilles, E.J., Smith, C.S., 2017. Unravelling infectious disease eco-epidemiology using Bayesian networks and scenario analysis: A case study of leptospirosis in Fiji. Environ. Model. Softw. 97, 271–286. https://doi.org/10.1016/j.envsoft.2017.08.004

Lu, L., Goerlandt, F., Valdez Banda, O.A., Kujala, P., Höglund, A., Arneborg, L., 2019. A Bayesian Network risk model for assessing oil spill recovery effectiveness in the ice-covered Northern Baltic Sea. Mar. Pollut. Bull. 139, 440–458. https://doi.org/10.1016/j.marpolbul.2018.12.018

Lucci, G.M., Nash, D., McDowell, R.W., Condron, L.M., 2014. Bayesian Network for Point and Diffuse Source Phosphorus Transfer from Dairy Pastures in South Otago, New Zealand. J. Environ. Qual. 43, 1370. https://doi.org/10.2134/jeq2013.11.0460

Mann, M.E., Lloyd, E.A., Oreskes, N., 2017. Assessing climate change impacts on extreme weather events: the case for an alternative (Bayesian) approach. Clim. Change 144, 131–142. https://doi.org/10.1007/s10584-017-2048-3

Marcot, B.G., Steventon, J.D., Sutherland, G.D., McCann, R.K., 2006. Guidelines for developing and updating Bayesian belief networks applied to ecological modeling and conservation. Can. J. For. Res. 36, 3063–3074. https://doi.org/10.1139/x06-135

Masante, D., 2019. Package "bnspatial": Spatial Implementation of Bayesian Networks and Mapping.

McDonald, N.T., Wall, D.P., Mellander, P.E., Buckley, C., Shore, M., Shortle, G., Leach, S., Burgess, E., O'Connell, T., Jordan, P., 2019a. Field scale phosphorus balances and legacy soil pressures in mixed-land use catchments. Agric. Ecosyst. Environ. 274, 14–23. https://doi.org/10.1016/j.agee.2018.12.014

McDonald, N.T., Wall, D.P., Mellander, P.E., Buckley, C., Shore, M., Shortle, G., Leach, S., Burgess, E., O'Connell, T., Jordan, P., 2019b. Field scale phosphorus balances and legacy soil pressures in mixed-land use catchments. Agric. Ecosyst. Environ. 274, 14–23. https://doi.org/10.1016/j.agee.2018.12.014

McDowell, R.W., Nash, D., George, A., Wang, Q.J., Duncan, R., 2009. Approaches for Quantifying and Managing Diffuse Phosphorus Exports at the Farm/Small Catchment Scale. J. Environ. Qual. 38, 1968–1980. https://doi.org/10.2134/jeq2007.0651

McVittie, A., Norton, L., Martin-Ortega, J., Siameti, I., Glenk, K., Aalders, I., 2015. Operationalizing an ecosystem services-based approach using Bayesian Belief Networks: An application to riparian buffer strips. Ecol. Econ. 110, 15–27. https://doi.org/10.1016/j.ecolecon.2014.12.004

Meals, D.W., Dressing, S.A., Davenport, T.E., 2010. Lag Time in Water Quality Response to Best Management Practices: A Review. J. Environ. Qual. 39, 85–96. https://doi.org/10.2134/jeq2009.0108

Mellander, P., Jordan, P., Melland, A.R., Murphy, P.N.C., Wall, D.P., Mechan, S., Meehan, R., Kelly, C., Shine, O., Shortle, G., 2013. Quantification of Phosphorus Transport from a Karstic Agricultural Watershed to Emerging Spring Water. Environ. Sci. Technol.

Mellander, P.-E., Galloway, J., Hawtree, D., 2022. Phosphorus mobilization and delivery estimated from long-term high frequency water quality and discharge data. Front. Water 4. https://doi.org/10.3389/frwa.2022.917813

Mellander, P.-E., Jordan, P., 2021. Charting a perfect storm of water quality pressures. Sci. Total Environ. 787, 147576. https://doi.org/10.1016/j.scitotenv.2021.147576

Mellander, P.-E., Jordan, P., Bechmann, M., Fovet, O., Shore, M.M., McDonald, N.T., Gascuel-Odoux, C., 2018. Integrated climate-chemical indicators of diffuse pollution from land to water. Sci. Rep. 8, 944. https://doi.org/10.1038/s41598-018-19143-1

Mellander, P.-E., Jordan, P., Shore, M., McDonald, N.T., Wall, D.P., Shortle, G., Daly, K., 2016. Identifying contrasting influences and surface water signals for specific groundwater phosphorus vulnerability. Sci. Total Environ. 541, 292–302. https://doi.org/10.1016/j.scitotenv.2015.09.082

Mellander, P.-E., Jordan, P., Shore, M., Melland, A.R., Shortle, G., 2015. Flow paths and phosphorus transfer pathways in two agricultural streams with contrasting flow controls. Hydrol. Process. 29, 3504–3518. https://doi.org/10.1002/hyp.10415

Mellander, P.-E., Melland, A.R., Jordan, P., Wall, D.P., Murphy, P.N.C., Shortle, G., 2012. Quantifying nutrient transfer pathways in agricultural catchments using high temporal

resolution data. Environ. Sci. Policy, CATCHMENT SCIENCE AND POLICY EVALUATION FOR AGRICULTURE AND WATER QUALITY 24, 44–57. https://doi.org/10.1016/j.envsci.2012.06.004
Mentzel, S., Grung, M., Holten, R., Tollefsen, K.E., Stenrød, M., Moe, S.J., 2022. Probabilistic risk assessment of pesticides under future agricultural and climate scenarios using a bayesian network. Front. Environ. Sci. 10.
Mieleitner, J., Reichert, P., 2006. Analysis of the transferability of a biogeochemical lake model to lakes of different trophic state. Ecol. Model., Special Issue on the Fourth European Conference on Ecological Modelling 194, 49–61. https://doi.org/10.1016/j.ecolmodel.2005.10.039
Mischler, J.A., Taylor, P.G., Townsend, A.R., 2014. Nitrogen Limitation of Pond Ecosystems on the Plains of Eastern Colorado. PLOS ONE 9, e95757. https://doi.org/10.1371/journal.pone.0095757
Mockler, E.M., Deakin, J., Archbold, M., Daly, D., Bruen, M., 2016a. Nutrient load apportionment to support the identification of appropriate water framework directive measures. Biol. Environ. Proc. R. Ir. Acad. 116B, 245–263. https://doi.org/10.3318/bioe.2016.22
Mockler, E.M., Deakin, J., Archbold, M., Gill, L., Daly, D., Bruen, M., 2017. Sources of nitrogen and phosphorus emissions to Irish rivers and coastal waters: Estimates from a nutrient load apportionment framework. Sci. Total Environ. 601–602, 326–339. https://doi.org/10.1016/j.scitotenv.2017.05.186
Mockler, E.M., O'Loughlin, F.E., Bruen, M., 2016b. Understanding hydrological flow paths in conceptual catchment models using uncertainty and sensitivity analysis. Comput. Geosci., Uncertainty and Sensitivity in Surface Dynamics Modeling 90, 66–77. https://doi.org/10.1016/j.cageo.2015.08.015
Moe, S.J., Benestad, R.E., Landis, W.G., 2022. Robust risk assessments require probabilistic approaches. Integr. Environ. Assess. Manag. 18, 1133–1134. https://doi.org/10.1002/ieam.4660
Moe, S.J., Carriger, J.F., Glendell, M., 2021. Increased Use of Bayesian Network Models Has Improved Environmental Risk Assessments. Integr. Environ. Assess. Manag. 17, 53–61. https://doi.org/10.1002/ieam.4369
Moe, S.J., Haande, S., Couture, R.-M., 2016. Climate change, cyanobacteria blooms and ecological status of lakes: A Bayesian network approach. Ecol. Model. 337, 330–347. https://doi.org/10.1016/j.ecolmodel.2016.07.004
Moloney, T., Fenton, O., Daly, K., 2020. Ranking connectivity risk for phosphorus loss along agricultural drainage ditches. Sci. Total Environ. 703, 134556. https://doi.org/10.1016/j.scitotenv.2019.134556
Moss, B., Jeppesen, E., Søndergaard, M., Lauridsen, T.L., Liu, Z., 2013. Nitrogen, macrophytes, shallow lakes and nutrient limitation: resolution of a current controversy? Hydrobiologia 710, 3–21. https://doi.org/10.1007/s10750-012-1033-0
Murphy, C., Kettle, A., Meresa, H., Golian, S., Bruen, M., O'Loughlin, F., Mellander, P.-E., 2023. Climate Change Impacts on Irish River Flows: High Resolution Scenarios and Comparison with CORDEX and CMIP6 Ensembles. Water Resour. Manag. 37, 1841–1858. https://doi.org/10.1007/s11269-023-03458-4
Mzyece, C.C., Glendell, M., Gagkas, Z., Quilliam, R.S., Jones, I., Pagaling, E., Akoumianaki, I., Newman, C., Oliver, D.M., 2024. Eliciting expert judgements to underpin our understanding of faecal indicator organism loss from septic tank systems. Sci. Total Environ. 171074. https://doi.org/10.1016/j.scitotenv.2024.171074
Neal, C., Hilton, J., Wade, A.J., Neal, M., Wickham, H., 2006. Chlorophyll-a in the rivers of eastern England. Sci. Total Environ., Monitoring and modelling the impacts of global change on European freshwater ecosystems 365, 84–104. https://doi.org/10.1016/j.scitotenv.2006.02.039
Negri, C., Mellander, P.-E., 2024. Evidence dossier for the workshop titled "In-stream phosphorus cycling in agricultural catchments: a workshop to quantify abiotic and biotic P uptake". https://doi.org/10.6084/m9.figshare.25055165.v1

Negri, C., Mellander, P.-E., Schurch, N.J., Wade, A.J., Gagkas, Z., Wardell-Johnson, D.H., Adams, K., Glendell, M., 2024a. Bayesian network modelling of phosphorus pollution in agricultural catchments with high-resolution data. Environ. Model. Softw. 106073. https://doi.org/10.1016/j.envsoft.2024.106073

Negri, Camilla, Schurch, N., Wade, A.J., Mellander, P.-E., Stutter, M.I., Bowes, M.J., Mzyece, C.C., Glendell, M., 2024b. Transferability of a Bayesian Belief Network Across Diverse Agricultural Catchments Using High-Frequency Hydrochemistry and Land Management Data. SSRN Electron. J. http://dx.doi.org/10.2139/ssrn.4780915

Neumann, A., Blukacz-Richards, E.A., Saha, R., Alberto Arnillas, C., Arhonditsis, G.B., 2023. A Bayesian hierarchical spatially explicit modelling framework to examine phosphorus export between contrasting flow regimes. J. Gt. Lakes Res. 49, 190–208. https://doi.org/10.1016/j.jglr.2022.10.003

Nojavan, F., Qian, S.S., Stow, C.A., 2017. Comparative analysis of discretization methods in Bayesian networks. Environ. Model. Softw. 87, 64–71. https://doi.org/10.1016/j.envsoft.2016.10.007

Nolan, P., Flanagan, J., 2020. Research 339: High-resolution Climate Projections for Ireland – A Multimodel Ensemble Approach (No. 339). Environmental Protection Agency, Co. Wexford, Ireland.

Norsys Software Corp, 2016. Netica - Bayes Net Software. Norsys Software Corp, Vancouver.

Oakley, J., 2020. SHELF: Tools to Support the Sheffield Elicitation Framework.

Ockenden, M.C., Deasy, C.E., Benskin, C.McW.H., Beven, K.J., Burke, S., Collins, A.L., Evans, R., Falloon, P.D., Forber, K.J., Hiscock, K.M., Hollaway, M.J., Kahana, R., Macleod, C.J.A., Reaney, S.M., Snell, M.A., Villamizar, M.L., Wearing, C., Withers, P.J.A., Zhou, J.G., Haygarth, P.M., 2016. Changing climate and nutrient transfers: Evidence from high temporal resolution concentration-flow dynamics in headwater catchments. Sci. Total Environ. 548–549, 325–339. https://doi.org/10.1016/j.scitotenv.2015.12.086

Ockenden, M.C., Hollaway, M.J., Beven, K.J., Collins, A.L., Evans, R., Falloon, P.D., Forber, K.J., Hiscock, K.M., Kahana, R., Macleod, C.J.A., Tych, W., Villamizar, M.L., Wearing, C., Withers, P.J.A., Zhou, J.G., Barker, P.A., Burke, S., Freer, J.E., Johnes, P.J., Snell, M.A., Surridge, B.W.J., Haygarth, P.M., 2017. Major agricultural changes required to mitigate phosphorus losses under climate change. Nat. Commun. 8, 161. https://doi.org/10.1038/s41467-017-00232-0

O'Hagan, A., 2019. Expert Knowledge Elicitation: Subjective but Scientific. Am. Stat. 73, 69–81. https://doi.org/10.1080/00031305.2018.1518265

Osawe, W., Curtis, J., 2024. An assessment of farmers' knowledge, attitudes and intentions towards water quality and pollution risk mitigation actions. Soc. Sci. Humanit. Open 9, 100858. https://doi.org/10.1016/j.ssaho.2024.100858

Packham, I., Mockler, E., Archbold, M., Mannix, A., Daly, D., Deakin, J., Bruen, M., 2020. Catchment Characterisation Tool: Prioritising Critical Source Areas for managing diffuse nitrate pollution. Environ. Model. Assess. 25, 23–39. https://doi.org/10.1007/s10666-019-09683-9

Pappenberger, F., Beven, K.J., 2006. Ignorance is bliss: Or seven reasons not to use uncertainty analysis. Water Resour. Res. 42. https://doi.org/10.1029/2005WR004820

Pascoe, S., 2018. Assessing relative potential economic impacts of an oil spill on commercial fisheries in the Great Australian Bight using a Bayesian Belief Network framework. Deep Sea Res. Part II Top. Stud. Oceanogr., Great Australian Bight Research Program - a whole of system investigation 157–158, 203–210. https://doi.org/10.1016/j.dsr2.2018.08.011

Pearl, J., 1986. Fusion, propagation, and structuring in belief networks. Artif. Intell. 29, 241–288. https://doi.org/10.1016/0004-3702(86)90072-X

Penk, M.R., Bruen, M., Feld, C.K., Piggott, J.J., Christie, M., Bullock, C., Kelly-Quinn, M., 2022. Using weighted expert judgement and nonlinear data analysis to improve Bayesian belief network models for riverine ecosystem services. Sci. Total Environ. 851, 158065. https://doi.org/10.1016/j.scitotenv.2022.158065

Pérez-Miñana, E., 2016. Improving ecosystem services modelling: Insights from a Bayesian network tools review. Environ. Model. Softw. 85, 184–201. https://doi.org/10.1016/j.envsoft.2016.07.007
Phan, T.D., Smart, J.C.R., Capon, S.J., Hadwen, W.L., Sahin, O., 2016. Applications of Bayesian belief networks in water resource management: A systematic review. Environ. Model. Softw. 85, 98–111. https://doi.org/10.1016/j.envsoft.2016.08.006
Phan, T.D., Smart, J.C.R., Stewart-Koster, B., Sahin, O., Hadwen, W.L., Dinh, L.T., Tahmasbian, I., Capon, S.J., 2019. Applications of Bayesian Networks as Decision Support Tools for Water Resource Management under Climate Change and Socio-Economic Stressors: A Critical Appraisal. Water 11, 2642. https://doi.org/10.3390/w11122642
Piffady, J., Carluer, N., Gouy, V., Henaff, G. le, Tormos, T., Bougon, N., Adoir, E., Mellac, K., 2021. ARPEGES: A Bayesian Belief Network to Assess the Risk of Pesticide Contamination for the River Network of France. Integr. Environ. Assess. Manag. 17, 188–201. https://doi.org/10.1002/ieam.4343
Powers, S.M., Bruulsema, T.W., Burt, T.P., Chan, N.I., Elser, J.J., Haygarth, P.M., Howden, N.J.K., Jarvie, H.P., Lyu, Y., Peterson, H.M., Sharpley, A.N., Shen, J., Worrall, F., Zhang, F., 2016. Long-term accumulation and transport of anthropogenic phosphorus in three river basins. Nat. Geosci. 9, 353–356. https://doi.org/10.1038/ngeo2693
Radcliffe, D.E., Freer, J., Schoumans, O., 2009. Diffuse phosphorus models in the United States and europe: their usages, scales, and uncertainties. J. Environ. Qual. 38, 1956–1967. https://doi.org/10.2134/jeq2008.0060
Refsgaard, J.C., van der Sluijs, J.P., Brown, J., van der Keur, P., 2006. A framework for dealing with uncertainty due to model structure error. Adv. Water Resour. 29, 1586–1597. https://doi.org/10.1016/j.advwatres.2005.11.013
Regan, J., Fenton, O., Healy, M., 2012. A Review of Phosphorus and Sediment Release from Irish Tillage Soils, the Methods Used to Quantify Losses and the Current State of Mitigation Practice. Biol. Environ. Proc. R. Ir. Acad. 112, 157–183. https://doi.org/10.3318/BIOE.2012.05
Rode, M., Arhonditsis, G., Balin, D., Kebede, T., Krysanova, V., Griensven, A. van, Zee, S.E.A.T.M. van der, 2010. New challenges in integrated water quality modelling. Hydrol. Process. 24, 3447–3461. https://doi.org/10.1002/hyp.7766
Rodrigues, P.P., Ferreira-Santos, D., Silva, A., Polónia, J., Ribeiro-Vaz, I., 2017. Implementing Guidelines for Causality Assessment of Adverse Drug Reaction Reports: A Bayesian Network Approach, in: ten Teije, A., Popow, C., Holmes, J.H., Sacchi, L. (Eds.), Artificial Intelligence in Medicine, Lecture Notes in Computer Science. Springer International Publishing, Cham, pp. 55–64. https://doi.org/10.1007/978-3-319-59758-4_6
Ropero, R.M.F., 2016. Hybrid Bayesian Networks: A Statistical Tool in Ecology and Environmental Sciences (PhD thesis). Dep. Biol. Geol. Univ. Almería.
Rowland, F.E., Stow, C.A., Johnson, L.T., Hirsch, R.M., 2021. Lake Erie tributary nutrient trend evaluation: Normalizing concentrations and loads to reduce flow variability. Ecol. Indic. 125, 107601. https://doi.org/10.1016/j.ecolind.2021.107601
Sahlin, U., Helle, I., Perepolkin, D., 2021. "This Is What We Don't Know": Treating Epistemic Uncertainty in Bayesian Networks for Risk Assessment. Integr. Environ. Assess. Manag. 17, 221–232. https://doi.org/10.1002/ieam.4367
Schulte, R.P.O., Melland, A.R., Fenton, O., Herlihy, M., Richards, K., Jordan, P., 2010. Modelling soil phosphorus decline: Expectations of Water Framework Directive policies. Environ. Sci. Policy 13, 472–484. https://doi.org/10.1016/j.envsci.2010.06.002
Schuwirth, N., Borgwardt, F., Domisch, S., Friedrichs, M., Kattwinkel, M., Kneis, D., Kuemmerlen, M., Langhans, S.D., Martínez-López, J., Vermeiren, P., 2019. How to make ecological models useful for environmental management. Ecol. Model. 411, 108784. https://doi.org/10.1016/j.ecolmodel.2019.108784
Scutari, M., 2010. Learning Bayesian Networks with the bnlearn R Package. J. Stat. Softw. 35, 1–22. https://doi.org/10.18637/jss.v035.i03

Seixas, A.A., Henclewood, D.A., Williams, S.K., Jagannathan, R., Ramos, A., Zizi, F., Jean-Louis, G., 2018. Sleep Duration and Physical Activity Profiles Associated With Self-Reported Stroke in the United States: Application of Bayesian Belief Network Modeling Techniques. Front. Neurol. 9. https://doi.org/10.3389/fneur.2018.00534

Sherriff, S., Rowan, J.S., Fenton, O., Jordan, P., hUallacháin, D.Ó., 2019. Influence of land management on soil erosion, connectivity, and sediment delivery in agricultural catchments: Closing the sediment budget. Land Degrad. Dev. 0. https://doi.org/10.1002/ldr.3413

Sherriff, S., Rowan, J.S., Melland, A.R., Jordan, P., Fenton, O., Ó hUallacháin, D., 2015. Investigating suspended sediment dynamics in contrasting agricultural catchments using ex situ turbidity-based suspended sediment monitoring. Hydrol. Earth Syst. Sci. 19, 3349–3363. https://doi.org/10.5194/hess-19-3349-2015

Shore, M., Jordan, P., Mellander, P.-E., Kelly-Quinn, M., Daly, K., Sims, J.T., Wall, D.P., Melland, A.R., 2016. Characterisation of agricultural drainage ditch sediments along the phosphorus transfer continuum in two contrasting headwater catchments. J. Soils Sediments 16, 1643–1654. https://doi.org/10.1007/s11368-015-1330-0

Shore, M., Jordan, P., Mellander, P.-E., Kelly-Quinn, M., Melland, A.R., 2015. An agricultural drainage channel classification system for phosphorus management. Agric. Ecosyst. Environ. 199, 207–215. https://doi.org/10.1016/j.agee.2014.09.003

Shore, M., Jordan, P., Mellander, P.-E., Kelly-Quinn, M., Wall, D.P., Murphy, P.N.C., Melland, A.R., 2014. Evaluating the critical source area concept of phosphorus loss from soils to water-bodies in agricultural catchments. Sci. Total Environ. 490, 405–415. https://doi.org/10.1016/j.scitotenv.2014.04.122

Smith, D.R., Jarvie, H.P., Bowes, M.J., 2017. Carbon, Nitrogen, and Phosphorus Stoichiometry and Eutrophication in River Thames Tributaries, UK. Agric. Environ. Lett. 2, ael2017.06.0020. https://doi.org/10.2134/ael2017.06.0020

South, A., 2017. rnaturalearthdata: World Vector Map Data from Natural Earth Used in "rnaturalearth."

Sperotto, A., Molina, J.-L., Torresan, S., Critto, A., Marcomini, A., 2017. Reviewing Bayesian Networks potentials for climate change impacts assessment and management: A multi-risk perspective. J. Environ. Manage. 202, 320–331. https://doi.org/10.1016/j.jenvman.2017.07.044

Sperotto, A., Molina, J.L., Torresan, S., Critto, A., Pulido-Velazquez, M., Marcomini, A., 2019a. A Bayesian Networks approach for the assessment of climate change impacts on nutrients loading. Environ. Sci. Policy 100, 21–36. https://doi.org/10.1016/j.envsci.2019.06.004

Sperotto, A., Molina, J.L., Torresan, S., Critto, A., Pulido-Velazquez, M., Marcomini, A., 2019b. Water Quality Sustainability Evaluation under Uncertainty: A Multi-Scenario Analysis Based on Bayesian Networks. Sustainability 11, 4764. https://doi.org/10.3390/su11174764

Stamm, C., Jarvie, H.P., Scott, T., 2014. What's More Important for Managing Phosphorus: Loads, Concentrations or Both? Environ. Sci. Technol. 48, 23–24. https://doi.org/10.1021/es405148c

Stewart, G., Glendell, M., McMorran, R., Troldborg, M., Gagkas, Z., Ovando, P., Roberts, M., Maynard, C., Williams, A., Clay, G., Reed, M., 2021. Uplandia: making better policy in complex upland systems. Final report.

Stritih, A., Rabe, S.-E., Robaina, O., Grêt-Regamey, A., Celio, E., 2020. An online platform for spatial and iterative modelling with Bayesian Networks. Environ. Model. Softw. 127, 104658. https://doi.org/10.1016/j.envsoft.2020.104658

Stutter, M., Barros Costa, F., O Huallachain, D., 2021a. Riparian buffer zone quantitative effectiveness review database 3. https://doi.org/10.17632/t64dbpv63x.3

Stutter, M., Glendell, M., Ibiyemi, A., Palarea-Albaladejo, J., May, L., 2022. Can Prediction and Understanding of Water Quality Variation Be Improved by Combining Phosphorus Source and Waterbody Condition Parameters? Front. Water 4, 852883. https://doi.org/10.3389/frwa.2022.852883

Stutter, M., Richards, S., Ibiyemi, A., Watson, H., 2021b. Spatial representation of in-stream sediment phosphorus release combining channel network approaches and in-situ experiments. Sci. Total Environ. 795, 148790. https://doi.org/10.1016/j.scitotenv.2021.148790

Stutter, M.I., Demars, B.O.L., Langan, S.J., 2010. River phosphorus cycling: Separating biotic and abiotic uptake during short-term changes in sewage effluent loading. Water Res. 44, 4425–4436. https://doi.org/10.1016/j.watres.2010.06.014

Tattari, S., Schultz, T., Kuussaari, M., 2003. Use of belief network modelling to assess the impact of buffer zones on water protection and biodiversity. Agric. Ecosyst. Environ. 96, 119–132. https://doi.org/10.1016/S0167-8809(02)00233-5

Teagasc - Agriculture and Food Development Authority, 2020. Teagasc Agricultural Catchments Programme phase 4 [WWW Document]. URL https://www.teagasc.ie/environment/water-quality/agricultural-catchments/ (accessed 5.20.24).

Teagasc - Agriculture and Food Development Authority, 2018. Agricultural Catchments Programme - Phase 2 Report.

Teagasc - Agriculture and Food Development Authority, 2017. Nutrient Management Planning (NMP) Online [WWW Document]. URL https://www.teagasc.ie/about/our-organisation/connected/online-tools/teagasc-nmp-online/ (accessed 1.28.20).

The European Commision, 2000. Directive 2000/60/EC of the European Parliament and of the Council of 23 October 2000 establishing a framework for Community action in the field of water policy.

The European Commision, 1991. The Council Directive 91/676/EEC concerning the protection of waters against pollution caused by nitrates from agricultural sources (the Nitrates Directive).

Thomas, I.A., Bruen, M., Mockler, E., Werner, C., Mellander, P.-E., Reaney, S., Rymszewicz, A., McGrath, G., Eder, E., Wade, A.J., Collins, A., Arheimer, B., 2021. Catchment Models and Management Tools for Diffuse Contaminants (Sediment, Phosphorus and Pesticides): DiffuseTools Project (No. 396). ENVIRONMENTAL PROTECTION AGENCY An Ghníomhaireacht um Chaomhnú Comhshaoil PO Box 3000, Johnstown Castle, Co. Wexford, Ireland.

Thomas, I.A., Bruen, M., Mockler, E.M., Kelly, E., Murphy, P., Al, E., 2019. Improving national mapping of critical source areas of phosphorus and nitrogen losses in Irish agricultural catchments to support policy. Presented at the LUWQ 2019: International Interdisciplinary Conference on Land Use and Water Quality. Agriculture and the Environment. Aarhus, Denmark, 3-6 June 2019.

Thomas, I.A., Jordan, P., Mellander, P.-E., Fenton, O., Shine, O., Ó hUallacháin, D., Creamer, R., McDonald, N.T., Dunlop, P., Murphy, P.N.C., 2016a. Improving the identification of hydrologically sensitive areas using LiDAR DEMs for the delineation and mitigation of critical source areas of diffuse pollution. Sci. Total Environ. 556, 276–290. https://doi.org/10.1016/j.scitotenv.2016.02.183

Thomas, I.A., Jordan, P., Shine, O., Fenton, O., Mellander, P.-E., Dunlop, P., Murphy, P.N.C., 2017. Defining optimal DEM resolutions and point densities for modelling hydrologically sensitive areas in agricultural catchments dominated by microtopography. Int. J. Appl. Earth Obs. Geoinformation 54, 38–52. https://doi.org/10.1016/j.jag.2016.08.012

Thomas, I.A., Mellander, P.-E., Murphy, P.N.C., Fenton, O., Shine, O., Djodjic, F., Dunlop, P., Jordan, P., 2016b. A sub-field scale critical source area index for legacy phosphorus management using high resolution data. Agric. Ecosyst. Environ. 233, 238–252. https://doi.org/10.1016/j.agee.2016.09.012

Troldborg, M., Gagkas, Z., Vinten, A., Lilly, A., Glendell, M., 2022. Probabilistic modelling of the inherent field-level pesticide pollution risk in a small drinking water catchment using spatial Bayesian belief networks. Hydrol. Earth Syst. Sci. 26, 1261–1293. https://doi.org/10.5194/hess-26-1261-2022

Ulén, B., Bechmann, M., Fölster, J., Jarvie, H.P., Tunney, H., 2007. Agriculture as a phosphorus source for eutrophication in the north-west European countries, Norway, Sweden, United Kingdom and Ireland: a review. Soil Use Manag. 23, 5–15. https://doi.org/10.1111/j.1475-2743.2007.00115.x

Uusitalo, L., 2007. Advantages and challenges of Bayesian networks in environmental modelling. Ecol. Model. 203, 312–318. https://doi.org/10.1016/j.ecolmodel.2006.11.033

Vadas, P.A., Bolster, C.H., Good, L.W., 2013. Critical evaluation of models used to study agricultural phosphorus and water quality. Soil Use Manag. 29, 36–44. https://doi.org/10.1111/j.1475-2743.2012.00431.x
Vero, S.E., Daly, K., McDonald, N.T., Leach, S., Sherriff, S., Mellander, P.-E., 2019. Sources and Mechanisms of Low-Flow River Phosphorus Elevations: A Repeated Synoptic Survey Approach. Water 11, 1497. https://doi.org/10.3390/w11071497
Vero, S.E., Doody, D., 2021. Applying the nutrient transfer continuum framework to phosphorus and nitrogen losses from livestock farmyards to watercourses. J. Environ. Qual. 50, 1290–1302. https://doi.org/10.1002/jeq2.20285
Villalba, G., Liu, Y., Schroder, H., Ayres, R.U., 2008. Global Phosphorus Flows in the Industrial Economy From a Production Perspective. J. Ind. Ecol. 12, 557–569. https://doi.org/10.1111/j.1530-9290.2008.00050.x
Voldoire, A., Sanchez-Gomez, E., Salas y Mélia, D., Decharme, B., Cassou, C., Sénési, S., Valcke, S., Beau, I., Alias, A., Chevallier, M., Déqué, M., Deshayes, J., Douville, H., Fernandez, E., Madec, G., Maisonnave, E., Moine, M.-P., Planton, S., Saint-Martin, D., Szopa, S., Tyteca, S., Alkama, R., Belamari, S., Braun, A., Coquart, L., Chauvin, F., 2013. The CNRM-CM5.1 global climate model: description and basic evaluation. Clim. Dyn. 40, 2091–2121. https://doi.org/10.1007/s00382-011-1259-y
Wade, A.J., Hornberger, G.M., Whitehead, P.G., Jarvie, H.P., Flynn, N., 2001. On modeling the mechanisms that control in-stream phosphorus, macrophyte, and epiphyte dynamics: An assessment of a new model using general sensitivity analysis. Water Resour. Res. 37, 2777–2792. https://doi.org/10.1029/2000WR000115
Wade, A.J., Jackson, B.M., Butterfield, D., 2008. Over-parameterised, uncertain 'mathematical marionettes' — How can we best use catchment water quality models? An example of an 80-year catchment-scale nutrient balance. Sci. Total Environ. 400, 52–74. https://doi.org/10.1016/j.scitotenv.2008.04.030
Wade, A.J., Skeffington, R.A., Couture, R.-M., Erlandsson Lampa, M., Groot, S., Halliday, S.J., Harezlak, V., Hejzlar, J., Jackson-Blake, L.A., Lepistö, A., Papastergiadou, E., Riera, J.L., Rankinen, K., Shahgedanova, M., Trolle, D., Whitehead, P.G., Psaltopoulos, D., Skuras, D., 2022. Land Use Change to Reduce Freshwater Nitrogen and Phosphorus will Be Effective Even with Projected Climate Change. Water 14, 829. https://doi.org/10.3390/w14050829
Wade, A.J., Whitehead, P.G., Butterfield, D., 2002. The Integrated Catchments model of Phosphorus dynamics (INCA-P), a new approach for multiple source assessment in heterogeneous river systems: model structure and equations. Hydrol. Earth Syst. Sci. 6, 583–606. https://doi.org/10.5194/hess-6-583-2002
Wall, D., Jordan, P., Melland, A.R., Mellander, P.-E., Buckley, C., Reaney, S.M., Shortle, G., 2011. Using the nutrient transfer continuum concept to evaluate the European Union Nitrates Directive National Action Programme. Environ. Sci. Policy 14, 664–674. https://doi.org/10.1016/j.envsci.2011.05.003
Wall, D.P., Jordan, P., Melland, A.R., Mellander, P.-E., Mechan, S., Shortle, G., 2013. Forecasting the decline of excess soil phosphorus in agricultural catchments. Soil Use Manag. 29, 147–154. https://doi.org/10.1111/j.1475-2743.2012.00413.x
Wall, D.P., Murphy, P.N.C., Melland, A.R., Mechan, S., Shine, O., Buckley, C., Mellander, P.-E., Shortle, G., Jordan, P., 2012. Evaluating nutrient source regulations at different scales in five agricultural catchments. Environ. Sci. Policy 24, 34–43. https://doi.org/10.1016/j.envsci.2012.06.007
Wall, D.P., Plunkett, M., 2020. Major and micro-nutrient advice for productive agricultural crops - 5th edition. Teagasc, Johnstown Castle, Co. Wexford.
Wall, D.P., Plunkett, M., 2016. Major and micro nutrient advice for productive agricultural crops.
Walsh, S., 2012. A Summary of Climate Averages 1981-2010 for Ireland, Climatological Note No.14. Met Éireann, Dublin.
Watanabe, M., Suzuki, T., O'ishi, R., Komuro, Y., Watanabe, S., Emori, S., Takemura, T., Chikira, M., Ogura, T., Sekiguchi, M., Takata, K., Yamazaki, D., Yokohata, T., Nozawa, T., Hasumi, H., Tatebe, H., Kimoto, M., 2010. Improved Climate Simulation by MIROC5: Mean States,

Variability, and Climate Sensitivity. J. Clim. 23, 6312–6335. https://doi.org/10.1175/2010JCLI3679.1
Wellen, C., Kamran-Disfani, A.-R., Arhonditsis, G.B., 2015. Evaluation of the Current State of Distributed Watershed Nutrient Water Quality Modeling. Environ. Sci. Technol. 49, 3278–3290. https://doi.org/10.1021/es5049557
Withers, P.J., Jordan, P., May, L., Jarvie, H.P., Deal, N.E., 2014. Do septic tank systems pose a hidden threat to water quality? Front. Ecol. Environ. 12, 123–130. https://doi.org/10.1890/130131
Withers, P.J.A., Jarvie, H.P., 2008. Delivery and cycling of phosphorus in rivers: A review. Sci. Total Environ. 400, 379–395. https://doi.org/10.1016/j.scitotenv.2008.08.002
Zambrano-Bigiarini, M., 2020. hydroGOF: Goodness-of-Fit Functions for Comparison of Simulated and Observed Hydrological Time Series. https://doi.org/10.5281/zenodo.839854
Zobrist, J., Reichert, P., 2006. Bayesian estimation of export coefficients from diffuse and point sources in Swiss watersheds. J. Hydrol. 329, 207–223. https://doi.org/10.1016/j.jhydrol.2006.02.014